NASA CR 71255

JET PROPULSION LABORATORY
CALIFORNIA INSTITUTE OF TECHNOLOGY
PASADENA, CALIFORNIA

GPO PRICE $ _____

CFSTI PRICE(S) $ _____

Hard copy (HC) $6.00

Microfiche (MF) 1.00

ff 653 July 65

RE-ORDER NO. 64-159

SURVEYOR
LUNAR ROVING VEHICLE, PHASE I

BSR-903

FINAL TECHNICAL REPORT

SUBMITTED TO

JET PROPULSION LABORATORY
CALIFORNIA INSTITUTE OF TECHNOLOGY

JPL CONTRACT
950656
under NAS 7-100

VOLUME II
MISSION AND SYSTEM STUDIES

APRIL 1964

Bendix SYSTEMS DIVISION

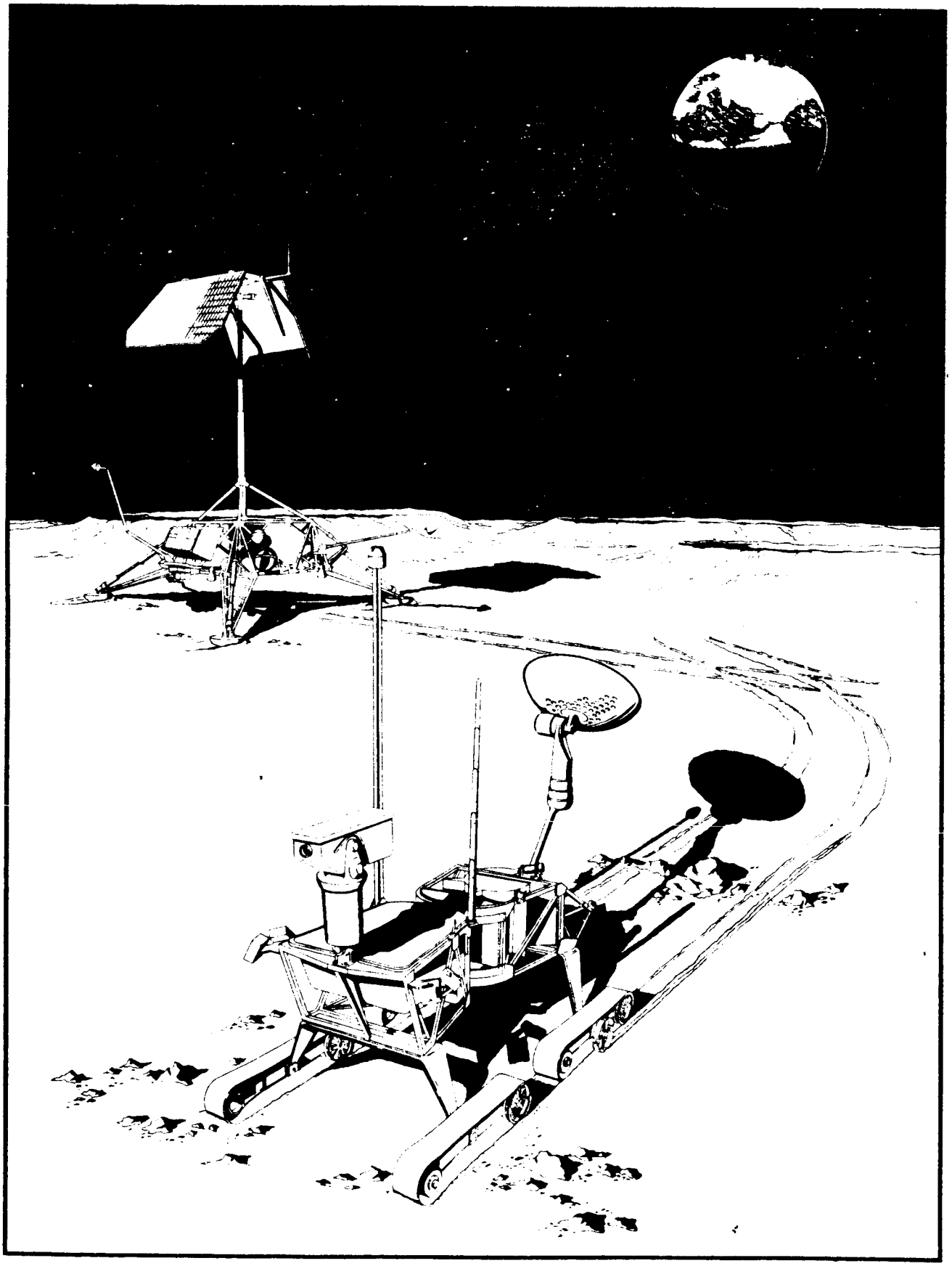

FOREWORD

As part of the continuing program of unmanned exploration of space, and to increase the effectiveness of the manned space program for exploring the moon, the Jet Propulsion Laboratory of the California Institute of Technology issued six-month study contracts to investigate the feasibility of a small, unmanned, lightweight, remotely controlled roving vehicle to be incorporated in the surveyor spacecraft to extend its data-gathering capabilities on the lunar surface. Specifically, the study program was to determine the feasibility of a 100-lb Surveyor Lunar Roving Vehicle (SLRV) system in gathering sufficient scientific information by surveying the lunar surface near the Surveyor spacecraft landing point to certify the area, in terms of specific hazards, as a potential Apollo LEM landing site.

This Final Technical Report, submitted in five volumes, presents the results and conclusions of the study program conducted by The Bendix Corporation under JPL Contract No. 950656. The volumes are organized to correspond to the specific objectives of the program: to conduct an analysis, to generate a preliminary design, and to fabricate and demonstrate an engineering test model in support of the over-all program objectives.

The results of Bendix's study show that the SLRV concept is not only feasible, but can make substantial contributions to the unmanned exploration of the moon in support of the manned Apollo program. The SLRV characteristics, the problems, and the initial trade-offs have been determined in sufficient detail to permit the definition of specific objectives and criteria for a follow-on development program. Program conclusions and recommendations are included in Volume V.

LIST OF VOLUMES

VOLUME I – PROGRAM SUMMARY

→ VOLUME II – MISSION AND SYSTEM STUDIES

VOLUME III – PRELIMINARY DESIGN AND SYSTEM DESCRIPTION

Book 1 – System Description and Performance Characteristics

Book 2 – Validation of Preliminary Design

VOLUME IV – RELIABILITY

VOLUME V – SYSTEM EVALUATION

THE DOCUMENT YOU ARE READING IS INDICATED BY THE ARROW

TABLE OF CONTENTS

		Page
1.	INTRODUCTION	1-1
2.	SUMMARY OF MISSION ANALYSIS AND REQUIREMENTS	2-1
2.1	PHYSICAL AND ENVIRONMENTAL CONSTRAINTS	2-1
2.2	PRIMARY OBJECTIVE	2-1
2.3	SECONDARY OBJECTIVES	2-2
2.4	PRIMARY MISSION REQUIREMENTS	2-2
2.4.1	Landing Site Diameter and Acceptability	2-2
2.4.2	Certified Landing Point Spacing	2-2
2.4.3	Landing Point Identifications	2-2
2.4.4	Soil Bearing Strength Measurements	2-3
2.4.5	Slope Measurements	2-3
2.4.6	Protuberances	2-3
2.4.7	Confidence in Acceptability of Certified Landing Points	2-3
2.4.8	Mission Probability of Success	2-3
2.5	MISSION ANALYSIS	2-3
2.5.1	Landing Point Pattern and Identification	2-4
2.5.2	Confidence in Landing Point Acceptability	2-15
2.5.3	Mission Probability of Success	2-19
3.	SUMMARY OF SYSTEM ANALYSIS AND REQUIREMENTS	3-1
3.1	SYSTEM DEFINITION	3-1
3.1.1	Surveyor Lunar Roving Vehicle	3-1
3.1.2	Surveyor Spacecraft Modifications	3-2
3.1.3	Ground Operating Equipment	3-2
3.1.4	Ground Support Equipment	3-3

TABLE OF CONTENTS (CONT.)

		Page
3.2	PRIMARY SYSTEM REQUIREMENTS	3-3
3.2.1	Landing Point Pattern	3-3
3.2.2	Landing Point Identification	3-3
3.2.3	Landing Point Certification Data	3-5
3.2.4	Traverse Capabilities	3-5
3.2.5	Data Transmission	3-6
3.2.6	Physical and Environmental Constraints	3-6
3.2.7	Reliability	3-6
3.3	SYSTEM ANALYSIS	3-6
3.3.1	Landing Point Verification and Mapping	3-6
3.3.2	Topographic Data Collection	3-9
3.3.3	Data Reduction	3-23
3.3.4	Topographic Data Coverage and Reduction from Fixed Baseline Stereo Images	3-30
3.3.5	Bearing Strength Measurements	3-35
3.3.6	Data and Landing Point Location Accuracy	3-36
3.3.7	Reliability	3-39
4.	SYSTEM DESIGN OF 100-lb VEHICLE	4-1
4.1	DESIGN METHODOLOGY	4-1
4.2	MOBILITY TRADE-OFFS AND SELECTIONS	4-4
4.2.1	Mobility Requirements	4-4
4.2.2	Mobility Concepts	4-11
4.2.3	Stability of Wheeled Vehicles	4-11
4.2.4	Weight Allocations	4-15
4.2.5	Friction and Step Heights	4-30
4.2.6	Figure of Merit Analysis	4-30
4.3	APOLLO SUPPORT SCIENTIFIC EXPERIMENTS	4-30
4.3.1	Bearing Strength Instrumentation	4-33
4.3.2	Topography Instrumentation	4-33
4.4	INFORMATION AND POWER	4-33
4.4.1	Mission Model	4-34
4.4.2	Design Selection	4-43

TABLE OF CONTENTS (CONT.)

		Page
4.5	OPERATION AND INTEGRATION	4-53
4.5.1	Functional Description	4-53
4.5.2	System Weight and Power	4-56
4.5.3	Operational Description	4-56
4.5.4	Mission Duration	4-60
4.6	CONCLUSION	4-63
5.	ADDITIONAL DESIGN ELEMENTS	5-1
5.1	MARKING	5-2
5.2	SAFETY	5-8
5.3	IMAGE SYSTEMS	5-14
5.3.1	Two-Tube Nonstereo TV	5-15
5.3.2	Two-Tube Stereo TV	5-15
5.3.3	Enhanced Monoptic Capabilities	5-16
5.3.4	Optical-Mechanical Scanner	5-19
5.4	SOIL BEARING STRENGTH INSTRUMENTATION	5-20
5.4.1	Soil Density Measurements	5-20
5.4.2	Vane Shear Meter	5-23
5.4.3	Jack Hammer	5-23
5.5	NIGHTTIME OPERATION	5-23
6.	SYSTEM DESIGN OF HEAVIER VEHICLES	6-1
6.1	DESIGN OBJECTIVES	6-1
6.2	PARAMETERS AFFECTING MISSION DURATION	6-4
6.2.1	Data Rate Effects	6-5
6.2.2	Vehicle Speed Effects	6-9
6.2.3	Continuous Driving Effect	6-9
6.2.4	Obstacle Traverse Capability Effect	6-11
6.2.5	Lunar Night Operation Effects	6-11
6.3	PARAMETERS AFFECTING OBSTACLE CLIMBING CAPABILITY	6-13
6.4	PARAMETERS AFFECTING RELIABILITY	6-18
6.5	TRADE-OFF RESULTS	6-21

TABLE OF CONTENTS (CONT.)

		Page
APPENDIX A	IDENTIFICATION OF ACCEPTABLE LANDING POINTS	A-1
APPENDIX B	PHOTOMETRIC DATA	B-1

LIST OF ILLUSTRATIONS

Figure	Title	Page
2-1	LEM Probability of Success vs Percent Acceptable Area in Site, LEM Crew Judgment, and Acceptable Area Distribution	2-5
2-2	Probability that Distance Between LEM Aiming Point and Hover Point is less than γ_e	2-8
2-3	Probability of Translating to Single Surveyed Point	2-9
2-4	Point Dispersion Patterns	2-10
2-5	Probability of Translating to a Surveyed Point	2-12
2-6	Probability that LEM Can Translate a Given Distance	2-13
2-7	Probability of Landing on Surveyed Point vs Diameter of Surveyed Point	2-16
2-8	Probability of LEM Translating to and Landing on Surveyed Point	2-17
2-9	Single-Shot Probability of Success vs Number of Vehicles	2-19
3-1	Landing Point Pattern	3-4
3-2	Limit of Terrain Masking	3-10
3-3	Typical Point Survey Patterns	3-11
3-4	Overlap of Convergent Images	3-13
3-5	Coverage of Overlapping Convergent Images	3-14
3-6	Normal Image Coverage Pattern	3-16
3-7	Coverage Pattern Distorted by Range Error	3-17
3-8	Coverage Pattern Distorted by Azimuth Error	3-18
3-9	Worst-Case Landing Point Camera Stations	3-19
3-10	Best-Case Landing Point Coverage and Camera Stations	3-21
3-11	Nominal Site Survey Pattern	3-22
3-12	Interpoint Topographic Data Collection	3-24
3-13	Perspective Grid	3-25
3-14	Object Measurement from Successive Images	3-27
3-15	Stereo Image Coverage	3-32
3-16	Stereo Camera Station Coverage	3-33
3-17	Stereo Landing Point Mapping Camera Stations	3-34
3-18	Point Diameter vs Point Location Error	3-37
3-19	Intrapoint Range vs Azimuth Uncertainty	3-40

LIST OF ILLUSTRATIONS (CONT.)

Figure	Title	Page
4-1	Functional Decisions	4-2
4-2	First-Order Effects Flow Diagram	4-3
4-3	Probability of Obstacle or Crevice Traverse vs SLRV Capability	4-7
4-4	Slope Traverse Probability vs SLRV Slope Traverse Capability	4-9
4-5	Soil Traverse Probability vs SLRV Bearing Strength Traverse Capability	4-10
4-6	Wheel Configurations	4-12
4-7	Three- and Four-Wheel Vehicle Geometry	4-13
4-8	Longitudinal Stability	4-14
4-9	Four- and Six-Wheel Vehicle Geometry	4-16
4-10	Lateral Stability	4-17
4-11	Three-Wheel Vehicle Geometry	4-18
4-12	Mobility Subsystem Wheel Weight	4-19
4-13	Motor, Transmission, Wheel, and Interconnection Assembly	4-21
4-14	Interconnecting Structure	4-21
4-15	Unit Drive Weight	4-23
4-16	Connecting Arms, Three- and Four-Wheel Vehicles	4-24
4-17	Mobility Subsystem Arm Weight	4-27
4-18	Mobility Subsystem Weight	4-28
4-19	Preliminary Weight Allocation	4-29
4-20	Friction and Step Capability	4-31
4-21	Figure of Merit Analysis	4-32
4-22	Crevice Crossing Capability vs Crevice Angle with Respect to Normal to Vehicle Heading	4-36
4-23	Crevice Detection Range vs Crevice Angle With Respect to Normal to Vehicle Heading	4-37
4-24	Crevice Detection Geometry	4-38
4-25	Parametric Relationships for Crevice Detection Range	4-39
4-26	Landing Point Survey and Marking Pattern	4-41
4-27	Number of Television Lines vs Traverse Spacing and Azimuth Sensing Accuracy Required	4-44
4-28	Preliminary SLRV Functional Block Diagram	4-54
4-29	SLRV Configuration Concept	4-55
4-30	Point Survey Pattern	4-58
4-31	Typical Intrapoint Power Profile	4-61

LIST OF ILLUSTRATIONS (CONT.)

Figure	Title	Page
4-32	Typical Interpoint Power Profile	4-62
4-33	SLRV Operational Periods as Function of Lunar and Earth Days	4-64
5-1	Marking Subsystem	5-3/5-4
5-2	Marking Deployment Technique	5-5
5-3	Safety Subsystem	5-11/5-12
5-4	Safety Mechanism Geometry	5-13
5-5	Two-Tube Stereo TV	5-17/5-18
5-6	SLRV Television Assembly (Zoom B)	5-25/5-26
6-1	Telecommunications Data Rate and Weight Trade-Off	6-6
6-2	Transmitter Weight and Mission Duration Trade-Off	6-8
6-3	Transport Weight and Mission Duration Trade-Off	6-10
6-4	Variation in Mission Duration With Obstacle-Climbing Capability	6-12
6-5	Mobility Weight and Obstacle-Climbing Capability	6-14
6-6	Structure Weight and Obstacle-Climbing Capability	6-15
6-7	Increase in Structure Weight for Vehicles Over 110 Lb	6-16
6-8	Deployment Weight vs Obstacle-Climbing Capability and Vehicle Weight	6-17
6-9	System Weight vs Obstacle-Climbing Capability for Various Composite Weights of Non-Transport Subsystems	6-19
6-10	Effects on System Reliability of Adding Weight in the Form of Redundancy	6-20
6-11	Trade-Off Results Between Data Rate and Vehicle Speed for Constant Obstacle Capability	6-23
6-12	Trade-Off Between Obstacle-Climbing Capability and Mission Duration	6-24
6-13	Figure of Merit vs Obstacle-Climbing Capability for 120-Lb System Design	6-26
6-14	Obstacle Capability and Mission Duration of Selected System Designs	6-29
A-1	Trajectory for Final 26 Sec of Main Retro Phase	A-3
A-2	Typical Landing Area	A-6
A-3	LEM Position Computation Geometry	A-6
A-4	Three-Point Geometry	A-9
A-5	Position Error as a Function of Relative Site Position Error	A-12

LIST OF ILLUSTRATIONS (CONT.)

Figure	Title	Page
A-6	Total Error as a Function of Relative Site Position Error	A-14
A-7	Minimum Point Diameter vs 3σ Total Error	A-15
A-8	Point Size as a Function of Relative Point Position Error	A-16
A-9	Optical Resolution vs Range	A-19
A-10	Required Diameter of Marking Circle as a Function of Range for Easy Visual Detection	A-21

LIST OF TABLES

Table	Title	Page
2-1	Translating Probabilities	2-14
4-1	Summary of Terrain Extremes	4-5
4-2	Mobility Subsystem Weight Breakdowns	4-26
4-3	Dual Mode Communications Summary	4-49
4-4	Antenna Coverage Required for Direct SLRV-To-Earth Link	4-51
4-5	System Weight and Power Summary	4-57
6-1	FOM Data Peaks	6-25
6-2	Selection Process	6-27
6-3	Selected Characteristics of Designs Over 100 Lb	6-28
A-1	Detection and Resolution Capabilities at Initial Correction Point	A-22

SECTION 1

INTRODUCTION

This volume of the Final Technical Report presents the results of the Phase I SLRV study program in accordance with Article 1, Section (a) (1) (i) of the Statement of Work of JPL Contract NO. 950656, Modification No. 1, which states:

> "Perform and present a system analysis, including the various system and subsystem trade-offs, leading to the proposed configuration. Subsystem trade-offs shall include, but not be limited to radioisotope thermoelectric generator (RTG) as a prime source of power, and a direct Rover-DSIF communications subsystem. Examine the various means of accomplishing the selected mission objectives and prepare data describing the extent to which the system meets the mission objectives and design criteria within applicable design restraints. These data shall provide a description of the system in sufficient detail so that the functions of the system and its subsystems can be identified."

In addition, this volume contains the results of system studies of vehicle concepts with a gross weight of more than 100 lb. These studies reflect trade-offs in terms of performance and reliability gains as a function of increased system weight.

SECTION 2

SUMMARY OF MISSION ANALYSIS AND REQUIREMENTS

At the outset of the study program, certain general mission objectives and requirements were evident. These lacked the necessary detail to permit meaningful conclusions to be drawn from the study. Accordingly, a mission analysis was conducted that resulted in specific mission requirements against which the preliminary design and evaluation were conducted. This section summarizes the results of this analysis and derivation of those results.

2.1 PHYSICAL AND ENVIRONMENTAL CONSTRAINTS

The physical and environmental constraints applicable to the SLRV are delineated in the following documents:

1. "Requirements for a Roving Vehicle for the Surveyor Spacecraft", Engineering Planning Document No. 98, Rev. 1, 18 November 1963, Jet Propulsion Laboratory, Pasadena, California.

2. "System Capabilities and Development Schedule of the Deep Space Instrumentation Facility", Technical Memorandum No. 33-83, 2 March 1962, Jet Propulsion Laboratory, Pasadena, California.

3. "Surveyor Basic Bus (2100 Lb) Payload Interface Requirements and Spacecraft System Description", HAC Specification No. 239503, Revision C, 20 November 1963. Hughes Aircraft Company, El Segundo, California.

2.2 PRIMARY OBJECTIVE

The primary objective of the SLRV is to provide a capability to obtain data which verify the suitability for manned landings in an area in the rear proximity of the Surveyor spacecraft.

2.3 SECONDARY OBJECTIVES

The secondary mission objectives are:

1. Provide a capability for the performance of additional scientific experiments and data collection beyond those required for manned landing site verification.

2. Demonstrate SLRV system operation in the actual lunar environment; perform the system functions of deployment, command and control, mobility, etc. and transmit data to earth which verify the performance of these functions.

3. Obtain data that will contribute to follow-on roving vehicle designs.

2.4 PRIMARY MISSION REQUIREMENTS

2.4.1 Landing Site Diameter and Acceptability

Measurement data shall identify and locate nineteen 40-meter diameter certified landing points in a site with a diameter of 3200 meters which includes the Surveyor touchdown point.

2.4.2 Certified Landing Point Spacing

Certified landing points shall be a maximum of 528 meters apart and nominally located at the apexes of continguous equilateral triangles. The center of the complex of landing points shall define the center of the 3200-meter site.

2.4.3 Landing Point Identifications

Three natural or artificial landmarks shall be identified within the site; these landmarks shall be spaced no less than 1500 meters apart and located, relative to each other, with an accuracy of 20 meters. Each of the LEM landing points shall be located relative to at least one of these landmarks with an accuracy of 20 meters. Orientation of the landing point pattern in lunar coordinates shall be provided.

The landmarks must be identifiable by the LEM crew during descent to the lunar surface from a slant range of up to 4400 meters and a minimum depression angle of 29 degrees. Artificial landmarks must retain their identifying characteristics for a period of at least one year.

2.4.4 Soil Bearing Strength Measurements

Measurements of the soil characteristics must verify that the landing points have an equivalent linear dynamic soil bearing strength gradient of at least 12 psi per foot for depths up to 50 cm at inpact velocities of up to 3 meters per second.

2.4.5 Slope Measurements

Measurement data must verify that the landing points contain effective slopes no greater than 12 degrees over any area greater than 10 meters in diameter. An effective slope is defined as the general surface slope over an area too large for the LEM to straddle, plus the combined effects of superimposed heights, depressions, and surface sinkage.

2.4.6 Protuberances

Measurements will verify that the landing points contain no effective protuberances greater than 50 cm. An effective protuberance is defined as the surface and subsurface relief within a horizontal distance of approximately 10 meters which might cause bottoming or tilting of the LEM. Effective protuberances may result from single objects, such as blocks, or complex combinations of heights, depressions, and surface sinkage.

2.4.7 Confidence in Acceptability of Certified Landing Points

The data derived from all measurements within each certified landing point provide a 0.99 confidence that 100 percent of the landing point area satisfies the acceptability criteria stated above.

2.4.8 Mission Probability of Success

The probability of achieving the primary mission objective shall be 0.50. This probability includes the launch vehicle and Surveyor Spacecraft success probabilities, and is applicable to a total of eight SLRV missions.

2.5 MISSION ANALYSIS

In Appendix A to EPD-98, Revision 1, it is stated that lunar reconnaissance systems employee for site verification be capable of:

1. Verifying with 90% confidence that 95% of the 3200-meter diameter site is acceptable.

2. Verifying with 99% confidence that 70% of the 3200-meter diameter site is acceptable.

The Phase I study requirements include determining the extent to which the SLRV can achieve this objective. At the outset, it was recognized that the SLRV could not verify an acceptable area greater than that which actually existed. It was further recognized that the percentage of acceptable area within the 3200-meter site might be considerably less than 95%. It was assumed that the primary purpose in establishing this objective in EPD-98 was to ensure a high degree of confidence in the probability of a successful LEM landing. Therefore the probability of success for LEM implied by this requirement was established and the extent to which the SLRV mission satisfied this level of LEM success was evaluated.

On a statistical basis, the probability of a successful LEM landing without prior site verification is directly proportional to the percentage of the site area which is actually acceptable, assuming uniform distribution of the acceptable area. Some improvement in this relationship could be expected by considering the ability of the LEM crew to maneuver during descent to avoid obviously hazardous areas. It can be shown that a significant improvement in this relationship may be achieved, even in sites where the acceptable area is down to a very small fraction of the total. This case is true if the distribution of the total acceptable area falls into a certain geometric pattern and that pattern is known. (Figure 2-1) Thus if a small percentage of the total site area can be verified in this pattern, then regardless of the total area actually acceptable, a high probability of a successful LEM can be achieved.

The derivation of the relationship between the percentage of total site area verified, the geometric pattern of the verified area, the pattern identification requirements, and the extent to which the resulting values for the probability of success for LEM satisfy the mission objective are presented in the following sections.

2.5.1 Landing Point Pattern and Identification

The probability of LEM mission success may be defined as:

$$P_s = P_{lem} P_{sa} P_{si}, \qquad (2\text{-}1)$$

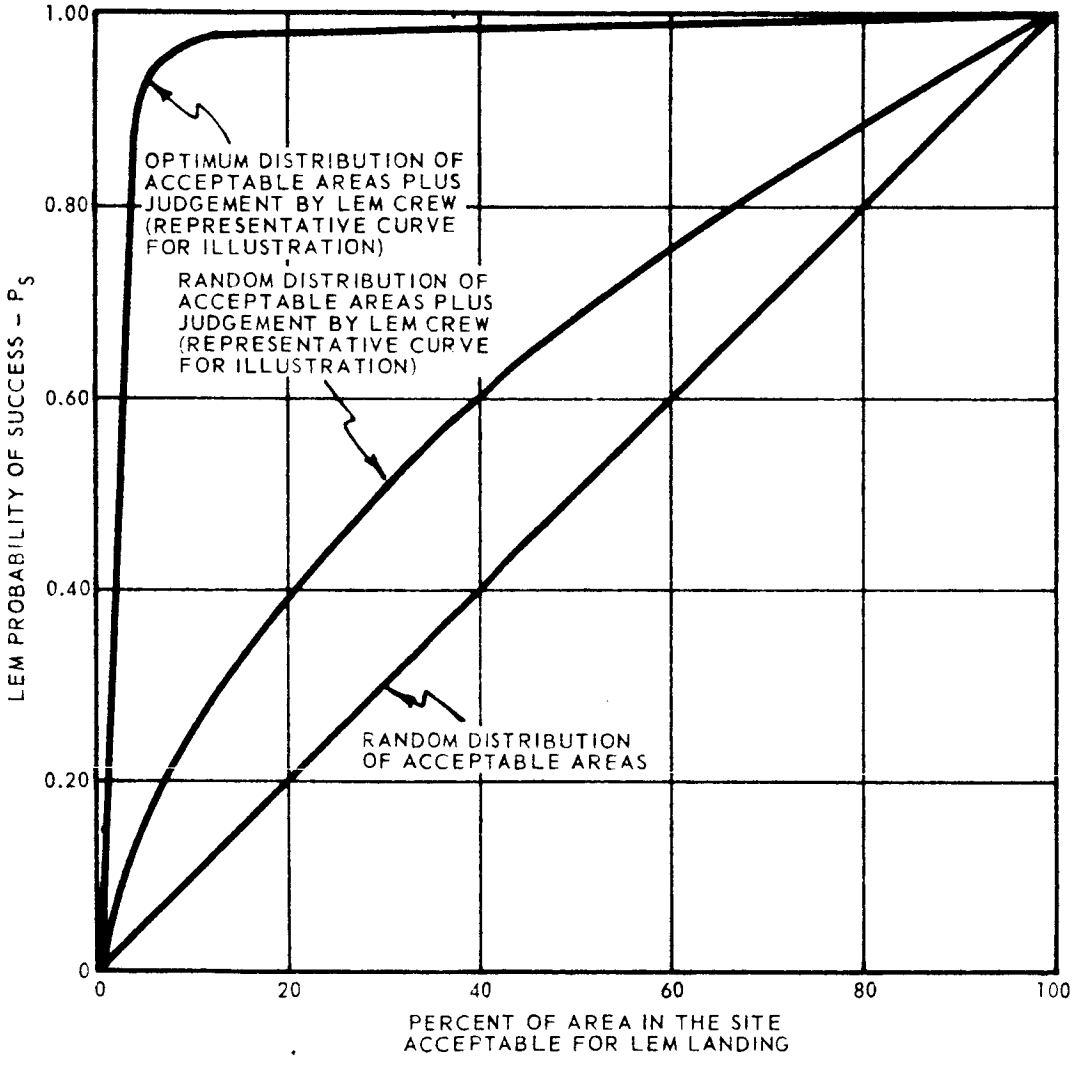

Figure 2-1 LEM Probability of Success vs Percent Acceptable Area in the Site, LEM Crew Judgment, and Acceptable Area Distribution

where P_{lem} is the probability that the LEM functions as required; P_{si} is the probability of identifying an acceptable landing point; and P_{sa} is the probability that the landing point on which the LEM attempts to land is acceptable.

The probability of successful LEM operation P_{lem} depends on the operation of the LEM and is independent of the characteristics of the site. Therefore, the SLRV can affect only P_s by providing improvement in the terms P_{sa} and P_{si}.

The probability, P_{sa}, that the LEM will land on an acceptable landing point is, in turn, dependent on:

1. P_{ts}: the probability that the LEM, after arriving at hover altitude, can translate to a verified landing point

2. P_{ls}: the probability of landing on the verified point, given that a translation to that point has been accomplished.

These probabilities combine to give:

$$P_{sa} = P_{ts} P_{ls}$$

The probability P_{ts} depends on the location error in the verified points. The LEM navigational errors (which are independent) may be combined to form an error in the position of the LEM hover point. Assuming that each of these errors are normally distributed with zero means and with standard deviations σ_l and σ_n respectively, the standard deviation σ_e of the combined error is

$$\sigma_e = \sqrt{\sigma_n^2 + \sigma_l^2} \qquad (2\text{-}2)$$

The probability P_e that the LEM hover point will be within a distance σ_e of the aiming point is given by

$$P_e = \frac{2}{\sigma_e^2 \pi} \int_0^{\gamma} e - \frac{\gamma^2}{2\sigma_e^2} \, d\gamma \qquad (2\text{-}3$$

A plot of P_e versus γ_e is shown in Figure 2-2 for

$$\sigma_e = 335 \text{ meters}$$

The LEM must translate from the hover point to a landing point verified by the LRV. If only a single point is verified by the SLRV, the LEM aiming point is in the center of this landing point and the translation required is the distance from the hover point to the edge of the verified landing point.

The probability P_{ts} that the LEM can translate from the hover point to the edge of the verified point is given by

$$P_{ts} = \frac{2}{\sigma_e \sqrt{2\pi}} \int_0^{T+1/2D} e^{-\frac{\gamma^2}{2\sigma_T^2}} d\gamma \qquad (2\text{-}4)$$

where (D) is the diameter of the verified landing point and (T) is the translational capability of the LEM. The value P_{ts} for any D and T can be determined from Figure 2-2 by computing γ_e from

$$\gamma_e = T + 1/2\ D \qquad (2\text{-}5)$$

Figure 2-3 shows the probability of translating to a single surveyed point as a function of point diameter and the translational capability of the LEM. It can be seen from Figure 2-3 that for the probability of translating to a single verified point to exceed 0.99, the diameter of the surveyed point must be greater than 1096 meters and the total area greater than 944,000 sq meters with a translational capability of 305 meters (3σ).

If more than one landing point is surveyed in patterns (Figure 2-4), the distance between each surveyed point should be such that the LEM can translate to a landing point from any point within a three-point triangular region. For a LEM with translational capabilities T, the distance L between the verified landing points should be

$$L = \sqrt{3}T \qquad (2\text{-}6)$$

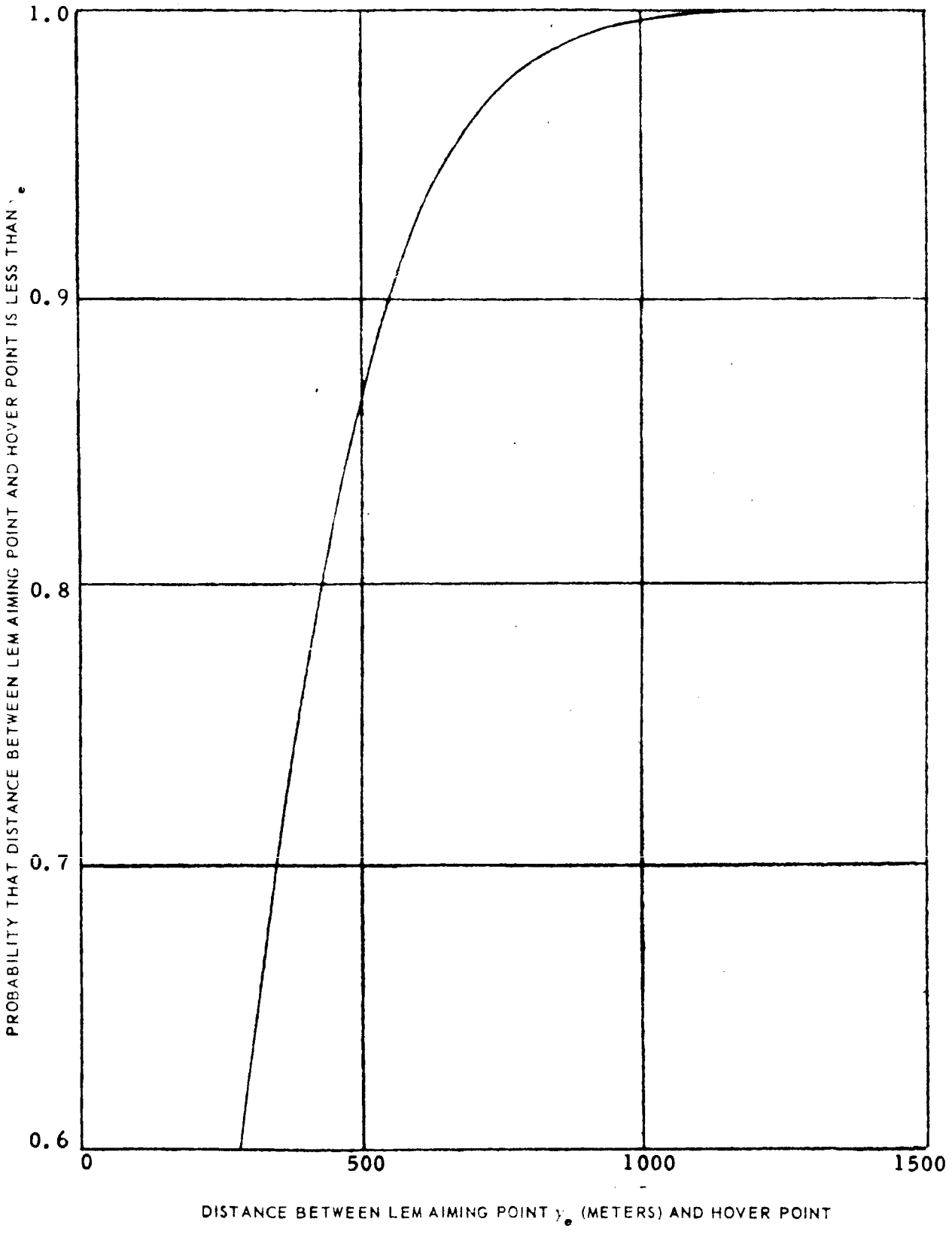

Figure 2-2 Probability That Distance Between LEM Aiming Point and Hover Point is Less Than γ_e

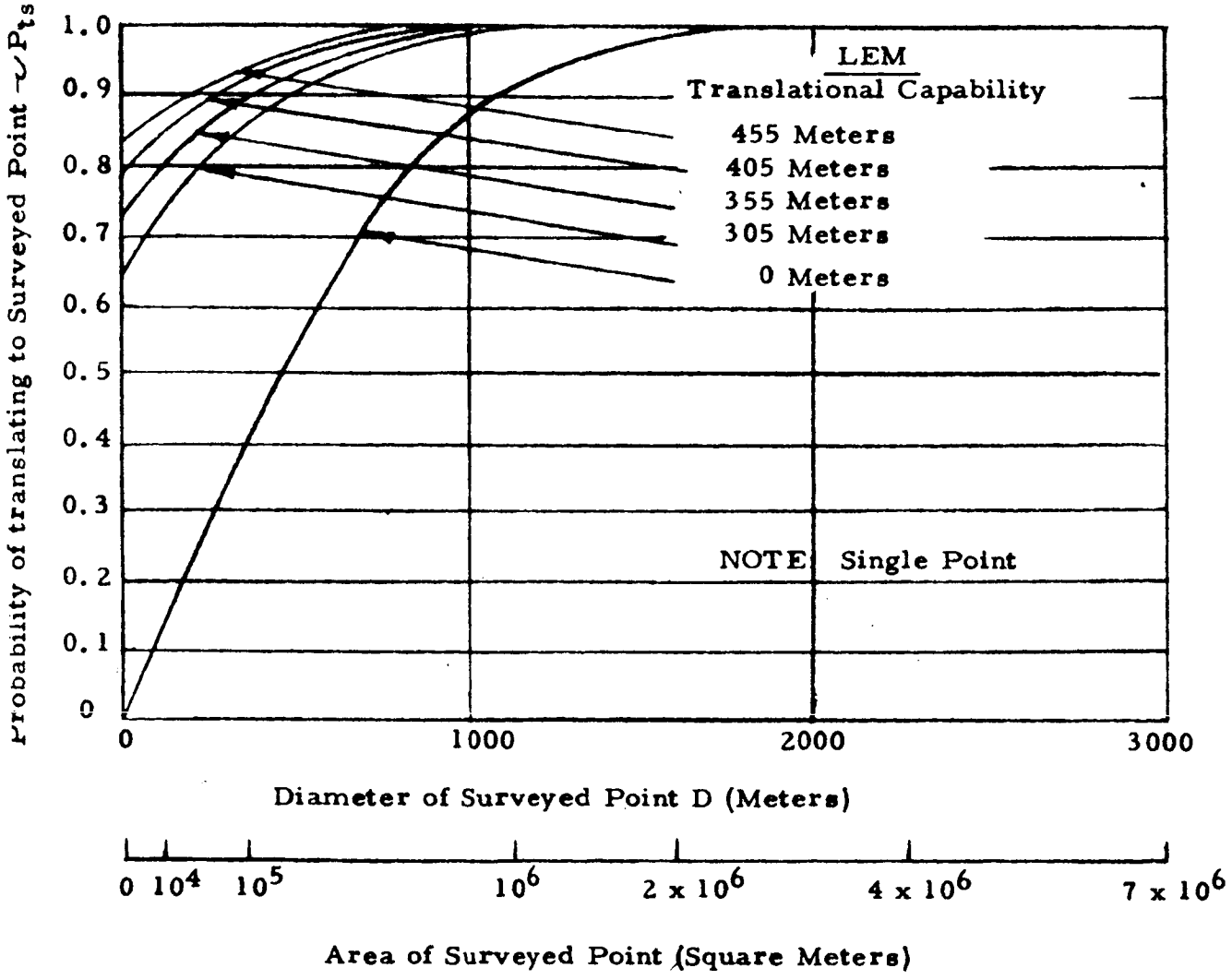

Figure 2-3 Probability of Translating to a Single Surveyed Point

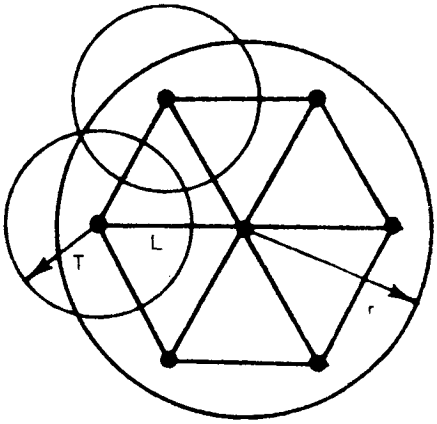

(a.) 7 POINTS

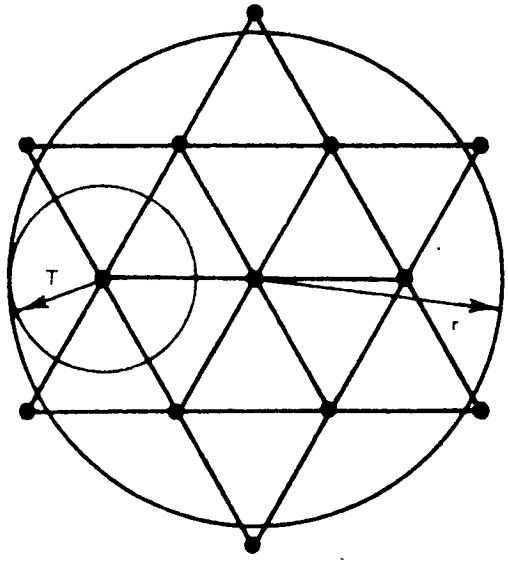

(b.) 13 POINTS

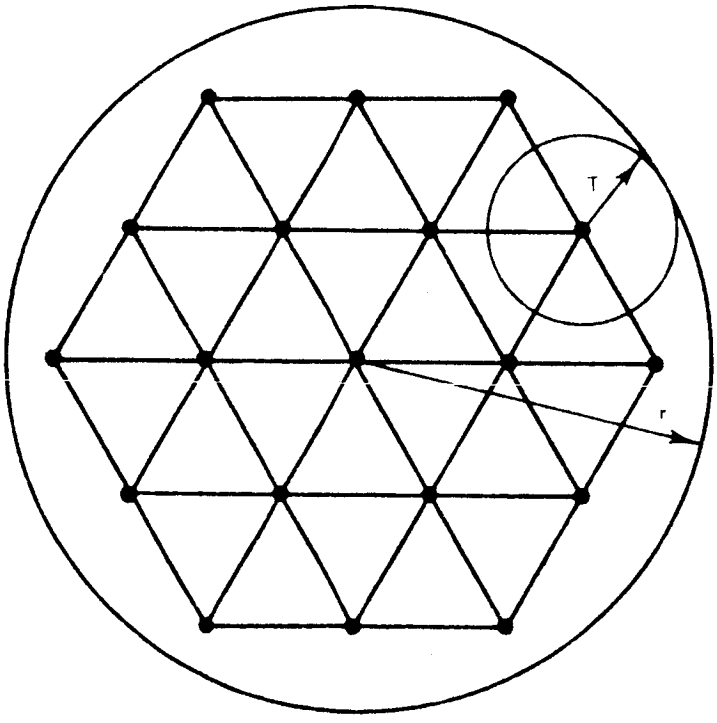

(c.) 19 POINTS

Figure 2-3 Point Dispersion Patterns

The LEM is then able to translate to at least one verified landing point from any point within the large circle of radius r as shown in Figure 2-4. For the seven-landing-point pattern, the radius of this circle is given by

$$r_7 = 2T \tag{2-7}$$

For the 13-point pattern

$$r_{13} = 2.732\ T \tag{2-8}$$

and for the 19-point pattern

$$r_{19} = 4T \tag{2-9}$$

Hence, a LEM with translational capability T will be able to reach at least one verified point if the hover point is within a circular region of radius r_i about the aiming point. The probability that the hover point is within this region is given by Equation (2-3), except that now the limits of integration are from 0 to r_i rather than 0 to γ. The probability is simply the probability P_{ts} of translation to a surveyed landing point. Plots of the probability P_{ts} as a function of the LEM translational capability are shown in Figure 2-5 for 7, 13, and 19 landing points.

In computing the probability P_{ts} as previously described, the LEM translation capability has been considered an independent variable. It can, however, be specified by a normal distribution with mean M_t and standard deviation σ_t. Hence, the probability of translating at least a distance γ_t is

$$P_t = \frac{1}{\sigma_t \sqrt{2\pi}} \int_{\gamma_t}^{\infty} e^{-\frac{(r-m)^2}{2\sigma_t^2}}\, d\gamma \tag{2-10}$$

A plot of P_t versus γ_t is shown in Figure 2-6 for:

$$M_t = 455 \text{ meters}$$

and

$$\sigma_t = 50 \text{ meters}$$

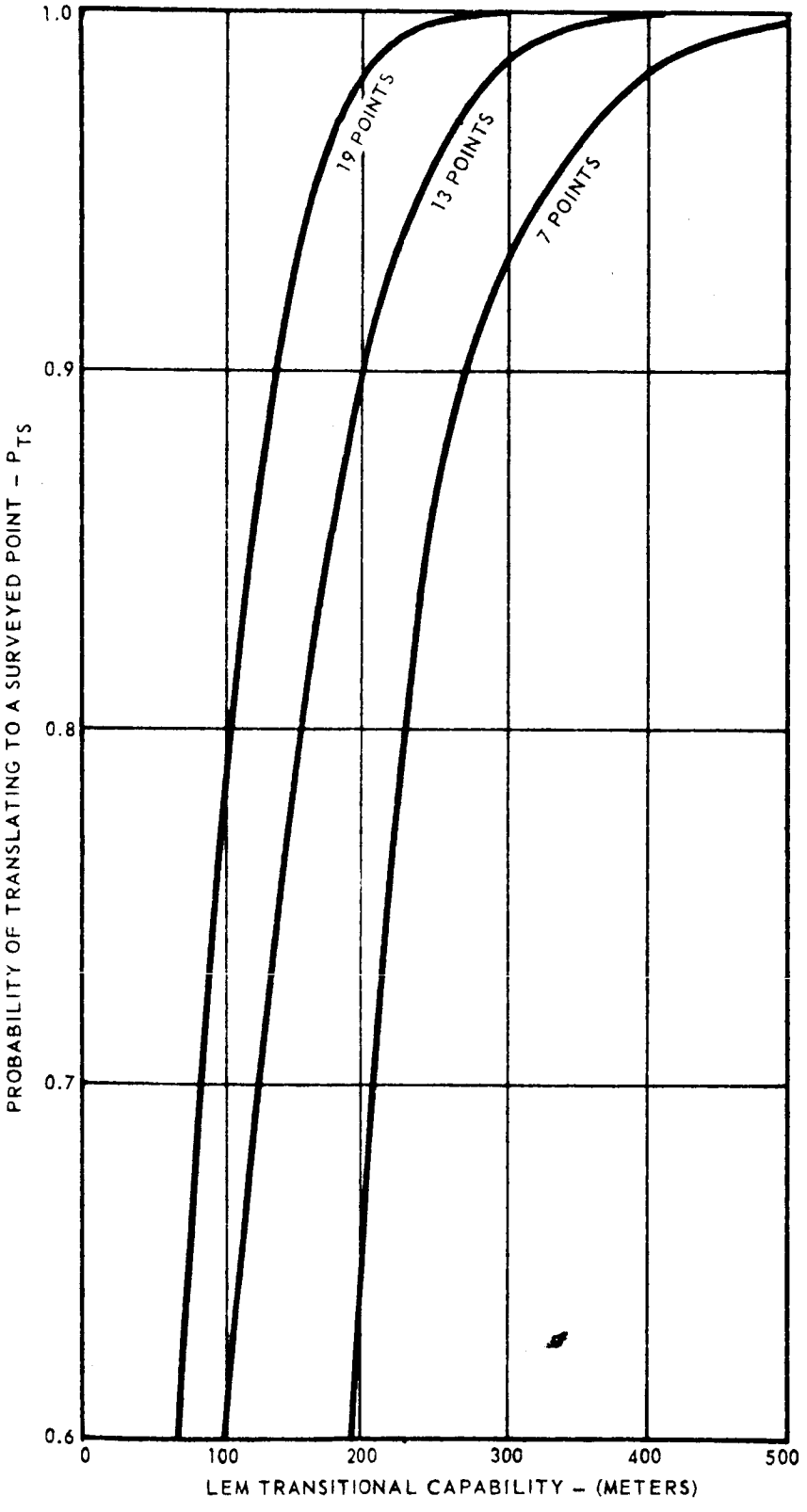

Figure 2-5 Probability of Translating to a Surveyed Point

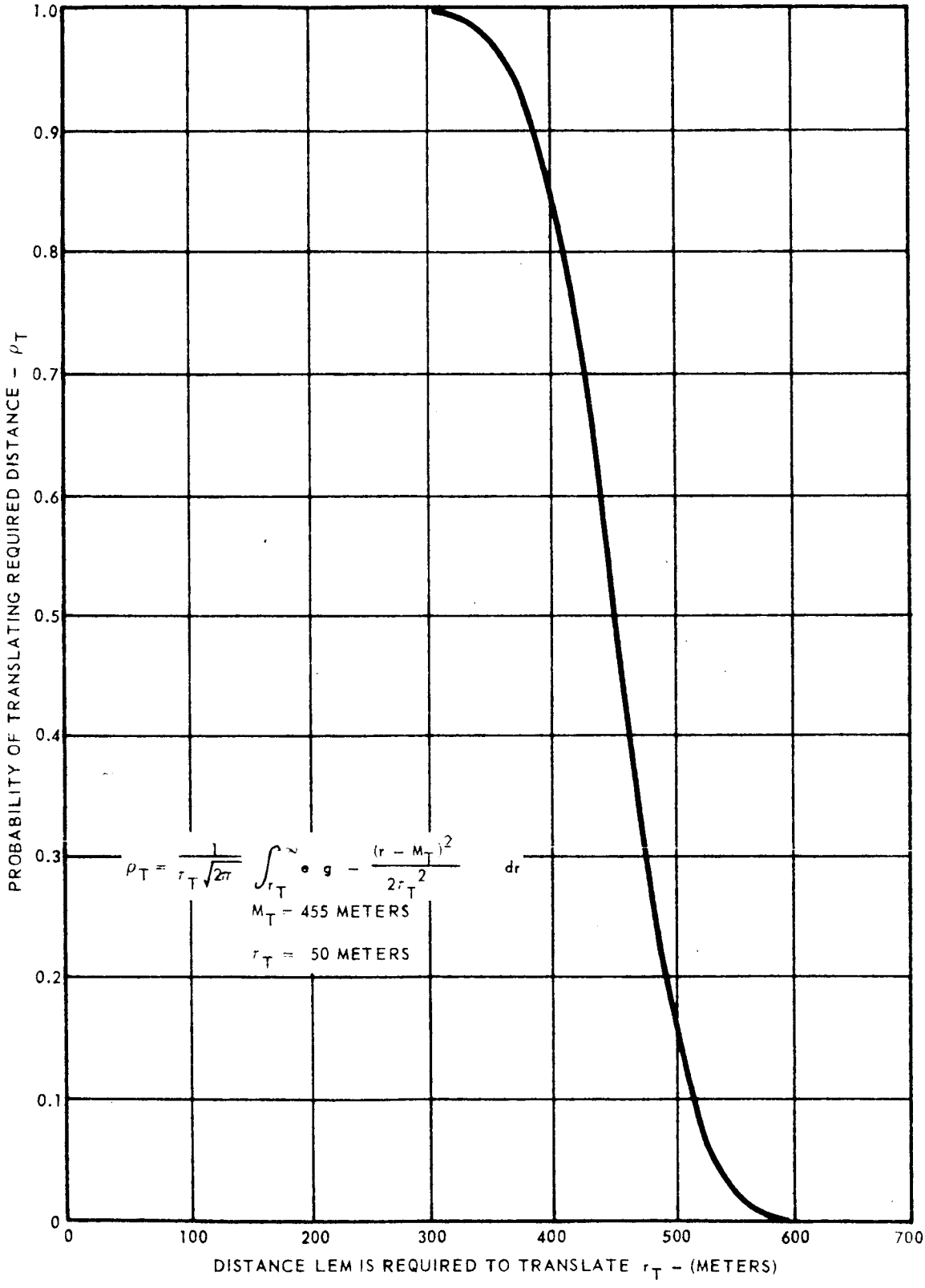

Figure 2-6 Probability that LEM can Translate a Given Distance

If the LEM translational capability is said to be T, this actually means that the LEM can translate at least the distance T with a probability given by Equation (2-10) where γ_t = T. Assuming P_t = 0.997, then T = 317 meters. The probabilities P_{ts} of translation to a verified point for the 7-, 13-, and 19-point patterns are given in Table 2-1.

TABLE 2-1

TRANSLATING PROBABILITIES

Number of Landing Points	P_{ts}
7	0.941
13	0.990
19	~ 1.000

The other major factor in determining P_{sa} is P_{ls} and is the probability that the LEM lands on the verified point, depending on the error in locating the landing point, the error in landing the LEM, and the diameter of the landing point. It is assumed that the error in locating the verified point is normally distributed with mean zero and a standard deviation, σ_{le}. It should be noted that $3\sigma_{le}$ is equivalent to the 3σ landing point location error. The LEM coordinate error is not included, since it is accounted for in the point diameter-point error relationship derived in Appendix A. It is assumed that the error in the LEM landing control is also normally distributed with mean zero and standard deviation σ_{ce}. These errors add vectorially to give the total error σ_{te} in landing of the LEM.

$$\sigma_{te} = \sqrt{\sigma_{le}^2 + \sigma_{ce}^2} \qquad (2\text{-}11)$$

The probability P_{ls} of landing within a verified point of diameter D is given by:

$$P_{ls} = \frac{2}{\sigma_{te}\sqrt{2\pi}} \int_0^{D/2} e^{-\frac{r^2}{2\sigma_{te}^2}} dr \qquad (2\text{-}12)$$

A plot of P_{ls} versus D for σ_{le} = 6.67 meters corresponding to a 20-meter point location error (see Appendix A) and σ_{ce} = 5 meters is shown in Figure 2-7. For these values of σ_{le} and σ_{ce}, σ_{te} = 8.34 meters.

In summary, the product of the probabilities P_{ts} and P_{ls} gives the combined probability P_{sa} of the LEM translating to and landing on an acceptable landing point. A plot of the probability P_{tl} is shown in Figure 2-8 as a function of the total area surveyed by the SLRV. Figure 2-8 shows that the probability P_m is low if only a single landing point is surveyed unless the diameter of that point is very large.

For a total acceptable area of less than 10,000 square meters, the seven-landing-point pattern gives a higher probability than either the 13-or 19-point pattern. In addition, the 13-point pattern gives a higher probability than the 19-point pattern for total acceptable areas less than approximately 25,000 square meters. This is explained by the fact that when equal areas are surveyed, the diameters of the individual landing points of the 7-point pattern are greater than those of the 13-point pattern. This decreases the overall probability due to the smaller diameter of each landing point in the 13-point pattern.

To obtain a probability of landing on an acceptable point of at least 0.98, 13 to 19 certified points are required, each with a minimum diameter of 40 meters, and, as derived in Appendix A, a point location accuracy of 20 meters. To aid in LEM point identification and landing the orientation of the landing point pattern must be established in lunar coordinates.

2.5.2 Confidence in Landing Point Acceptability

The previous analysis indicated that certification of 19 landing points properly distributed throughout the landing site will provide a high probability of success of an LEM landing within the site. The confidence in this probability figure is achieved by the confidence in the degree to which the landing points have been verified and located. Since, in a small landing point of the order of 40 meters in diameter, there is little or no room for maneuvering the LEM, 100% of the landing point must be acceptable with as high a confidence level as possible. Therefore it has been established as a mission requirement that a 99% confidence should be obtained that 100% of a certified landing point is acceptable.

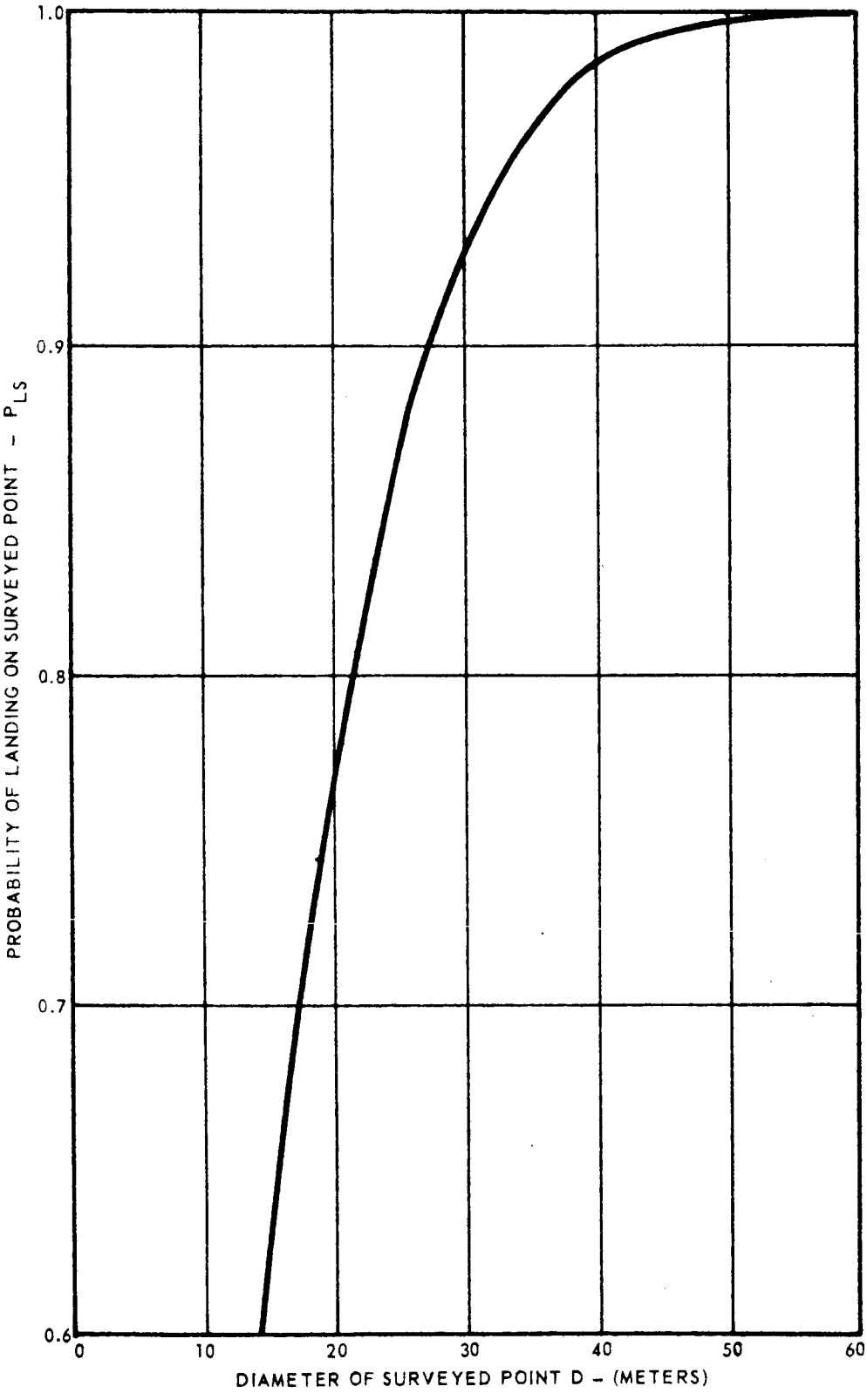

Figure 2-7 Probability of Landing on Surveyed Point vs Diameter of Surveyed Point

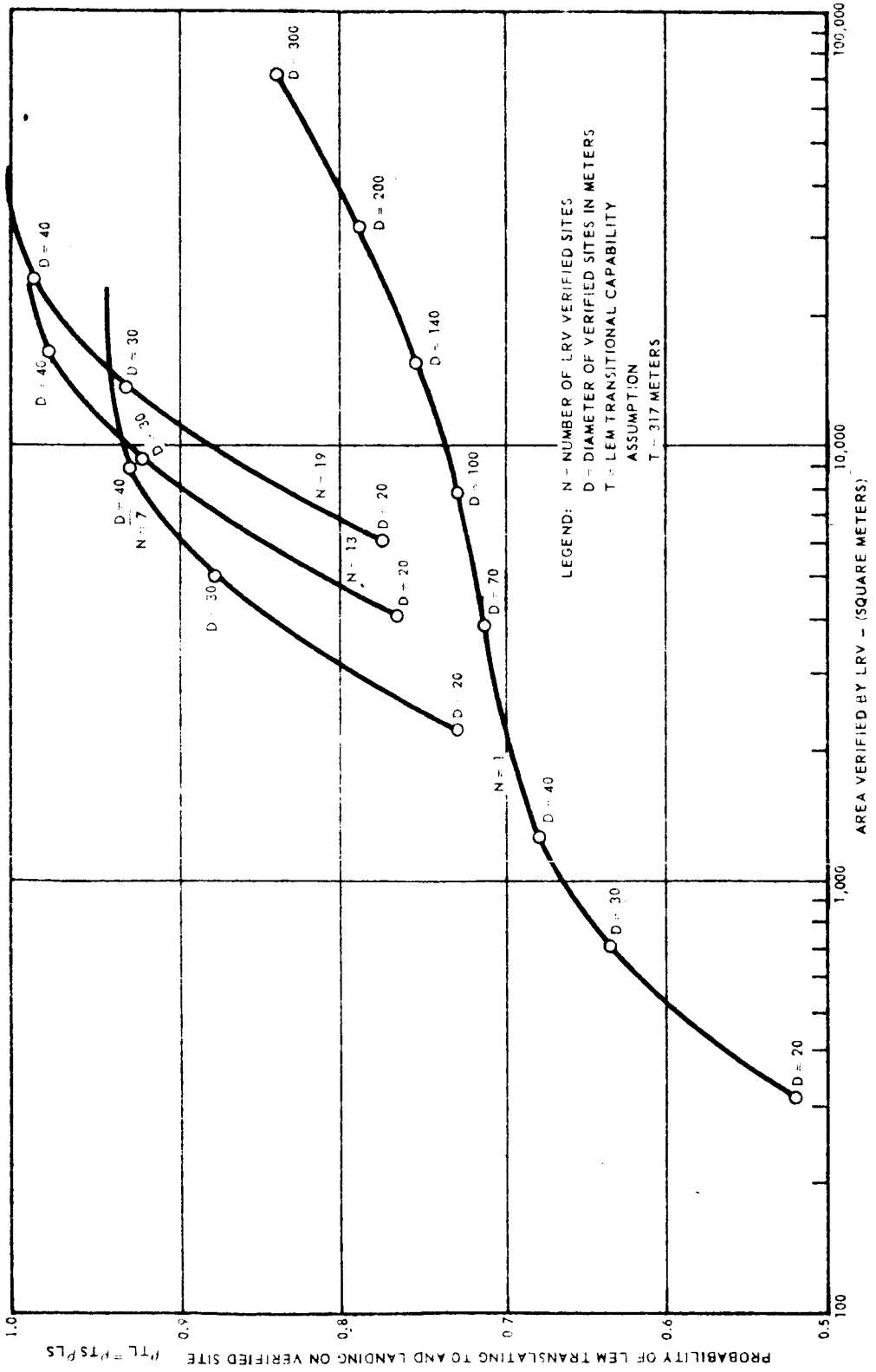

Figure 2-8 Probability of LEM Translating to and Landing on Surveyed Point

2.5.3 Mission Probability of Success

The SLRV Program consists of a number of vehicles, each designed to complete the primary mission objective of surveying the LEM landing area. The probability of successfully completing this program is dependent on the probability of success of each vehicle and the number of vehicles. Denoting the probability of success by P_{ps}, the single-shot mission success probability by P_{ss}, and the number of vehicles by N, then (provided the probability of mission success is the same for each vehicle).

$$P_{ps} = 1 - (1 - P_{ss})^N \qquad (2\text{-}13)$$

The required single shot probability as a function of the number of vehicles is shown in Figure 2-9 for a program success probability requirement of 0.99.

If it is assumed that each vehicle provides follow-on design data, the probability of successfully completing the mission increases with each vehicle.

Hence,

$$P_{ps} > 1 - (1-P_{ss_1})(1-P_{ss_2}) \ldots (1-P_{ss_N}), \qquad (2\text{-}14)$$

where P_{ss_i} is the probability of mission success of the i^{th} vehicle and

$P_{ss_i} \leq P_{ss_i} + 1$.

Three methods are suggested as bases for the relative values of the single-shot probabilities:

1. A constant percentage increase in the probability of success of each vehicle. Hence,

$$P_{ss_i} = \left(1 + \frac{K_1}{100}\right) P_{ss_{i-1}}$$

where K_1 is the percentage increase in the probability of each vehicle.

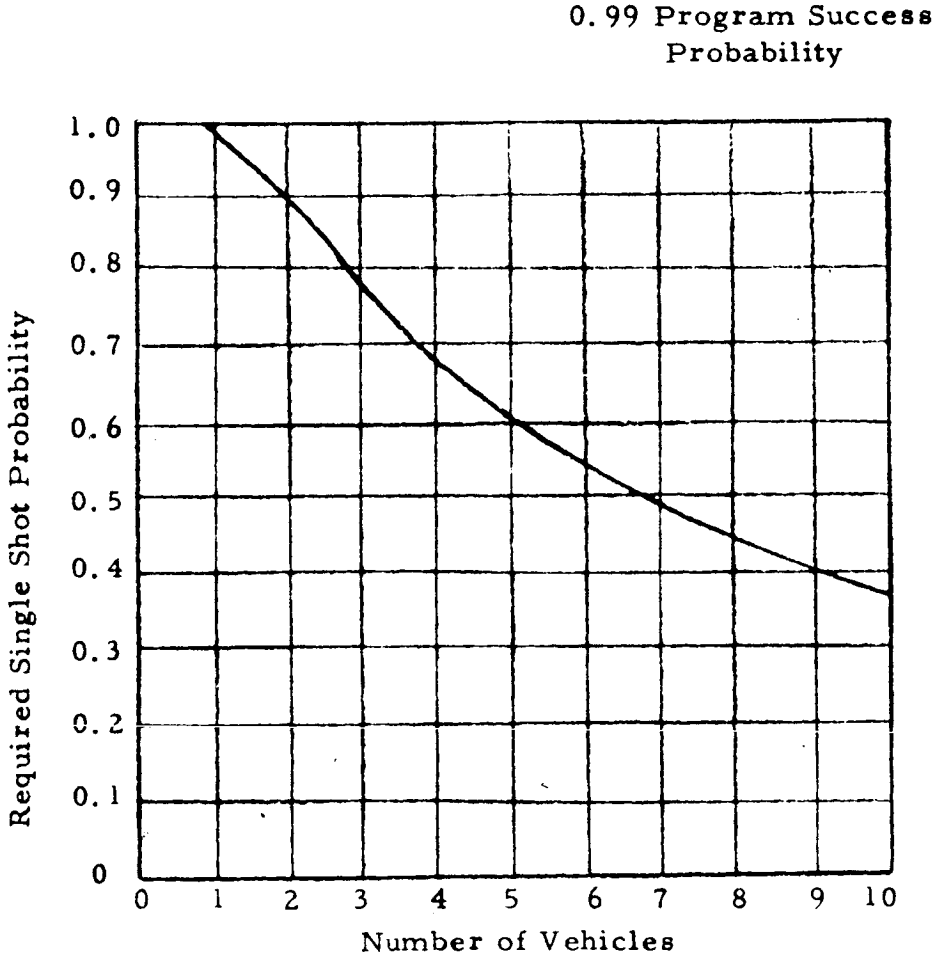

Figure 2-10 Single-Shot Probability of Success vs Number of Vehicles

2. The increase in probability of success is an exponential decay,

$$P_{ssi} = \left(1 + e - \frac{i}{K_2} \right) P_{ss_{i-1}} \qquad (2\text{-}16)$$

where K_2 is a constant which affects the rate of exponential decay.

3. The first (M-1) vehicles have zero probability of success while all succeeding vehicles increase the probability of success by the exponential decay. Thus,

$$P_{ss_i} = 0 \quad i < M$$

$$P_{ss_i} = \left(1 < 3 - \frac{i}{K_3} \right) P_{ss_{i-1}} \quad i \geq M \qquad (2\text{-}17)$$

The first approach is not realistic. It seems more reasonable that the percentage increase in P_{ss} will diminish as more vehicles are launched. Follow-on vehicle design data should decrease so that the probability of a successful mission will remain essentially constant after the first few vehicles. The second method is designed to show this trend. The third method considers an initial vehicle design which decreases the over-all range of the vehicle while increasing the design margin on mobility, data collection, etc. These initial vehicles would be unable to survey completely a LEM landing area because of limited range capabilities, but are more likely to satisfy the secondary objective of system demonstration and providing follow-on vehicle design data.

If a given number of vehicles are allocated for the SLRV Program and the required probability of program success is designated, then the single shot probability required for each vehicle can be determined by the methods described.

SECTION 3

SUMMARY OF SYSTEM ANALYSIS AND REQUIREMENTS

To implement the specified mission objectives, an analysis was performed which resulted in a set of system requirements. These requirements define the accuracies required of the system data gathering and support function elements necessary to assure a maximum probability of SLRV mission success.

This section summarizes the system requirements and their derivations.

3.1 SYSTEM DEFINITION

The complete SLRV System (Surveyor Lunar Roving Vehicle) is composed of the following elements:

1. SLRV
2. Surveyor Spacecraft Modifications
3. Ground Operating Equipment (GOE)
4. Ground Support Equipment (GSE)

These elements are operated in conjunction with the DSIF and SFOF facilities and the Atlas/Centaur launch vehicle.

3.1.1 Surveyor Lunar Roving Vehicle

The SLRV is composed of the following subsystems:

1. Mobility
2. Structure

3. Information and Sensors

4. Prime Power

5. Navigation and Control

6. Experiment Payload.

3.1.2 Surveyor Spacecraft Modifications

The SLRV will perform all required mobile surface operations via remote commands from earth and will be as independent of the Surveyor Spacecraft as practical.

Any Surveyor functions which are required by the SLRV beyond those normally provided must be charged against the SLRV System; i.e., any additional weight will be subtracted from the 100 lb allotted for the SLRV.

3.1.3 Ground Operating Equipment

Ground operating equipment is defined as all ground equipment, including DSIF or SFOF equipment, required to perform the following functions:

1. Remote control of SLRV deployment and operational checkout.

2. Examination and evaluation of spacecraft-gathered data to determine likely LEM landing points for verification by the SLRV.

3. Remote control of the mobile surface operations, including steering the SLRV, manipulating the soil testing devices, and controlling the observation systems aboard the SLRV.

4. Process and display SLRV-gathered data to allow real-time decisions of landing point acceptability.

5. Correlation and processing of the SLRV data so that detailed maps of the survey points and adjacent portions of the site are obtained.

Major ground operating equipment subsystems are: communications, displays and controls, data analysis computers, command computers, and recording devices.

3.1.4 Ground Support Equipment

Ground support equipment is that equipment used for assembly, integration, test, evaluation, transportation, and handling of the SLRV.

3.2 PRIMARY SYSTEM REQUIREMENTS

The following primary system requirements were derived to satisfy the primary mission objective and requirements specified in Section 2.6.

3.2.1 Landing Point Pattern

The desired pattern of certified points in the site is shown in Figure 3-1. Terrain conditions may not allow the certification of points precisely in the indicated pattern, but the pattern can be adjusted where necessary with closer spacing between points.

3.2.1.1 Landing Point Spacing and Location Accuracy

Although the pattern of points may be altered to compensate for terrain conditions, the maximum allowable distance between any two adjacent points is 528 meters, center to center.

All landing points shall be located with an accuracy of 20 meters (3σ) with respect to one of the LEM navigational aid marks.

3.2.1.2 Landing Point Diameter

Consistant with the above point location accuracy, the landing points shall have a minimum surveyed and certified acceptable area contained within a diameter of 40 meters.

3.2.2 Landing Point Identification

The SLRV must be able to locate and identify natural, or emplace three artificial marks to serve as navigational aids to the LEM crew. The marks must have the visual qualities specified in Appendix A.

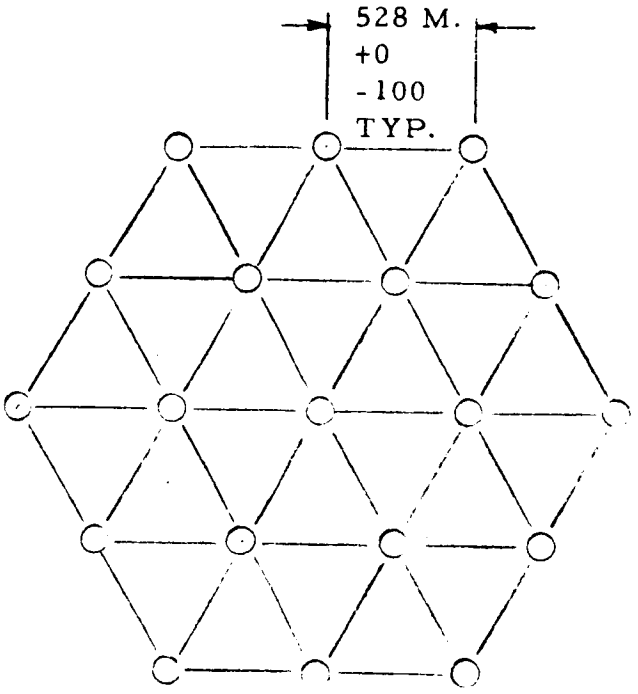

Figure 3-1 Landing Point Pattern

Minimum spacing between any two marks shall be 1500 meters. Each mark shall be located with respect to the other two with an accuracy of 20 meters.

3.2.3 Landing Point Certification Data

The landing point certification data requirements summarized below are those derived to satisfy the soil bearing strength, effective protuberance, and effective slope measurements specified in Section 2.1.

3.2.3.1 Effective Protuberance Data

All surface discontinuities of 20 cm or more change in elevation within the landing point shall be identified with an accuracy of 5 cm minimum.

3.2.3.2 Effective Slpe Data

The system shall be capable of providing elevation, protuberance, and bearing strength data so that there is a 99% confidence that there are no effective slopes of 12^{o} or greater in a certified landing point.

3.2.3.3 Soil Bearing Strength Data

Soil bearing strength is defined as the force per unit area that the soil will support at a given level of sinkage. The test data collected should be capable of extrapolation to areas larger than 0.30 meter in diameter.

Measurements for bearing strength shall be taken at a minimum of 45 locations distributed over the survey area. The data measurement range shall be sufficient to be correlated to bearing strengths of 0.5 to 12 psi with a tolerance of ± 20% within this range.

The depth of measurements shall be at least 50 cm unless a force of 12 pounds per square inch is encountered.

3.2.4 Traverse Capabilities

The SLRV shall be capable of traversing the surface models specified in EPO-98, Revision 1 commensurate with a 0.5 probability of successfully certifying 19 acceptable landing points and identifying or emplacing three marks.

3.2.5 Data Transmission

Data transmission shall be compatible with the DSIF capabilities as specified in JPL Technical Memorandum No. 33-83.

3.2.6 Physical and Environmental Constraints

The SLRV shall be compatible with the physical and environmental contraints specified in Section 2.

3.2.7 Reliability

The SLRV system reliability shall be commensurate with 0.5 probability of successfully certifying 19 acceptable landing points and identifying or emplacing three land marks.

3.3 SYSTEM ANALYSIS

The analyses conducted to determine system requirements which assure subsequent system design and to incorporate characteristics and capabilities which satisfy the mission requirements and objectives are discussed in this section.

3.3.1 Landing Point Verification and Mapping

This section describes and analyzes methods of measuring the lunar topographic relief within a landing point to verify its acceptability for an Apollo landing.

The mission analysis (Section 2) concluded that a mission based on certifying the acceptability of 19 landing points within a site produces a confidence in the probability of the LEM landing essentially equal to that produced by mapping the entire site; the astronauts need only guide the LEM to a certified point one of which will always be within the LEM translational capability. Consequently a chart of the 3200-meter site would be prepared. The chart would contain easily identified terrain hazards and the location of the certified landing points with respect to the referenced landmarks, either natural or artificial. Within this chart, a 25-cm contour map of the certified landing points would not be of significant value to the astronaut since by definition it would show virtually no topographic relief. Thus the usefulness of a map as a navigation aid can be satisfied

by the production of a chart of the 3200-meter area based on the primary mission defined. That the actual certification of the landing points should result from an analysis of the data returned by the SLRV in real-time, or from analysis of the data processed into the form of a contour map is the next consideration.

The time required to produce the contour map of a landing point must be considered if it is to be used for certification. The impact of this time on the overall mission must then be evaluated. Only two techniques appear to offer a reasonable chance of success in obtaining the necessary data. First, profile data derived from direct measurement sensors as the SLRV is guided over the surface to be surveyed should be obtained. Profile data obtained in this manner would require an extensive range requirement on the vehicle to get data sufficiently fine grained to produce a 25-cm contour map. The time required to obtain these data would drive the total mission time to a length which is considered to be unacceptable.

Second, data necessary to produce the map through the stereo-photogrammetric reduction of television or other image pictures obtained by a sensor as it surveys the landing point must be obtained. However, the time required to reduce a pair of photographs to a topographic map will increase as the complexity of the lunar surface increases to the point where, for a marginally acceptable surface, it is estimated that upwards of four hours would be required to reduce one stereo pair of photographs. The fact that production of an accurate contour map is not a real-time function is important from an operational viewpoint. Before the SLRV leaves the vicinity of a surveyed landing point to search for the next point, the first point should be classified as acceptable or unacceptable (it is undesirable to return later to the vicinity of a surveyed point which subsequent photogrammetric analysis has proved unacceptable). Every operation mistake of this type will add a minimum of 1 km to the SLRV range requirement, and 10 to 20 hours are added to the mission time every time a replacement landing point must be verified.

Therefore, to ensure mission success, a set of techniques should be devised which will yield, in as many cases as possible, verification of terrain suitability as a real-time operation. Subsequent rendition of these data in contour map form will provide a permanent record of the validation.

Section 3.3.2 presents techniques for gathering the topographic data; analysis of the requirements for soil bearing strength data is contained in Section 3.3.5. Real-time analysis of topographic data derived

from stereo image pairs from a fixed base binocular television system is discussed in Section 3.3.4.

In summary, the analysis of real-time topographic data reduction techniques shows that they are useful on surfaces which range from smooth to medium difficulty; e.g. smooth with scattered obstacles. In difficult terrain, (typified by the Bonito lava flow) the uncertainties in these techniques for slope and elevation measurement are so large that stereophotogrammetric reduction of the image data would be required for certification despite the operational objections noted previously. The alternate to this would be to reject all potentially good points which required accurate measurement and instead, search for obviously good landing points. Further operational analysis in Phase II will determine which is the more reasonable strategy on given lunar surface models. In addition, further study may reveal real-time evaluation techniques which are acceptable in rugged terrain.

The relationship of charts and contour maps to site certification are summarized as follows:

1. The value to the astronauts of a 25-cm contour map of certified acceptable 40-meter diameter landing point is questionable.

2. Since such a map cannot be produced in real-time, its usefulness as an aid to landing point verification is limited to those terrains in which faster techniques are not sufficiently accurate.

3. Complete contour maps of each certified landing point, which are of great scientific interest, can be produced at a later time if not required for verification.

4. Within the 100-lb SLRV design, the operational capability exists to obtain sufficient convergent television images to produce a 25-cm contour map of the landing point by stereophotogrammetric analysis. (Mission times are based on obtaining these images but not on reducing them to a map).

5. A chart of the landing site which identifies all major hazards and as many minor hazards as possible in addition to the location of acceptable landing points is of value to the astronauts during an LEM landing. The value of this chart would

not be as great as a 25-cm contour map of the entire 3200-meter site if a large percentage of the site is actually acceptable. Therefore, after completion of the primary objective, the SLRV if operable, would be used to extend the collection of fine-grained topographic data to as large a percentage of the site as possible.

3.3.2 Topographic Data Collection

This section describes operational techniques which may be employed in collecting sufficient data to verify the acceptability of the landing point and produce a contour map.

To obtain the necessary data for contour maps, or a real-time decision with respect to landing point verification, requires some type of image forming system such as a TV camera or flying spot scanner. In the following paragraphs, it is assumed that a TV system can be used.

To comply with the mission requirement that 100% of the point is acceptable with a confidence of 99%, 100% of the potential landing point must be surveyed with respect to obstacles, crevices, depressions, and slopes. It is therefore necessary to define the minimum allowable distance between inspection points in terms of potential surface contours and the height of the TV camera above the surface to ensure 100% coverage of potential hazards. Figure 3-2 illustrates one of the more limiting cases of terrain masking involving acceptable surface conditions in terms of slopes and depressions. In this case, the depth of the depression must be determined to determine its acceptability. This and other similar examples of terrain masking indicates that a TV camera located 0.9 meter above the local surface (a height compatible with the packaging of the 100-lb SLRV on Surveyor) must be capable of viewing features from two positions spaced no more than approximately 3 meters apart. As Figure 3-2 illustrates, a wider spacing would result in the inability to measure the depth of the 25-cm depression. To ensure complete coverage of the point with the specified confidence level in the results, the requirement for a closely spaced survey pattern is evident at least in marginally acceptable terrains. This pattern may take various forms, (Figure 3-3). The factors involved in the choice of a pattern include the ease of maneuverability, navigation accuracies, the effect of the sun's position with respect to the pattern, and the position of landmarks or the Surveyor Spacecraft for ranging information. Pattern B provides the most desirable characteristics with respect

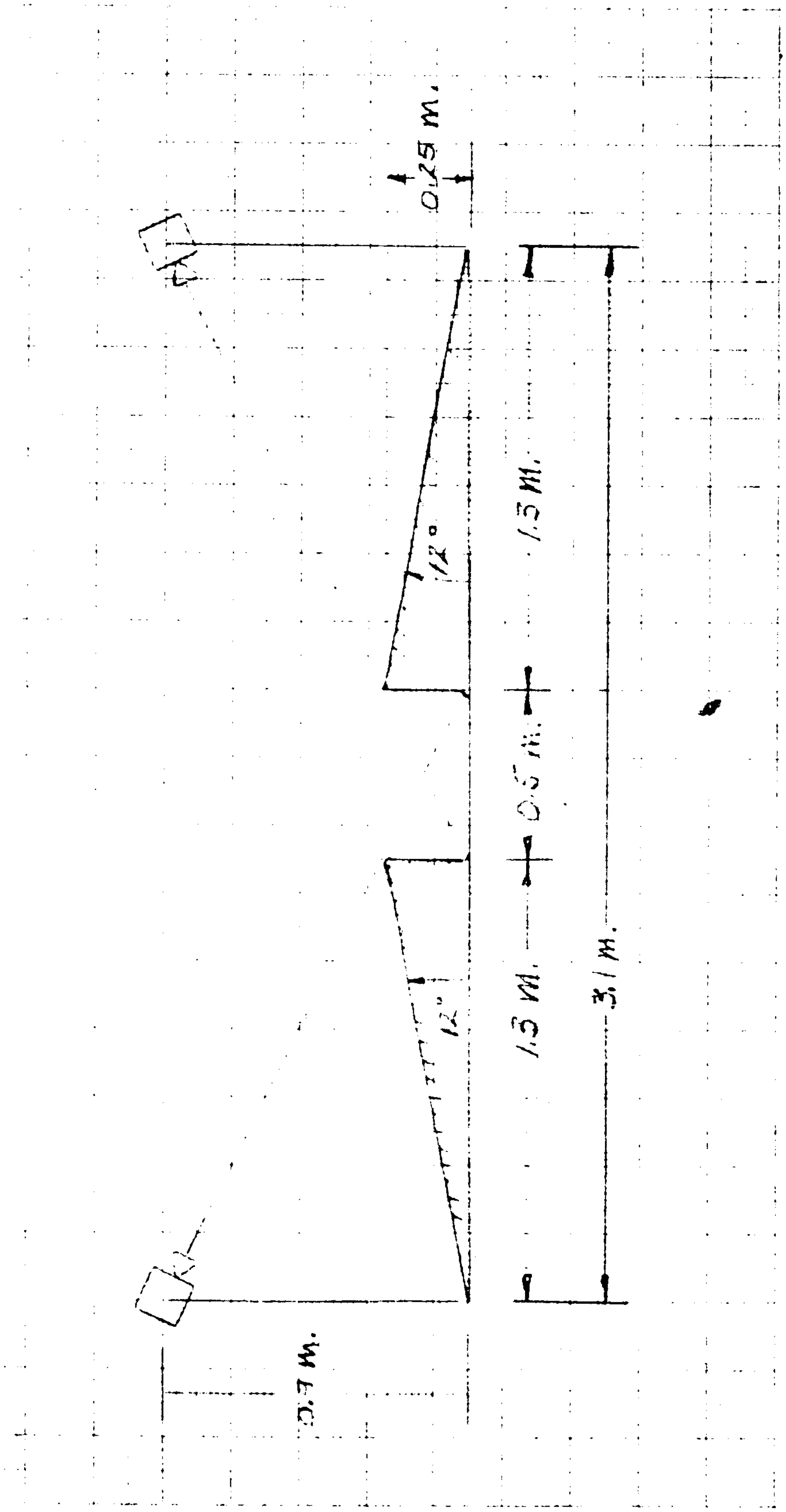

Figure 3-2 Limit of Terrain Masking

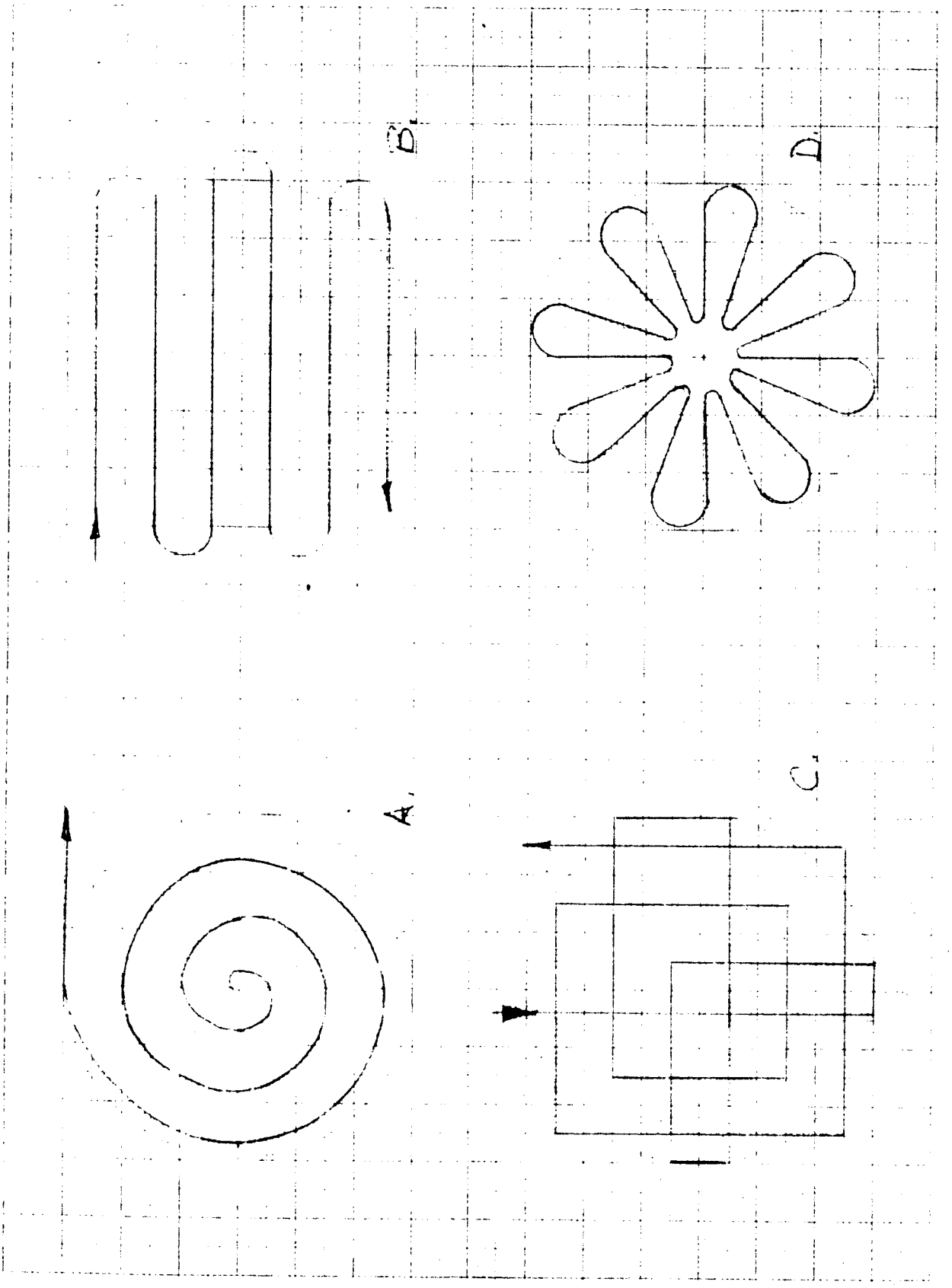

Figure 3-3 Typical Point Survey Patterns

to these considerations. Patterns A and B require the least amount of maneuvering; pattern B places the least stringent requirements on navigation, represents the pattern with the most consistent vehicle heading with respect to solar orientation; and represents the pattern with the most consistent vehicle heading with respect to identifiable landmarks, or the Surveyor Spacecraft, for ranging purposes.

Since the spacing of the traverses of pattern B should be of the order of two to three meters, a wide field-of-view lens would be desirable to minimize the total number of images required to survey a point.

From the results of the photogrammetric error analysis contained in Volume III, Book 2, Section 6, a 50° field-of-view lens will produce a 4.8-cmuncertainty in the elevation of a point of range of six meters from the vehicle baseline. This represents approximately a 20% error in establishing the 2.5-cm-contour intervals, and is considered to be a practical maximum allowable error. This then establishes approximately 6 meters as a reasonable maximum range to be achieved in operating with a wide angle lens for the purpose of stereo mapping the landing point. Since current automatic processing equipment will handle photographs of high convergence angles, the advantage of this mode of operation is that it makes the most efficient coverage pattern for a monocular TV camera. Coverage requirements for fixed base stereo systems are presented in Section 3.3.4.

Figure 3-4 presents a pattern of overlapping convergent images taken along the parallel traverses of pattern B of Figure 3-3. At each of three-meter steps along the travers, 50° field-of-view images are taken at azimuth angles of 80°, 100°, 260°, and 280° with respect to the vehicle heading. The image taken at 80° from position 1 (1-i) and that taken at 100° from position 2 (2-ii) form overlapping coverage of the fan shaped area between points 4, 6, and 7 as illustrated. The optical axes of the two camera positions intersect at a convergence angle of 20° and thus at the near point of intersection the convergence angle reaches a maximum of 70°. The images taken at 260° and 280° at each position provide stereo coverage to the other side of the traverse. These pairs serve two purposes: (1) to "fill in" the small gaps left between the pairs of images at 80° and 100° at each position, and (2) to provide redundant coverage to ensure that any potential hazards masked in the other sets of images are examined. If this process is repeated at each of a series of points on the traverse at three-meter intervals, complete and overlapping coverage of the landing point will be provided (Figure 3-5). The spacing of traverse paths at 2.6 meters and camera location spacing along each traverse of 3 meters are compatible with the maximum camera separation of approximately 3 meters established to ensure 100% coverage of all potential hazards.

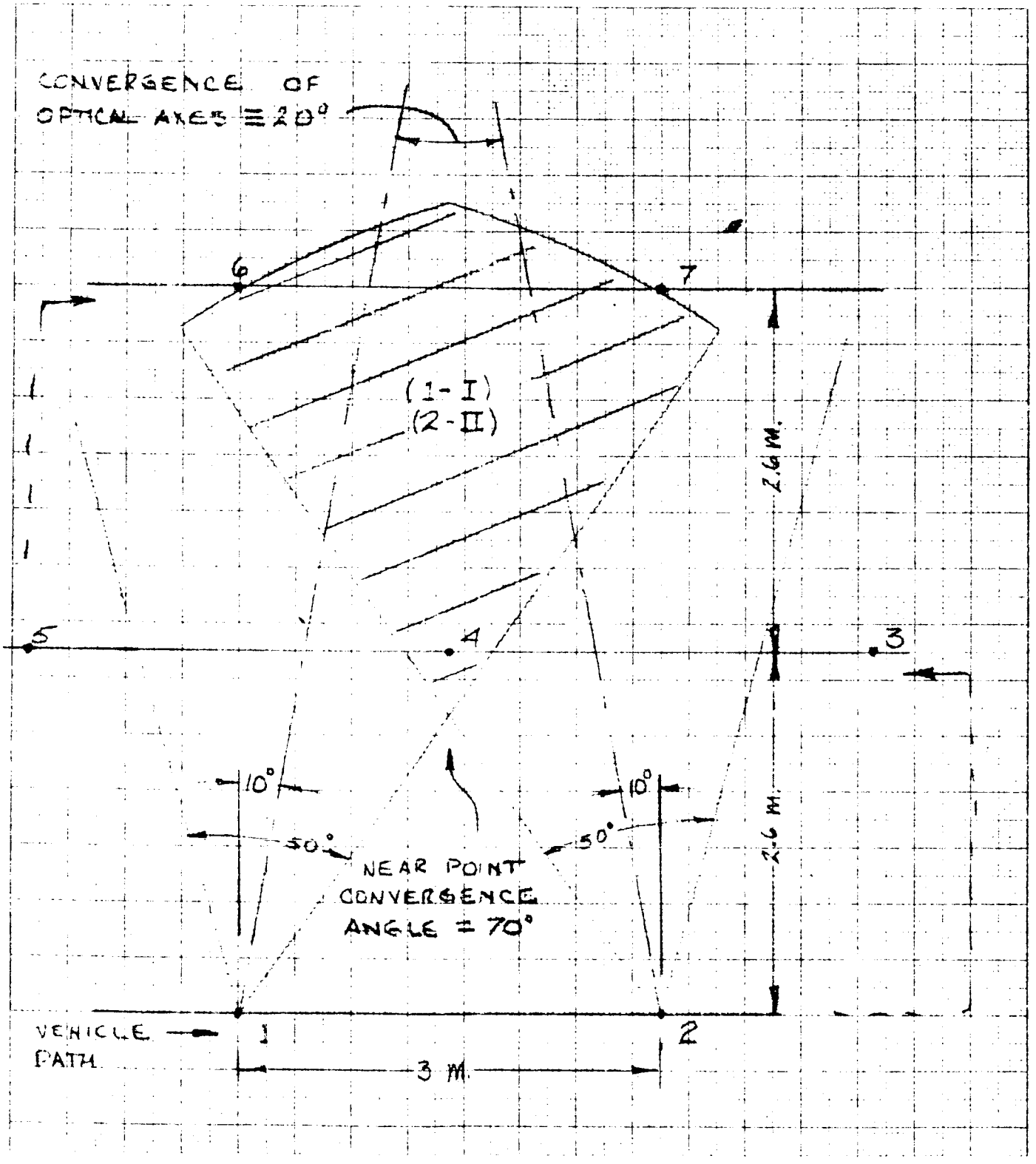

Figure 3-4 Overlap of Convergent Images

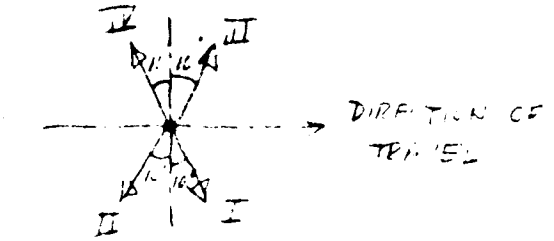

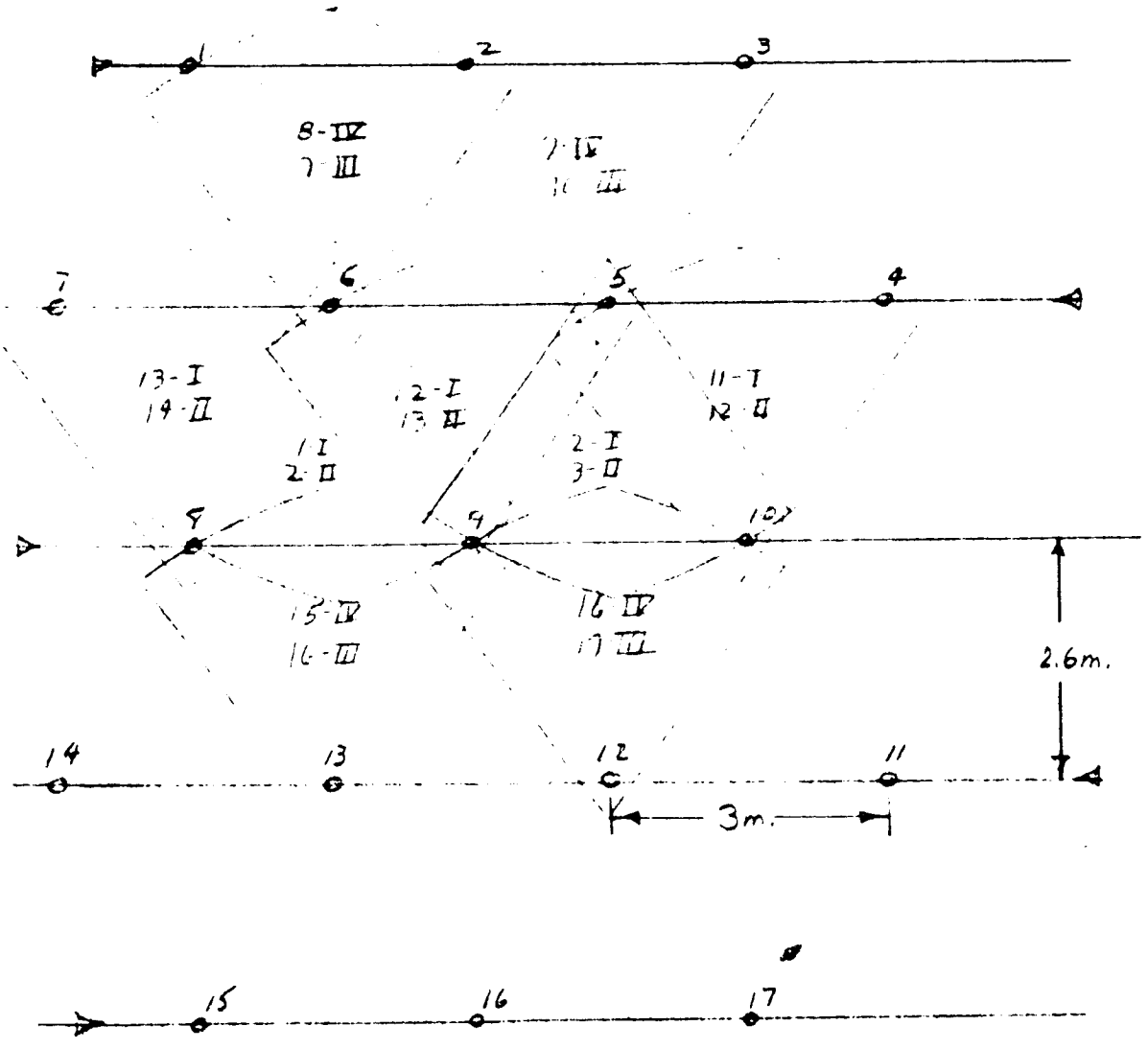

Figure 3-5 Coverage of Overlapping Convergent Images

The azimuth orientation of the images allows sufficient overlap between coverage areas so that control points are established in the overlapping strips to orient adjacent coverage areas. To provide data for driving along the traverse path, single 50° field-of-view images will be taken at each three-meter interval in the direction of travel.

To ensure that complete stereo image coverage of the landing point is provided, a tolerance on SLRV range measurement accuracy must be established.

Figure 3-6 illustrates the typical coverage pattern obtained when no navigation errors exist. The shaded areas are gaps in coverage from either the images oriented upward or downward on the page. With normal coverage these are the gaps that are covered by images taken in the opposite direction as illustrated.

If a range measurement error exists, these two patterns will be shifted with respect to each other (Figure 3-7). When this shift reached 0.9 meter between traverse rows 2 and 5, the shaded areas or coverage gaps will just begin to overlap, and in this overlap area no coverage from either direction will exist.

Then the SLRV range must be measured with an error not to exceed ±0.9 m over five traverse paths, or approximately 160 m.

If the distance between traverse paths is varied, overlapping of coverage gaps also occurs (Figure 3-8). Here a deviation of 0.6 m over a span of four traverse paths can produce a gap in stereo coverage. This would then allow only an rms error of ±0.3 m in the lateral position of each traverse path. Increased error could be accommodated by closing up the path spacing by 0.05 m for the center traverses. However, in reality 0.05 m is well below other system uncertainties and therefore 2.6 m ±0.5 m will be considered the spacing required between traverses.

The pattern of camera stations within each landing point required to provide total coverage is shown in Figure 3-9. There are 167 camera stations within this pattern. Four television images at each station would yield a total of 668 images; however, approximately 40 images which would cover area outside the landing point may be eliminated. Thus a maximum of 628 images are required to collect sufficient data to ensure certification of the most marginal landing points. In addition, 167 images would be required for driving, making a total of 795 images required per landing point.

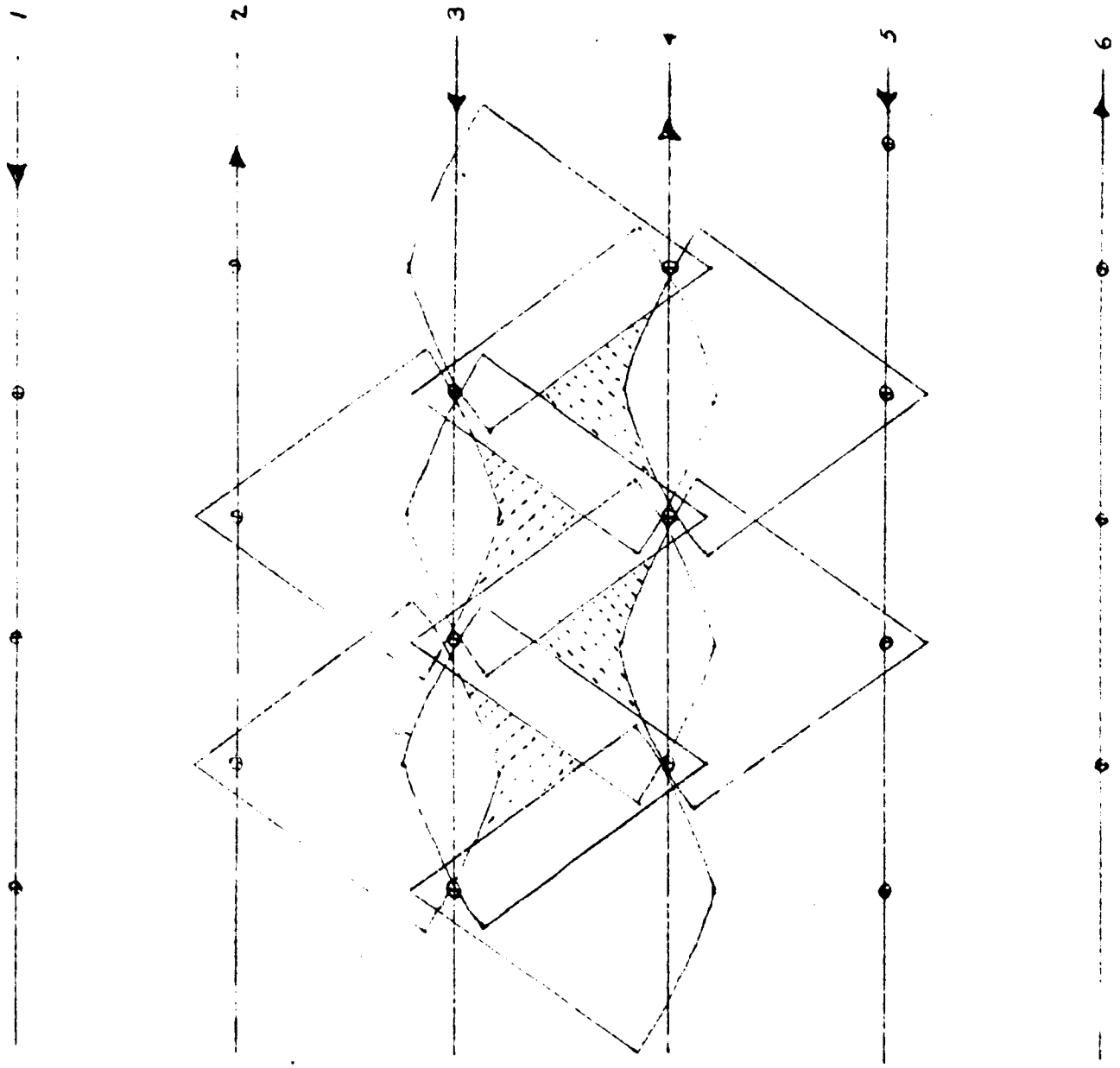

Figure 3-6 Normal Image Coverage Pattern

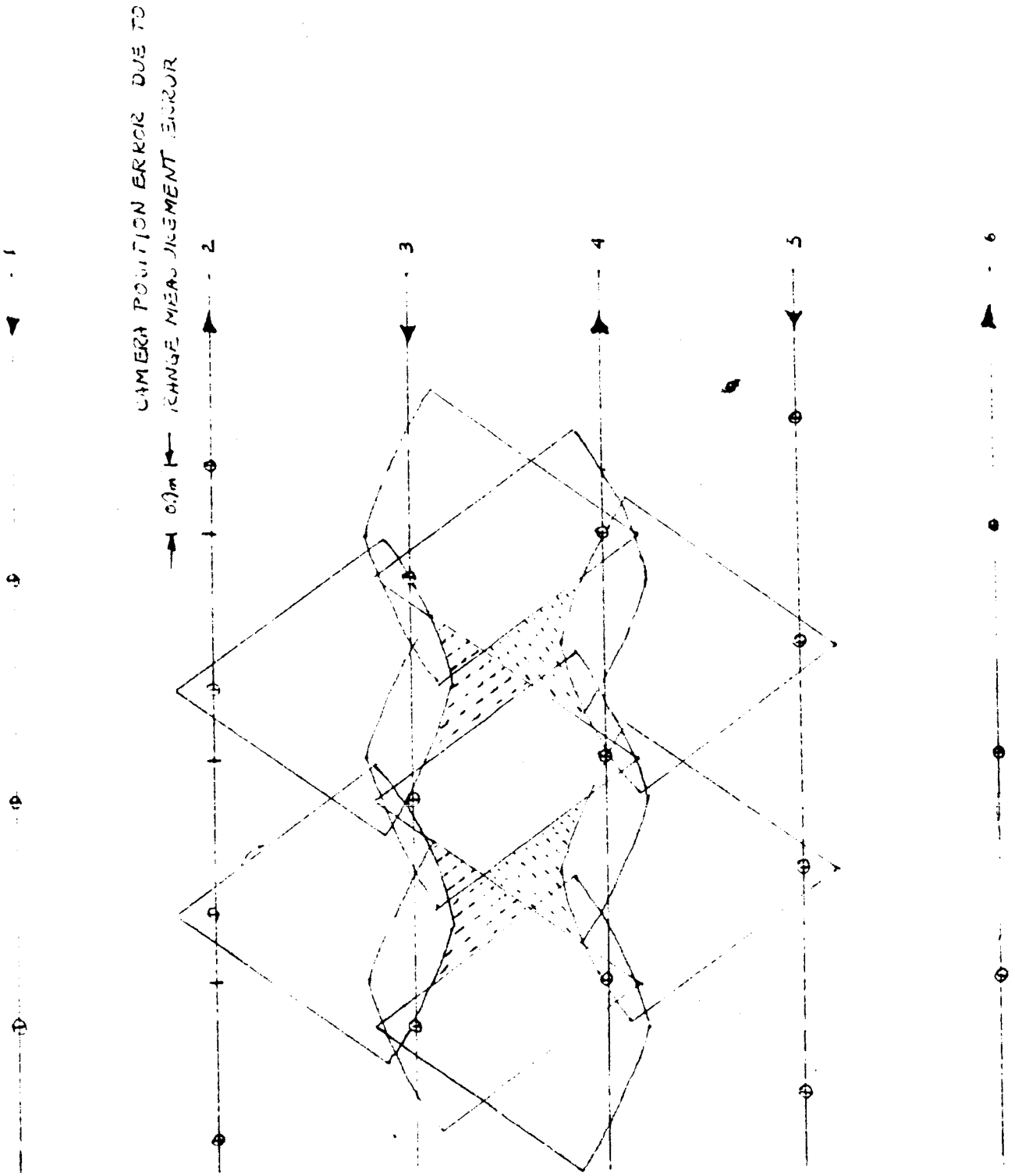

Figure 3-7 Coverage Pattern Distorted by Range Error

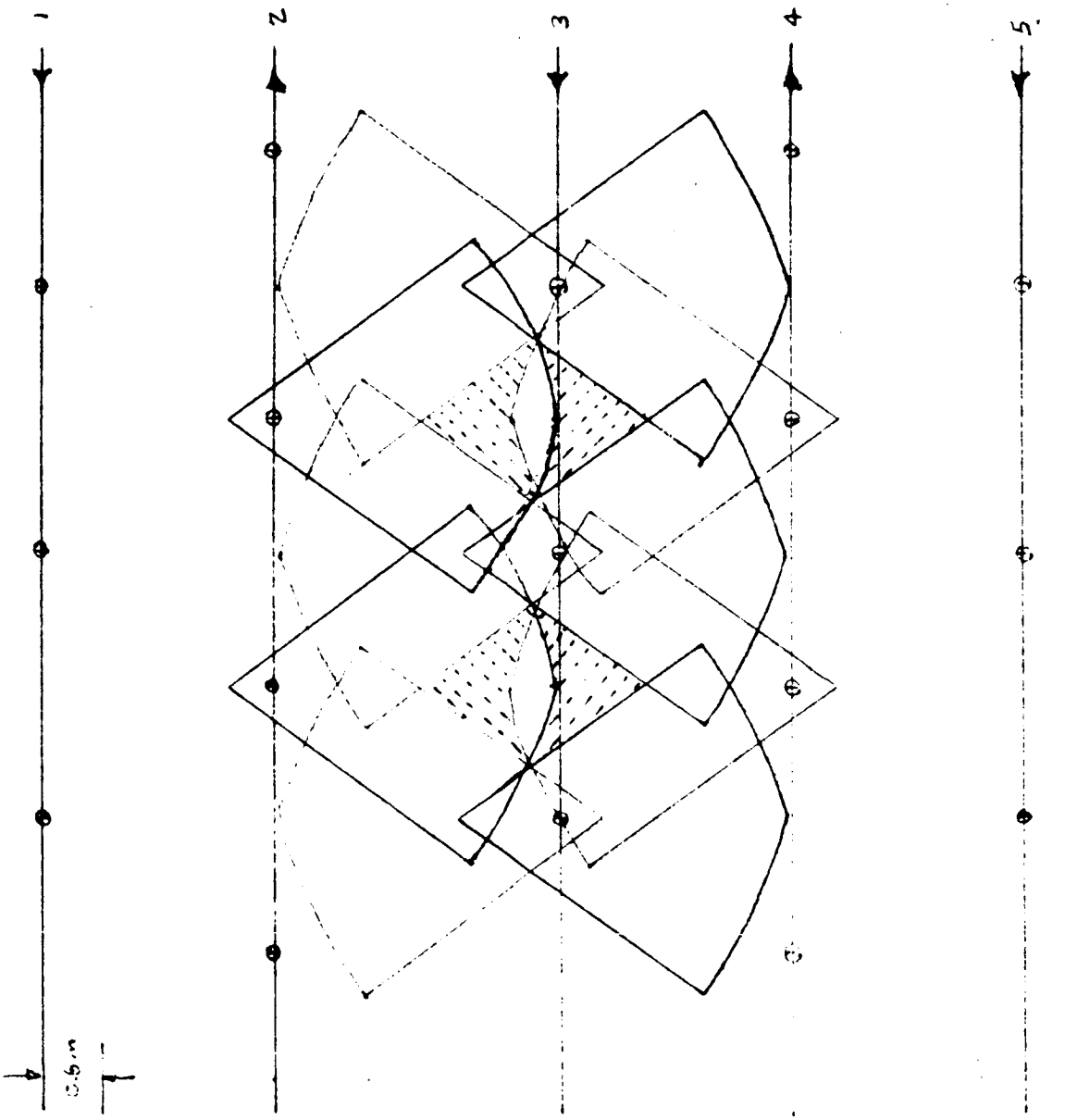

Figure 3-8 Coverage Pattern Distorted by Azimuth Error

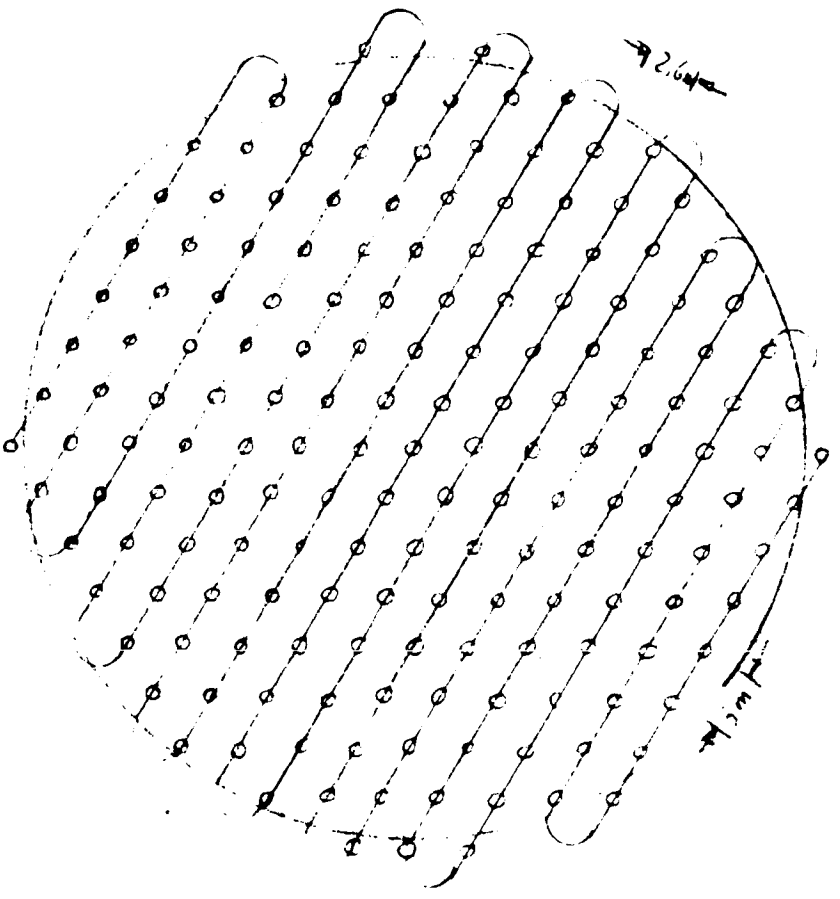

Figure 3-9 Worst-Case Landing Point Camera Stations

Since the photogrammetric operating range is established by the anticipated spatial measurement errors, in theory the number of TV images per landing point cannot be reduced without further compromising the map accuracy. However, this entire mode of operation was derived for a worst case terrain in which there is a high density of obstacles between 25 and 50 cm. In such a terrain, each point must be spatially located. However, if a surface is considered which is relatively smooth (slopes less than 5°), free of significant crevices or depressions, and with only occasional obstacles appearing, a different mode of operation would be employed. This procedure reduces the requirement on photogrammetry to locating in x and y coordinates and determining the height of a relatively few obstacles.

Considering the use of the 10° field-of-view lens (f = 72.58 mm) and the same image and baseline measurement errors used for the previous mode of operation, the photogrammetric error analysis in Volume III, Book 2, Section 6 shows that the height dimension of an 18-cm obstacle can be measured to ±2.1 cm at a 20-m range.

Referring to Figure 3-10, the three camera stations shown provide the required coverage for a nearpoint focus of 4.5 m (f22 at 10° FOV). If a larger aperture is required, the camera stations are moved out to provide for the longer near point focus point with an attendant increase in maximum range. For this coverage pattern, 27 TV images are required from each camera station to provide azimuth coverage with adequate overlap. If the ground were absolutely flat, these would provide adequate elevation coverage; however, even a 5° general slope requires two images in elevation at each azimuth stop. Thus this mode of operation imposes a lower limit of 162 TV images to obtain certification data in a landing point. Ten additional 50° field-of-view images would be required for driving, making a total of 172 images.

To gather necessary data to prepare a chart of the 3200-meter site which identifies and locates major hazards within the site, topographic data will be obtained from TV images taken from the vehicle during interpoint travel. The basic site survey pattern is illustrated in Figure 3-11. This figure indicates that it would be necessary to obtain terrain coverage out to a maximum range of 500 meters between the outer periphery of the landing point pattern and the site periphery. Within the landing point pattern, coverage of the area between interpoint traverses requires coverage out to a maximum of 250 meters on either side of the traverse.

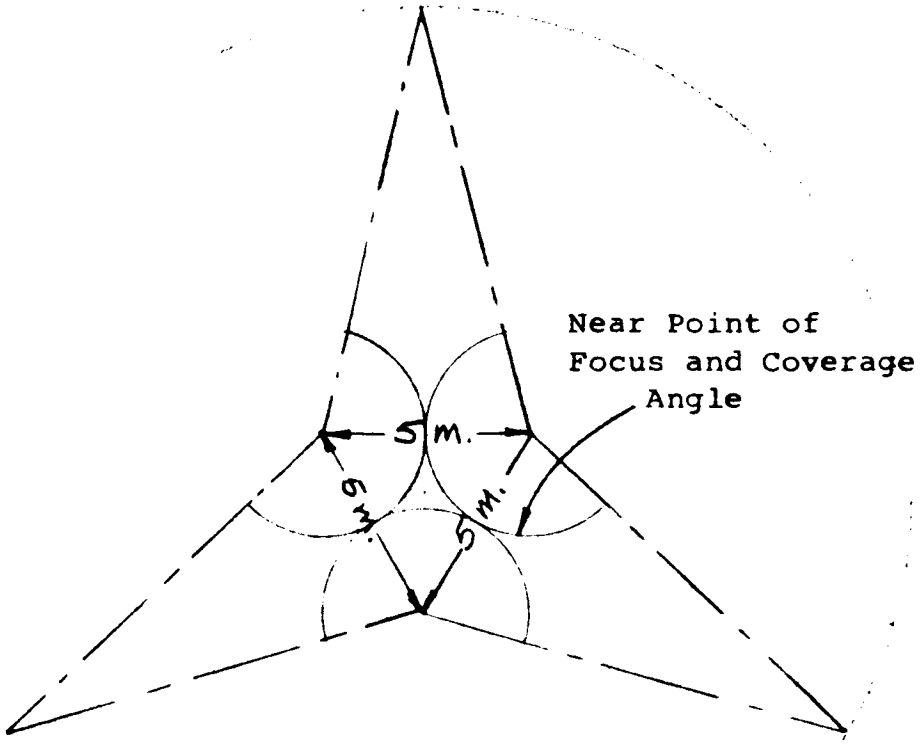

Figure 3-10 Best-Case Landing Point Coverage and Camera Stations

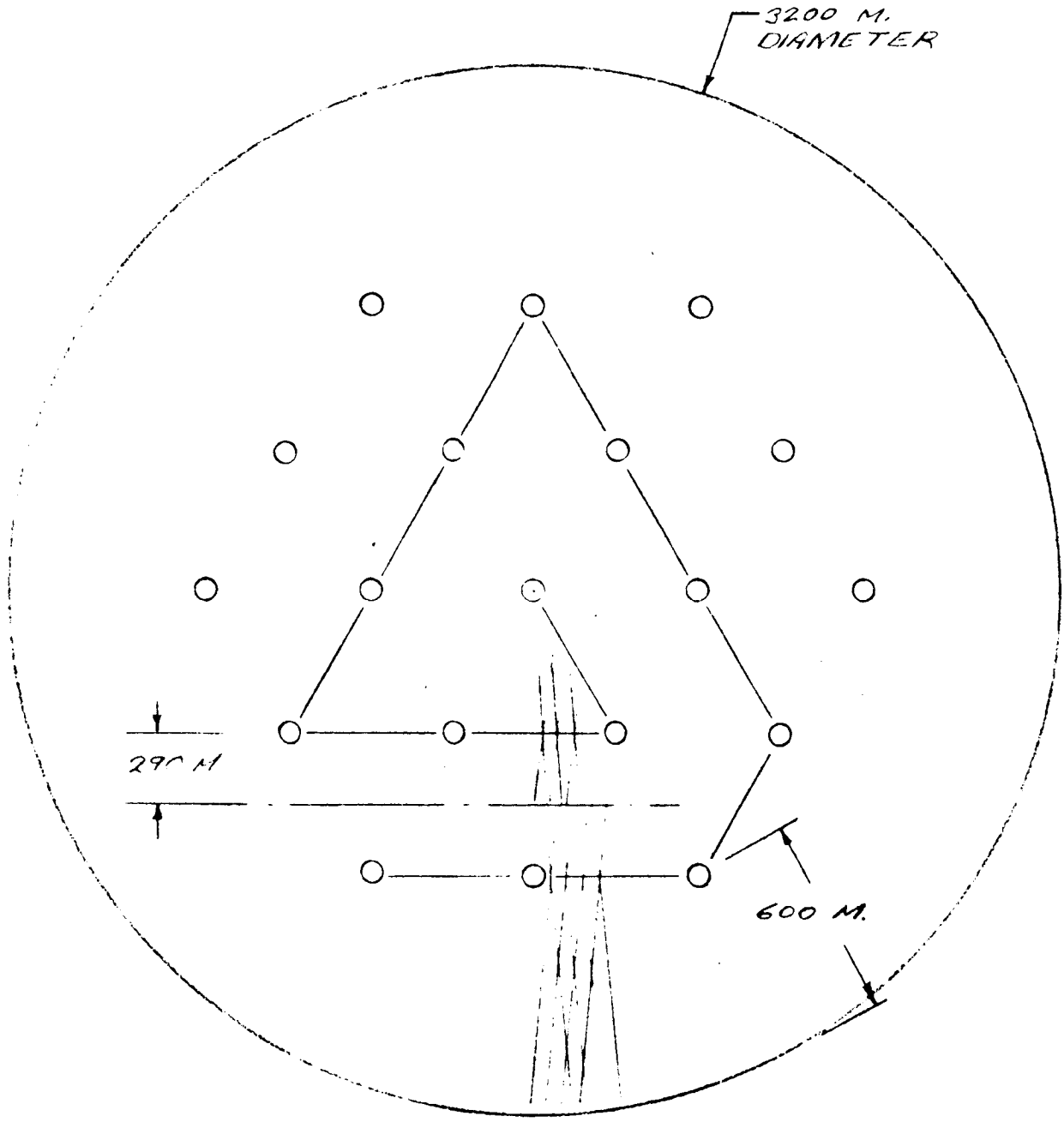

Figure 3-11 Nominal Site Survey Pattern

Figure 3-12 illustrates the proposed operational procedure which results in the maximum site coverage without deviating from the nominal exploration survey pattern. Ten degree field-of-view images are taken at every 9 meters to provide coverage at the extreme range. The gap between these images if covered by 50° images taken along the traverse at each stop which are also used for interpoint driving, and by 22.5 field-of-view images taken every nine meters in conjunction with the 10° images. This technique results in better than 99% coverage of the site. Objects 25 cm or greater can be identified at a distance of 7 meters to either side of the traverse, objects greater than 35 cm to a range of 50 meters on either side of the raverse, and obstacles of 0.75 meter to the 250-meter range, and 1.8 meters to the 600-meter range. Figure 3-12 illustrates three-meter stops for driving during interpoint travel required in the more rugged terrains. In more level terrains, the stop length would be increased to 9 meters with a substitution of 22.5° field-of-view images for driving rather than 50°.

3.3.3 Topographic Data Reduction

Accurate real-time topographic measurement of protuberances and depressions from the TV images are not feasible; however, approximate measurements can be made in real-time.

An operating console can be provided in the SFOF. On this console would be displayed the previously described mapping and driving images as they are received from the SLRV. Superimposed on this display would be a computer generated perspective grid similar to that shown in Figure 3-13. The perspective of Canadian grid is a well known photogrammetric technique for obtaining a planimetric map from an oblique aerial or terrestrial photograph. In terrain of low relief, the X and Y coordinates of any obstacle of interest are estimated with respect to the grid lines which are spaced at one-meter intervals. The range to the obstacle is then,

$$R = x^2 + y^2 + 0.9^2 \text{ meter}$$

and the vertical dimension (h) of the obstacle is estimated from

$$h = \frac{R\delta z}{f}$$

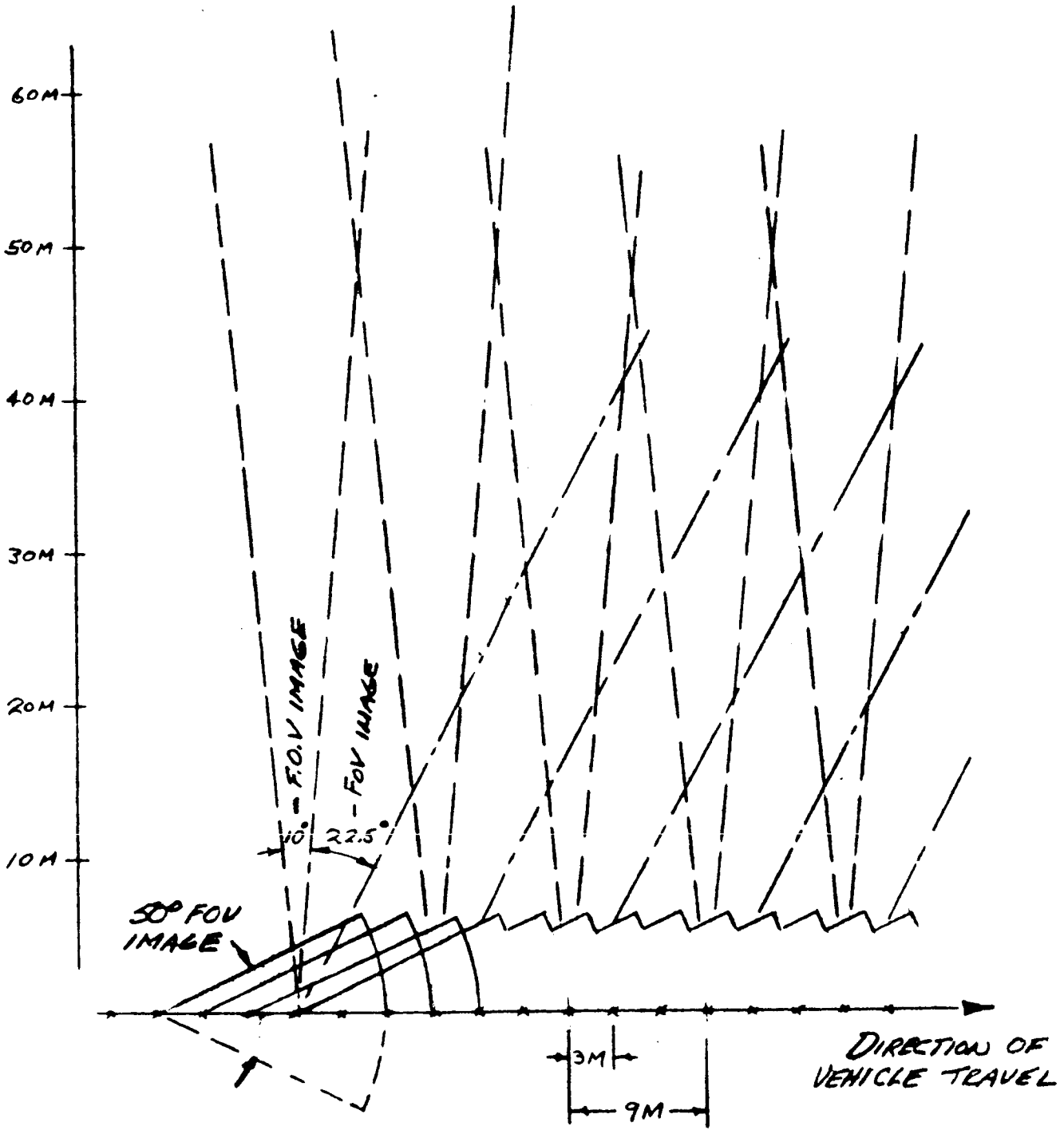

Figure 3-12 Interpoint Topographic Data Collection

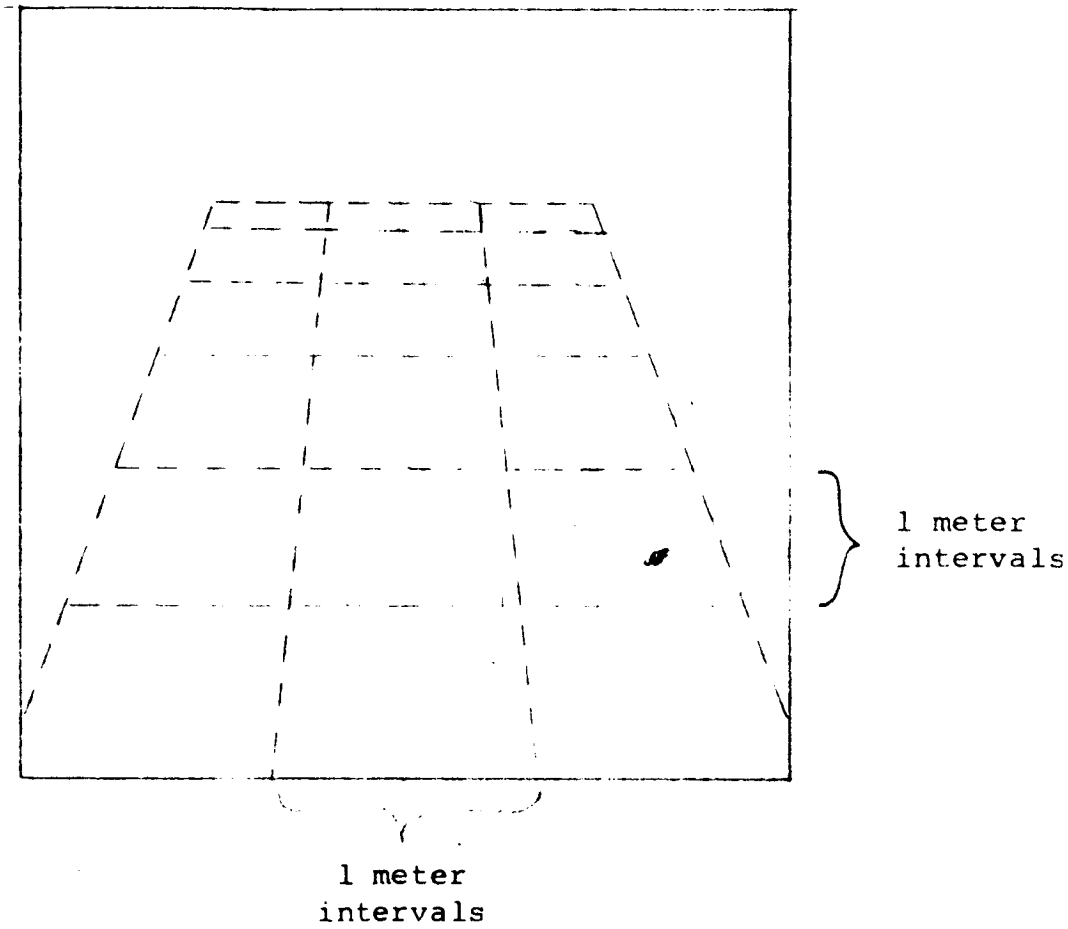

Figure 3-13 Perspective Grid

where

δz = vertical dimension of the obstacle on the image

f = focal length.

The computer generated grid can be oriented on the image to correspond to the orientation of the TV line-of-sight vector as determined from an inclinometer readout and television camera gimbal angle readout.

The size of objects appearing within successive TV images may also be estimated from measurement of their apparent size on each image and of SLRV displacement between images.

Referring to the simplified geometry shown in Figure 3-14.

$$z_1 = \frac{fz}{y_1}$$

$$z_2 = \frac{fz}{yz}$$

where

f = focal length of camera

Z = height of object

z_1, z_2 = dimension of object on succeeding image

then

$$y_1, y_2 = S = fz \left(\frac{1}{z_1} - \frac{1}{z_2}\right.$$

or

$$z = \frac{z_1 z_2 S}{f(z_1 - z_2)}$$

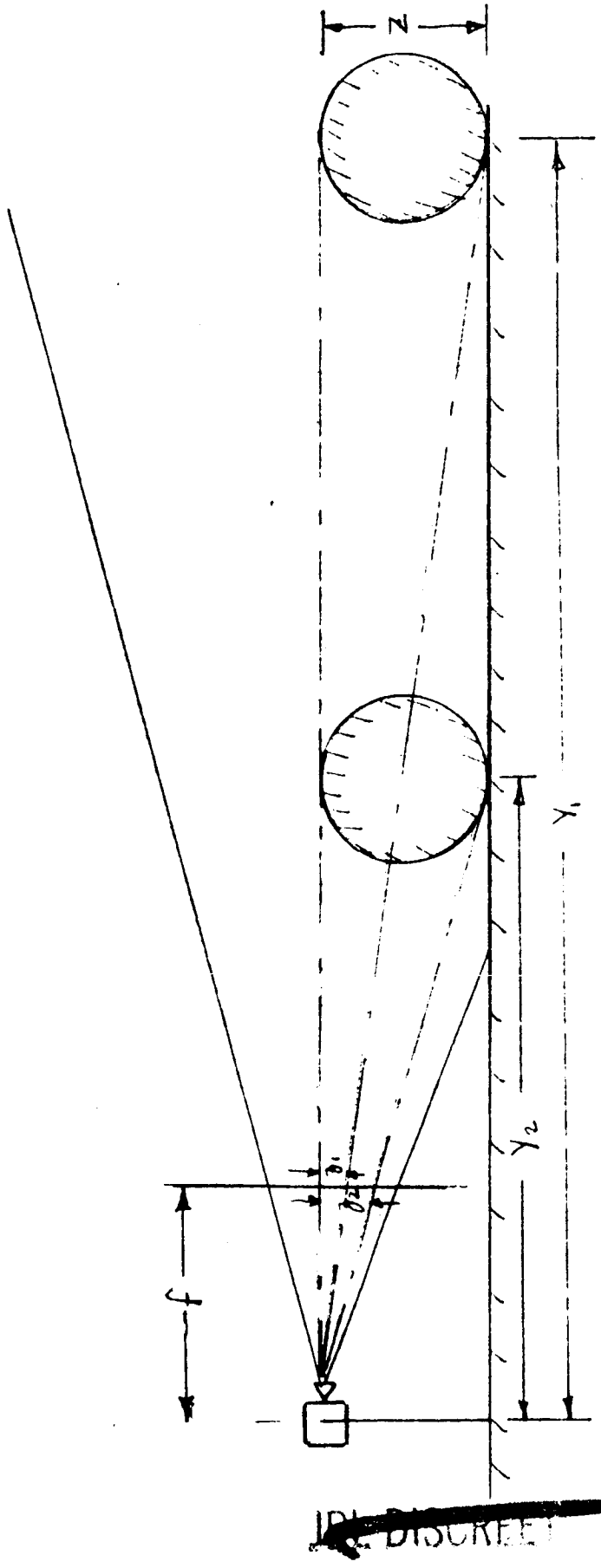

Figure 3-14 Object Measurement From Successive Images

where

S = SLRV displacement between images

The accuracy of this measurement may be estimated from;

$$\Delta Z = \frac{dZ}{dz} \Delta z, + \frac{dZ}{dz2} \Delta z2 + \frac{JZ}{JS} \Delta S$$

performing the indicated differentiations:

$$\Delta Z = \frac{-S_{z2}^{2}}{f(z1 - z2)^{2}} \Delta z1 + \frac{-S_{z1}^{2}}{f(z1 - z2)^{2}} \Delta Z^{2} + \frac{z1\, z2}{f(z1 - z2)} \Delta S$$

For a 50° field-of-view lens, an SLRV displacement of 3 m ±3%, and an average 50μ image measurement error, this equation yields an RMS error of ±4.6 cm in measureing a 25-cm object which appeared at ranges of 6 and 3meters respectively in each of two successive images.

Since the images taken for driving provide complete coverage of the landing point, although not in stereo, the grid can be applied to just the driving images for the purpose of verification of the point in terms of obstacles, depressions, and crevices. It would not be necessary to use the four additional images taken at each stopping point; hence, these images would be used only for subsequent photogrammetric analysis and preparation of a contour map.

As the terrain relief and slope uncertainties become greater, these techniques become less effective. Eventually, in marginally acceptable terrain where accurate measurements are required, stereophotogrammetric analysis of the convergent TV images must be employed.

A major objective of Phase II would be to refine the technique of analyzing the driving photographs, particularly if they are taken with a fixed base stereo system. Thus sufficient confidence in verification of the point could be achieved by these techniques in marginal surface conditions. If this becomes possible, then at the potential sacrifice of a 25-cm contour map of the landing point, the mission time could be reduced due to the reduction in the total number of images from 795 to 167.

Various measurement instruments exist which will accept convergent images of the type which would be obtained by the SLRV; e.g., the Wild A-7 Autograph, Zeiss C8 Stereoplanigraph. However, the OMI-Nistri AP-2 Analytic Plotter appears best suited to the requirement for rapid data reduction.

Essentially, the analytical stereoplotter is a stereo comparator linked to a digital computer in which computations are performed on the measured image coordinates to yield the corrected spatial coordinates of the objects within the image pair. These output coordinates drive an automatic coordinatograph or x-y plotter.

The major advantage of the analytical stereoplotter is the relative speed and ease of set-up time. Aside from the manual elimination of parallax by the operator, the relative orientation of the two images is handled entirely by computation within the computer linked to the stereo comparator.

The overlapping feature of the stereo pairs would permit elevation data to be derived from these images photogrammetrically with an accuracy that would permit the calculation of slopes to a tolerance of $\pm 0.5^{\circ}$ over any 10-meter length.

In addition, since the obstacle identification capability at 6 meters is 20 cm with a 5-cm accuracy, a maximum additional elevation uncertainty between any two locations 10 meters apart of approximately 45 cm is incurred. A further contributing factor to the effective slope is differential LEM footpad sinkage. This differential sinkage may range from zero to 30 cm (one footpad on infinitely hard surface, another on the minimum acceptable surface bearing strength.) Therefore, the total maximum relative uncertainty between any two locations 10 meters apart to be added to 0.5° slope measurement tolerance to obtain the effective slope is 45 to 75 cm, depending upon the surface bearing strength measurement range.

Since the maxmimum and minimum bearing strength within a point are statistically predictable values, they will be used to determine the contribution of differential sinkage to the effective slope.

The total uncertainty in the slope measurements must be subtracted from 12° to give the acceptable measured slope for point cerfitication.

The acceptable measured slope is therefore

$$\theta \text{ accp.} = 12^{o} - 0.5 - \tan^{-1}\frac{45}{1000} - \tan^{-1}\frac{\Delta s}{1000}$$

$$\approx 8.8^{o} - \tan^{-1}\frac{\Delta s}{1000}$$

where

Δs = sinkage differential in cm

To obtain slope data on a real-time basis, elevation must be measured by some means other than photogrammetric analysis. At this time the most feasible means of doing this would be the continuous integration of a combined odometer - inclinometer readout. The accumulated errors in this type of measurement are only marginally acceptable in the very best surface conditions and totally unacceptable in the more rugged terrains. Thus, currently, it must be stated that photogrammetric analysis of the stereo image pairs must be used for point verification in terms of slope as well as obstacles in the more rugged terrains.

Measurements to obtain slope data may be augmented, depending upon sun/vehicle geometry, by photometric interpretation and analysis of the TV images. This process is described in Appendix B.

3.3.4 Topographic Data Coverage and Reduction from Fixed Baseline Stereo Images

If a fixed baseline stereo image system is used, the following mode of operation would be employed to obtain the topographic data. Since the stereo images would be used for both the operator driving display and mapping, a compromise would have to be made between the photogrammetrist's desire for the best range finder (maximum fixed bas) and the operator's requirement for a geometrically true stereo image (baseline 6 cm). The optimum stereo picture for viewing would also require that the images be convergent at the near point. Here the baseline is assumed to be 1 ft (30.5 cm) and the image axes parallel.

From the error coefficients presented in Volume III, Book 2 and changing only the baselength from 3 m to 0.305 m and eliminating the baselength error, the total RMS errors at 6 m from the camera become

$\Delta Z = \pm 3.5$ cm

$\Delta x = \pm 16.0$ cm

$\Delta y = \pm 3.4$ cm

The error performance, then, would be better than the monocular system. This performance however, would not represent a significant advantage.

The stereoptic system presents a distinct advantage of greater coverage. The terrain area included within each pair of convergent 50° field monoptic images is approximately 5.5 square meters. Each pair of fixed baseline stereo images (Figure 3-15) will contain, however, about 10.9 square meters.

This coverage would allow the step between camera stations to increase to 4 meters. At each camera station a set of 5 stereo pairs of images taken as shown in Figure 3-16 provide overlapping coverage out to 5 meters either side of the SLRV line of travel. As Figure 3-17 shows this results in 34 camera stations or 350 total images for worst case coverage. Fortunately, this number also includes forward directed images which serve for driving.

The second major advantage of a fixed base stereo system is the increased ease of reducing the photogrammetric data. Since the baseline is rigid, the relative orientation of each pair of images is constant, eliminating most of the set-up procedure.

Also, since each pair of images may be fused without further adjustment throughout the field when presented to the operator, the real-time landing point verification procedure may be speeded. This is accomplished by displaying a computer generated stereo perspective grid on the stereo TV image display. When the stereo model is viewed through this grid (which appears to form a horizontal plane in the object space), objects intersecting and passing through the plane are easily determined. The relative height of the grid with respect to the model plane can be controlled by the operator who can thus estimate the height and position of obstacles in the field of view.

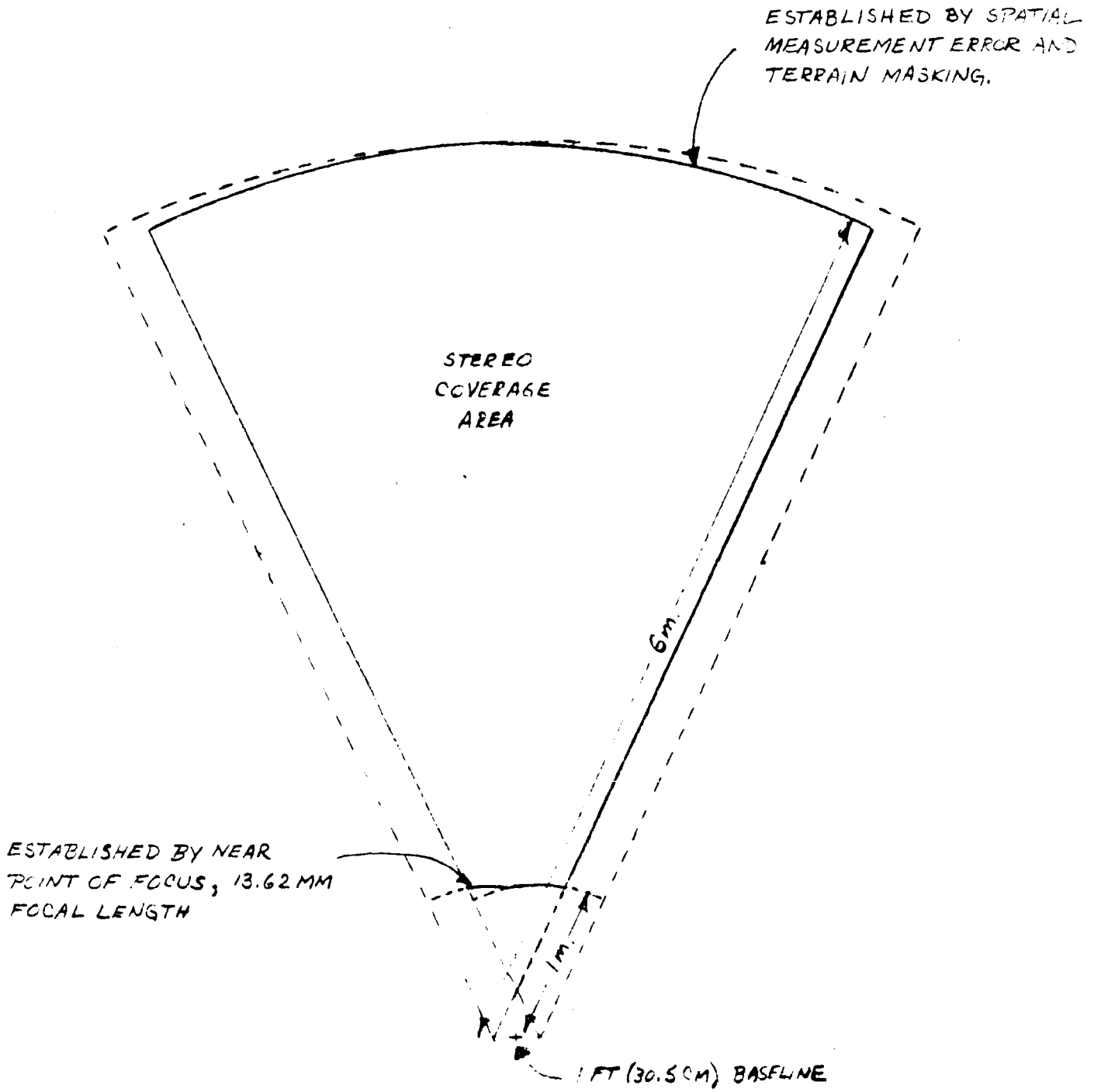

Figure 3-15 Stereo Image Coverage

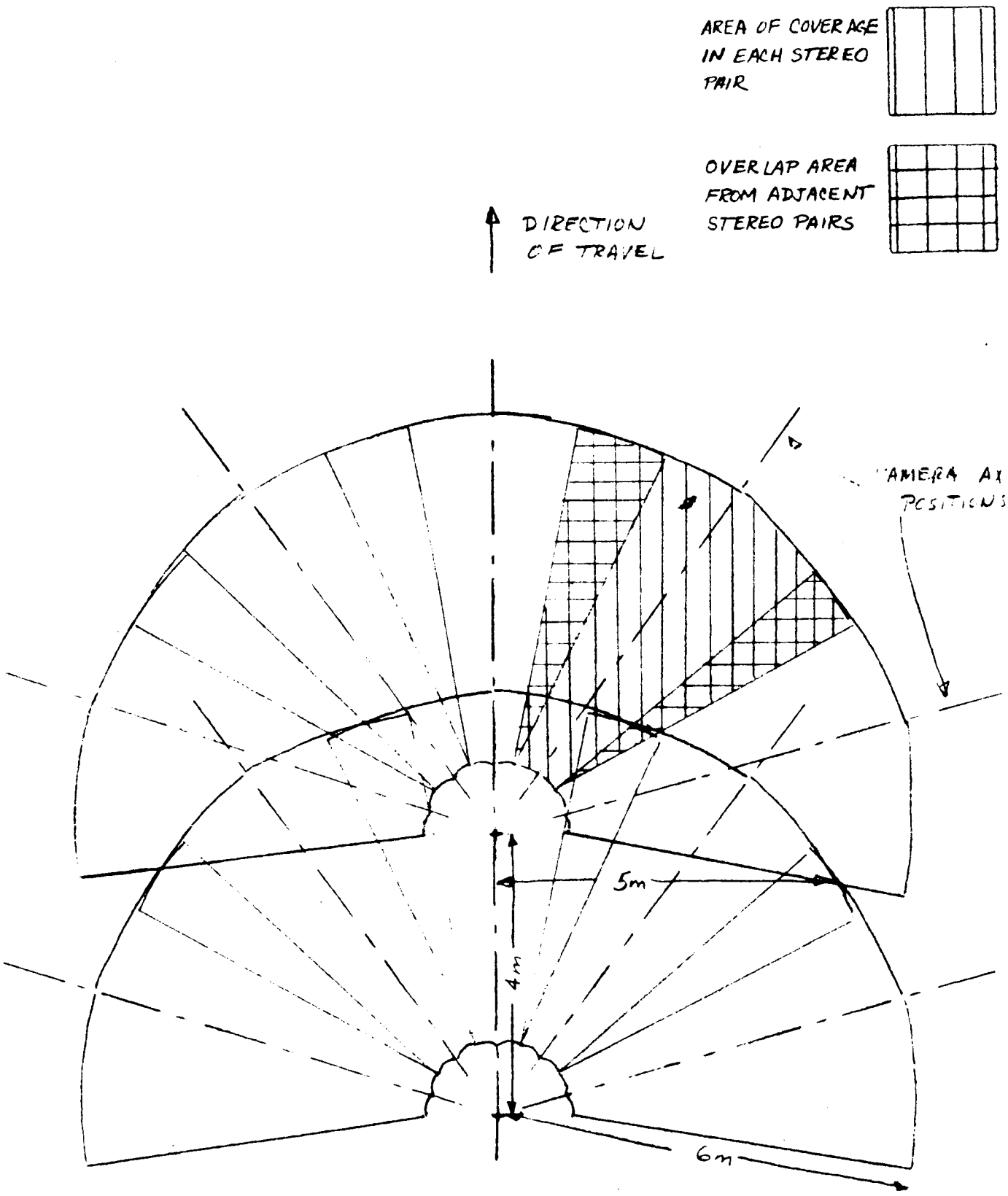

Figure 3-16 Stereo Camera Station Coverage

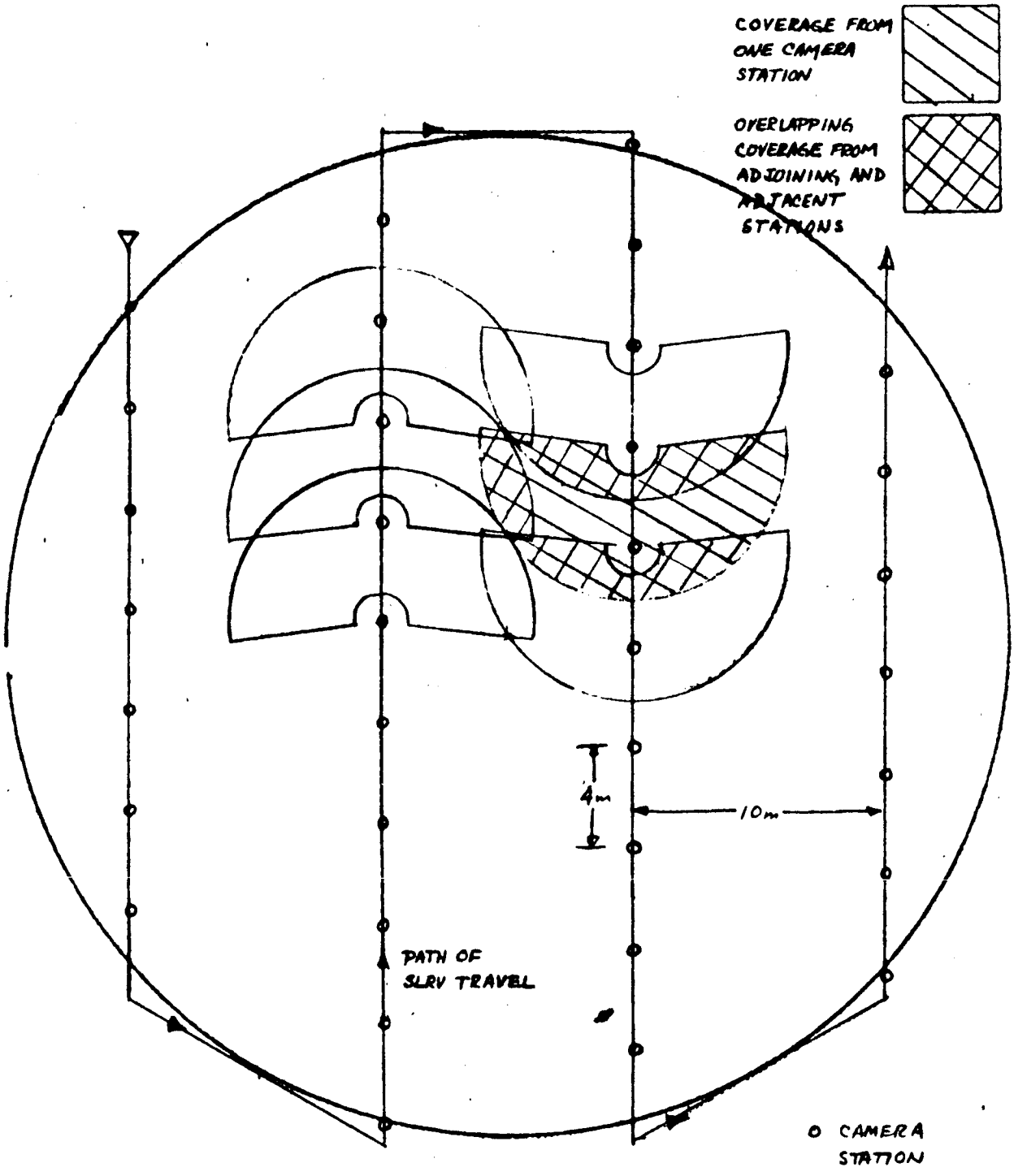

Figure 3-17 Stereo Landing Point Mapping Camera Stations

The site coverage during interpoint travel, using a fixed base stereo image system, would differ from the coverage obtained by a monocular system (Section 3.3.2). If the increase in mission time could be tolerated, all single image pictures noted in Figure 3-12 would be produced in stereo.

As a minimum, the images taken along the direction of travel would be stereo pairs with images taken to the left and right of the interpoint traverse consisting of monocular images from one of the two stereo elements. The increase in mission time caused by taking stereo instead of monocular pictures along the direction of travel would be offset by the increase in mission time resulting from the confidence in path selection derived from the stereo pair.

3.3.5 Bearing Strength Measurements

To comply with the mission requirement (99% confidence that 100% of the certified landing point is acceptable in terms of bearing strength), the system requirement on data derived from the SLRV has been based on a classical statistical sampling formula. This formula relates the number of sequentially acceptable measurements to the confidence levels in percentage of the area that satisfies the acceptability criteria.

$$N = \frac{\ln (1 - C)}{\ln (1 - P)}$$

where

N = number of sequential acceptable measurements

C = confidence level

P = percent of landing point area

This relationship is presented graphically in Figure 2-9, Section 2. It is seen that 45 sequential acceptable measurements of the soil bearing strength are required to verify that 95% of the landing point is acceptable, with a 90% confidence. It is further evident that on a purely statistical basis, to provide a 99% confidence that 100% of the area is acceptable, would require an unacceptably large number of data measurements. The appearance of obstacles and depressions within the landing point may randomly occur without any reason or logic and thus requiring 100% coverage.

However, the quality of the soil with respect to bearing strength is subject to verification by extrapolation of known data based on a knowledge of soil formation processes. It is therefore reasonable to assume that if 45 sequentially acceptable measurements are obtained in a landing point spaced reasonably uniformly over the landing point, then the actual confidence that 100% of the landing point is acceptable would be higher than 90%, possibly approaching 99% as a function of the specific type of lunar surface under examination.

3.3.6 Data and Landing Point Location Accuracy

The system navigation function is to provide throughout the mission a continuous indication of the vehicle's position and attitude with respect to Surveyor or other identifiable landmarks. This indication must satisfy the landing point and data location tolerances. This function must be performed in two different modes of operation during the mission: navigation between the landing points (interpoint) and navigation within each point (intrapoint). The requirements and constraints of each mode differ, placing separate requirements on the elements that comprise the navigation function.

3.3.6.1 Data Location Accuracy

To assure that the entire point receives adequate image coverage, the diversion between the nominally parallel traverses within the point, must not exceed one meter. The vehicle therefore cannot deviate from the parallel path more than ±0.5 meter over a 40-meter length; this is equivalent to an azimuth uncertainty (vehicle heading error) of 43 arc-minutes.

The intrepoint navigation range accuracy requirement of ±0.9 meters per 160 meters of SLRV travel is set by the topographic data collection requirement (Section 3.3.2).

3.3.6.2 Landing Point Location Accuracy

The mission requirements provide a relationship between the landing point location accuracy with respect to one of the mark or identifiable surface features and the point diameter. This expression, (Figure 3-18) is

$$D = 2\left[(\Delta d)^2 + (16.4)^2\right]^{1/2} + 10 \text{ meters}$$

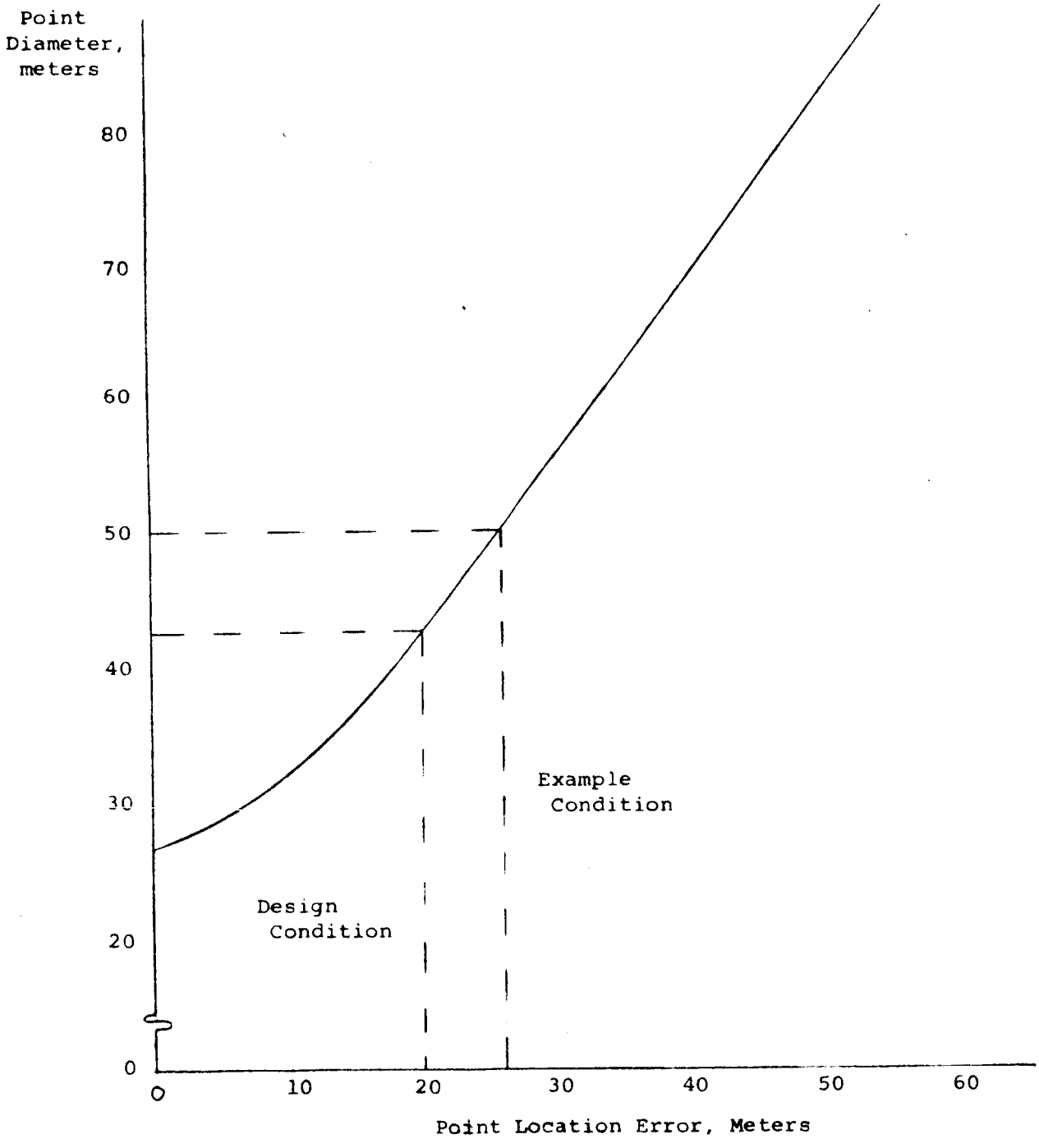

Figure 3-18 Point Diameter vs Point Location Error

where

D = point diameter

Ld = point location uncertainty with respect to one mark

It may be necessary to situate and locate three artificial site reference markers for use during LEM descent if the Surveyor Spacecraft or suitable natural landmarks are not available. The markers are to be placed in an approximate equilateral triangle with sides of 1500 meters to an accuracy of 20 meters between marks. For the case in which Surveyor is at the site center, the maximum range from Surveyor to each marker is approximately 870 meters. For the worst case situation in which Surveyor is at the side of the site, the distance to the markers is approximately 1500 meters. For this situation, the 43 arc-minute azimuth accuracy produces a 18.8-meter cross-range component. This is acceptable if the range component tolerance is tightened accordingly; a range error of approximately 4 meters is allowable.

The 20-meter tolerance on the landing point (as discussed in Appendix A) location with respect to one of the reference landmarks can be examined in terms of range and cross-range accuracy tolerances. Assuming a rms relationship, each component becomes

$$\epsilon_1 = \epsilon_2 = 14.1 \text{ meters}$$

The outermost landing point centers are located on a 2100-meter diameter circle, concentric with the 3200-meter site. Applying the 43 arc-minute azimuth accuracy intrapoint requirement to interpoint navigation, a cross-range error of 13.1 meters results at the 2100-meter circle, satisfying the cross-range tolerance established above. To satisfy the range component tolerance, a range measurement accuracy of 1.34% is required at the 2100-meter circle.

3.3.6.3 Summary

For intrapoint navigation, a 43 arc-minute azimuth accuracy and 0.56% range measurement accuracy is required. For interpoint navigation, the 43 arc-minute azimuth accuracy is also satisfactory. A range measurement accuracy of 1.3% at 1050 meters is required. This is also satisfactory for marker location tolerances when Surveyor is at the site center. When Surveyor is at the side of the site, a range error of no more than 4 meters in 1500 is allowable.

To illustrate the importance of the navigation accuracy on the mission, several instances will be considered. In the parallel point traverse procedure if the paths cannot be kept within the 0.5-meter tolerance, then the nominal spacing must be reduced accordingly.

This is seen by the relationshipL

$$X + 2D \tan \psi = 3.6 \text{ meters}$$

where

X = traverse spacing

D = point diameter

ψ = navigation azimuth error

If the spacing between paths is reduced, more travel is required to complete the point survey. This relationship was solved for the limiting case and plotted in Figure 3-19, which relates total intrapoint vehicle travel to azimuth error. It can be seen that azimuth error has relatively little effect on intrapoint travel for a 40-meter point diameter. However, as the point diamter increases due to interpoint navigation error, azimuth error contributes an increasing range penalty.

Now, if a 60 arc-minute azimuth accuracy is considered, the added intrapoint range can quickly be illustrated. At the outermost point distance of 1050 meters, the cross-range error component is 18.4 meters. If the 14.1-meter range error is held unchanged, the rms point location error is 23.4 meters. Relating this through Figure 3-18, a point diameter of 46 meters is required. The resultant intrapoint range is shown on Figure 3-19.

3.3.7 Reliability

The SLRV range is basically the determinant of reliability from the system analysis standpoint, since it is this requirement, together with the terrain models, data requirements, and physical constraints, upon which the design is based. The range requirement must be sufficiently higher than the absolute, ideal minimum, to allow for maneuvering around

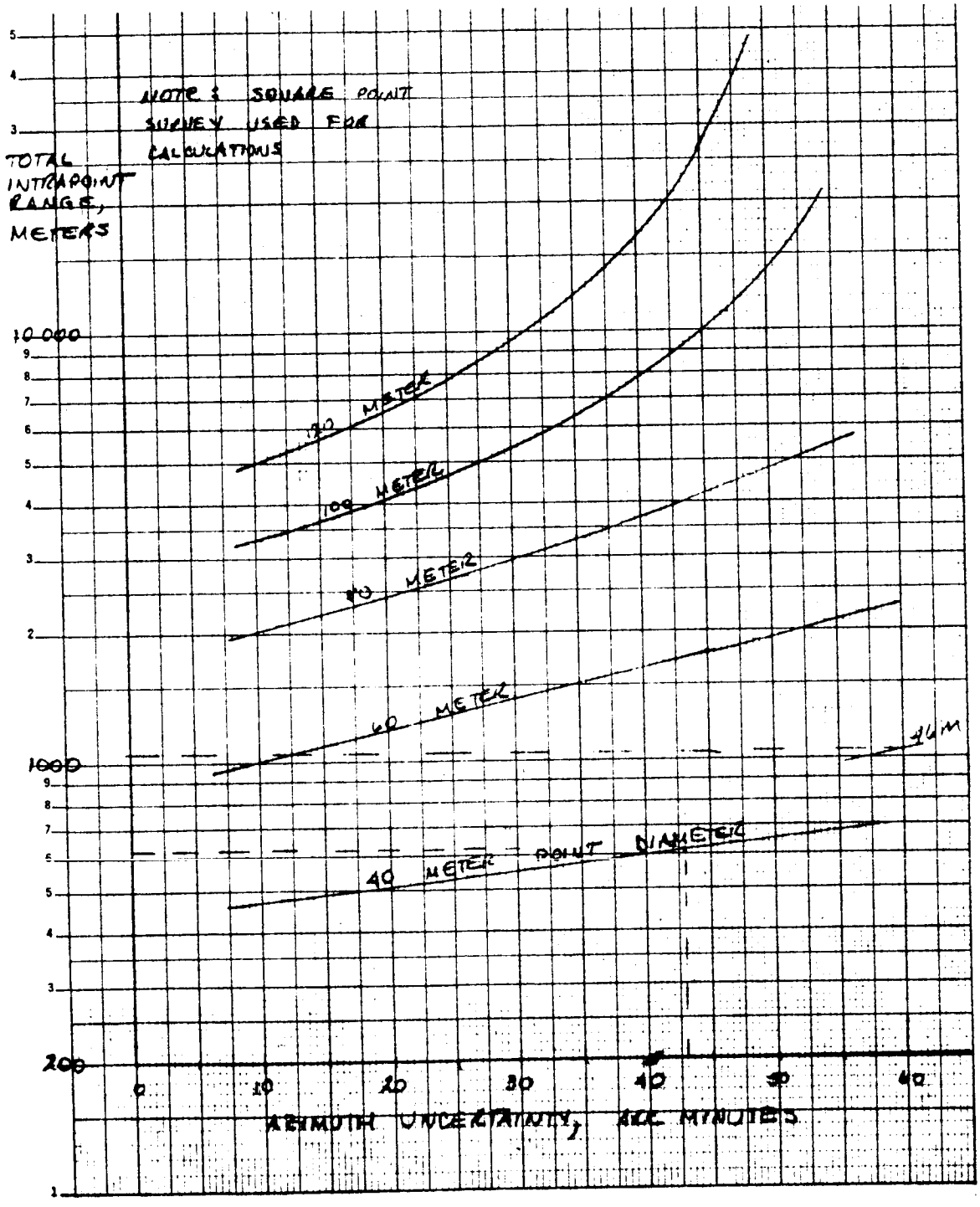

Figure 3-19 Intrapoint Range vs Azimuth Uncertainty

hazards and searching for secondary sites after the primary proves unacceptable. To maintain the best possible reliability, the range allowance for this maneuvering must be carefully selected. Computation of the allowance is discussed in the following paragraphs.

3.3.7.1 Interpoint Range

An analysis was presented in the First Bi-monthly SLRV Progress Report for determining the increase in travel distance necessary to avoid large hazards, small hazards, and to allow for moving to another nearby point when one proves unacceptable. A factor of $k_1 = 1.29$ was determined as the path increase in the form of a semicircular arc between points to avoid large hazards. A second factor of the same magnitude, $k_2 = 1.29$, was determined for the avoidance of small obstacles by making small semicircular path changes. A third factor of $k_3 = 1.08$ was included to allow for moving to another point when one proves unacceptable. This factor was based on the assumption that, for every good point, there is an equal probability of an unacceptable one, thus increasing the total interpoint traverse distance by one point diameter for every good point.

Since each of these factors is independent, their combined effect is determined in an rms manner as:

$$K_T = 1 + \sqrt{(k_1 - 1)^2 + (k_2 - 1)^2 + (k_3 - 1)^2} = 1.417 \tilde{=} 1.4$$

The total traverse distance outside of the point surveys can be expressed as:

$$D_T = K_T \left[(n-1) D_{pp} + D_{sp} \right]$$

where

n = number of acceptable points

D_{pp} = straight-line interpoint traverse distance

D_{sp} = straight-line distance from Surveyor to the first point to be surveyed.

3.3.7.2 Intrapoint Range

The distance traversed within a point in performing the point survey consists of the nominal "straight-line" distance modified by factors to account for obstacle and crevice avoidance and for unacceptable points which are abandoned part way through.

An initial check is made of a prospective landing point at a range of 40-to 100-meters distance using a narrow angle field-of-view capability of the TV camera. This eliminates areas having large hazards; hence, the k_1 factor in the interpoint traverse is not necessary here. However, the $k_2 = 1.29$ factor for small obstacles and crevices is still applicable.

Allowance must be made for the partial distance traveled in points that are abandoned part way through. Points may be abandoned for the following basic reasons:

1. Obstacles are too large and crevices too wide for LEM
2. Crevices are too wide for the SLRV to negotiate
3. Slopes are too steep for an LEM landing
4. Soil is too soft for an LEM landing.

There is an equal probability of occurrence of the first three reasons anywhere within the point; hence, the average occurrence is for 50% of the point survey to be completed. A fairly good indication of the soil strength characteristics (reason 4) will be obtained before completion of the first half of a point survey as it is very unlikely that there will be abrupt changes in the soil bearing strength properties. Thus, finding the first half acceptable will provide a high confidence that the entire point is acceptable. Therefore, the average occurrence of point rejection for inadequate soil bearing strength will occur at about 25% completion of the point survey. Taking the average of the occurrences of the four reasons for rejecting a point,

$$K_1 = \frac{1.5 + 1.5 + 1.5 + 1.25}{4} \simeq 1.4.$$

Therefore, a factor of 40% will be used for the average portion of each abandoned point that is surveyed.

In addition to these factors, allowance must be made for navigation errors resulting in increased path lengths. This is more critical in the point survey than it is in the interpoint traverse because, in the former, the survey pattern depends on maintaining parallel equally-spaced traverse paths through the point. A maximum of 5% increase in intrapoint path length will be assumed for navigation error. Since the probability of occurrence of this error is independent of path length, number of good points, and number of abandoned points, its effect combines with the product of the previous factors in an rms manner to determine the total increase in intrapoint travel distance.

$$K_P = 1 + \sqrt{(1.4 \times 1.29 - 1)^2 + (1.05 - 1)^2} \cong 1.8$$

The total travel distance inside points can be expressed as:

$$D_p = 1.8\ n\ D_1$$

where:

n = number of acceptable points

D_1 = straight-line travel distance within a point.

3.5.4.3 Total Range

The total distance traveled in performing the point survey mission is the sum of the previous results:

$$D_M = D_T + D_P$$

$$= 1.4 \left[(n - 1)\ D_{pp} + D_{sp} \right] + 1.8\ n\ D_1$$

If the reasonable assumption is made that the distance traveled from the Surveyor to the first survey point is approximately the same as the interpoint distance, $D_{sp} = D_{pp}$, and the equation simplifies to:

$$D_M = n\,(1.4\,D_{pp} + 1.8\,D_l)\,.$$

This equation does not include extra travel distance for placing markers as this is assumed to be accomplished during the traverse of the normal point-to-point pattern.

The total range is computed to be 34.4 km for values of:

D_{pp} = 500 meters

D_l = 558 meters.

The reliability requirement placed on the system is therefore that value sufficient to ensure the mission goal for probability of success of 0.5 for a total vehicle range of 34.4 meters. The system requirement on performance is to achieve the specified operating characteristics with a probability of 0.997. Therefore the value for reliability for the mission is established to be 0.50.

SECTION 4

SYSTEM DESIGN OF 100-POUND VEHICLE

4.1 DESIGN METHODOLOGY

To ensure that all feasible system concepts were investigated potential subsystem concepts were arranged in a matrix for evaluation (Figure 4-1). Thus many concepts were examined. An initial screening reduced the number of concepts to a manageable level (some combinations were intrinsically incompatible, and others could be eliminated on the basis of previous evaluations).

A mission model (Section 4.4.1) was generated to facilitate further analysis of the system concepts; a more advanced model was used in the subsequent system evaluation program (See Volume V). The mission model considered the functions to be performed by the SLRV and the characteristics of the lunar surface. It consists of two primary operational elements: (1) landing point survey and verification, and (2) traverse between landing points. In addition, a sensitivity study was conducted to determine system elements having a first-order effect on the design. Second-order effects are defined as those not sufficient in magnitude to affect system functional decisions. The interaction between functional elements of the system, represented by the flow lines of Figure 4-2, are of three distinct types:

1. Those dependent solely upon the mission requirements.

2. Those dependent upon both the mission requirements and other subsystems.

3. Those dependent solely upon other subsystems or elements of the system.

It is evident from Figure 4-2 that the mobility subsystem is of the first type and hence can be analyzed independently.

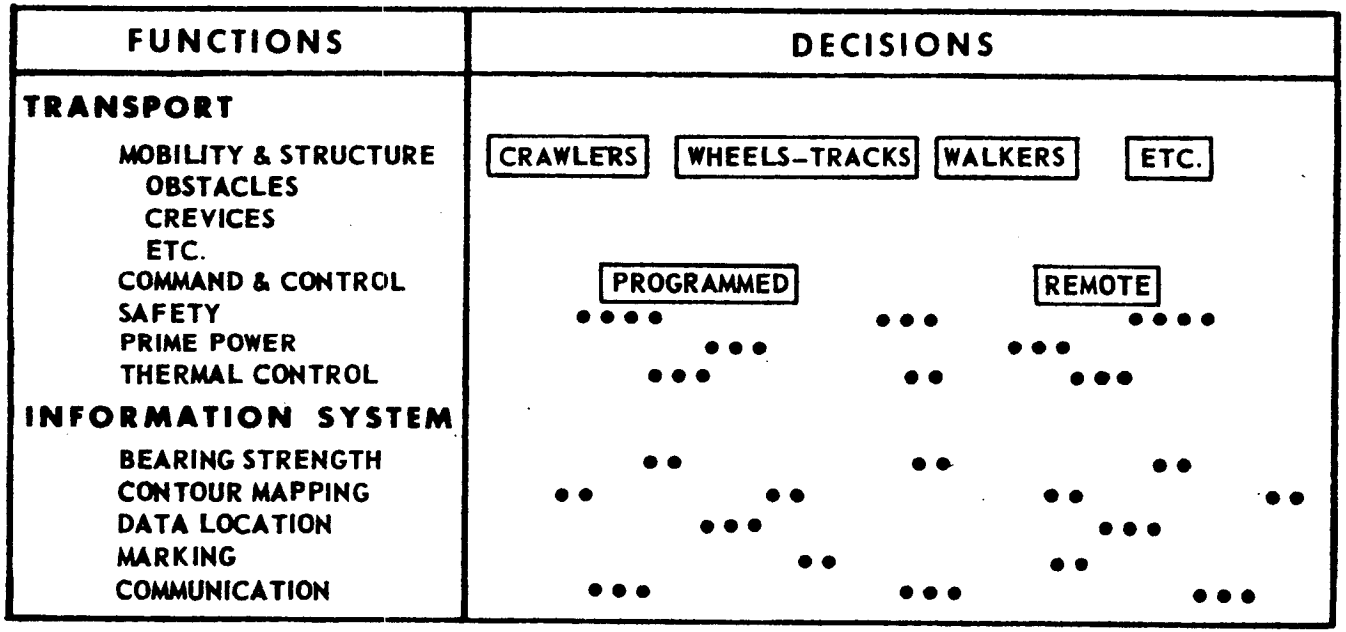

Figure 4-1 Functional Decisions

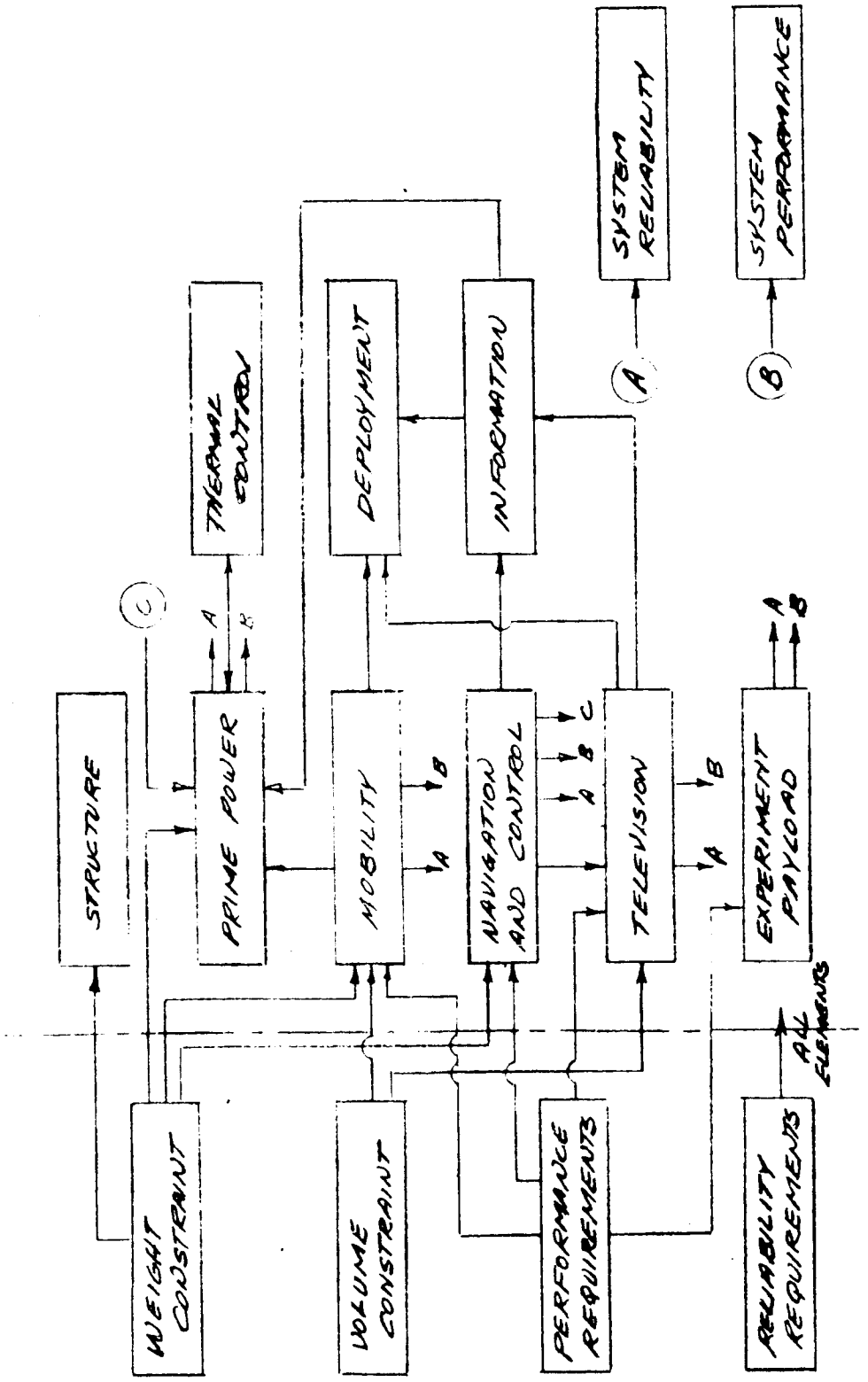

Figure 4-2 First Order Effects Flow Diagram

4.2 MOBILITY TRADE-OFFS AND SELECTION

4.2.1 Mobility Requirements

The movement of the SLRV, given a degree of control, is a function of the probability of terrain negotiability, P_t. This probability is in turn dependent upon the lunar terrain and the SLRV's mobility capability. Thus P_t should be based on the requirement that the SLRV be able to negotiate any randomly-selected site because a landing site with a high percentage (perhaps 95%) of bad terrain can conceivably be negotiated well enough to satisfy mission requirements. (The vehicle can choose and change its direction of travel to avoid bad areas.) The minimum good area for mission completion is, in addition to the area within the points, a strip of vehicle width running somewhat irregularly between successive points; i.e., a path winding in some devious fashion around bad spots is the minimum good area required between points. However, the probability that the Surveyor will land on some part of the path or within one of the not-yet-certified points is remote.

P_t should reflect, then, the SLRV's ability to negotiate a randomly-selected site whose roughness is defined by the terrain models. The probability should not allow the vehicle a choice of direction, but should reflect the probability that deployment may occur in a bad area, where all directions may be non-negotiable. Terrain negotiability therefore may be written as the product of the probabilities of negotiating individual hazards defined by the terrain models. To make the problem more tractable, it is assumed that these individual probabilities are mutually independent. Thus:

$$P_t = P_o \times P_c \times P_{sn} \times P_{os}$$

where:

P_o = probability of obstacle negotiation

P_c = probability of crevice negotiation

P_{sn} = probability of terrain slope negotiation

P_{bs} = probability of soil negotiation

These probabilities must be based upon both the terrain models and the SLRV's capability. The extremes of terrain expected are summarized in Table 4-1.

TABLE 4-1

Hazard	Model	
	Soft	Hard
Obstacles	< 10 cm	10 cm to 1 meter
Crevices	None	10 cm to 1 meter
Slopes	± 15°	± 15°
Bearing Strength Gradient	> 1 psi/ft	Infinitely hard

4.2.1.1 Obstacle and Crevice Negotiation

The probability of obstacle negotiation, P_o, may be derived by assuming that:

1. The hard and soft models are equally likely.

2. An obstacle has dimensions equal to or greater than 10 cm for the hard model and from zero to 10 cm for the soft model.

3. The probability of encountering an obstacle of a given size within the dimensions of assumption 2 (above) is a constant for either model.

The obstacle negotiation probability may then be writen as:

$$P_o = P_{soft} \times P_{\substack{negotiable \\ area,\ soft}} + P_{hard} \times P_{\substack{negotiable \\ area,\ hard}}$$

$$P_o = \begin{cases} \frac{H}{20} & 0 \leq H \leq 10 \text{ cm} \\ 0.5 + \frac{H-10}{180} & 0 < H \leq 100 \text{ cm} \\ 1.0 & H > 100 \text{ cm} \end{cases}$$

where H is the SLRV obstacle-climbing capability in centimeters. Figure 4-2 shows a plot of this function. Obstacle negotiation capability includes not only the vehicle's capability of climbing obstacles, but also its capability of straddling an obstacle with sufficient clearance to pass over it. Thus, the parameter H of Figure 4-3 is equally applicable to both obstacle-climbing and obstacle-straddling capabilities.

Crevice-climbing capability will enter the terrain negotiation probability in the same manner as obstacle-climbing. The crevice width is substituted for the climbing capability, resulting in a function as follows:

$$P_c = \begin{cases} \frac{W}{20} & 0 \leq W \leq 10 \text{ cm} \\ 0.5 + \frac{H-10}{180} & 0 \leq H \leq 100 \text{ cm} \\ 1.0 & H \geq 100 \text{ cm} \end{cases}$$

where W is the crevice width the SLRV can successfully negotiate. Figure 4-3 also applies here. The soft model contains no crevices (by assumed definition) and therefore contributes a full 0.50 probability.

4.2.1.2 Slope Negotiation

P_{sn}, the probability of negotiating any given terrain slope, is dependent upon the distribution of slopes in any site. If this distribution is assumed constant from 0^o to 15^o and zero beyond these limits, the probability of slope negotiation is the ratio of the range of negotiable slopes to the total range of slopes.

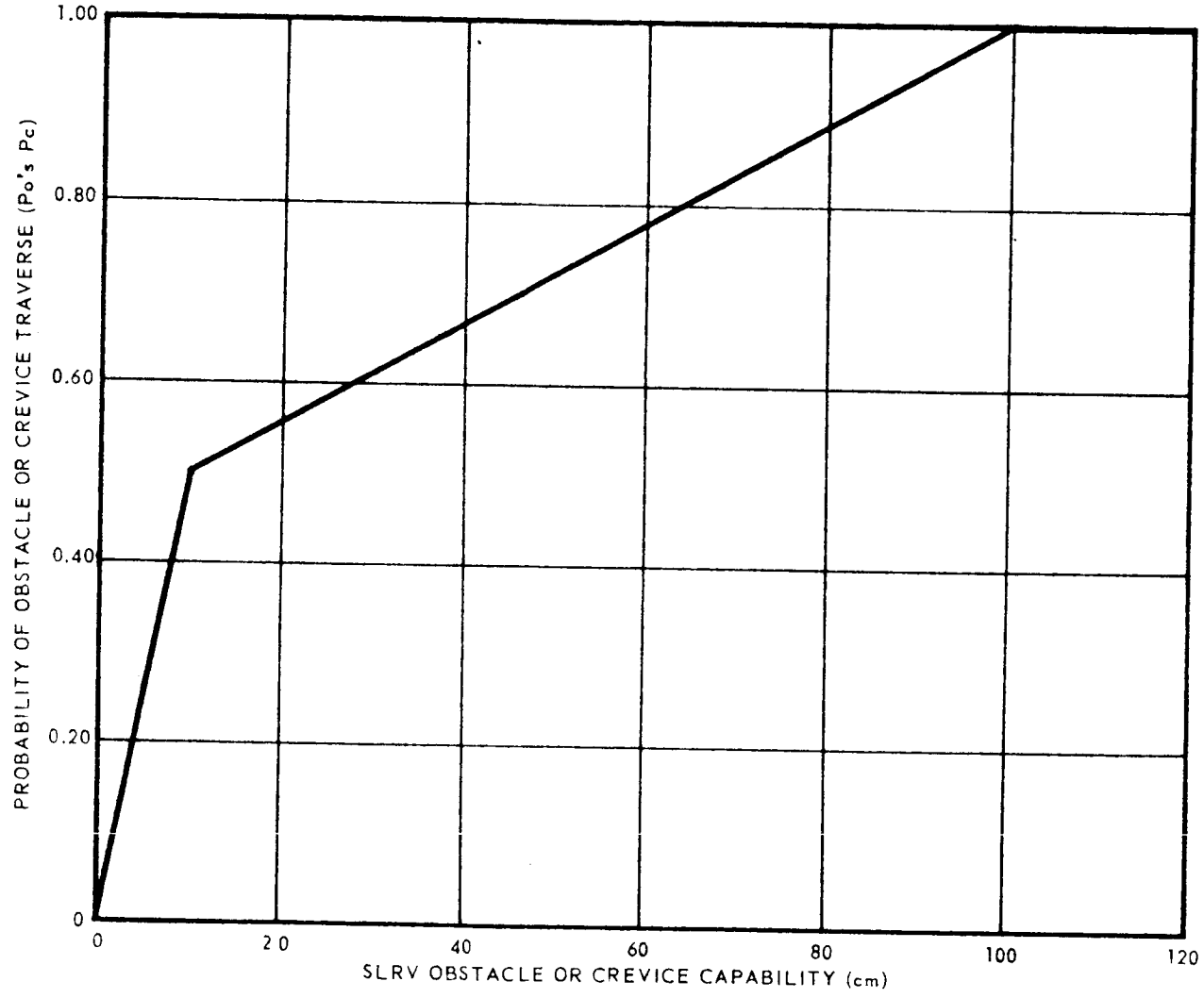

Figure 4-3 Probability of Obstacle or Crevice Traverse vs. SLRV Capability

$$P_{sn} \begin{cases} \frac{B}{15} & 0 \leq B \leq 15 \text{ deg} \\ 1.0 & B > 15 \text{ deg} \end{cases}$$

where B is the maximum slope which the SLRV can negotiate. The straight-line dependency shown in Figure 4-4.

4.2.1.3 Soft Soil Traverse

The final contributor to terrain negotiation, and possibly the most important, is the bearing strength negotiation probability P_{bs}. The bearing strength of interest here is the static bearing strength. This differs from the dynamic bearing strength, which refers to the resistance of the soil to rapid penetration (e. g., under landing loads). The dyanmic bearing strength depends upon static friction, cohesion, and on the foil viscosity (comparable to viscous resistance in fluids). The relation between static and dynamic friction is not clear and probably varies with soil conditions. The lower limit on static bearing strength for SLRV should consider the soft model with static bearing strength gradient of 1.0 psi/ft.

An expression for the SLRV probability of bearing strength traverse may be derived in the following manner. The upper limit on the soft model is assumed to be 9 psi/ft. Assuming that the probability of bearing strength gradients between 1 psi/ft and 9 psi/ft is constant, then P_{bs} may be expressed as:

$$P_{bs} \begin{cases} 1.0 & 0 \leq F \leq \text{psi/ft} \\ 0.5 + \frac{9-F}{16} & 1F \leq 9 \text{ psi/ft} \\ 0.5 & F > 9 \text{ psi/ft} \end{cases}$$

where F is the minimum bearing strength gradient over which the SLRV can travel. This relationship is shown in Figure 4-5.

The probabilities of negotiating the four types of hazards contained in the terrain model have been derived. The overall probability of terrain negotiation may then be computed as the product of the individual probabilities. The variables entering the final expression are the capabilities of the LRV in negotiating each type of obstacle. By relating the capability variables to parameters of a specific LRV design, the trade-offs between terrain negotiability and system design parameters may be established.

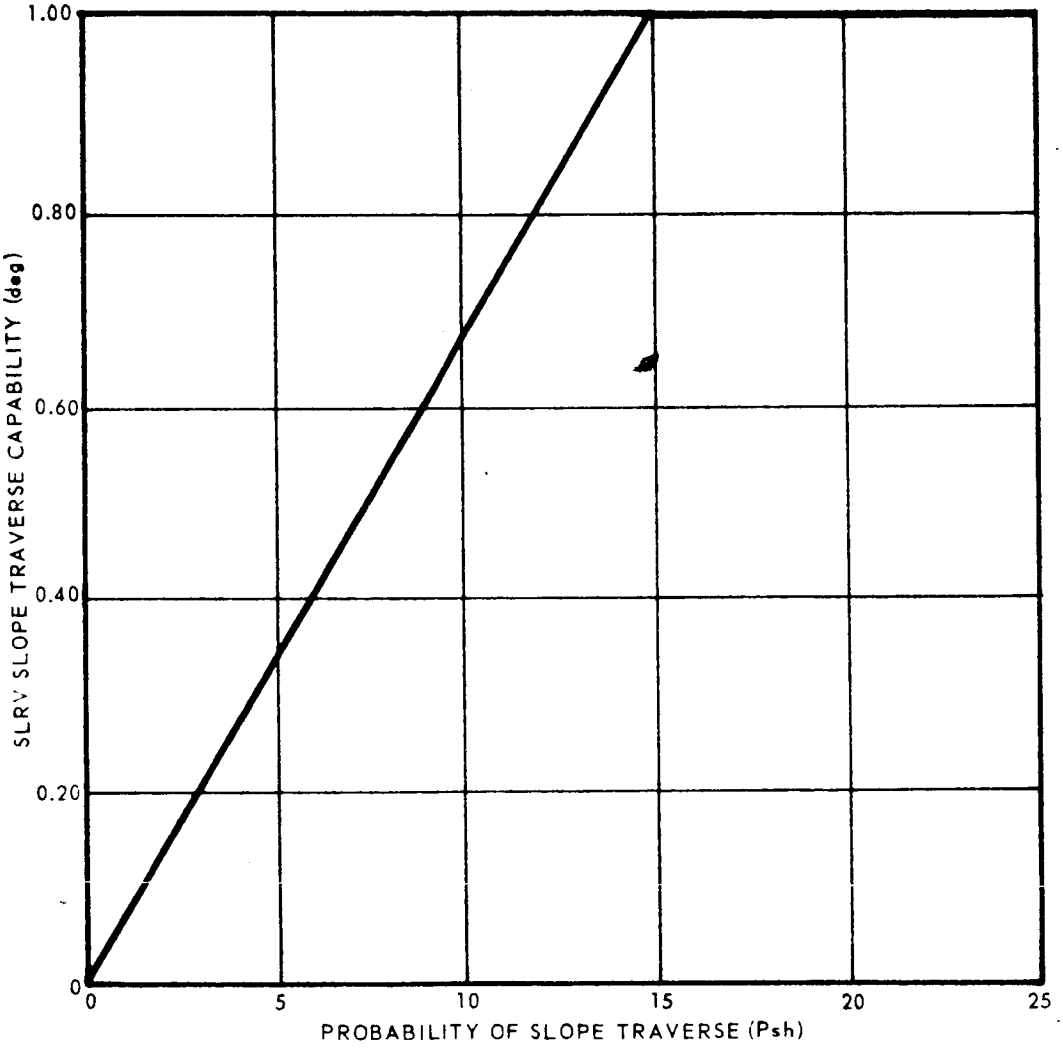

Figure 4-4 Slope Traverse Probability vs SLRV Slope Traverse Capability

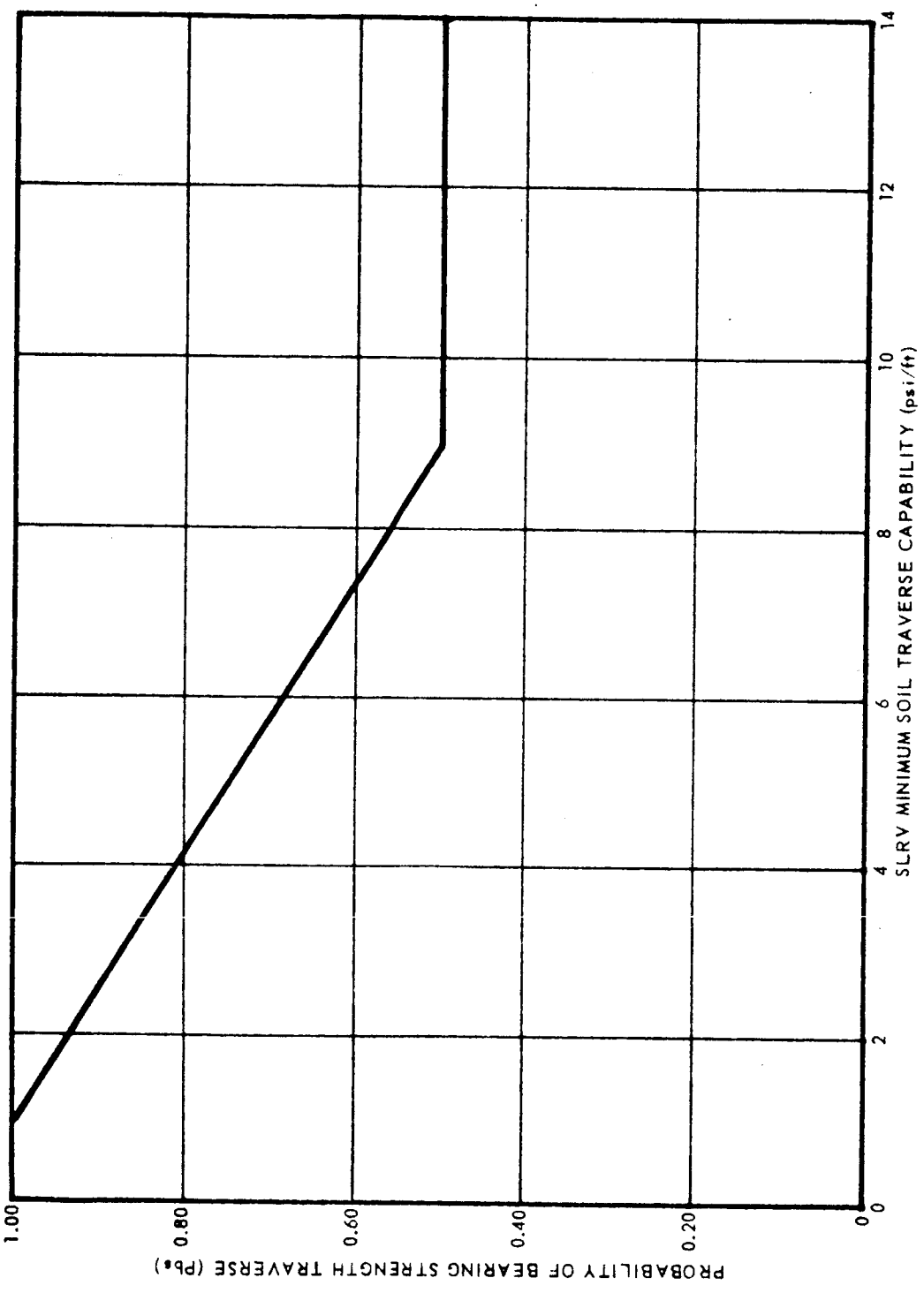

Figure 4-5 Soil Traverse Probability vs. SLRV Bearing Strength Traverse Capability

4.2.2 Mobility Concepts

There are many methods of moving the SLRV over the lunar surface. Crawling, walking, and hopping devices could move the vehicle. However, these devices pose numerous design problems, especially in the areas of complexity and reliability. In the following discussion, only wheel and track devices are considered.

Possible wheeled vehicles are shown in Figure 4-6. The sizes of the wheels in the illustration are somewhat relative and it is assumed that all have the same vehicle weight and packaged volume.

The multiwheel vehicle poses complexity and weight distribution problems; the 10-wheel vehicle approaches the multi-wheel vehicle in complexity. The two-wheel (dumbell shaped) and one-wheel (a simple ball) vehicles present problems in achieving any meaningful degree of mobility.

The choice for the SLRV mobility subsystem then appears to be between the six-wheel vehicle and the three- or four-wheel vehicle.

4.2.3 Stability of Wheeled Vehicles

4.2.3.1 Longitudinal Stability

The geometry of a three- or four-wheel vehicle climbing an obstacle is shown in Figure 4-7. Actually, $a = 0.9949R$, but $a = R$ is used for convenience. The maximum obstacle height is taken to be $0.90R$, $\overline{Z} = (6 - 1/10\,R)$, $N = 1/3$ for the three wheel vehicle. The margin of safety is derived as

$$S = n\sqrt{L^2 - (0.90R)^2} + (0.09)\frac{R^2}{L} - R\left(1 + \frac{5.4}{L}\right)$$

Setting S equal to zero (or a small positive value) yields the relationship between minimum wheel base and wheel radius (or diameter).

The six-wheel vehicle presents no problems of longitudinal stability. The wheel base (L) is equal to twice the wheel diameter plus a small clearance, which is sufficient to provide adequate steering capability.

The results of this analysis are shown in Figure 4-8. The curves provide the minimum wheel base required for longitudinal stability as a function of wheel diameter.

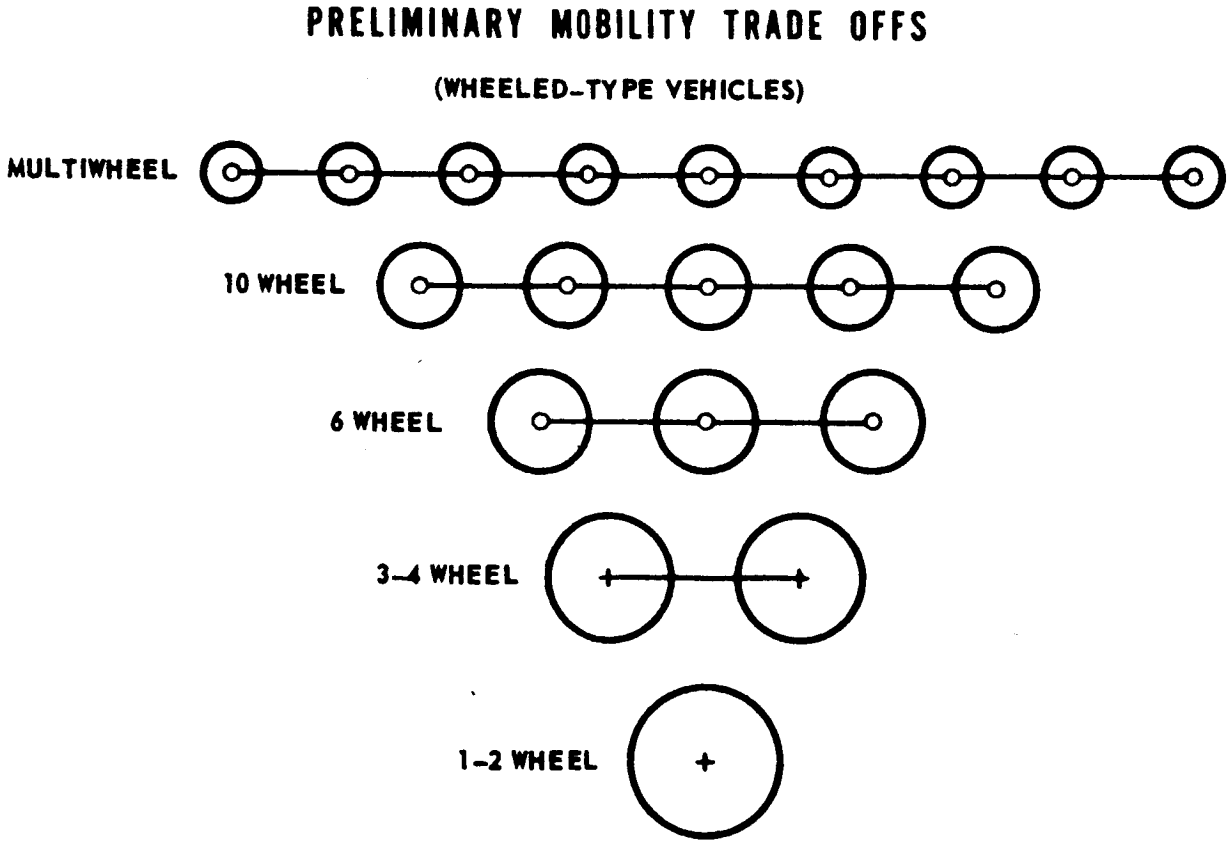

Figure 4-6 Wheel Configuration

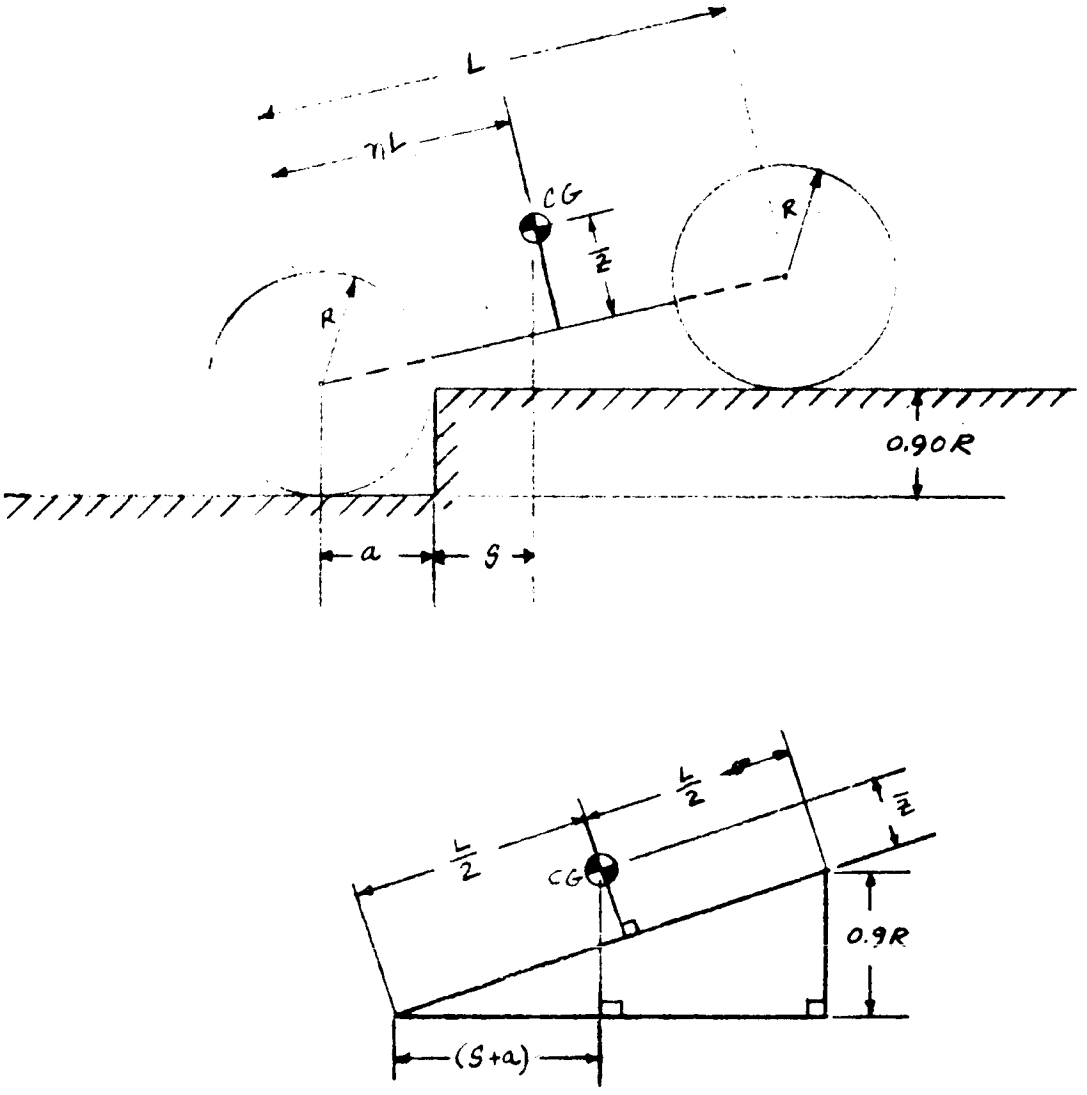

Figure 4-7 Three and Four Wheel Vehicle Geometry

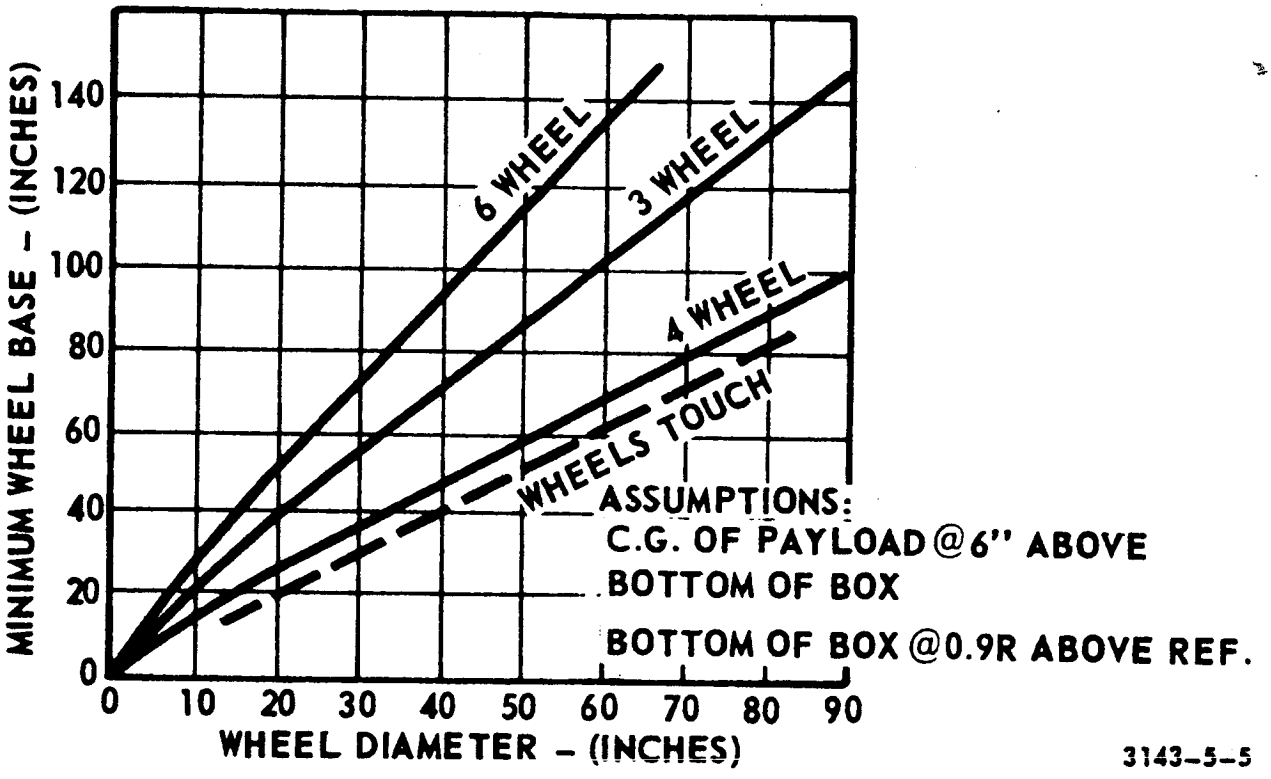

Figure 4-8 Longitudinal Stability

4.2.3.2 Lateral Stability

Figure 4-9 defines the 4- or 6-wheel vehicle configuration when lateral stability is considered. It is assumed that the maximum obstacle height is 0.90R and that $\bar{Z} = (6\text{-}1/10R)$. The geometry of Figure 4-8 reveals the lateral stability margin to be

$$S = \frac{1}{2}\sqrt{6^2 - (0.9R)^2} - \frac{R}{6}(5.4 + 0.81R).$$

Defining S as a small positive number provides a relationship between minimum wheel span (trend) and wheel radius (or diameter). This relationship is shown in Figure 4-10.

The configuration for lateral stability of the 3-wheel vehicle is shown in Figure 4-11. The same assumptions are made concerning obstacle height and $\bar{Z}$ as were made for the 4-wheel vehicle. It can be shown that the stability margin is given by

$$S = \frac{1}{3}\sqrt{\frac{b^2 L^2}{L^2 + \left(\frac{b}{2}\right)^2} - (0.81)R^2} - \frac{(0..90)R\,(6 + 0.90R)}{bL}\sqrt{L^2 + \left(\frac{b}{2}\right)^2}$$

Again, S is set equal to a small positive number so that the center of gravity is just within the stable base area. For each choice of wheel radius (R) the value of wheel base (L) is used which is the minimum required for longitudinal stability. Thus, the above equation plus the 3-wheel curve of Figure 4-8 allow the determination of minimum wheel span (b) required for lateral stability for each value of wheel diameter. The locus of such points is shown in Figure 4-10.

4.2.4 Weight Allocations

4.2.4.1 Mobility Subsystem Wheel Weight

The weight per wheel of the 3-, 4-, and 6-wheeled vehicle given in Figure 4-12 is based on two opposing spiral, elastic-spoked wheels, and

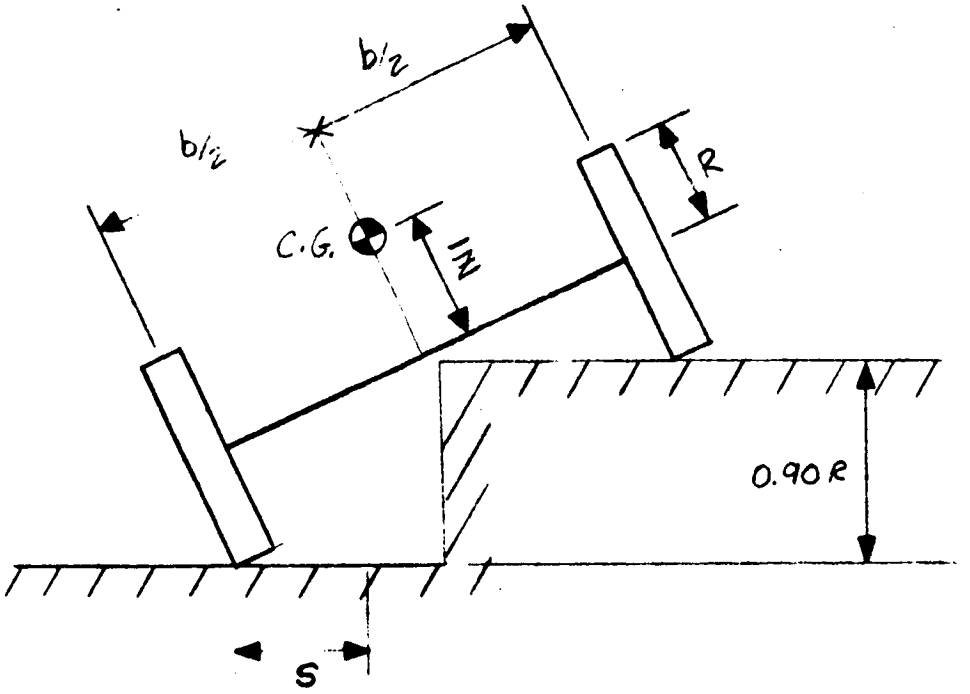

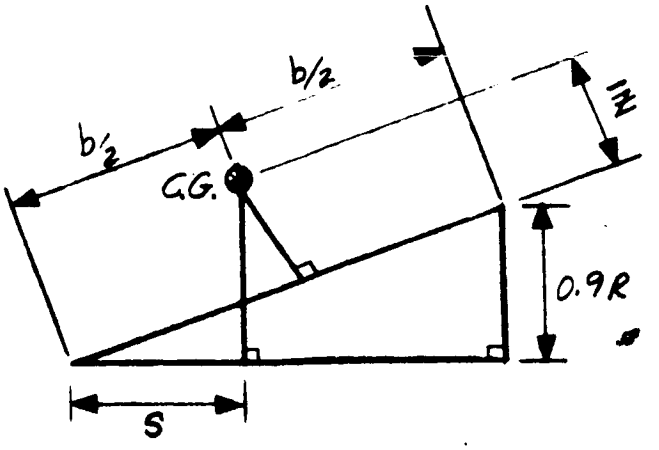

Figure 4-9 Four and Six Wheel Vehicle Geometry

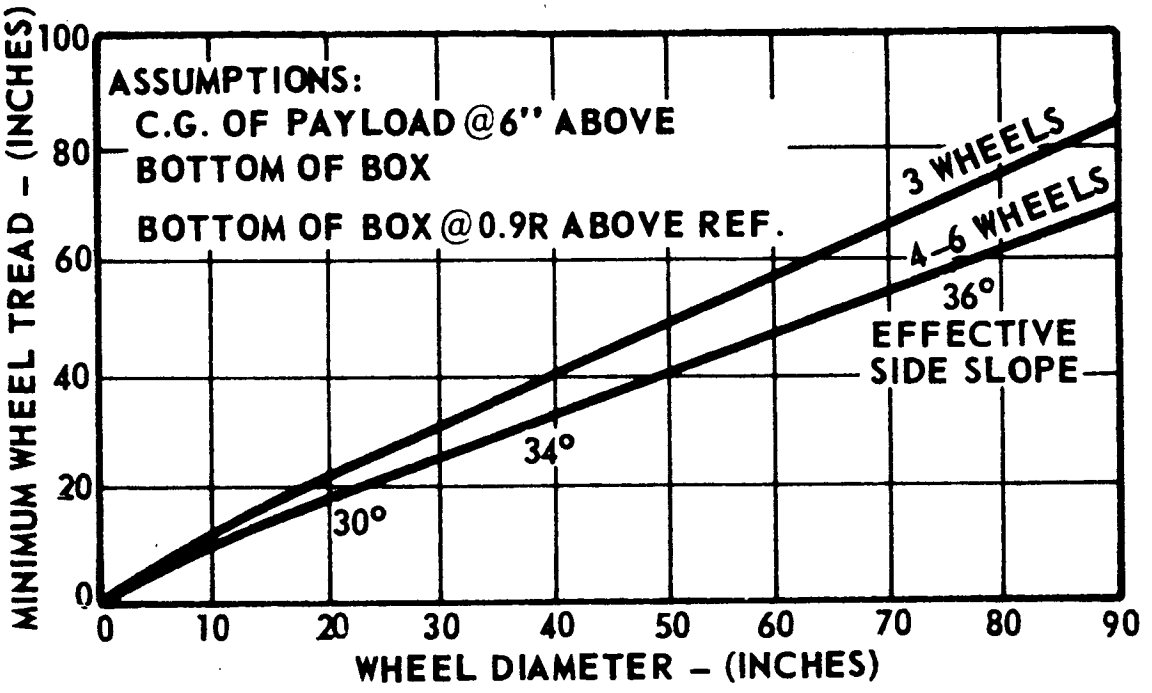

Figure 4-10 Lateral Stability

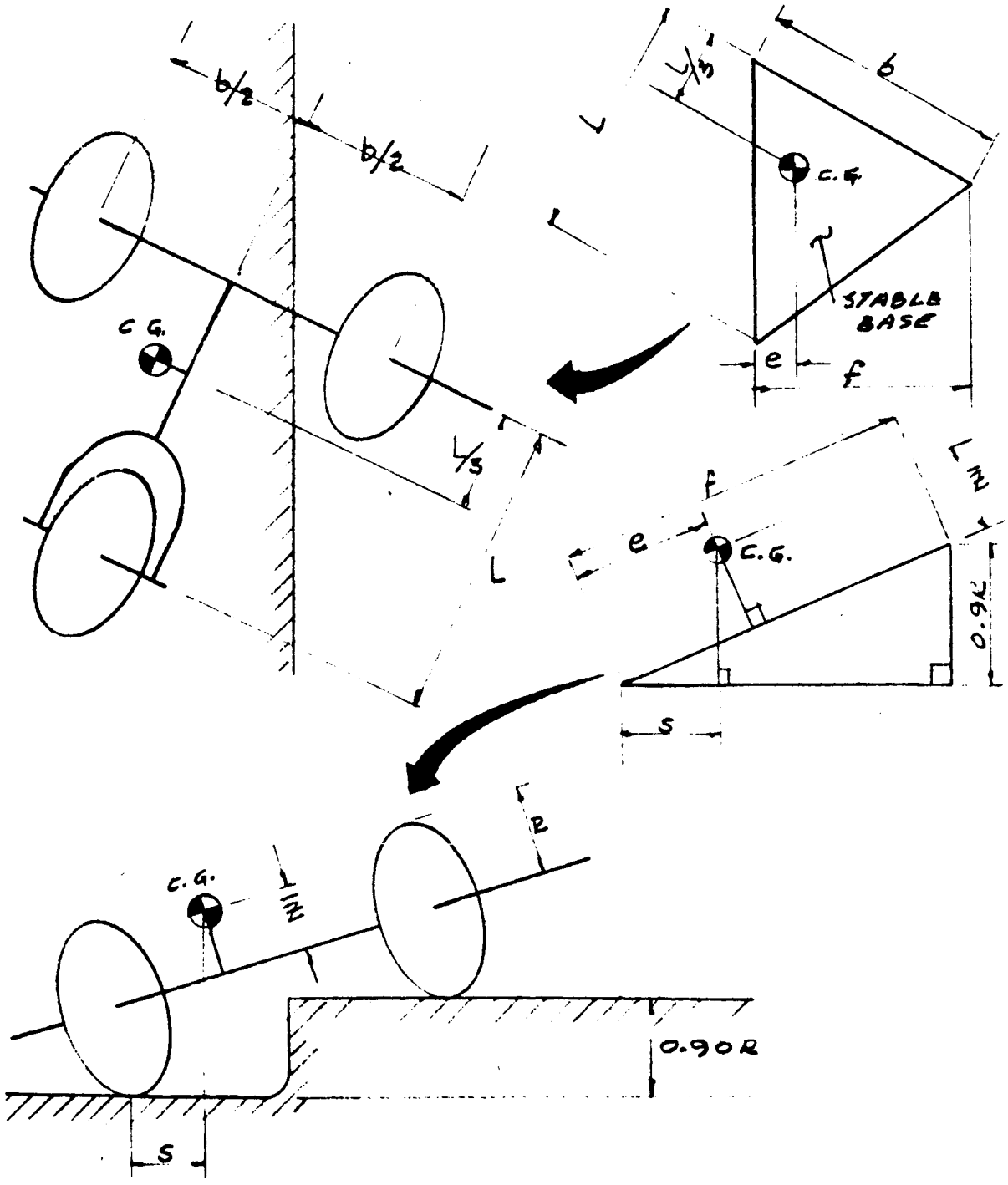

Figure 4-11 Three Wheel Vehicle Geometry

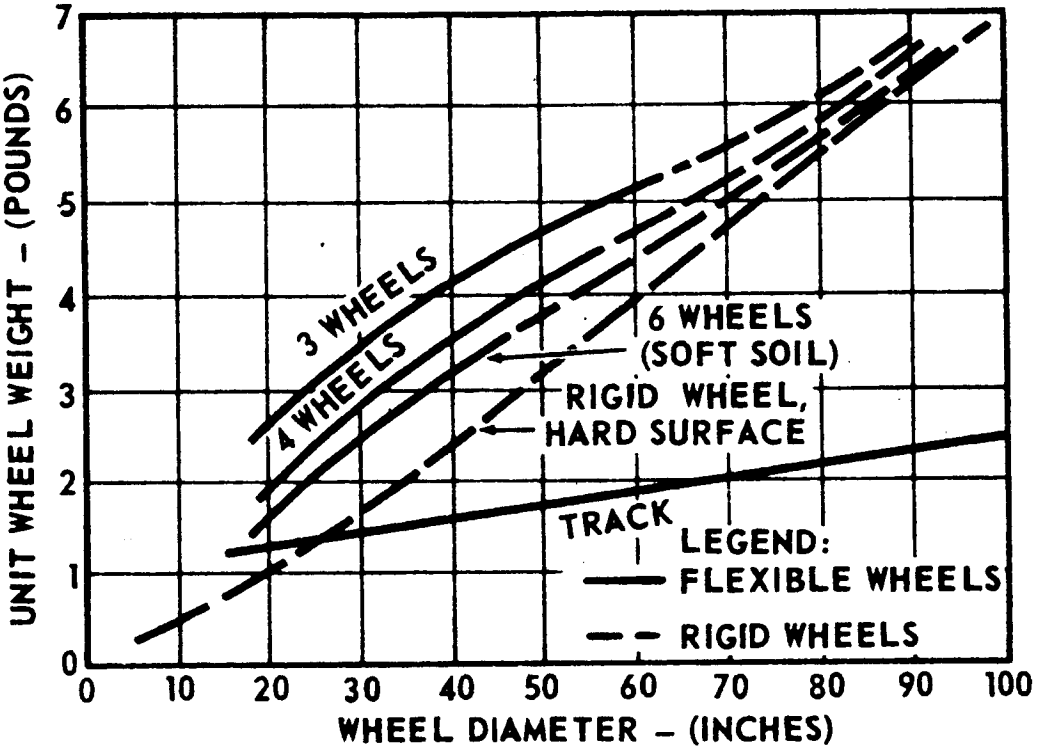

Figure 4-12 Mobility Subsystem Wheel Weight

a wire-spoked wheel for the rigid wheel. The approach used for this comparison was to use a constant spring rate for a given wheel diameter, and to adjust the width of the wheel to compensate for varying loads between the 3-, 4-, and 6-wheeled vehicles so that all the flexible wheels operate at the ground pressure equivalent to a one-inch sinkage in a 1 psi/ft soil. The rigid wheels are sized so that their maximum sinkage is one inch in the 1 psi/ft soil.

The track was held at the 3-inch width which is required to maintain a 1-inch sinkage for the smallest track considered. Theoretically, this width should be reduced for longer tracks, but physical implementation of a narrower track is not considered realistic. The abscissa of the graph is an equivalent wheel diameter for the track. The normalizing factor is the obstacle height (h) which is 0.9R for the flexible wheel and L sin 30° for the track. Therefore, the equivalent wheel radius of the track is

$$R_{e_T} = \frac{L}{0.9} \sin 30^\circ$$

4.2.4.2 Unit Drive Weight

Power requirements demand that the motor and transmission (Figure 4-13) weight for the 3-wheel, 4-wheel, and 6-wheel vehicles be approximately 3.0 lb, 2.7 lb, and 2.5 lb.

Sprocket diameter (Figure 4-12) is taken as 5% of wheel diameter with the condition that the minimum sprocket diameter is 2 in. For an average sprocket thickness of 0.25 in., and aluminum as the sprocket material, the following weights are obtained:

Wheel Diameter (in.)	Sprocket Weight (lb)
18	0.079
36	0.079
54	0.143
72	0.255
90	0.398

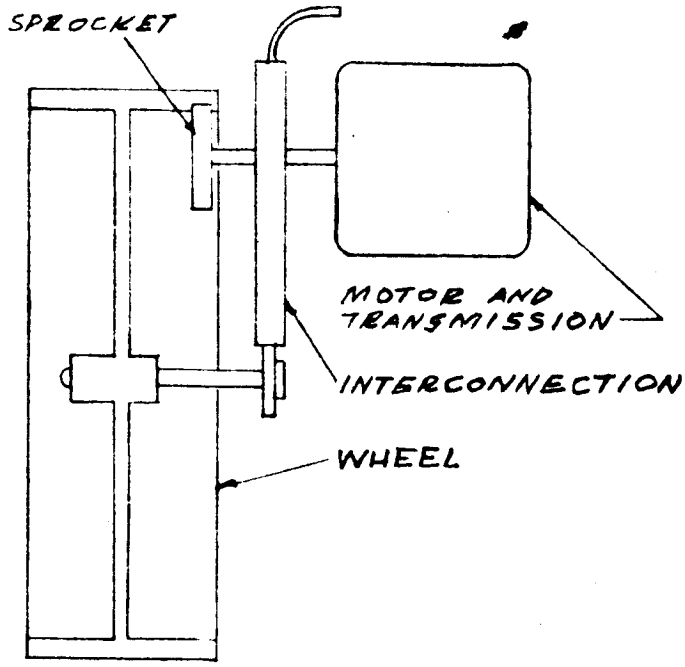

Figure 4-13 Motor, Transmission, Wheel, and Interconnection Assembly

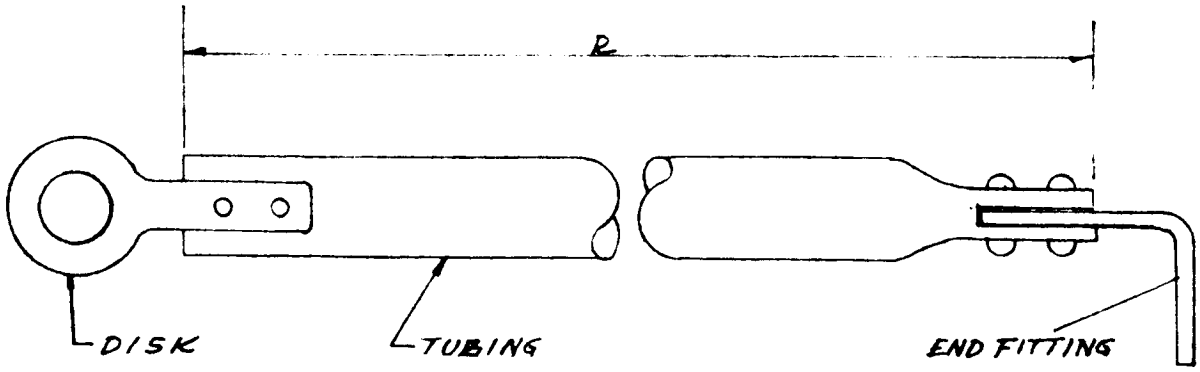

Figure 4-14 Interconnecting Structure

The interconnecting structure is shown in Figure 4-14 where the tubing length, R, is equal to the wheel radius. The material is aluminum. The weight of the disk and fasteners is approximated by 0.00165R lb. Using 1-in. OD x 0.030-in. tubing results in a tubing weight of 0.092R lb. The end fitting is the same for all wheel diameters and is a 1- x 1-in. angle, 0.100-in. thick, and 1.30-in. wide.

Wheel Diameter (in.)	Interconnection Weight (lb)
18	0.880
36	1.722
54	2.600
72	3.519
90	4.420

Summing all component weights yields the following

Wheel diameter (in.)	Unit Drive Weight (lb)		
	3-wheel	4-wheel	6-wheel
18	3.959	3.659	3.459
36	4.801	4.501	4.301
54	5.743	5.443	5.243
72	6.774	6.474	6.274
90	7.818	7.518	7.318

The above tabulation is shown graphically in Figure 4-15.

4.2.4.3 Mobility Subsystem Arm Weight

The arms for the 3- and 4-wheel vehicles (Figure 4-16) are fabricated from 1 in. OD x 0.40 in. aluminum tubing with a fitting attached to both ends of each arm. These end fittings are the same as those on the interconnecting structure shown in Figure 4-14. Arm lengths are given by

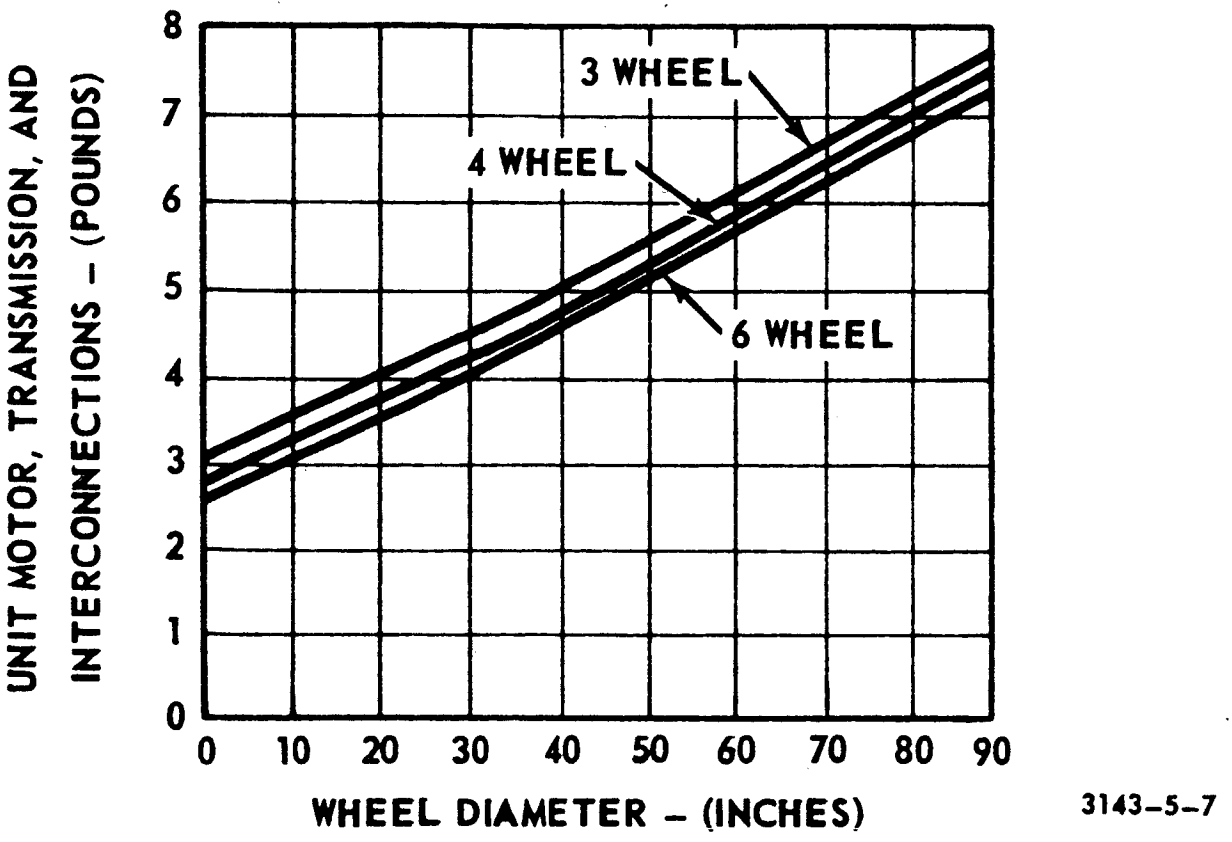

Figure 4-15 Unit Drive Weight

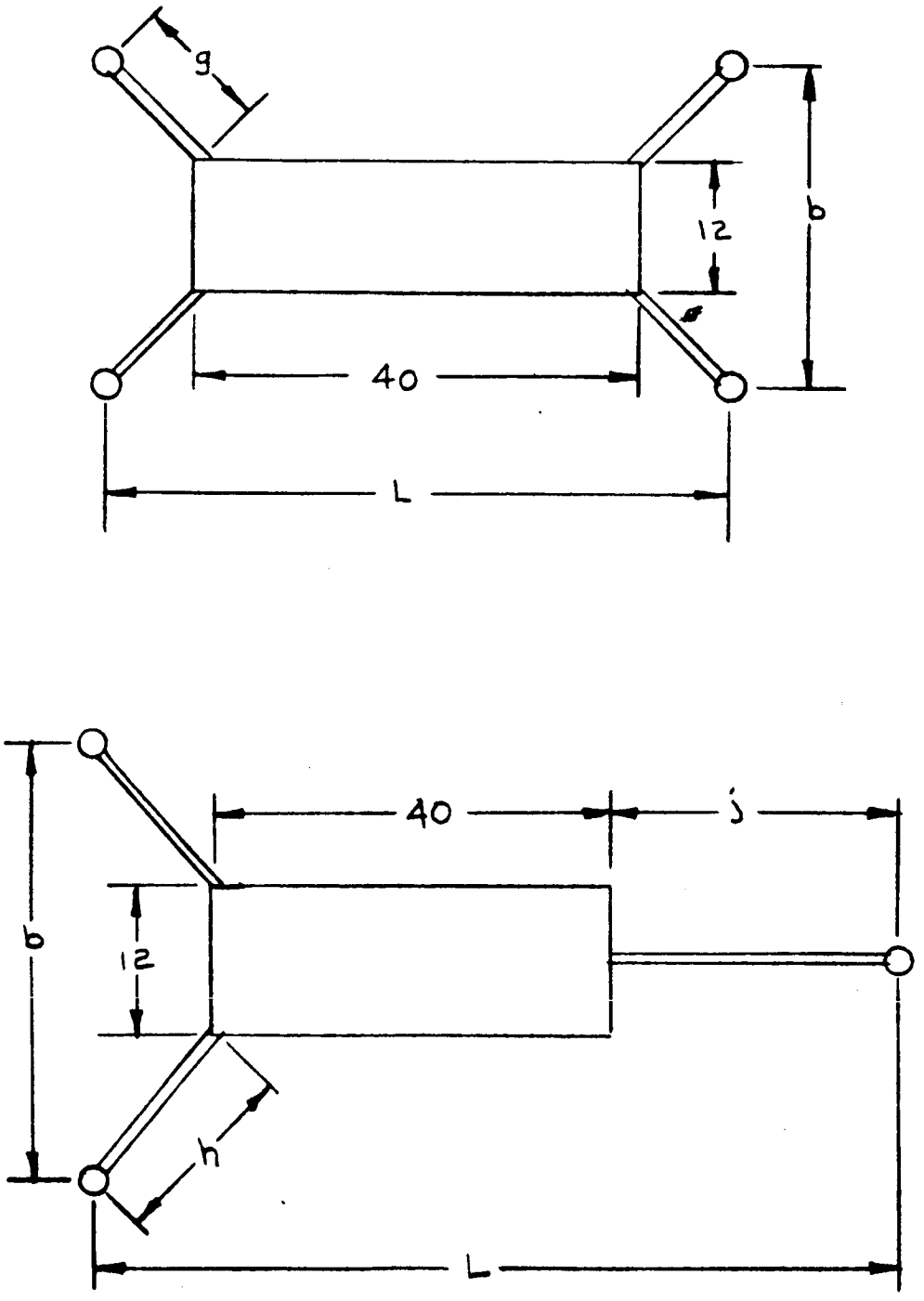

Figure 4-16 Connecting Arms,
Three-and Four-Wheel Vehicles

$$g = \frac{1}{2}\sqrt{(L-40)^2 + (b-12)^2}$$

$$h = \sqrt{\left(\frac{L}{3} - 20\right)^2 - \left(\frac{b}{2} - 6\right)^2}$$

$$j = \frac{2}{3}L - 20)$$

The weight of each end fitting plus fasteners is approximated by (0.0214 lb) + (0.00214 lb/in.) x (arm length). The tubing weight is 0.124 lb/in.

The total arm weight for the 6-wheel vehicle was taken as 1.5 times the total arm weight for the 4-wheel vehicle. The sum of the arm weights for each vehicle is tabulated below and shown graphically in Figure 4-17.

	Total Arm Weight (lb)		
Wheel diameter/(in.)	3 wheel	4 wheel	6 wheel
18	1.57	1.26	1.89
36	6.04	4.64	6.96
54	11.24	9.44	14.16
72	16.66	15.32	22.98
90	21.98	20.92	31.38

4.2.4.4 Mobility Subsystem Weight

Table 4-2 summarizes the weights which constitute the mobility subsystem weight, and these data are plotted in Figure 4-18. Again, as in the wheel and track weight comparison, the track length is sized to climb steps equal to 0.9 wheel radius at a friction coefficient of $\mu = 0.58$.

Figure 4-19 shows a subsystem weight allocation for the 100-lb SLRV System. The weight of 18.3 lb allocated to mobility is considered to be a high average value. The upper limit of this allocation must be considered as 25 lb (extensive studies have indicated that serious degradation in the performance of other subsystems occurs beyond a 25-lb mobility weight). Therefore, a range of approximately 13 to 25 lb is a reasonable span for the mobility subsystem.

TABLE 4-2

MOBILITY SUBSYSTEM WEIGHT BREAKDOWNS

Wheel diameter (in.)	18	36	54	72	90
Obstacle Height	20.6	41.2	61.8	82.4	100
3-Wheeled vehicle					
Arms	1.7	5.8	11.2	16.8	22.0
Motor, trans., interconnections	12.0	14.4	17.4	20.4	23.4
Wheels	7.5	11.9	15.0	17.5	20.7
Steering	2.5	2.5	2.5	2.5	2.5
TOTAL	23.7 lb	34.6 lb	46.1 lb	57.2 lb	68.6 lb
4-Wheeled vehicle					
Arms	1.2	4.7	9.5	15.0	21.2
motor, trans., interconnections	14.6	18.0	21.8	25.8	30.0
wheels	7.0	13.2	18.0	22.5	26.8
TOTAL	22.8 lb	35.9 lb	49.3 lb	63.3 lb	78.0 lb
6-Wheeled vehicle					
Arms	2.0	7.2	14.4	23.0	31.2
motors, trans., interconnections	20.7	25.8	31.7	37.8	43.8
wheels	9.0	17.7	24.9	31.4	39.0
TOTAL	31.7 lb	50.7 lb	71.0 lb	92.2 lb	114.0 lb
3-Tracked vehicle					
Arms	1.7	5.8	11.2	16.8	22.0
motor, trans., interconnections	12.0	14.4	17.4	20.4	23.4
steering	2.5	2.5	2.5	2.5	2.5
TOTAL	19.8 lb	27.2 lb	36.5 lb	45.9 lb	54.9 lb
4-Tracked vehicle					
Arms	1.2	4.7	9.5	15.0	21.2
Motor, trans., interconnections	14.6	18.0	21.8	25.8	30.0
Tracks	4.8	6.0	7.2	8.3	9.3
TOTAL	22.6 lb	28.7 lb	38.5 lb	49.1 lb	69.5 lb

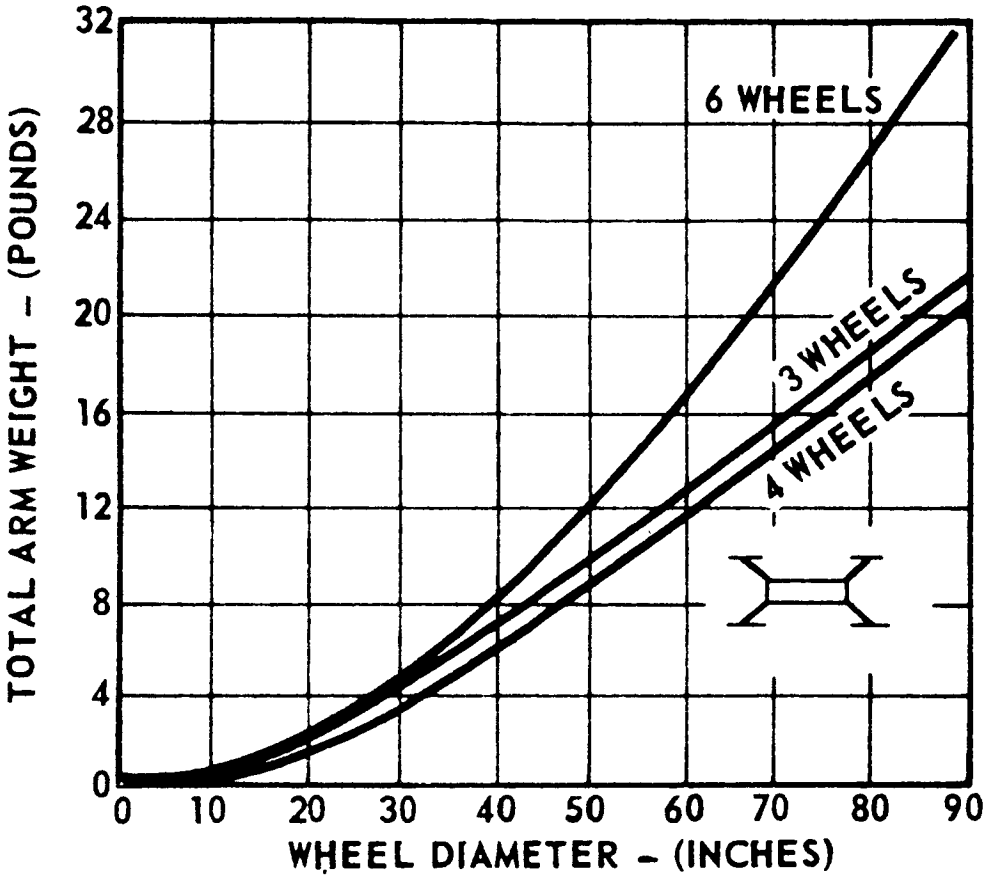

3143-5-10

Figure 4-17 Mobility Subsystem Arm Weight

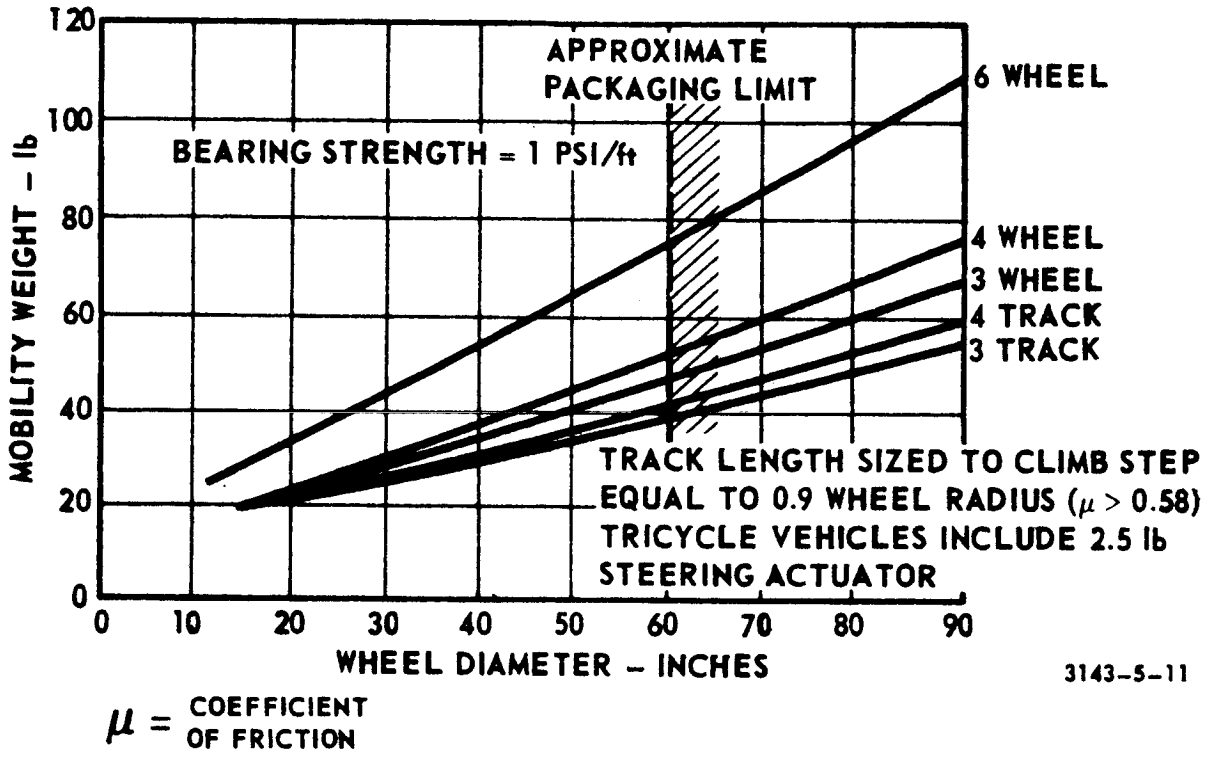

Figure 4-18 Mobility Subsystem Weight

SUBSYSTEM	WEIGHT, LB	
PRIME POWER	35.2	64.5
ELECTRONICS	18.2	
TELEVISION	8.5	
PENETROMETER	2.6	
MOBILITY	18.3	35.5
STRUCTURE	10.5	
DEPLOYMENT	6.7	
TOTAL	100.0	

Figure 4-19 Preliminary Weight Allocation

4.2.5 Friction and Step Heights

For a 25-lb system, the 6-wheel vehicle appears to be preferable because of the higher step-climbing capability at a higher coefficient of friction, as shown in Figure 4-20. There appears to be little to choose from between the 3-or 4-track vehicles and 3-or 4-wheel vehicles based on step climbing capabilities.

4.2.6 Figure of Merit Analysis

To rate the vehicles being considered, a figure of merit was established that is the product of several partial probabilities (Figure 4-21). Below 18 lb for the 3-or 4-wheel or track vehicles and below 25 lb for the 6-wheel vehicle, all figures of merit are zero. Up to a mobility weight of 25 lb, the 3-or 4-wheel or track vehicles always have a higher figure of merit than the 6-wheel vehicle. Adjustments could be made in the systems so that there would probably be little difference in the figures of merit. Neither reliability nor weight are included, but both would reduce all figures of merit proportionally.

Between the tracked and wheeled systems, Figure 4-21 shows that the tracked systems consistently indicate a higher figure of merit than their wheeled counterparts. Therefore, the choice resolves to either 3-or 4-tracked systems. A reliability analysis conducted for these two systems (see Volume IV, Section 2) shows superior reliability for 4-tracked systems. The results of this system design effort, including reliability, indicate the same functional choice (4 track) over the specified weight range of 13 to 25 lb. Since the process of freezing the rest of the subsystems could not reasonably be expected to result in a mobility subsystem greater than 25 lb, it was a valid engineering decision to select the 4-track concept at this point, regardless of the final over-all system configuration.

The selection of obstacle-traversing capability and design speed for the 100-lb SLRV is described in Section 4.4.2 where trade-offs with communication data rate and system power are considered.

4.3 APOLLO SUPPORT SCIENTIFIC EXPERIMENTS

The SLRV Apollo-support mission objectives include the determination of:

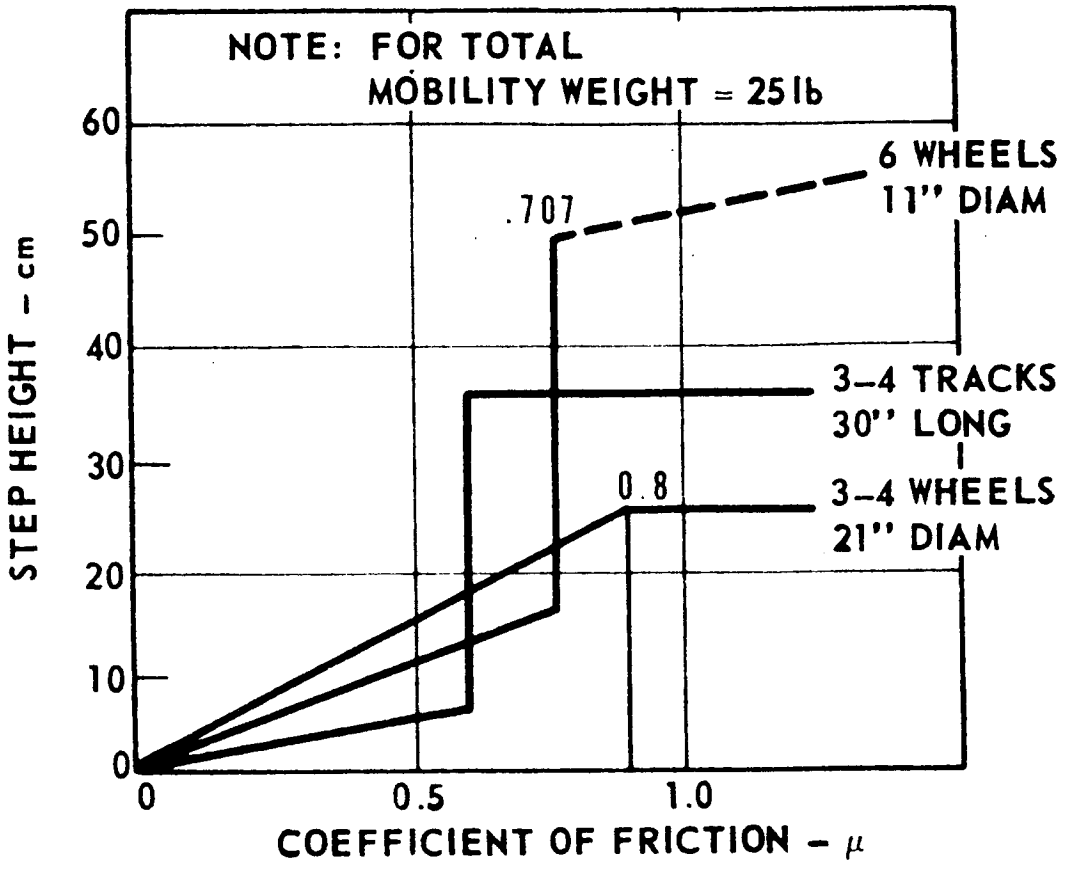

3143-5-12a

Figure 4-20 Friction and Step Capability

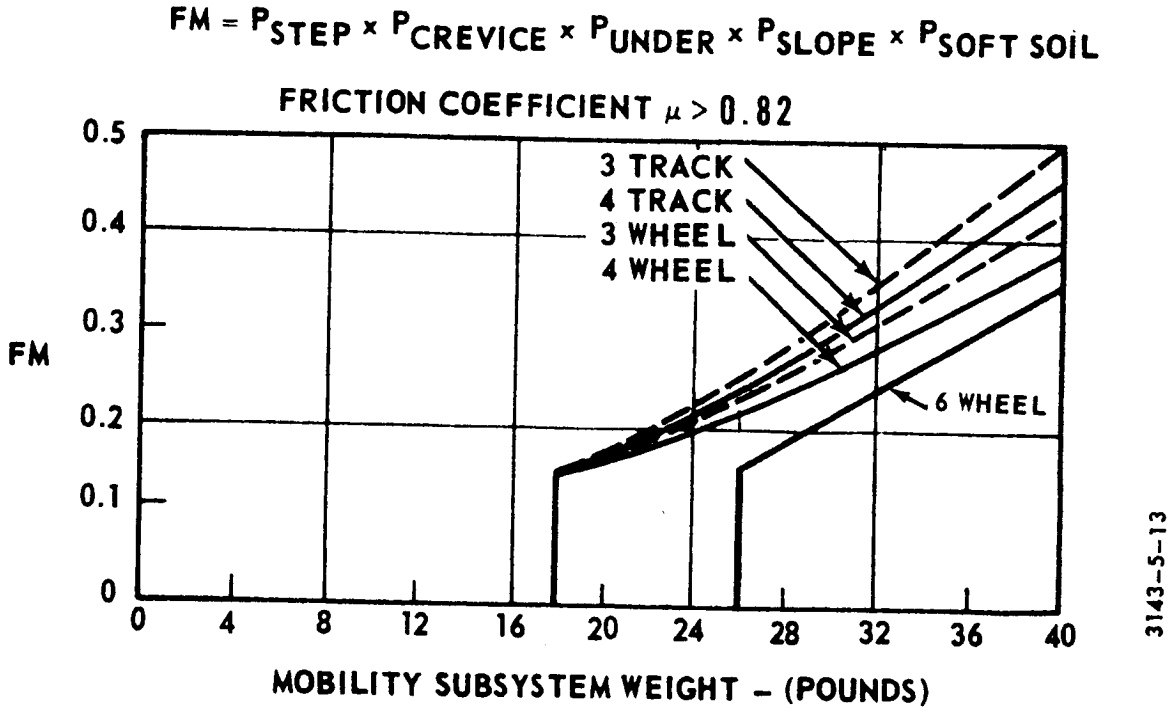

Figure 4-21 Figure of Merit Analysis

1. Topography of the lunar surface.
2. Bearing strength and soil properties.

These requirements are analyzed in Section 3. The system design to satisfy these requirements is based on the first-order effects flow diagram (Figure 4-2), which shows that the soil bearing strength instrumentation depends primarily on the performance requirement and has little effect on the rest of the system.

4.3.1 Bearing Strength Instrumentation

The bearing strength performance requirement can be considered to be of two degrees: (1) obtain quantitative measurements of the bearing strength which would satisfy both the LEM landing point verification and acquisition of scientific data, or (2) obtain qualitative data for a simple go/no-go decision on the landing point acceptability. Since the first-order outputs of this trade-off are to the system reliability and performance only, it may be treated as functionally independent of other elements of the system. Parametric studies showed that the weight and power requirements for a quantitative measuring device (penetrometer) were modest. The primary drawback of the penetrometer is it greater complexity and lower reliability as compared to a qualitative sampling device. However, the increased performance of the penetrometer more than offsets its lower reliability, thereby giving it the higher figure of merit.

4.3.2 Topography Instrumentation

Site verification and mapping analysis (Section 3) indicate that no specific instrumentation is required for topographic data, but requirements are placed on the navigation and control subsystem and the TV subsystem. These requirements are applied in the selection of an information system design (Section 4.4).

4.4 INFORMATION AND POWER

The first-order effects flow diagram (Figure 4-2) shows that the remaining first-order effect trade-offs of a functional nature are between:

1. TV total data content per frame and the information subsystem data rate.

2. TV frame rate and the information subsystem data rate.

3. Navigation accuracy and navigation subsystem weight.

4. Navigation technique and information subsystem data rate.

5. Information subsystem data rate and prime power.

6. Mobility performance and mobility subsystem weight.

7. Mobility performance and prime power.

8. Prime power and thermal control.

These functions have a high degree of interaction and depend on the selected mission model. Therefore, they will be treated as a combination after the mission model definition.

4.4.1 Mission Model

4.4.1.1 Video Requirements

To establish the TV requirements, an analysis was made of the data-gathering procedure within the landing point and the video implementation required for control of the vehicle (a function of mobility performance).

The maximum range at which crevices can be detected must be known to determine vehicle traverse step length and the number of pictures required for the photogrammetric survey at a point. The range at which a crevice can be detected depends on the following factors:

1. Lines per frame.
2. Field of view.
3. TV camera height.
4. Number of lines required for detection.
5. Crevice width.
6. Angle of crivice to line of sight.
7. Number of grey levels.
8. Illumination conditions.
9. Surface texture.
10. Operator experience.

This analysis treats only factors 1 through 6, with suitable adjustments made for factors 7, 8, 9, and 10.

The maximum width of a crevice which can be crossed is a function of the crevice crossing angle for a given design. This relationship is shown in Figure 4-22. The crevice width and corresponding crossing angle from Figure 4-22 were used to compute the crevice detection range in terms of crevice crossing angle as shown in Figure 4-23. This curve shows that the minimum detection range occurs for crevices at right angles to the TV camera line of sight. Therefore, the remaining discussion will be limited to detecting crevices at right angles to the line of sight.

The crevice detection range for crevices at right angles to the line of sight can be expressed as

$$D + 0.96 \sqrt{\frac{57.3\, hSN}{K_\theta} - h^2}$$

where:

D = detection range (meters)

K = number of TV lines required for detection

N = TV lines per frame

θ = TV field of view (degrees)

S = crevice width

h = TV camera height above surface.

The geometric relationship is shown in Figure 4-24.

Figure 4-25 presents the parametric relationship for detection range, camera height above the surface, and $\frac{NS}{\theta}$.

A similar analysis and parametric output was made for obstacle identification and size determination required for safe vehicle traverse and landing point certification. It was determined from this that crevice identification was the governing factor in establishing the maximum vehicle step length.

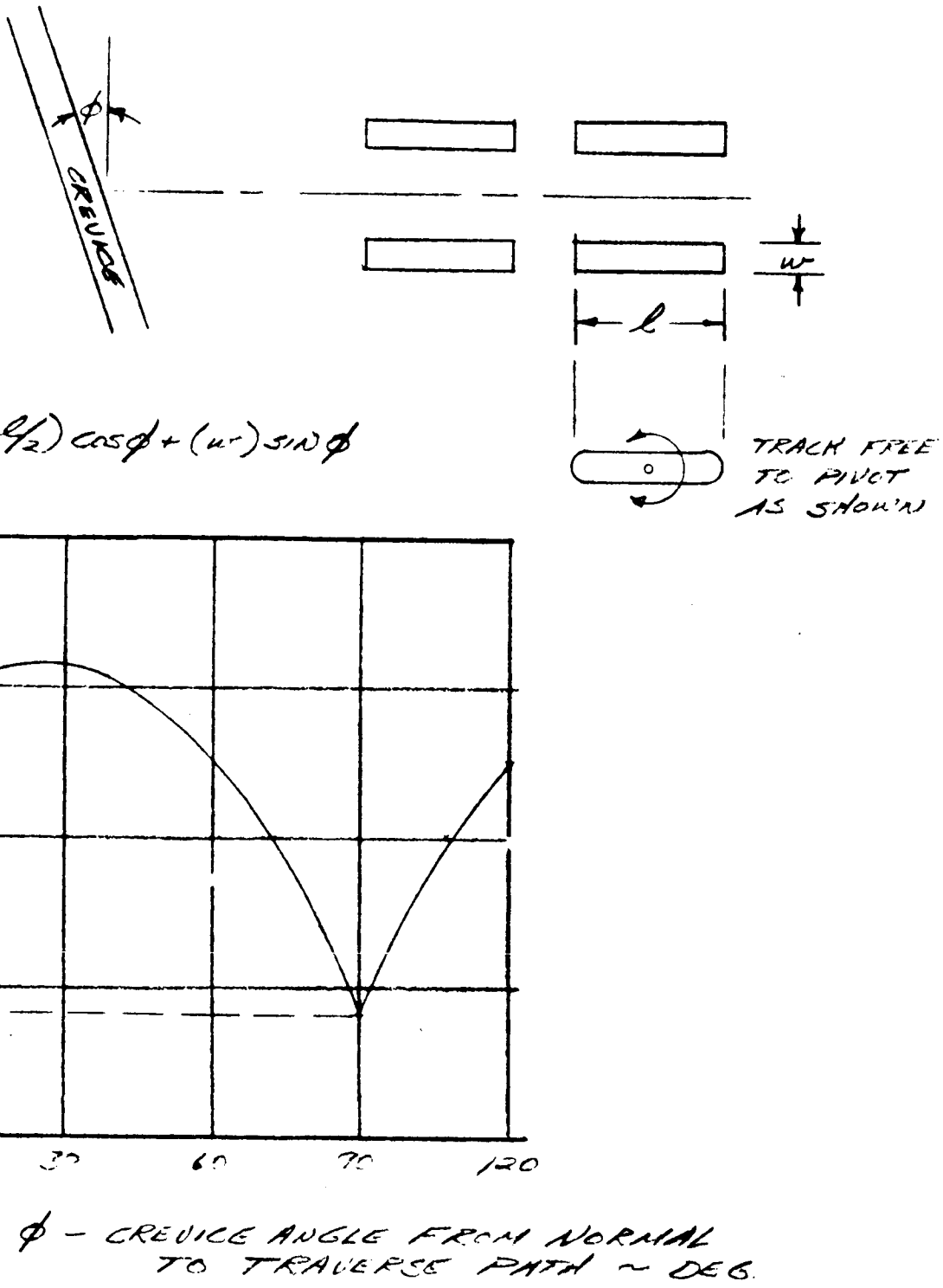

Figure 4-22 Crevice Crossing Capability vs Crevice Angle With Respect to Normal to Vehicle Heading

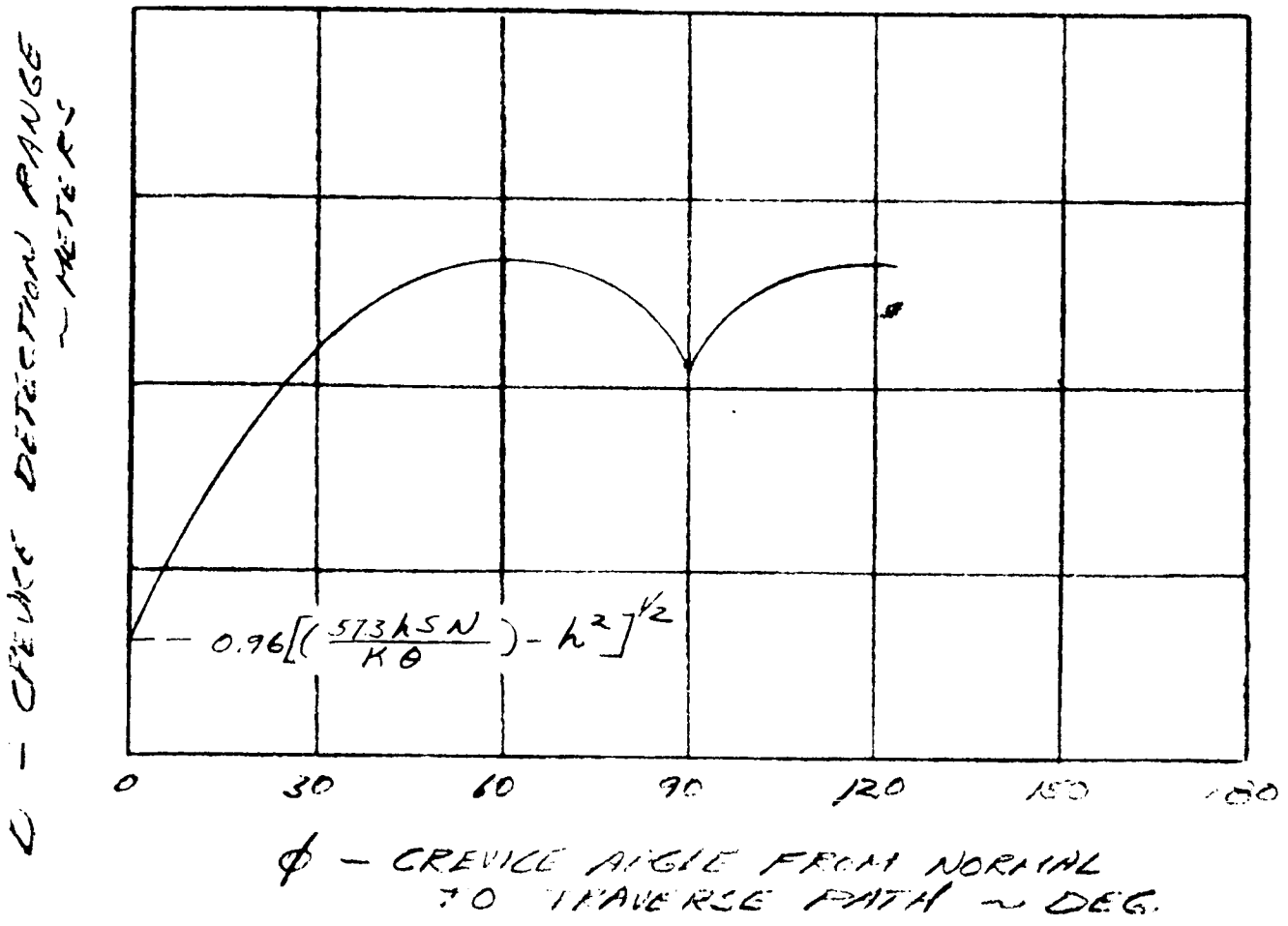

Figure 4-23 Crevice Detection Range vs Crevice Angle With Respect to Normal to Vehicle Heading

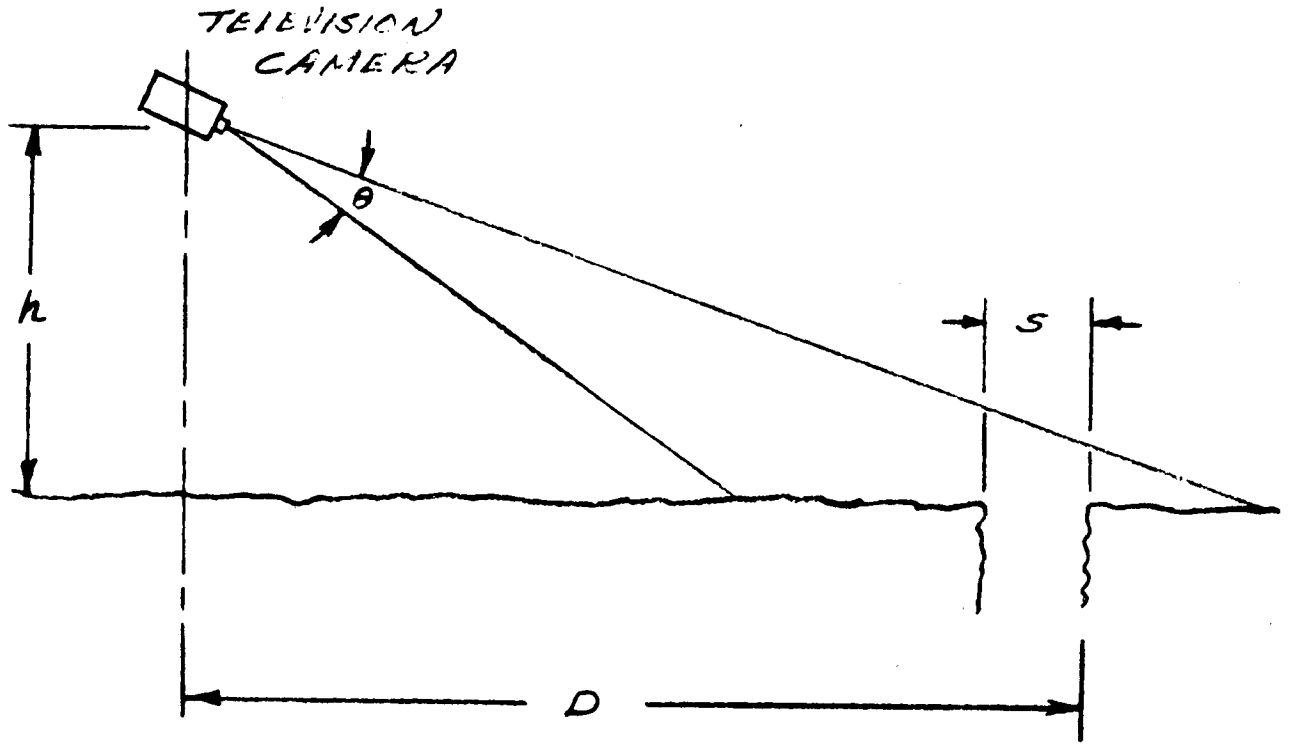

Figure 4-24 Crevice Detection Geometry

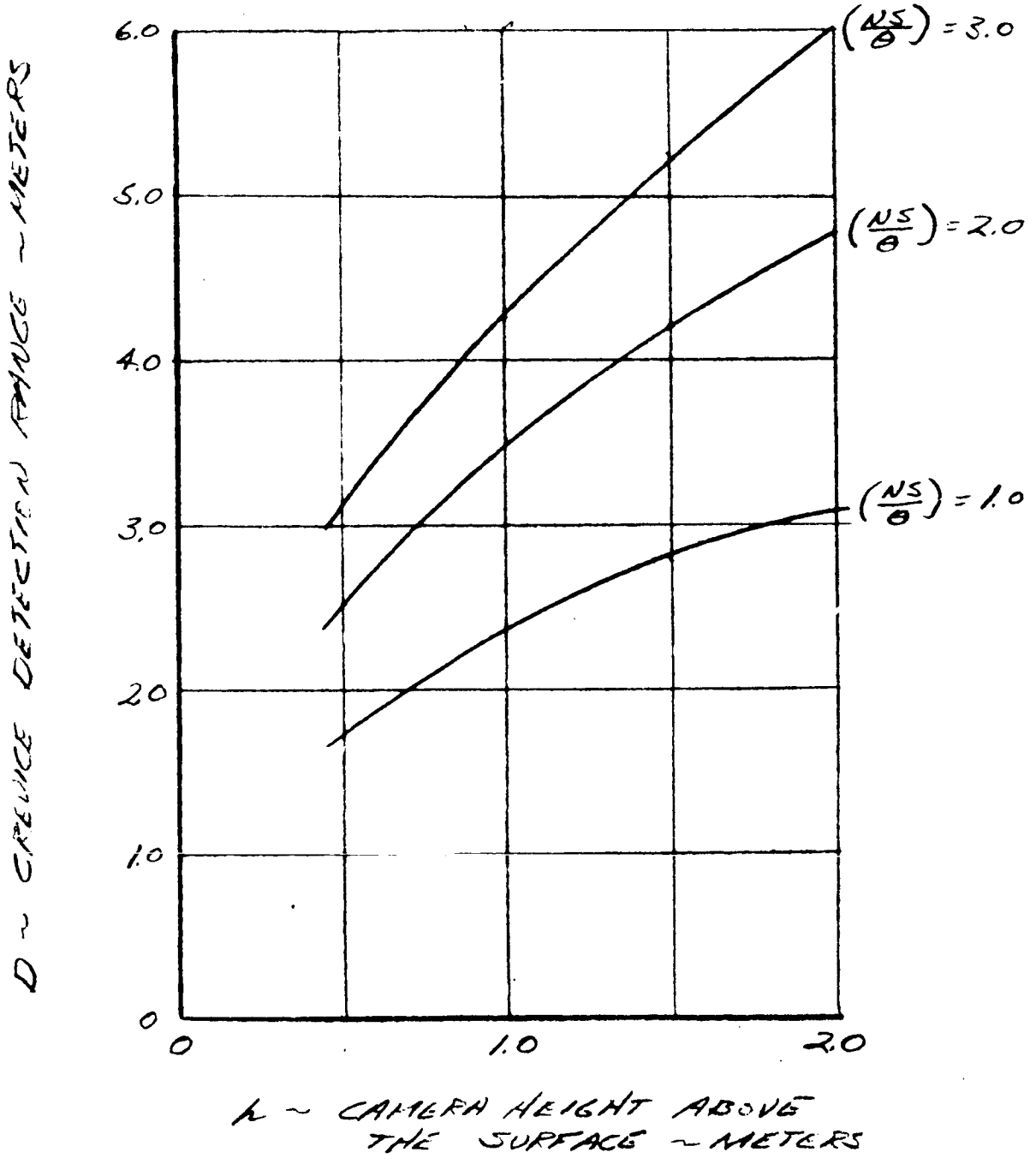

Figure 4-25 Parametric Relationship for Crevice Detection Range

Since the number of lines per degree and number of grey levels employed do not significantly affect the TV subsystem weight, no first order effect or trade-off exists here. However, as was shown by the analysis above, the TV height above the surface has a direct and significant relationship to the vehicle operating characteristics and is indirectly related to the mission duration and system reliability. Therefore, the volume constraint within the Surveyor Spacecraft has a direct effect on the system via the TV stowage-height-above-the-surface relationship. The same consideration is true with respect to the deployment subsystem weight. Study of packing concepts resulted in a TV camera height above the lunar surface of approximately 1 meter maximum.

4.4.1.2 Landing Point Diameter

The landing point diameter is a function of the location accuracy, (Section 2) and therefore directly dependent upon the navigation subsystem. The relationship is:

$$D + \left[2\,(\Delta\, d)^2 + (16.4)^2\right]^{1/2} + 10$$

where

D = landing point diameter (meters)

Δd = landing point location accuracy (meters)

Thus, the point location accuracy will have a large influence on the mission duration and the required value of system reliability.

4.4.1.3 Interpoint Traverse Pattern

An idealized pattern for surveying the 19 landing points is presented in Figure 4-26. This pattern is dependent upon a highly accurate navigation subsystem to keep the landing point diameters of reasonable size. Several extra interpoint traverses are included in the pattern to allow placement of marking devices during the early portion of the mission while the system reliability is still near maximum.

If a lower accuracy navigation subsystem is used, it may be necessary to return periodically to the Surveyor Spacecraft or landmarks to update the navigational data. Lunar surface features may degrade the

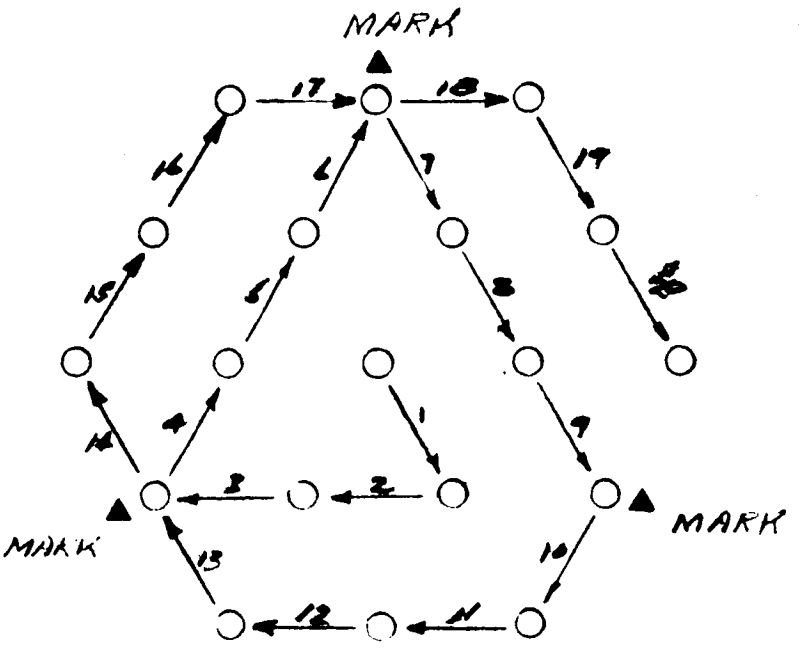

Figure 4-26 Landing Point Survey and Marking Pattern

idealized pattern to various degrees. These factors must be considered prior to calculating the SLRV range required to complete the mission.

4.4.1.4 Total Mission Time

There is approximately a one-to-one relationship between the total distance traveled during a mission and the operational mission time. (An increase in path length causes a corresponding increase in number of TV pictures, slewing times, etc.) Therefore, the total operational mission time can be expressed as:

$$T_M = n\,(1.4\,T_{pp} + 1.8\,T_l)$$

where

T_{pp} = time to survey one point based on straight-line distances

T_l = time for interpoint traverse based on straight-line paths

n = number of acceptable points.

The constants of 1.4 and 1.8 are derived in the same manner as the equivalent constants in the total distance formula presented in Section 3.

4.4.1.5 Bearing Strength Sampling

It has been assumed that penetrometer readings are made only within the landing points.

Forty percent of every abandoned landing point would be surveyed (Section 3). Hence, an average of 40% of the number of penetrometer readings made in an acceptable point will be made at every abandoned point. It was also assumed that there would be an equal number of abandoned and good points.

Therefore, the total number of penetrometer readings made during a mission is:

$$N_p + 1.4\,(n)\,(n_p)$$

where

n = number of good points surveyed

n_p = number of penetrometer readings in a good point

System analysis has established 45 as the minimum number of good penetrometer readings necessary to declare a point acceptable.

Therefore, the minimum number of readings expected for the mission is:

$$N_p + 1.4\,(19)\,(45) \cong 1200$$

This number may increase if additional readings are made between points.

4.4.1.6 Advanced Mission Model

A more advanced model was developed during the subsequent system evaluation. This model (Volume V) differs primarily in the refinement of distance and time calculations as a function of specific surface models. Some faster surveys are also made at points late in the mission based on confidence gained from data obtained at early points.

4.4.2 Design Selection

Based on the preliminary mission model, a combined selection was made of the various functional concepts available for the television, navigation, information, and prime power subsystems.

The landing point survey places some requirements on the navigation and control subsystem and the TV. The spacing between the parallel traverses through the point is a function of the TV resolution. Also, the azimuth dispersion of these traverses must be limited to ensure complete coverage of the landing point. This relationship is shown in Figure 4-27 which plots the number of TV lines vs traverse spacing; azimuth sensing will become proportionally more stringent with increasing landing point diameter. The time required to survey a point will increase at a rate inversely proportional to the traverse spacing and directly proportional to the square of the landing point diameter.

In the study of azimuth sensing concepts, both analog and digital solar aspect sensors were considered. The digital sensor has an accuracy

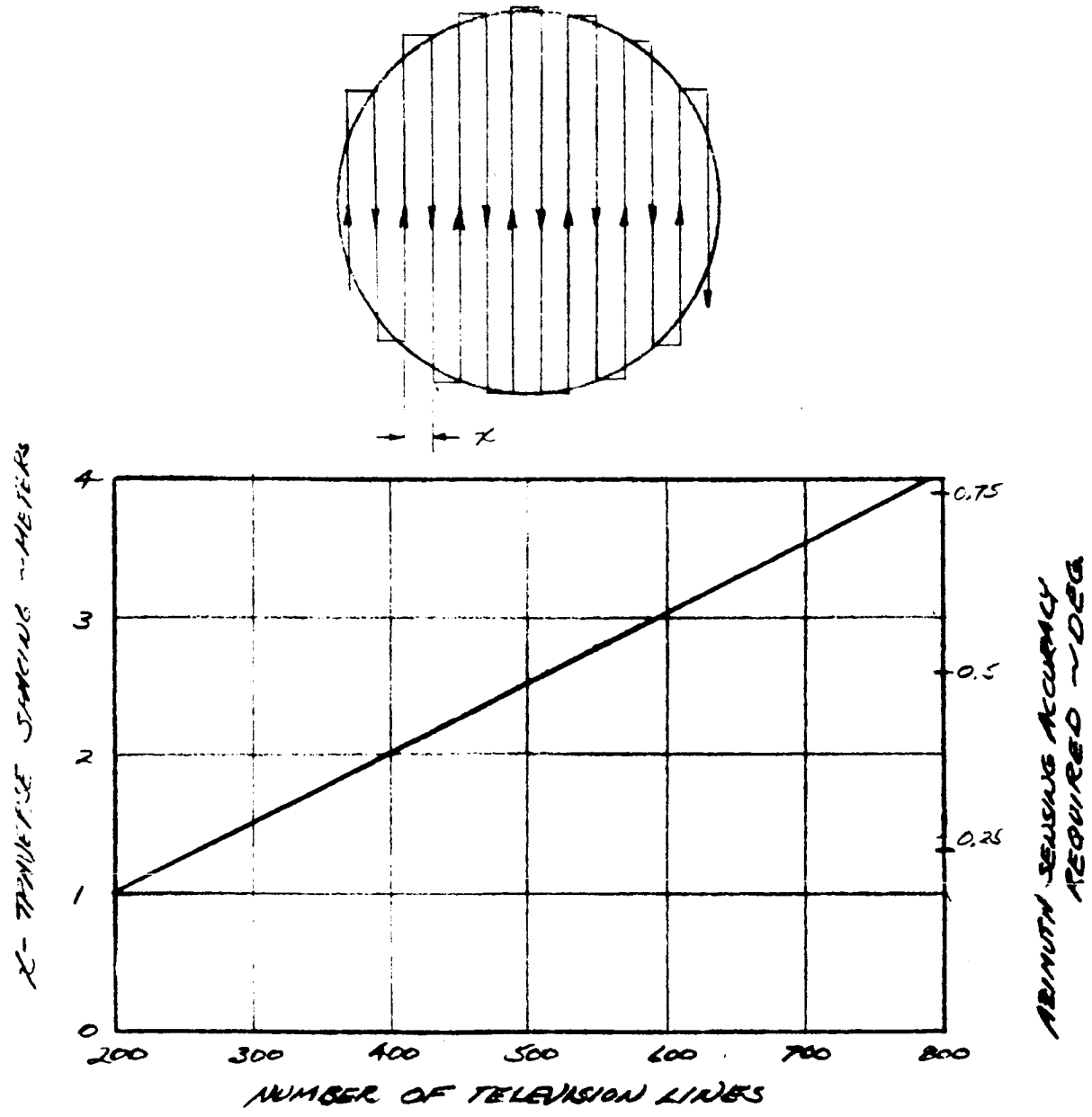

Figure 4-27 Number of Television Lines vs Traverse Spacing and Azimuth Sensing Accuracy Required

of approximately 0.5° while the analog accuracy is in excess of 1.0°. It is not feasible to obtain the number of TV elements required to be compatible with a 1° accuracy. Thus, the digital sensor was chosen for this application. Approximately 500 TV elements are required. The 20% safety factor accounts for losses in accuracy associated with transformation of solar azimuth to vehicle azimuth using the inclinometer reading of vehicle tilt.

Of the navigation techniques considered, two were attainable within reasonable weight and power bounds: (1) dead reckoning using the solar aspect sensor, an odometer, and an inclinometer, (2) dead reckoning supplemented by RF ranging to the Surveyor when in line of sight. The accuracy of the basic dead reckoning technique is approximately 5%. If this system were employed, the points could not be located to the required accuracy by direct traverse. It would then be necessary to make extra traverses back to Surveyor or known lunar landmarks. As the locations of the point are further removed from the Surveyor or known landmark, the error in its location would increase. Since the size of the point must increase to compensate for the location error and satisfy the LEM landing position requirements, some points may be as large as 80 meters. Consequently, the total mission travel distance would be more than 100 kilometers with an attendant increase in mission duration.

If the dead reckoning navigation system is supplemented by RF ranging (when RF line of sight is available) the range from the point to the Surveyor is determined with an accuracy of at least ± 20 meters without having to return to the Surveyor. Thus, traverse can be directly from point to point. This navigation technique, combined with a TV capability of approximately 500 lines per frame, gives a total range of about 40 kilometers. The selection of navigation techniques includes a digital sun sensor, inclinometer, odometer, and RF ranging.

These considerations also lead to the conclusion that the 512- x 512-element TV system with 50° FOV and 8 lines for identification provides the best vehicle step length. With a 50° FOV camera tilted 30° below the horizontal, 30-cm obstacles are resolved at 10 meters; in the same picture, 22-cm crevices are detected out to 0.74 meter. The blind spot in front of the vehicle is 0.7 meter. (If the TV is depressed to its limit in elevation, the blind spot is reduced to 0.36 meter).

Consequently, navigation can be 3-meter steps with one TV picture at each stop, using 50° FOV, and 512 lines for a crevice-crossing capability of 22 cm. Occasionally, long-range pictures at 10° FOV are desired for detecting large obstacles and crevices that may necessitate a path change or the abandoning of a point. The choice of 3-meter step lengths is compatible with the spacing, (Section 2) required for 100% coverage of the point with 50° images in stereo pairs.

The data content per TV frame is $(512)^2 \times (4)$, or 1,048,576 bits based on 16 gray levels. The vidicon can hold the image more than seconds without restrictive degradation. However, a minimum time compatible with the weight and power constraints is desired. The telemetry data rate is largely determined by the digital solar aspect sensors. Four of these units are required for the coverage desired and a 960 bit/second telemetry rate is required for proper operation.

Three modes of communication are possible: (1) direct, where the SLRV transmits directly to earth, (2) cooperative, when data are transmitted to the Surveyor Spacecraft for relay to earth, and (3) dual, where the cooperative technique is used when the Surveyor Spacecraft is in line of sight of the SLRV, and direct transmission is used when the Spacecraft is not in line of sight.

The cooperative mode, although offering a high data rate capability cannot be employed because the line-of-sight availability shows that the presence of a moderate amount of large size obstacles or slopes would prohibit the SLRV from examining and certifying landing points in the nominal pattern.

The dual mode takes advantage of the Surveyor spacecraft directional antenna to obtain a high data rate when in line of sight, but can also operate in non-line-of-sight areas by use of a direct link to earth. This direct link would require a fixed antenna on the SLRV (weight limitations would preclude a steerable antenna plus all other dual mode equipment).

Information from Hughes Aircraft Company on the Surveyor lunar-day capability indicates that, for an equatorial landing, the Surveyor cannot be used for a period of 5.42 earth days out of each lunar day. (Reference: HAC Document 2256/70, 24 October 1963, "Reference Figures for Descriptive Presentation of Surveyor Spacecraft Design and Performance in Support of a Roving Vehicle Payload".)

For an additional period of five days (2.5 days each side of zenith), the Surveyor may be used for TV transmission at an average duty cycle of 50%. For the remaining 3.58 days, the Surveyor may be used continuously. These operational imitations are summarized as follows:

Event	Duration (earth days)
Start of Lunar Day	----------
Operate Continuously	1.79
Operate at 50% Duty (Average)	2.50
Non-operative	5.42
Operate Continuously	1.79
End of Lunar Day	----------
Total	14

Based on these considerations, the Surveyor may be used for cooperative SLRV communications for 43.5% of the lunar day, or a total period of 6.08 earth days. If the 210-ft and 85-ft DSIF facilitiees are used on a 24-hour basis, the indirect mode may be used for 146 operational hours each lunar day.

In arriving at the portion of the total landing site accessible to the SLRV for line-of-sight communications with the Surveyor Spacecraft, an analysis was made assuming four lunar surface models whose characteristics ranged from smooth level surfaces to surfaces having a high incidence of 10-meter high rock piles and slopes greater than 10^{o}. Since little is known about the lunar surface, it is difficult to assign weighting factors favoring one surface model over another in arriving at an estimate of inaccessible line-of-sight communications areas. Consequently, for this study the four models were weighted equally. A SLRV antenna height of 4-ft was assumed. The average of the four surface models indicates that 43% of the area of interest is accessible to the SLRV for line-of-sight communications with the Surveyor.

In the absence of precise lunar surface data, 50% of the lunar surface is assumed to be soft soil and the remaining 50% is hard surface. The soft soil is defined such that all of it is negotiable by the SLRV. Only 22% of the hard surface is not negotiable by the LRV (with 30-cm obstacles climbing capability). Therefore, 89% of the lunar terrain in the landing site is negotiable by the LRV). Combining this information with the previous information about line-of-sight communications leads to the following lunar surface conditions:

1. 38% of the total landing site is both line-of-sight (LOS) and negotiable.

2. 51% of the landing site is negotiable, but not LOS.

3. 4.7% of the landing site is LOS, but not negotiable.

4. 6.3% of the landing site is neither LOS nor neogitable.

The portions of landing site covered in conditions (3) and (4) are useless for the SLRV mission. Conditions (1) and (2) provide an input in determining the division of the mission time between direct and indirect modes of communications. The likelihood of the SLRV being in either of the areas described by conditions (1) and (2) is in proportion to the percentage of the negotiable area found in each of these categories. Therefore, the SLRV will be 42.5% of the time in the area of condition (1) and 57.5% of the time in the area of condition (2). Combining this information with that on the use of the Surveyor provides the division of time between the direct and indirect communications modes. The Surveyor data determined that indirect communications could be maintained for 43.5% of the lunar day. This, combined with 42.5% of the time being spent in the LOS area, results in obtaining indirect communications for 18.% of the operating time and direct communications for the remaining 81.5% of the operating time.

Employing the above use factors in the mission model gives a total mission duration of approximately seven months when using the cooperative communications 24 hours/day (210' -85' -85' ground receiving antennas) and the direct link in conjunction with 210' Goldstone antenna only with a radiated power of approximately 2.75 watts.

Another arrangement, which would simplify the SLRV somewhat by a reduction in the number of data rates, would utilize the Goldstone 210-ft antenna only. In this case, the mission duration would be approximately 12 months.

If the Surveyor Spacecraft were capable of continuous communications, the mission times would be reduced. Table 4-3 summarizes these cases.

TABLE 4-3

DUAL MODE COMMUNICATIONS SUMMARY

Surveyor Utilization (%)	Cooperative Mode Ground Antennas (ft)	Mission Duration (Months)	Reliability Estimate
43.5	210'-85'-85'	7	0.85
43.5	210'	12	0.80
100	210'-85'-85'	4.5	0.86
100	210'	8	0.80

These results must be compared with the direct mode. A steerable antenna having a gain of 17 db can be packaged on the SLRV. This will yield a data rate less than that of the cooperative mode, but considerably higher than that achieved in the direct link of the dual mode using a fixed antenna. For a 512 x 512 line, 16 grey level TV frame, the transmission time is 8.5 seconds with two watts of radiated power. The mission duration for this capability will be 3.9 months and will have a reliability of approximately 0.90.

Examination of the weights associated with the dual and direct communications modes indicates that they are roughly equivalent, considering an inpug of 8.8 watts in the direct mode and 11.5 watts in the dual mode.

Two other factors deserve consideration before reaching a conclusion on the information subsystem functional arrangement: (1) the cooperative mode is extremely sensitive to line of sight; i. e., a smooth surface would yield a greatly reduced mission, and a highly irregular surface would extend the mission time considerably from the stated value, and (2) use of the Goldstone ground facility only will simplify the SLRV control and decision functions.

The direct mode, having a greater reliability, shorter mission duration (with higher confidence in the calculated value since the information function is independent of the lunar surface), and using only the Goldstone Ground Station is a functional choice.

The coverage required on an SLRV-mounted steerable antenna communications link is a function of link geometry and the lunar topography.

The nominal earth elevation angle with respect to the lunar local horizontal plane is a function of SLRV latitude and longitude. Irrespective of landing position, the earth's surface subtends a total angle of 1.9 at the lunar surface, neglecting atmospheric refraction effects. However, the Surveyor Spacecraft landing point may vary from 0° to 75° in longitude. Thus, the axis of the SLRV normal to a smooth flat lunar surface may be inclined as much as 75° with respect to the line of sight to the moon, and the antenna coverage must be increased to 150° to allow for this. For the present study, the Surveyor landing position is considered to be in the nominal location of $43 \pm 10^{\circ}$ W longitude.

The SLRV must be capable of traversing slopes and obstacles up to its stability angle of 35°. To account for this, the antenna coverage must be increased another 70°.

Allowances must also be made for the periodic variation in the earth elevation angle (approximately $\pm 7^{\circ}$) caused by lunar libration. Hence, this factor also contributes to the problem of providing antenna coverage.

These factors are summarized in Table 4-4.

TABLE 4-4

ANTENNA COVERAGE REQUIRED FOR DIRECT SLRV-TO-EARTH LINK

Source of Antenna Coverage Requirement	Total Angle (degrees)
Angle subtended by earth at lunar surface	1.9
Location of Surveyor landing point	106.0
Terrain slope and obstacles	70.0
Lunar libration (negligible over short-term)	14.0
Total Antenna Coverage Required	190.0

Thus, the steerable antenna must be capable of an elevation variation of $\pm 95^{\circ}$ less one-half the beam width with respect to the local vertical axis, and an azimuth variation of 360°.

Referring to the first-order effects flow diagram, (Figure 4-2) it is seen that mobility, information, and thermal control are the subsytems having a direct bearing on the prime power subsystem functional decision.

Since lunar night survival is required, a power source is required for thermal control during this period. A battery - solar cell combination is prohibitively heavy because of the long discharge period. If an RTG is used, no battery is required for lunar night since the RTG produces thermal and electrical energy continouously. A battery could be used to implement a high power communications system since most of the electrical energy delivered will be used only 10 hours/day. This technique would incur a weight penalty because of the charge regulators and heater to sustain the battery through lunar night. In addition, introduction of a battery into the system causes a reduction in reliability. Therefore, the RTG alone is the most desirable prime power choice since it has minimum weight and highest reliability.

With regard to the mobility subsystem, several trade-offs exist. A functional decision to use a 4-track configuration was made in Section 4.2. Two other first-order decisions were yet to be made:

1. Obstacle traversing capability of the mobility subsystem.

2. Speed of the SLRV.

The first decision is a function primarily of the subsystem weight. It was found that only by compromising severly in the navigation or information subsystem could more than approximately 18 lb be made available for the mobility subsystem. Either of these two trade-offs would result in long missinn duration. The 4-track, 18-lb mobility subsystem will be capable of traversing obstacles 30-cm high and crevices 22.5-cm wide.

The second trade-off is primarily power. Since telemetry data are required continuously, transmitter and mobility power occur simulataneously. The optimum division of power (for minimum mission duration) between data rate and vehicle speed is determined thus:

1. Parametric data were determined relating vehicle speed vs power and data rate vs power

2. The relationships of speed and data rate to the mission duration was expressed as

$$T = \frac{R}{V} + \frac{N}{b} + c$$

where:

T = mission duration
R = total range of the SLRV to mission completion
V = vehicle speed
N = total number of video bit transmitted during the mission
b = video data rate
c = a constant (decision time, etc.).

From the mission model and subsequent decision, R, N, and c were determined. The total power available for mobility and the transmitter within the weight constraint was also known. Therefore, the mission duration can be expressed as the sum of two functions of the power (from the parametric data) and a constant. Solution of the expression for minimum time was approximately at the minimum acceptable transmitter power required for telemetry (2.0 watts radiated), and indicated the mobility subsystem was to operate at 6.0 watts for maximum SLRV mission efficiency.

4.5 OPERATION AND INTEGRATION

4.5.1 Functional Description

A functional block diagram is shown in Figure 4-28, and the configuration is shown in Figure 4-29.

The design interfaces functionally with the Surveyor Spacecraft in two areas. During the flight, telemetry will be transmitted by the Surveyor Spacecraft via an umbilical since the SLRV fixed antenna will be at least partially screened by the Surveyor. Secondly, a transponder will be located aboard the Surveyor to implement the RF ranging navigational technique. The transponder will necessarily be dependent upon the Surveyor power supply.

The ground complex will consist of the Goldstone facility plus control and ground data handling equipment. Utilization duty cycle of the Goldstone facility will be 10 hr/day on 11 of every 28 days.

A common fixed antenna will be used for reception of commands and telemetry transmission. If the steerable antenna fails, the fixed antenna could be used to transmit video data in a degraded mode. Deployment will be controlled by command to the Surveyor Spacecraft.

The steerable antenna will be directed by ground command while the SLRV is not traversing. All transmission of video data will be by the steerable antenna while the vehicle is stationary.

Slewing of the TV camera and change of FOV will also be by ground command. The TV is to employ three fields of view (10°, 22°, and 50°) which are also selected by ground command.

Steering control of the vehicle is to be achieved by floating pivot in the center of the SLRV and differential and directional control of the track drive motors.

Elevation profiles within the landing points will be determined by data from the three axes inclinometer and the TV. The inclimometer accuracy is 2° to 3° while traversing and better than 0.5° when the SLRV is stationary.

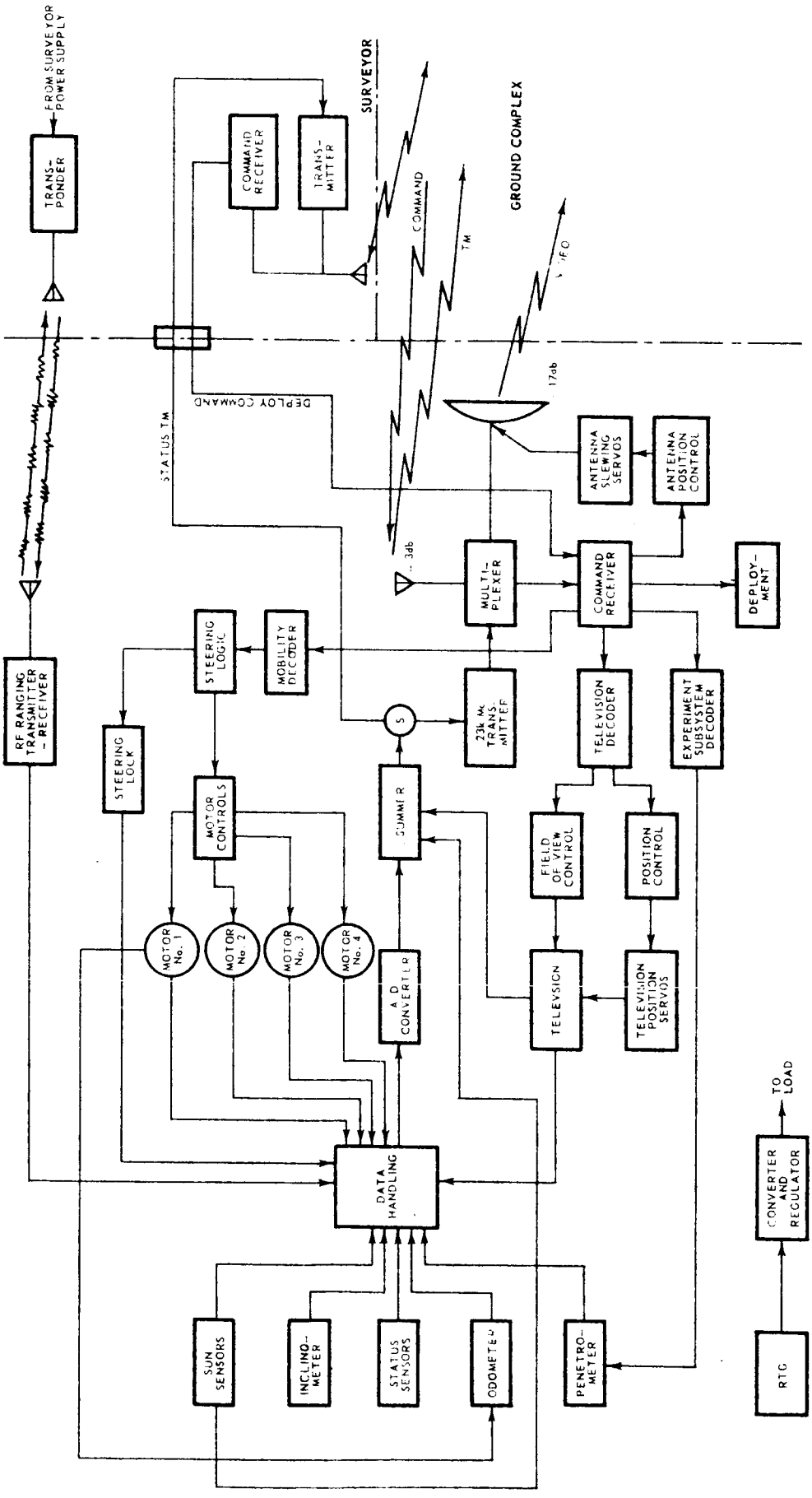

Figure 4-28 Preliminary SLRV Functional Block Diagram

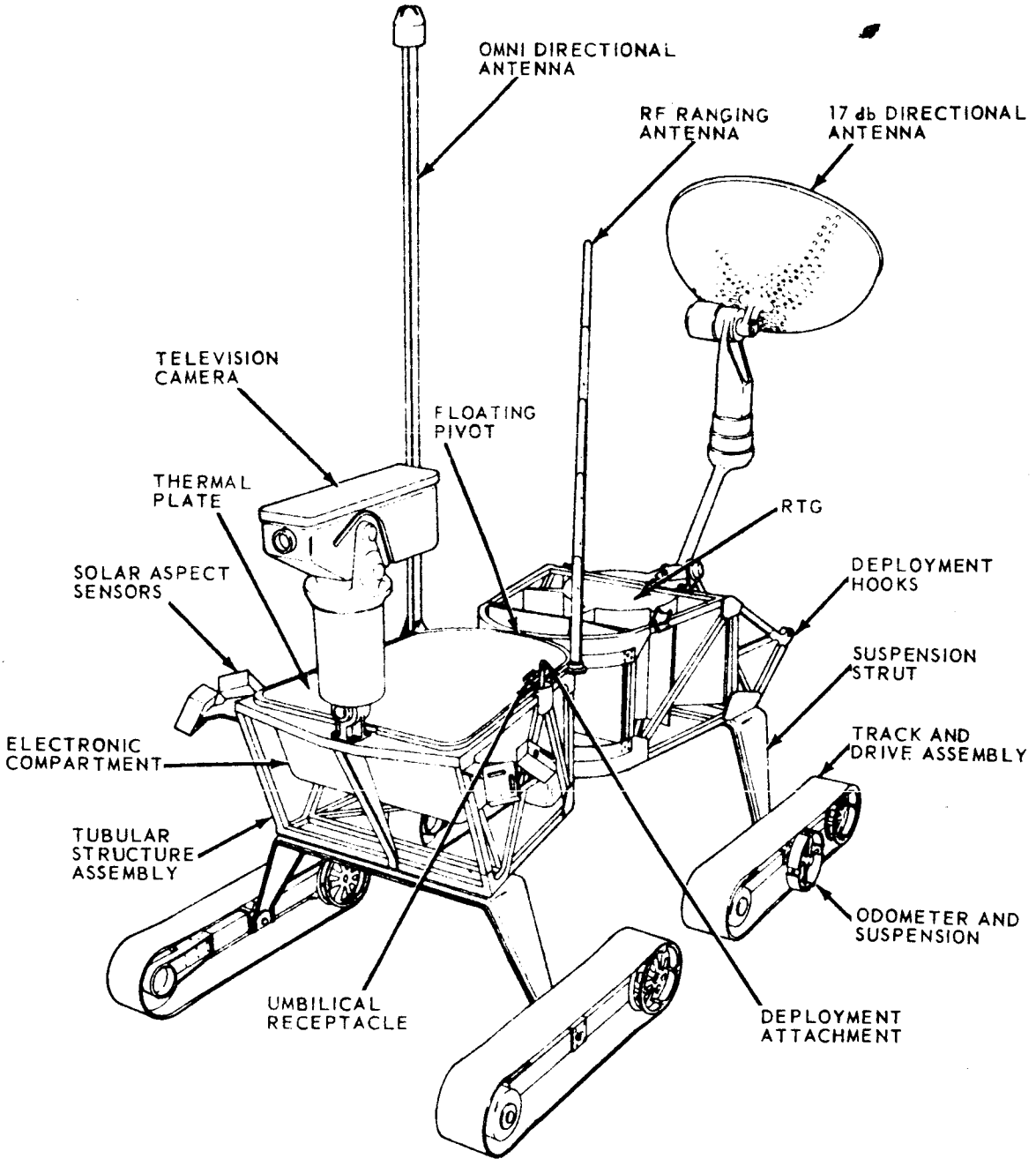

Figure 4-29 SLRV Configuration Concept

Navigation will be achieved by a combination of RF ranging to Surveyor and dead reckoning. RF ranging will be used when line of sight to the spacecraft exists, and dead reckoning will be employed in other areas. The RF ranging will also be used to calibrate the dead reckoning technique which is dependent upon an odometer. The odometer will be mounted on the track. Additional odometer data are available from the controlled speed of the drive units. Four digital solar aspect sensors will provide vehicle heading inputs with an accuracy of 0.5°. Thermal control will be passive during lunar day and both passive and semiactive during lunar night.

The mission duration is short enough to permit use of a short (145 days) half-life RTG.

4.5.2 System Weight and Power

The SLRV and Surveyor Spacecraft mounted equipment weight, power, and characteristics are presented in Table 4-5.

These values are based on parametric data, and small deviations are expected as detailed engineering progresses. More definite weight and power values for the various subsystems and elements of the system are contained in Book III of this report.

4.5.3 Operational Description

As previously noted, the SLRV mission is comprised of two basic functional parts: (1) survey and certify acceptable landing points for the LEM, and (2) traverse between landing point. The operational characteristics of the selected preliminary design in performing each of these functions are described below.

4.5.3.1 LEM Landing Point Survey

The point survey pattern for a 40-meter diameter point is shown in Figure 4-30. This pattern is based on utilization of the equilateral triangular arrangement of stereo pairs of TV pictures for survey. The spacing is based on the use of a 512-line TV system at 50° FOV. Such a system can detect 50-cm crevices at 5.7 meters, within the stereo coverage afforded by the 3-meter baseline. Also, for the safety of the SLRV, the TV system can detect (8 lines for detection) 22-cm crevices at 3.75 meters, or 0.75 meter beyond the step length.

TABLE 4-5

SYSTEM WEIGHT AND POWER SUMMARY

Subsystem	Description	Requirements	Weight (lb)	*Peak Power (watts)
Mobility	Four track	30 cm obstacle climbing capability 22 cm crevice crossing capability 15° slope climbing capability	17.7	6.0
Communications	Direct mode only			
Command RCVR & Antenna			2.5	1.0
Transmitter	S-Band TWT		4.0	8.8
Transmitting Antenna	Directional	17 db gain, ±95° Elevation slewing, 360° Azimuth slewing	8.0	3.0
Navigation	Sun sensor Inclinometer Odometer & RF ranging	Azimuth bearing to ±0.5° Slope to ±0.5° Range to ±20 meters	8.0	7.5
Structure			9.5	
Deployment			6.8	
Power Supply	RTG with > 3 month useful life			30.0 gross output 24.0 net output
RTG	30.0 watts gross output		16.7	
Converter, Regulator, Misc.	24.0 watts net output		3.7	
Data Handling	Command decoders & TM processing		3.8	4.3
Television	Monocular Galilean Telescope	10°, 22°, 50° Field-of-view f-7 to f-22 512 x 512 lines, 2 to 4 bits encoding ±200° Azimuth slewing +15° to -45° Elevation slewing 6° per second slewing rate	8.3	7.8
Thermal Control			4.9	
Penetrometer		1200 readings, minimum 0.5 inch per second retraction rate	2.6	6.0
Cabling & Umbilical			3.5	
			TOTAL 100.0	*System Peak Power Requirement = 24.0 watts

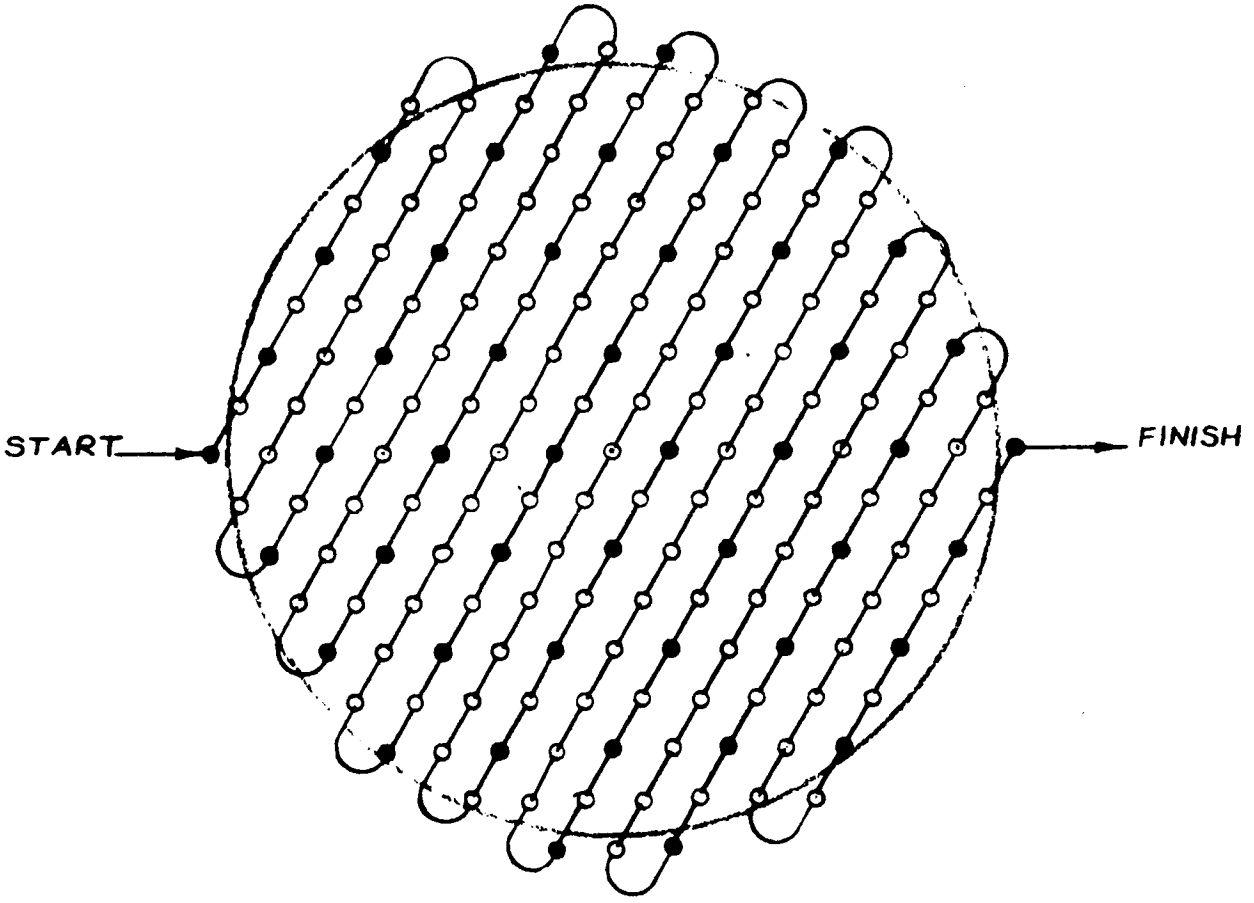

Figure 4-30 Point Survey Pattern

To maintain the equilateral triangle arrangement for the stereo pictures, the spacing between traverse paths within the point is 2.6 meters. With spacing this close, a single pass through the pattern is sufficient to obtain elevation profile data, and no orthogonal retrace is required. A turning radius of 1.3 meters is required at the end of each path.

For uniform coverage, there are 49 penetrometer readings spaced approximately 6 meters apart. Thus, penetrometer readings will be taken only on alternate paths and at alternate stops on these paths.

The total length of travel within the point(not allowing for the avoidance of obstacles, crevices, and navigation errors) is 558 meters. The necessary increase in this distance to allow for obstacles, etc., is discussed in the previous section where the necessary correction factors are derived.

At each internal stop, five TV pictures will be taken, at 50^{o} FOV. Four of these are used for survey, and one is used for navigation in the direction of travel. Along the outer edges of the point, fewer pictures are required. An additional 10^{o} FOV picture is taken looking down the path to be traversed at the completion of each end turn to observe any potential hazards which may require a path change, or possibly abandoning the point. The number of TV pictures are summarized as follows:

Survey at 50^{o} FOV	628
Naviation at 50^{o} FOV	187
Naviation at 10^{o} FOC	15

Continuous elevation data will be derived from the inclinometer and odometer readings. These data, together with TV data, will be used to construct the topographical map of the landing point. Obstacles and crevices or depressions which present a hazard to a LEM landing will be identified by TV. Slopes over any 10-meter length in the point will be obtained from interpolation from the constructed elevation profiles. The effective slope will then be known since it is the sum of all the terrain elements.

Figure 4-31 is a typical power profile for operations within a landing point. Referring to Figure 4-30, it is seen that the power profile will be irregular because of the irregular sequential spacing of penetrometer readings. Other deviations will be caused by the vehicle turnaround maneuver where additional TV pictures may be needed, and the lunar surface variations. However, with an RTG prime power source, the power profile is significant primarily to the thermal control subsystem.

4.5.3.2 Interpoint Traverse

Interpoint traverse will be accomplished by movement in 3-meter increments. This is required so that crevices which cannot be safely crossed (22 cm) will be identified before they are reached. In some types of terrain where there is a high confidence that no crevices exist, the mobility increments may be increased to greater than 5 meters. However, for purposes of determination of the mission duration, it will be assumed that the SLRV will always be confied to 3-meter mobility increments.

Navigation from one landing point to the next will be achieved by RF ranging and solar aspect sensing when line of sight to Surveyor Spacecraft exists. In non-line-of-sight areas, navigation will be by dead reckoning using the solar aspect sensors, odometer, and inclinometer.

A typical power profile for the interpoint traverse operations is presented in Figure 4-32.

4.5.4 Mission Duration

The operation periods of the SLRV are constrained by the Goldstone ground complex availability and the time of lunar day.

Lunar night operation is not feasible with a vidicon, and the weight required for an orthicon capable of surviving the launch and landing environment makes it prohibitive. Therefore, the mission time calculation takes into account operation only when illumination conditions are favorable.

RE-ORDER No. 64-54

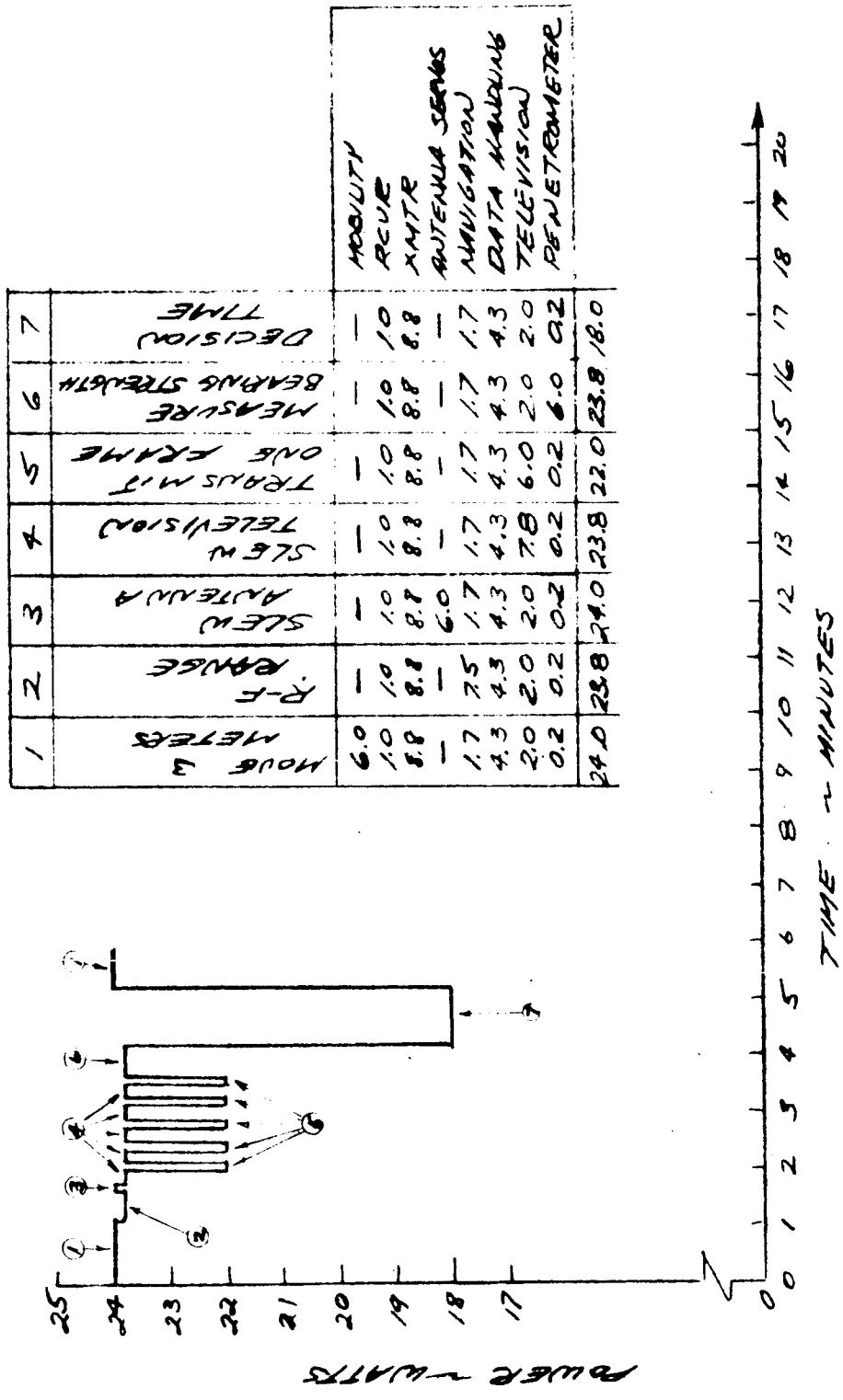

Figure 4-31 Typical Intrapoint Power

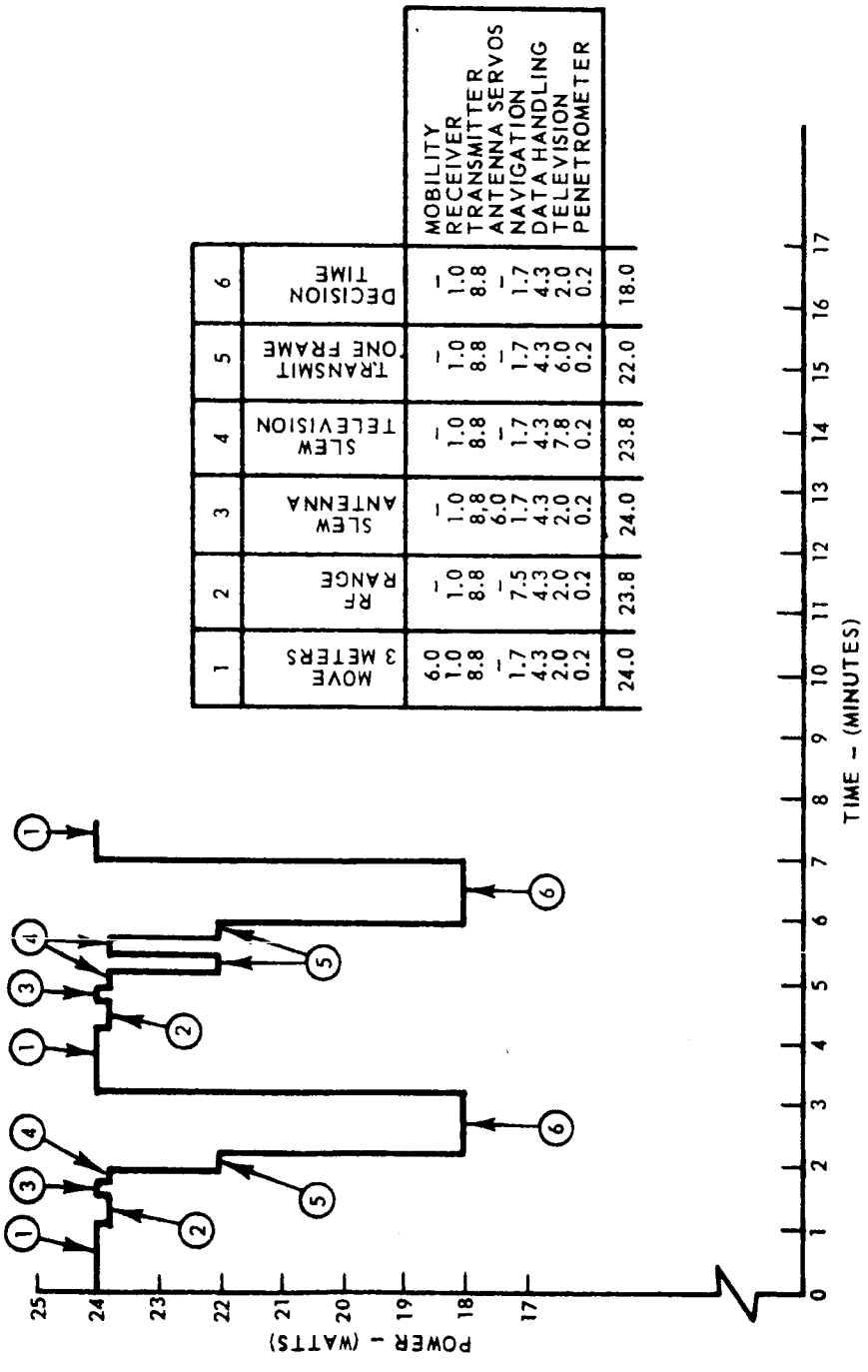

1	2	3	4	5	6	
MOVE 3 METERS	RF RANGE	SLEW ANTENNA	SLEW TELEVISION	TRANSMIT ONE FRAME	DECISION TIME	
6.0	–	–	–	–	–	MOBILITY
1.0	1.0	1.0	1.0	1.0	1.0	RECEIVER
8.8	8.8	8.8	8.8	8.8	8.8	TRANSMITTER
–	–	6.0	–	–	–	ANTENNA SERVOS
1.7	7.5	1.7	1.7	1.7	1.7	NAVIGATION
4.3	4.3	4.3	4.3	4.3	4.3	DATA HANDLING
2.0	2.0	2.0	7.8	6.0	2.0	TELEVISION
0.2	0.2	0.2	0.2	0.2	0.2	PENETROMETER
24.0	23.8	24.0	23.8	22.0	18.0	

Figure 4-32 Typical Interpoint Power Profile

II

Figure 4-33 is a time schematic of SLRV operational days. The first earth day after lunar sunrise and the last before lunar sunset are considered non-operational because of the thermal environment and illumination conditions. A 24-hour period centered about noon of the lunar day will be a non-operational period since the sun will be nearly directly over the SLRV and the solar aspect sensor will not function. With this exclusion, the sun will always be more than 6° from the zenith during operations.

In addition, it is considered that the ground complex will be usable for 10 hours per operational day.

Using these operational periods, an SLRV average speed of 3.22 meters/minute, a TV frame rate of 8.5 second/frame, an average of one minute for decisions following each vehicle stop, and the appropriate factor derived in Section 4.4.1 to account for surface conditions, a mission duration of approximately 3.9 months is required.

Surface characteristics and partial failures will influence calculations of mission duration. The system evaluation (Volume V) accounts for various types of surfaces and partial failure in determining the overall and partial probabilities of success. These results show that the average mission is slightly shorter than the duration estimated above.

4.6 CONCLUSION

The selected 100-lb preliminary design cannot perform the marking function; the mission success will be a function of existence of natural landmarks.

If the Surveyor Spacecraft were made available for cooperative mode communication on 100% duty cycle, the dual mode communications would permit completion of the mission in approximately 4.5 months. Preliminary reliability numbers showed this to be inferior to the selected preliminary system design.

Marking, more redundancy in critical elements, stereo TV, and other enhancements of the system are considered in the trade-off analysis of systems up to 150 lb (see Sections 5 and 6).

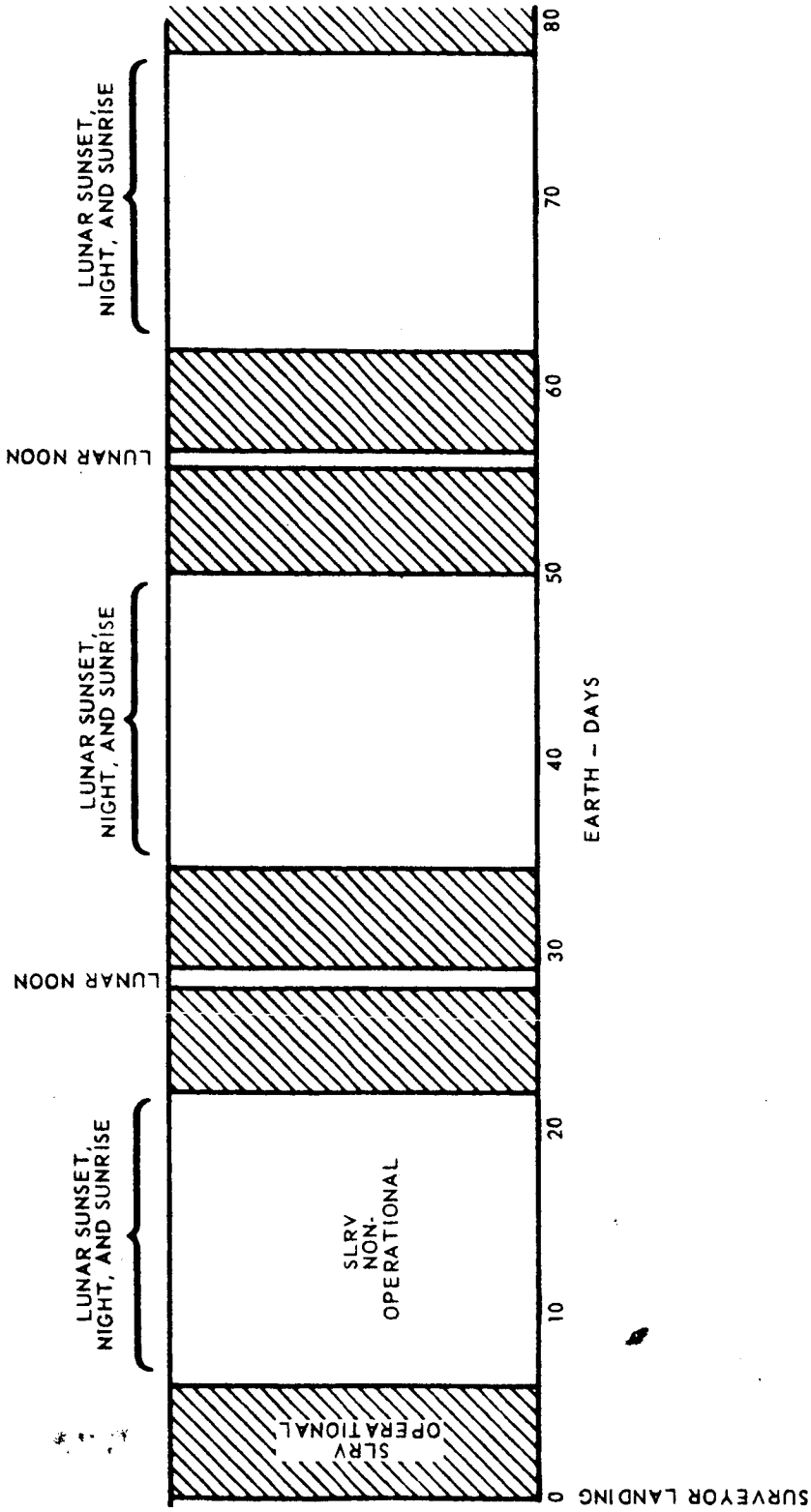

Figure 4-33 SLRV Operational Periods as Function of Lunar and Earth Days

SECTION 5

ADDITIONAL DESIGN ELEMENTS

In arriving at the system design presented in Section 4, it was evident that certain elements required to satisfy fully the system requirements could not be included within the 100 lb weight constraint. Three principal elements not included were:(1).equipment to place an artificial mark on the lunar surface, (2) a mechanical safety device for obstacle detection, and (3) a stereo image–sensing system to enhance vehicle control. These were not included because trade-off studies indicated that some provisions did exist to implement the system requirements in these areas. On the other hand, deletion of other elements such as the directional antenna would reduce the probability of the SLRV completing its mission to an unacceptable degree.

To complete the mission successfully as defined in Section 2, three landmarks must be identified for use by the astronauts in navigating the LEM to one of the certified landing points. Although the capability to provide artificial marks in the 100-lb system would ensure mission success, the possibility still exists that enough natural landmarks will be available within the site, including the Surveyor Spacecraft itself. Thus, the addition of an artificial marking subsystem is highly desirable but not mandatory.

The addition of a mechanical safety device to detect surface features that constitute a hazard to the SLRV would partially relieve the ground operator of subjective decisions. However, such a device is not mandatory because the operator can control the vehicle using only the video and telemetry information available from the 100 lb design. Therefore, no safety devices (feelers) were provided and, for similar reasons, the fixed-based stereo imaging system was not included.

If the system gross weight is increased, these three functions would be included in the design. The following sections briefly describe approaches to the design of such equipments.

5.1 MARKING

Three artificial landmarks must be visible from the Apollo LEM for use as navigation aids in reaching the selected landing point. Based on visibility requirements specified in Appendix A, an annulus of 20 ft O. D. and 16 ft I. D. has been selected. It would be constructed from 2 sheets of mylar (see Figure 5-1) each 0. 0005 inch thick; these were fused along the inner and outer diameter and along two intermediate diameter seams. The mark is unfolded after emplacement on the lunar surface. The external surfaces are coated with anodic deposited aluminum for better visibility. Unfolding is by expansion of trapped air within the annulus.

The mark is slit along a radius and packaged in a canister as shown in Figure 5-1. The canister includes a pressurized rolling diaphragm which acts as a mark ejector.

Ejection occurs when the cover is released by a command that actuates the explosive connection in the Marman-type clamp mounted on the canister. The mark exits from the canister and unfolds as it strikes the lunar surface. The method of deploying the mark is shown in Figure 5-2.

Three marks are packaged in individual pressurized canisters mounted to the forward end of the SLRV structure.

It has been calculated that the mark should land about 30 ft from the vehicle. This establishes a minimum velocity for the mark as it leaves the canister. The angle between the canister center line and the local horizontal is 60° (see Figure 5-1). Thus, the ejection velocity can be calculated as follows:

$$x = 360 \text{ in. } M\, t\, V_o \cos 60^{\circ}$$

$$\therefore t\, V_o = \frac{360}{0.5} = 720 \text{ (in.)}$$

$$V_o = 720/t \text{ (in/sec)}$$

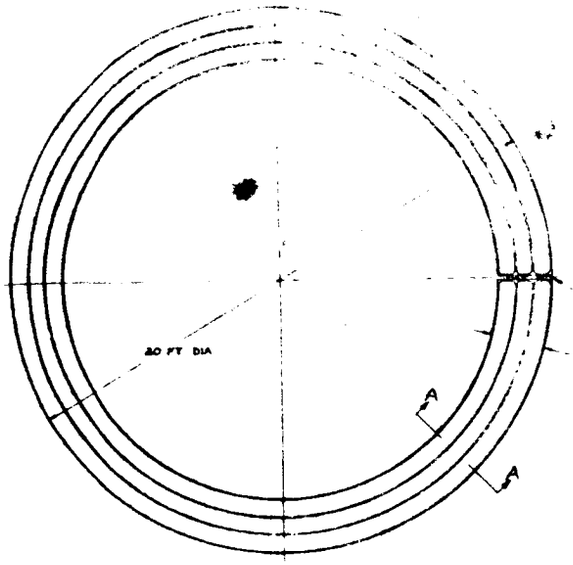

MARKER

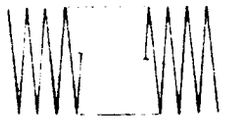

TOP VIEW - FOLDS

MARKER - ACCORDION FOLDS
SCALE 1=4

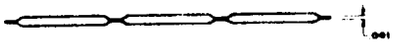

SECTION A-A
NO SCALE
MAT'L .0005 THK MYLAR - ALUM ANODIC COATING

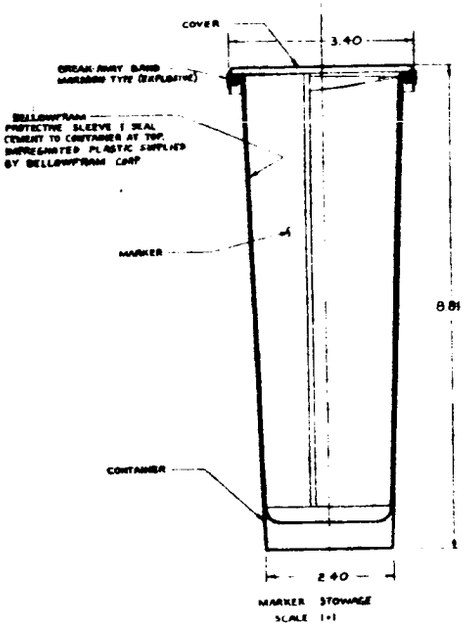

MARKER STOWAGE
SCALE 1=1
MAT'L .005 THICK ALUM

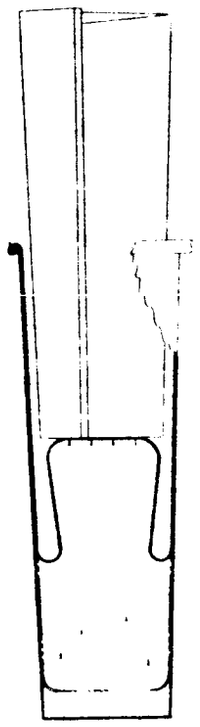

MARKER PARTIALLY DEPLOYED

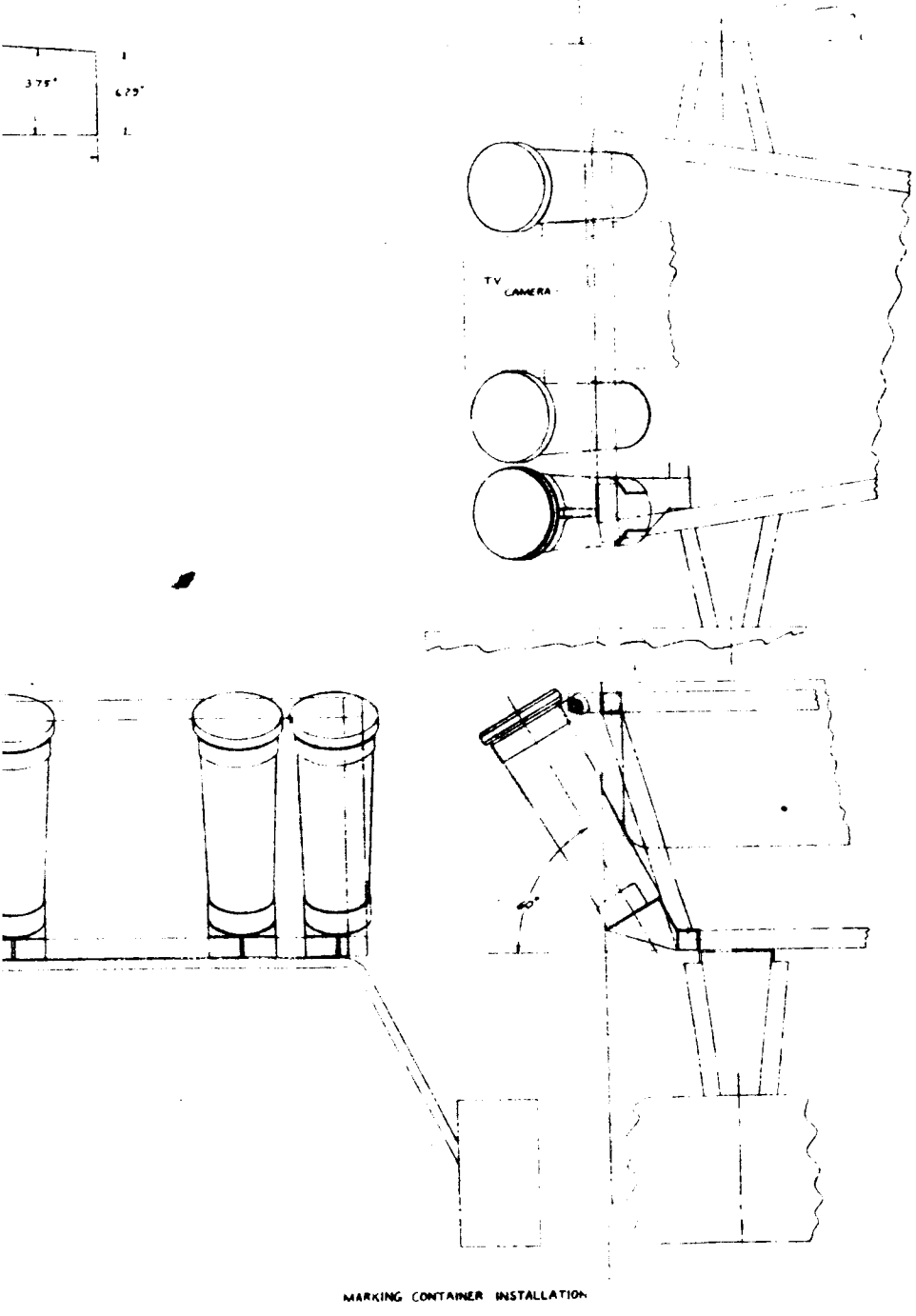

Figure 5-1 Marking Subsystem

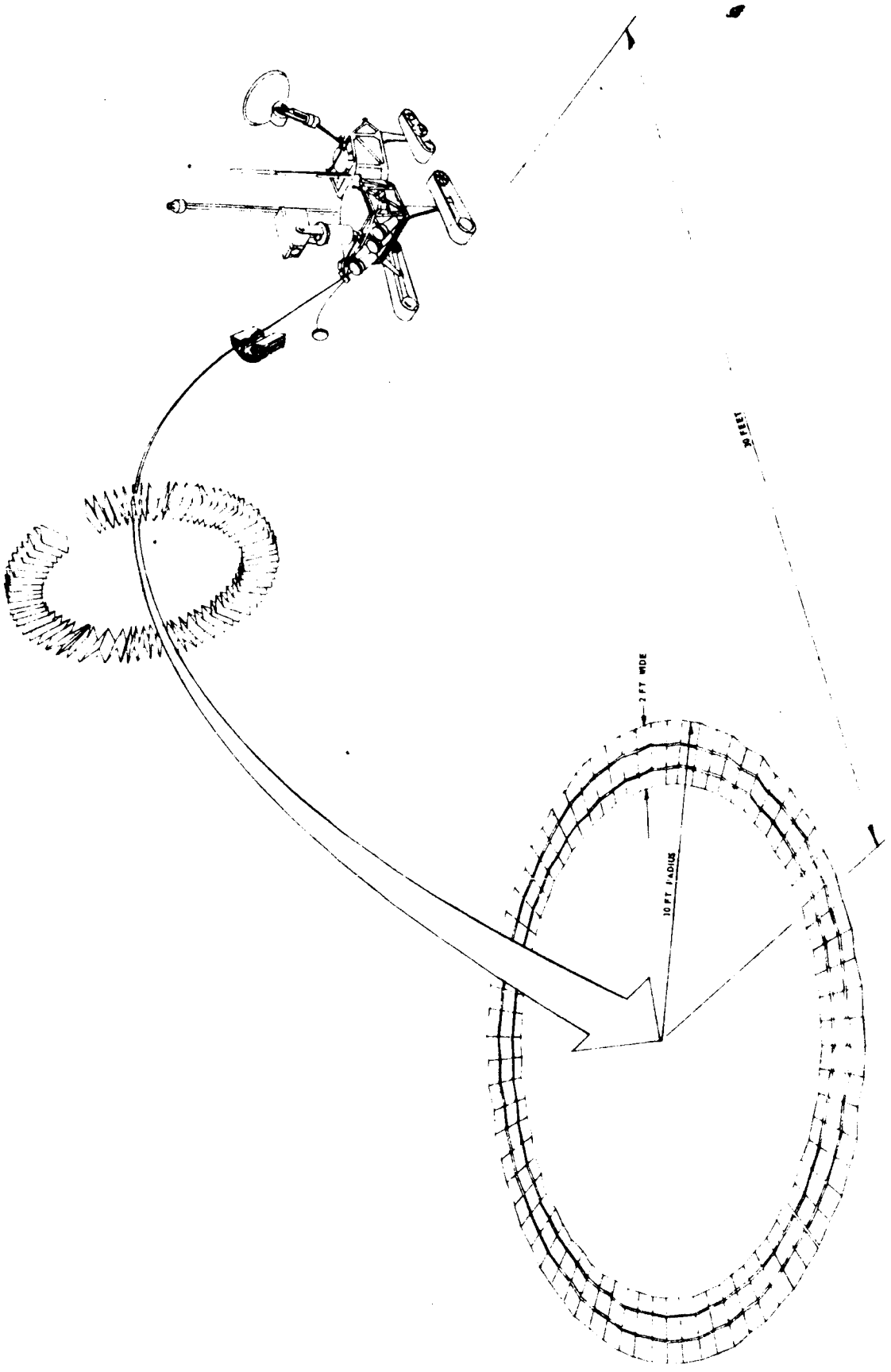

Figure 5-2 Marking Deployment Technique

at $x = \text{max.},\ y = o$

$$y = o = V_o\, t \sin 60^o - 1/2\, g_m\, t^2$$

$$\frac{V_o}{t} = \frac{g_m}{2 \sin 60} = \frac{(32.2)(12)}{(6)(2)(0.866)} = 37.2 \text{ in./sec}^2$$

$$t = \frac{V_o}{37.2 \text{ in./sec}^2}$$

$$\therefore\ V_o = \frac{720}{V_o/37.2}$$

$$V_o = \left[(720)(37.2)\right]^{1/2} = 164 \text{ in./sec}$$

where

x = distance (in.)

t = time to reach lunar surface (seconds)

g_m = lunar acceleration due to gravity

V_o = initial velocity

The weight of the marks and dispensers has been calculated as follows:

$$A_{\text{Marker}} = (2)(\tfrac{\pi}{4})\,(D_{OD}^{\ 2} - D_{ID}^{\ 2}) = \frac{\pi}{2}\,(\overline{20}^2 - \overline{16}^2)\ \text{M 226 ft}^2$$

$$= 3.26 \times 10^4 \text{ in.}^2$$

$$V = At\ M\ (3.26 \times 10^{4})\ (5 \times 10^{-4}) = 16.3\ in.^{3}$$

$$W = \rho V = (6 \times 10^{-2})\ (16.3) = 0.98\ lb$$

From Echo data (including captive air for deployment).

$$A_{Echo} = \pi D^{2} = \pi \quad (100)(12) \quad ^{2} = 4.5 \times 10^{6}\ in.^{2}$$

$$W/in.^{2} = \frac{136}{4.5 \times 10^{6}} = 30 \times 10^{-6}\ lb.in.^{2}$$

$$W_{Marker + air} = (W/in.^{2})\ (A) = (30 \times 10^{-6})\ (3.26 \times 10^{4}) = 1.08\ lb$$

$$W_{canister} = 0.2\ lb$$

$$W_{Structure} = 0.1\ lb$$

Total weight: 3 markers + 3 canisters + structure ≈ 4.0 lb

where:

W = weight (lb)

V = volume ($in.^{3}$)

A = surface area ($in.^{2}$)

W_{Echo} = 136 lb

Dia_{Echo} = 100 ft

To establish the pressure required to eject the mark at the calculated velocity, it was assumed that the air will follow a polytropic expansion process. The change in potential energy of the air thus released will all be converted to kinetic energy.

$$\Delta PE = \frac{P_1V_1 - P_2V_2}{k-1} = 1/2\ mv^2$$

$$V_1 = 2.50\ in.^3$$

$$V_2 = 44.6\ in.^3$$

$$\frac{V_2}{V_1} = \left(\frac{P_1}{P_2}\right)^{\frac{1}{k}}$$

where k = 1.4 for air

$$\frac{44.6}{2.5} = 17.9 = \left(\frac{P_1}{P_2}\right)^{\frac{1}{1.4}}$$

$$P_2 = \frac{P_1}{(17.9)^{1.4}}$$

$$m = \frac{0.98}{386}\ \frac{lb\ sec^2}{in.}$$

With appropriate subsititutions in the energy equation, the P_1 required was calculated to be 8 psi. A more thorough analysis will be accomplished for the detail design to account for frictional losses, variation in temperature, etc.

The aluminized surface would provide sufficient contrast with the lunar background to ensure detection by the astronauts from their position above the lunar surface. It has not yet been determined to what extent this type of marking device would be degraded over a one-year period when subjected to the long-term effects of hard vacuum and solar radiation. This will be the subject of more detailed analysis during Phase II.

5.2 SAFETY

Certain safety features are inherent in the 100-lb design. Among these are the design of the mobility and structure subsystems, which provide for both lateral and longitudinal stability of the vehicle compatible

with the vehicle's ability to climb discrete obstacles. In addition, the design provides undercariage clearance compatible with the largest obstacle the vehicle can climb. Since the vehicle tracks lead all other portions of the vehicle in either direction of travel, the probability is high that the vehicle will not hang up on a protuberance. The TV imaging system also provides a degree of safety in that the ground operator can determine to some extent, the size and shape of hazards in the vehicle's path, and thus choose a path compatible with the vehicle's capabilities. There are two potential hazards. One is the probability that in a terrain consisting of random obstacles the vehicle could exceed its stability limits by climbing over a series of small obstacles that eventually cause a sufficient difference of elevation between the left and right side to overturn the vehicle. To guard against this condition, the inclinometer mounted within the vehicle contains limit switches which automatically stop the vehicle if it approaches stability limits.

The second potential hazard is crevices. The results of the Phase I study how that, even with a stereo imaging system, it may not be possible to detect a crevice in the vehicle's path which constitutes a catastrophic hazard. The following paragraphs describe the implementation of a safety sensor that will detect hazardous crevices in time to prevent a catastrophe.

The mechanism shown in Figure 5-3 has been designed:

1. To detect crevices wider than one-half the track length.

2. To measure the depth of crevices wider than one-half the track length.

The safety mechanism consists of a pair of independently suspended motorized tracks 2 inches wide and of the same length and height as the SLRV drive tracks. The drive mechanism is similar to, but of much less mass (since the power required is slight) than those used in the SLRV drive tracks. Each safety track is connected to the SLRV by a self-erecting tube (see Figure 5-3) which serves both as an articulating suspension arm and as a deployment mechanism.

The rotation of the suspension arms is limited to ± 30 degrees in the vertical plane and the rotation of the safety tracks is limited to ± 50 degrees rotation in the vertical plane with respect to the suspension arms. These restrictions will ensure proper erection and positioning of the safety mechanism while allowing crevice depth measurement of at least 40 cm.

Each suspension arm is equipped with a potentiometer whose output is proportional to the angular position of the arm relative to the SLRV. Each safety track is mounted a potentiometer whose output is proportional to the pitch angle of the track relative to the suspension arm (see Figure 5-4). By monitoring the potentiometer outputs, the angular positions of the tracks and suspension arms are determined, which then define the lunar surface irregularities being encountered by the safety mechanism. The potentiometer outputs are continuously sampled. A reading that indicates an unsafe condition will automatically stop the SLRV.

The safety tracks have a passive steering ability due to the caster built into the suspension system. The caster reverses automatically when the vehicle reverses, allowing the vehicle to move in both directions. The safety track motors are equipped to reverse direction whenever the SLRV reverses direction. The change from positive to negative caster as the vehicle direction reverses is accomplished by operating the safety tracks at a slightly slower velocity than the SLRV driving tracks. This causes an axial force to be transmitted along the suspension arm whenever the SLRV is moving. This force moves the suspension arm attachment point either forward or backward (depending on the SLRV direction of motion) to a stop in the ball joint track (see Figure 5-3).

The articulated suspension arm is a foldable, self-erecting column which is square in cross section and consists of four thin straps of spring steel. The straps have a slight cross-sectional curvature. Rigid supports are spaced every nine inches along the length of the column as shown in Figure 5-4. When the safety system is retraced, the safety tracks are stowed between the main driving tracks with the suspension arms stowed in the available space. The suspension arms in the retracted position are very flexible and can be manipulated easily for stowage. Upon deployment, the safety system is quite stiff and cannot be accidentally folded again. The weight of the safety system is 4.8 lb.

If the SLRV is proceeding along the lunar surface (zero slope) and encounters a crevice that is wider than one-half the track length then for the vehicle-crevice configuration shown in Figure 5-4 (b) and (c), the relationship between crevice depth and the measured angular position of the suspension arms and safety tracks is:

$$h = R \sin \alpha - C (1 - \cos \alpha) + \frac{1-d}{2} \sin (\alpha+\beta)$$

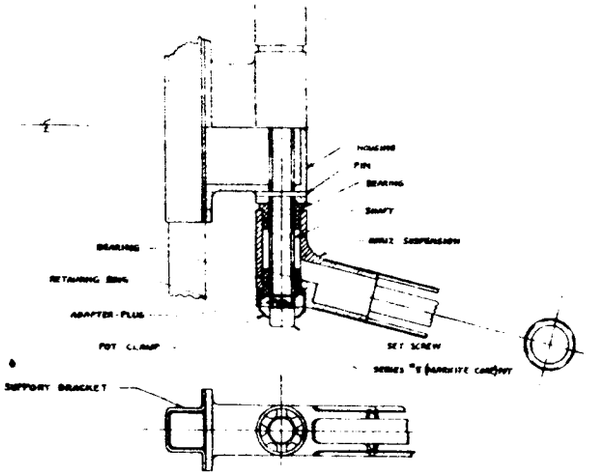

VIEW F-F
SUSPENSION PIVOT
SCALE 1:1

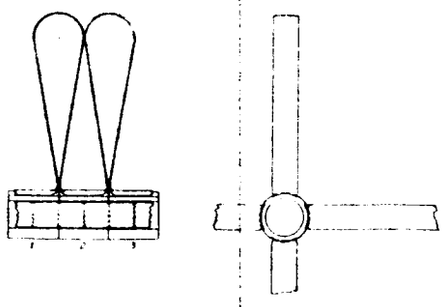

VIEW E-E
SUSPENSION ARM RETRACTED
FULL SCALE

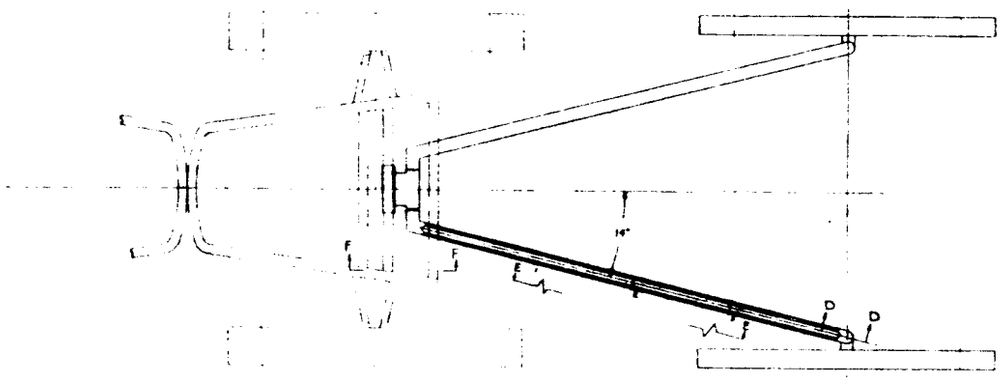

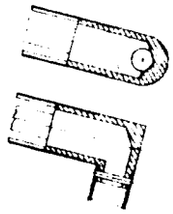

SECTION D-D
SCALE 1:1

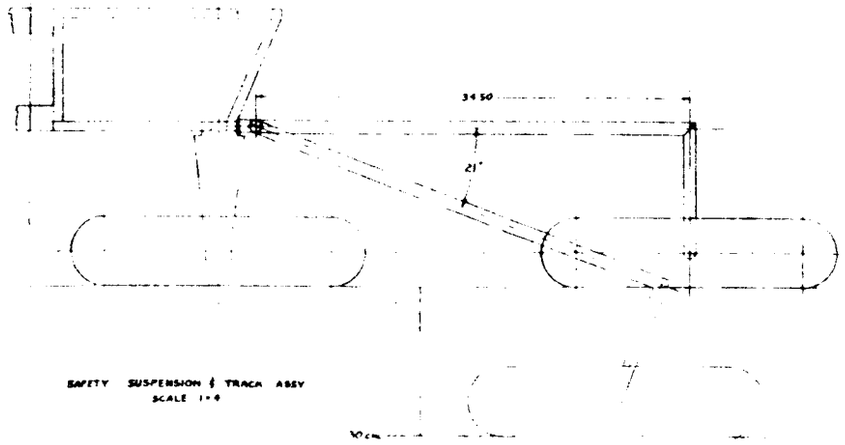

SAFETY SUSPENSION & TRACK ASSY
SCALE 1:4

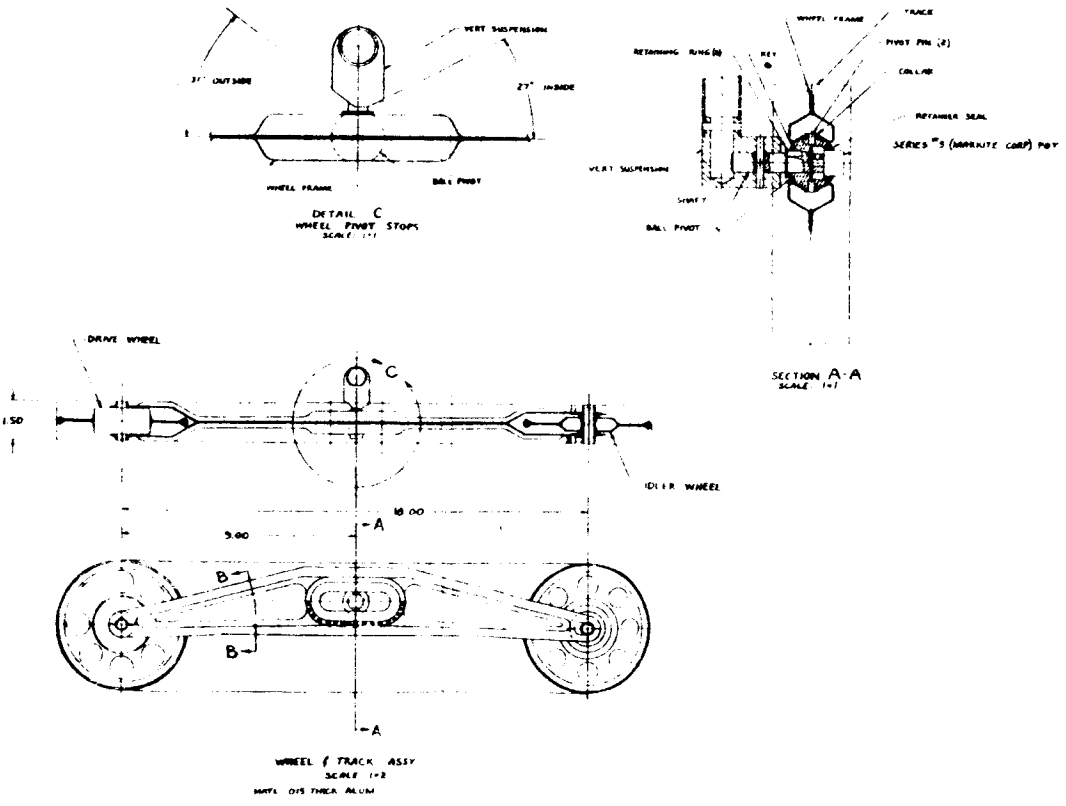

Figure 5-3 Safety Subsystems

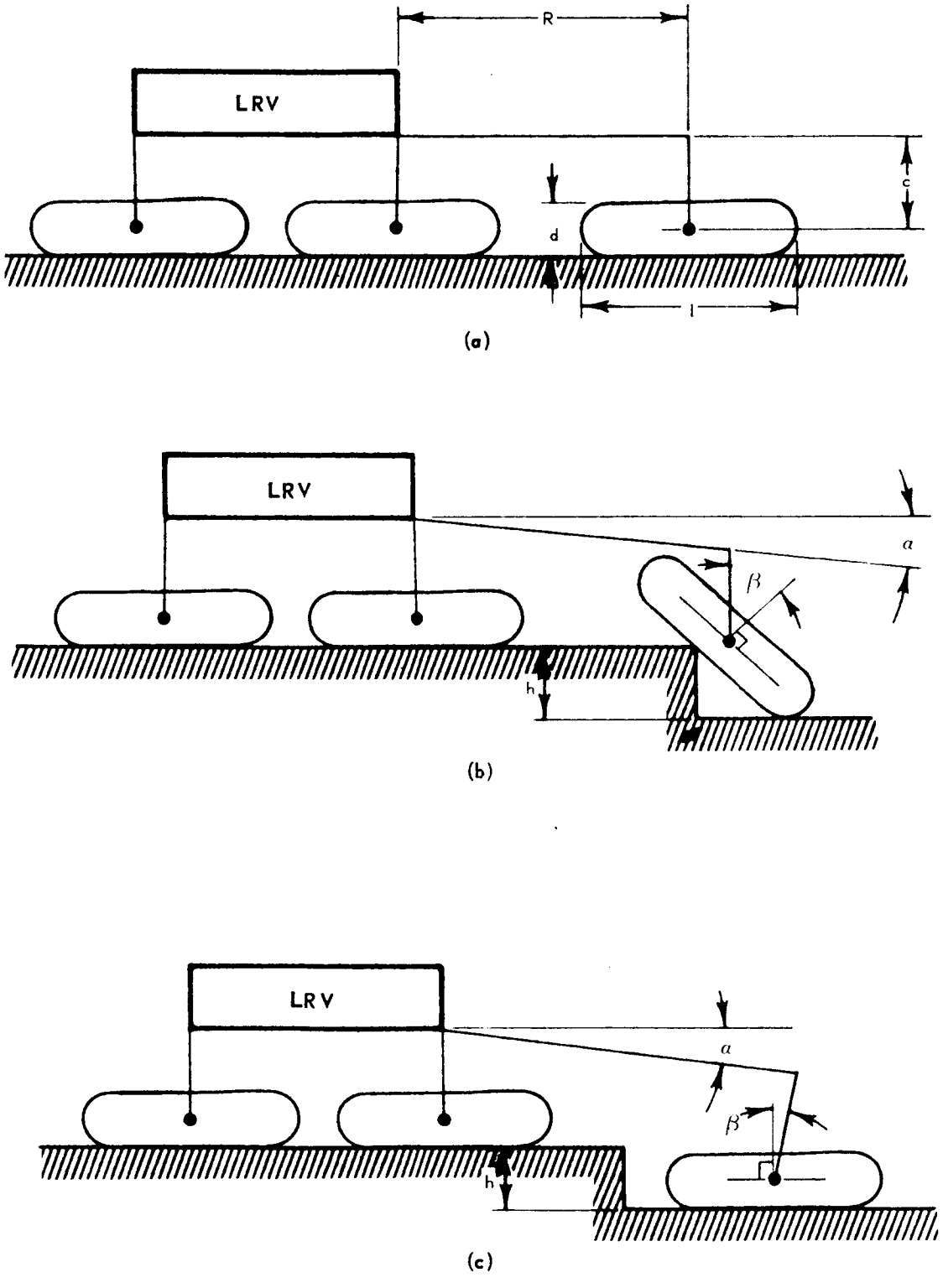

Figure 5-4 Safety Mechanism Geometry

where

h = crevice depth

l = track length

d = track height

R and C = suspension arm dimensions (see Figure 5-4 (a))

α = angular displacement of the suspension arm relative to the SLRV

β = angular displacement of the safety tracks relative to the suspension arm. Initial values of α and β are zero.

When the SLRV is operating on a slope, the voltages from the four potentiometers must be integrated with the outputs from the two-axis inclinometer to detect unsafe mobility conditions.

The full range of potentially hazardous surface conditions has not been evaluated during this study; therefore, it is recognized that certain limitations to the safety mechanism described here may exist. The study has resulted in the conclusion that, at best, the design of a terrain detection device will require considerable investigation and design ingenuity. This design represents simply an approach to the solution of the problem for the purpose of establishing initial weight and power requirements for the study of heavier vehicles.

The weight, exclusive of additional data-handling electronics, is estimated to be from 4.0 to 4.5 lb and the required power is approximately 2 watts.

5.3 IMAGE SYSTEMS

To increase confidence in the ability of the ground operator to control the SLRV in the face of terrain hazards, an increase in the amount and quality of image information provided by the 100 lb design is highly desirable. In addition, the success of the SLRV mission is dependent upon this image information to the extent that the imaging device is considered to be one of the most critical system elements in terms of failure mode. Thus, it is desirable to improve not only the amount and quality of video information but also the reliability.

The following discussion covers several techniques for increasing the quantity and quality of data and the reliability of the imaging system which were not included in the 100 lb design because of weight limiations or insufficient design detail.

5.3.1 Two-Tube Nonstereo TV

There are many variations of a two-tube design. If a two-tube design has two electrostatic tubes with minimum displacement between them and with like optics, the resulting configurations will provide increased reliability but not a stero capability. The additional tube would mean the addition of a lens turret, iris control, shutter, lens and tube, which totals approximately 1.80 lb, and some added structural weight which might amount to 0.5 lb. If only the electronic deflection amplifier and the video preamps are duplicated, and the remaining electronics are time shared, only 0.034 lb of additional electronics are required. The total weight addition is approximately 2.5 lb and would bring the design to an estimated 10 lb weight.

This configuration requires only a small amount of additional power (estimated at 200 milliwatts) to operate control circuits required to switch between tubes.

The thermal problems associated with two tubes would require further investigation, but since the two tubes would be enclosed in the same insulated thermal environment, a conventional approach may prove satisfactory.

If the telescope can be relinquished and fixed optics can be used for the two tubes, the weight saving is approximately 1 lb. It is important to realize that the bulk of the weight for the basic system is in the azimuth and elevation drives (2.5 lb), structure (2.3 lb), and optical accessories (1.67 lb). The tube plus its electronics weigh 1.18 lb. Thus, complete redundancy in tube circuitry would cost 1.18 lb.

5.3.2 Two-Tube Stero TV

When the two-tube design is a stereo arrangement (see Figure 5-5), the added requirement is a substantial baseline and continuous power to each tube. The addition of the baseline length would add little weight if the severe vibration problem associated with launch was not present.

A preliminary estimate is that the penalty would be 2 lb, for a baseline length of approximately one foot. In addition, if the baseline is large, separate thermal problems may arise. The total weight of the stereo configuration is estimated at 12.0 lb.

A stereo pair would probably require 1.120 watts for dual filament operation to eliminate warmup time. If only one tube were used at a time, the power could be switched from one tube to the other; hence, an additional power increment would be required for switching.

5.3.3 Enchance Monoptic Capabilities

In considering the monoptic hybrid tube designs, the increased power, not weight, is the predominant consideration. A hybrid tube (GEC 1335A) would require 6 watts peak power and 2 watts average for the deflection drive circuits as contrasted to 0.8 watt peak for electrostatic. The hybrid requirement for peak power is, in effect, an average requirement since the readout times of hundreds of seconds involve prolonged operation at near peak powers. In essence, the power requirement for the TV electronics would increase from the present 5 watts to approximately 10 watts. In addition to the power, the hybrid deflection coil weight approximately one-half pound. In total, the hybrid vs all electrostatic selection depends on whether the anticipated edge resolution improvement of 40 to 50 percent at the 50 percent aperture response point is worth the 5 watt and one-half pound weight penalties.

In addition to major TV alternatives, there are possibilities of enhanced capabilities for the basic monoptic design. With little difficulty theoutput encoding levels could also include 5 and 6 bit capability. This capability might be desirable when the vidicon operates in the degraded communications mode (256 lines at 2 bit encoding) where the video amplifier has a dynamic range of ≈200:1. The added power would be approximately 1.2 watt and the weight increase would be negligible.

The added capability of $(1024)^2$ elements is a possibility. This might be desirable to assure that all the resolution capability of the tube is being obtained. It is important to indicate that since the electrostatic tube's aperture response is down to 20 percent at 350 TV lines, per 3/8-inch raster, the $(525)^2$ element scan with a 350 line resolution handles most of the situation. The $(1024)^2$ element scan requires little additional power or weight,

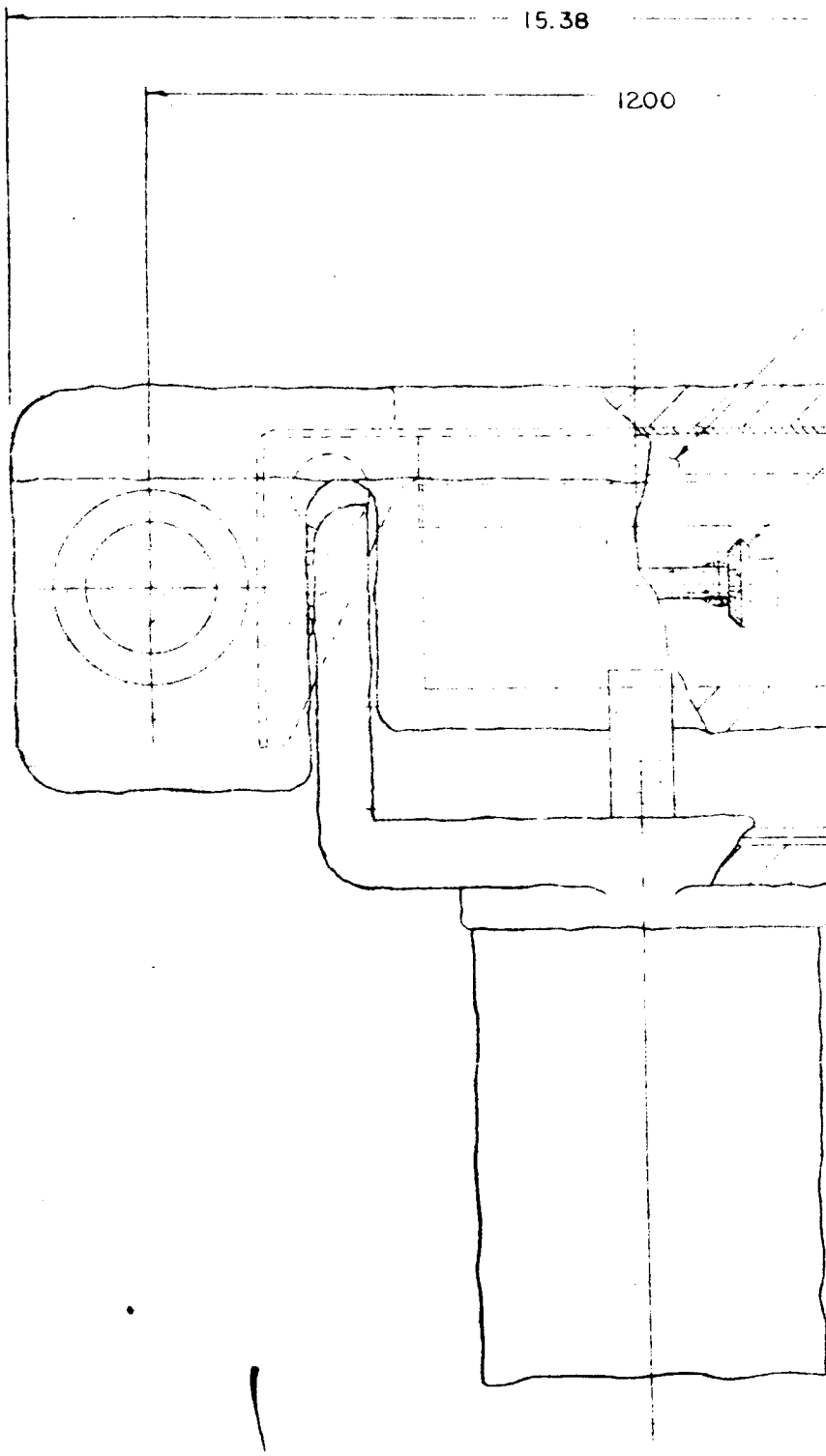

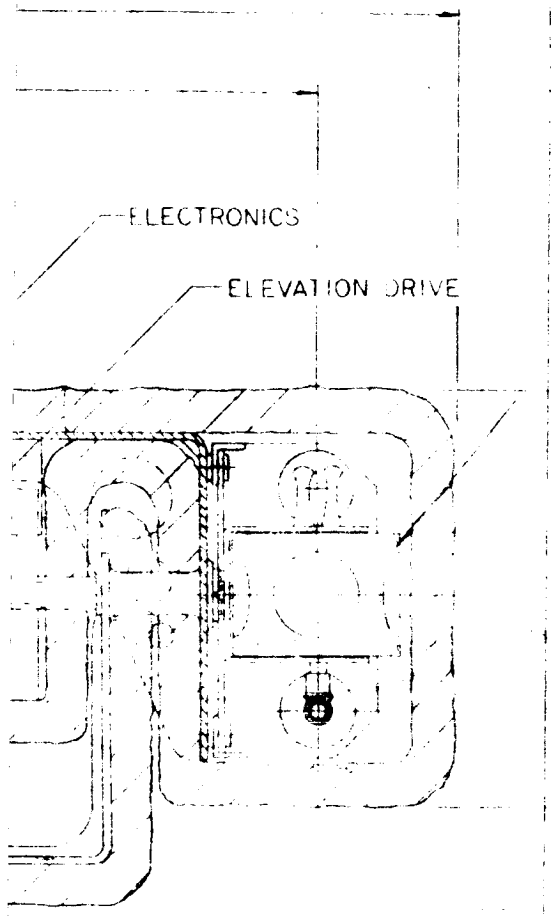

—GA LEAN LESCOPE

SHUTTER

TELESCOPE DR

AZIMUTH DRIVE

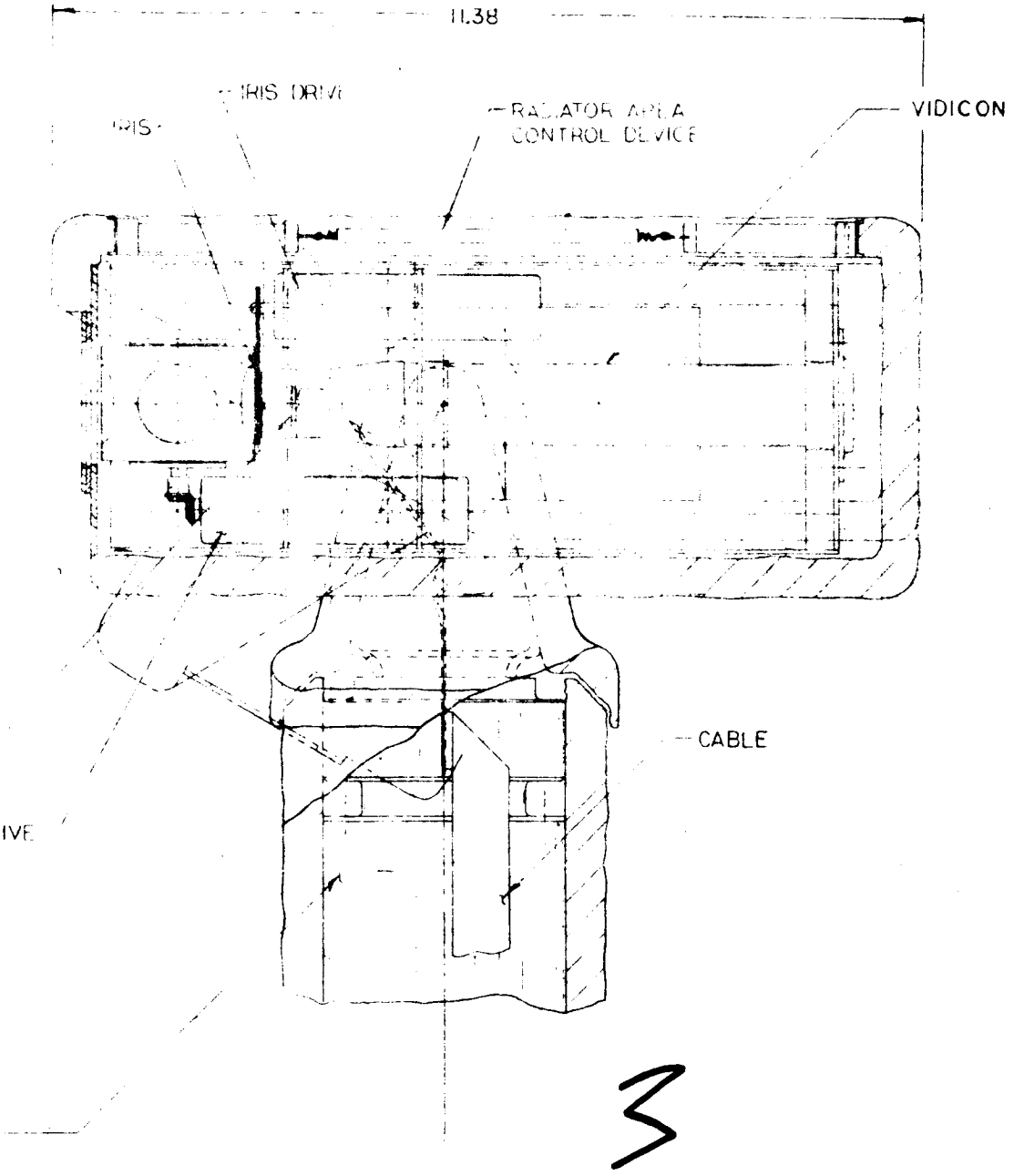

Figure 5-5 Two-Tube Stereo TV

and for this reason may well be worthwhile. There are several drawbacks involved in increasing the number of elements. First, for the same data rate the frame time increases with the increase in number of elements. Thus, the frame time for 4 bit, $(1024)^2$ element frame at 122.88 k bit/sec, would be 32 seconds instead of 8, a fourfold increase. For this large increase in frame time, the only benefit is slightly better resolution in the center of the scene.

5.3.4 Optical-Mechanical Scanner

An optical-mechanical scanner such as the high-resolution facsimile sensor for slow scan applications has certain advantages over television sensors. It can provide 360° field-of-view coverage in azimuth and more versatility in the choice of scanning mode. The problems associated with mechanically moving parts under the severe lunar environmental conditions and the weight and power requirements must be traded off against the electronic complexity and the modes of failure associated with slow-scan vidicon television systems.

Scanners have been satisfactorily developed for airborne and space applications. In these systems, the object space is scanned both in azimuth and elevation across a single detecting element and the image is reconstituted in a pseudo-facsimile fashion. Each specific application requires a specially designed scanner system, and corrections for the scanning mode such as curvature of field, non-linear rates across the field, and sequential data handling must be incorporated.

An optical mechanical scanner has been developed for Ranger with a field of view of 360° in azimuth and 50° in elevation. The weight is approximately 5 lb. Although, the high power requirement of 15 watts and extremely low frame time of 8 hr make the device unfeasible for SLRV, the angular resolution of 0.1° is better than that achieved by the SLRV TV with the narrow (10°) field of view.

Performance improvements such as reduced frame time and power requirements are anticipated by several suppliers. These improvements could result in an optical-mechanical scanner that is definitely competitive with a vidicon sensor. However, significant development problems are expected which are associated mainly with the high-speed, extremely accurate mechanical positioning of a mirror or prism in an extreme environment. Such devices have not yet been developed, whereas vidicons have been proved in space applications.

5.4 SOIL BEARING STRENGTH INSTRUMENTATION

JPL Document EPD-98, Revision 1, specified that the acceptability of an LEM landing point includes knowledge of the bearing strength of the surface in terms of its ability to support the LEM during and after touchdown. This document also specifies that, as a minimum, the SLRV can measure force versus penetration characteristics of the soil. The 100-lb design contains a penetrometer which satisfies the basic requirement of providing force versus penetration data. The ability to inerpret these data and extract information relating to bearing strength is limited to determining the lower boundary of a range of possible bearing strengths. The techniques developed for determining this boundary condition are sufficient to satisfy the objectives stated in Appendix A of EPD-98 with respect to soil static bearing strength. Since the establishment of a boundary condition may be inefficient in terms of mission time, it may be desirable to obtain a closer correlation to the actual static bearing strength characteristic of the soil.

The following sections discuss the other instrumentation which might be added to a higher gross-weight vehicle to improve the interpretation of bearing strength properties.

5.4.1 Soil Density Measurements

The second most important lunar soil measurement is that of density. For a soil which derives its strength from arrangement of particles rather than cementation, whether limited by shear strength or compressibility, the bearing capacity is largely a function of density; thus the settlement of a particular loaded area on a non-cemented material will vary with the bulk density. This is also true for a material which fails by an upward displacement of soil around the loaded area. The density measurements, coupled with the penetrometer measurements, will give the best information for the purpose needed of the properties of the lunar surface.

In general, the shear strength of a material is greatly dependent upon its grain structure, which is reflected in the porosity. The porosity, in turn, is a function of the bulk density of the material and also the specific gravity of the individual soil particles or absolute specific gravity. Thus, the porosity cannot be calculated from the density without knowledge of the type of material composing the soil. However, penetrometer measurements and observation of both the soil and the performance of the vehicle

would give an indication of the order of magnitude of the porosity (i.e., loose, dense, etc.). One could then draw conclusions as to the type of material composing the lunar soil on the basis of the density measurements. For example, a material such as silica flour (SiO_2) — which has a negligible, if any, concentration of iron or magnesium — would have a density of approximately 0.9 g/cc in the loose state. A material having a high metallic content such as olivine or pyroxene (meteoritic minerals) would have a density of approximately 1.1 g/cc at the same porosity.

In addition, the bearing capacity of a material is a function of its density. This would be particularly true for a dense material which requires upward displacement of the material in shear failure under the footing. Also, for any one material the settlement of a particular footing will vary with the bulk density in the form,

$$S = k\,(q/\gamma)^m \quad .$$

where

S = settlement

q = bearing pressure

γ = density of the soil

k, m = parameters dependent upon the size of the footing, the environmental atmospheric pressure, and the soil density.

It can be seen that the relationship between the settlement and the density is not a simple one. However, measurements of the variation in the density on the lunar surface will give indications as to the variation of the settlement characteristics of the soil at various points over the surface.

The proposed subsurface density instrument would be designed to measure the density of the subsurface material at various depths as the penetrometer is driven into the lunar material. In general, a radiation source would be located a known distance from a Geiger-Mueller counter tube. The radiation would be directed so that it impinges on the lunar material located between the source and the detector. Shielding would be

arranged so that little radiation passes directly from the source or from other sources, such as the RTG, to the detector. As radiation scatters into the lunar material, portions are radiated to the region of the Geiger-Mueller counter tube and would be detected. Because the scattering and absorption of radiation in a material is related to the density of that material, the density of the lunar subsurface material can be derived from the detector output pulses.

The sensor assembly would be made up of a radiation source and a G-M counter tube and located in the tip of the penetrometer probe. It may be necessary to have the radiation source attached to a positioning mechanism so that effects of natural formation radiation can be accounted for.

The electronics unit would contain a DC-DC converter to provide the high voltage for the counter tube, and signal conditioning circuits to match the counter tube to the telemetry equipment.

Design Characteristics:

Size	Sensor: 0.75 in. dia., 3 to 5 in. length Electronics unit: 1-3/4 x 3 x 1 in.
Weight	Sensor: 1.1 lb Electronics unit: 0.45 lb
Power	22 ± 2 volts DC 10.2 ma nominal
Measurement range	0.3 to 3.0 g/cc
Repeatability	± 20% of reading or 0.1 g/cc, whichever is larger
Output pulse repetition rate	5-2000 cps

5.4.2 Vane Shear Meter

A vane shear device would measure the horizontal or rotary displacement torque property of the soil, thus providing additional data relative to the soil's frictional and cohesive characteristics. The device consists of a probe head having a series of teeth protruding from its periphery which is rotated into the material. The force exerted to turn the device is a measure of the shear strength, which can be interperted to determine bearing strength properties of a given type of soil.

It is estimated that a shear vane and associated drive mechanisms would weigh 1.0 lb and require 8 watts for operation. The degree of confidence in the bearing strength determination would be increased by providing this additional information on the soil properties; further experimentation will be required to determine to what extent.

5.4.3 Jack Hammer

The jack hammer may be used exclusively to provide data for bearing strength properties, but of a somewhat different nature than the force vs sinkage penetrometer. A measure is made of the sinkage or resistive force exerted when a given load is permitted to free fall or impact the surface material which gives dynamic bearing strength information. If performed in a repetitive fashion, the force data must be integrated and processed for telemetry. If performed by one impact, which is necessarily of extremely short duration, the data must be stored and then transmitted. It is conceivable that adequate designs and interpretion data can be generated, but the device and data processing would become complex, heavy, and power-consuming.

5.5 NIGHTTIME OPERATION

In order to survive the lunar night environmental conditions it is necessary to supply power to most of the electronic equipment in order to maintain that equipment at a reasonable minimum temperature. Night operation would permit faster operation, hence a shorter mission time, thus enhancing the reliability of the operating equipment to achieve the primary objectives. The 100-lb vehicle is designed to operate during a lunar day and survive at night thus no useful information other than status data is obtained during one half of the total mission time. It would be desirable, therefore, to provide an operational capability for the SLRV during lunar night as well as lunar day. The two major drawbacks to lunar night operation stem from the low thermal environment and the absence of solar illumination.

The absence of solar illumination affects several functions of the vehicle; e. g., the image sensing system and the navigation system. Figure 5-6 shows the design for a camera with nighttime operating capability using an electrostatic image orthicon and a fully controlled zoom lens. The use of a zoom optics for nighttime operation provides the ability to set the field of view to an optimum value for the particular scene. This allows maximum utilization of the light sensor's resolution capability; however zoom lenses with sufficient precision for photogrammetry pose a serious development problem.

Incorporated with the optics in this design are focus control, iris control, focal length control, and a filter wheel having color and polarization filters. Of these controls, the focal length is by far the most critical. Forcus control is required to overcome temperature effects and to improve the near point of the narrow-field position of the lens. The estimated total weight for this method of implementing nighttime imaging is 17.25 lb. The minimum peak power requirement would be approximately 7 watts.

The image orthicon sensors are not as fuly developed as vidicons. Thus, a sizable tube development program would be involved. Westinghouse's secondary emission conduction tube and General Electric's electrostatic image orthicon are distinct possibilities. The electrostatic versions of these tubes weigh 12 to 14 ounces as compared to the 2.6 ounces for vidicon. Their limiting resolutions, upon cursory investigation, appear to be roughly one-half to three-quarters that of the electrostatic vidicon.

The sensitivity of both tubes appears adequate for starlight operation. The mode of operation with each of these devices would differ from the vidicon, because these devices can be electronically shorted and because their high sensitivity and electronic shutter interval may possibly be combined to permit a fixed f-number operation. Each of these would require a power supply in the 4- to 7-kilovolt range. Although these tubes have less resolution, they have larger surfaces which compensate for this lack of resolution. To the optics, this means a larger diameter lens to maintain the same f-numbers and fields of view.

Another possible method of implementing a nighttime sensor would be to add channel mutlipliers to conventional or modified vidicons. The resulting increase in sensitivity would not be as great as that achieved with the image orthicon; however, the resulting tube would be far more rugged than current orthicon designs and would require a less comprehensive development program.

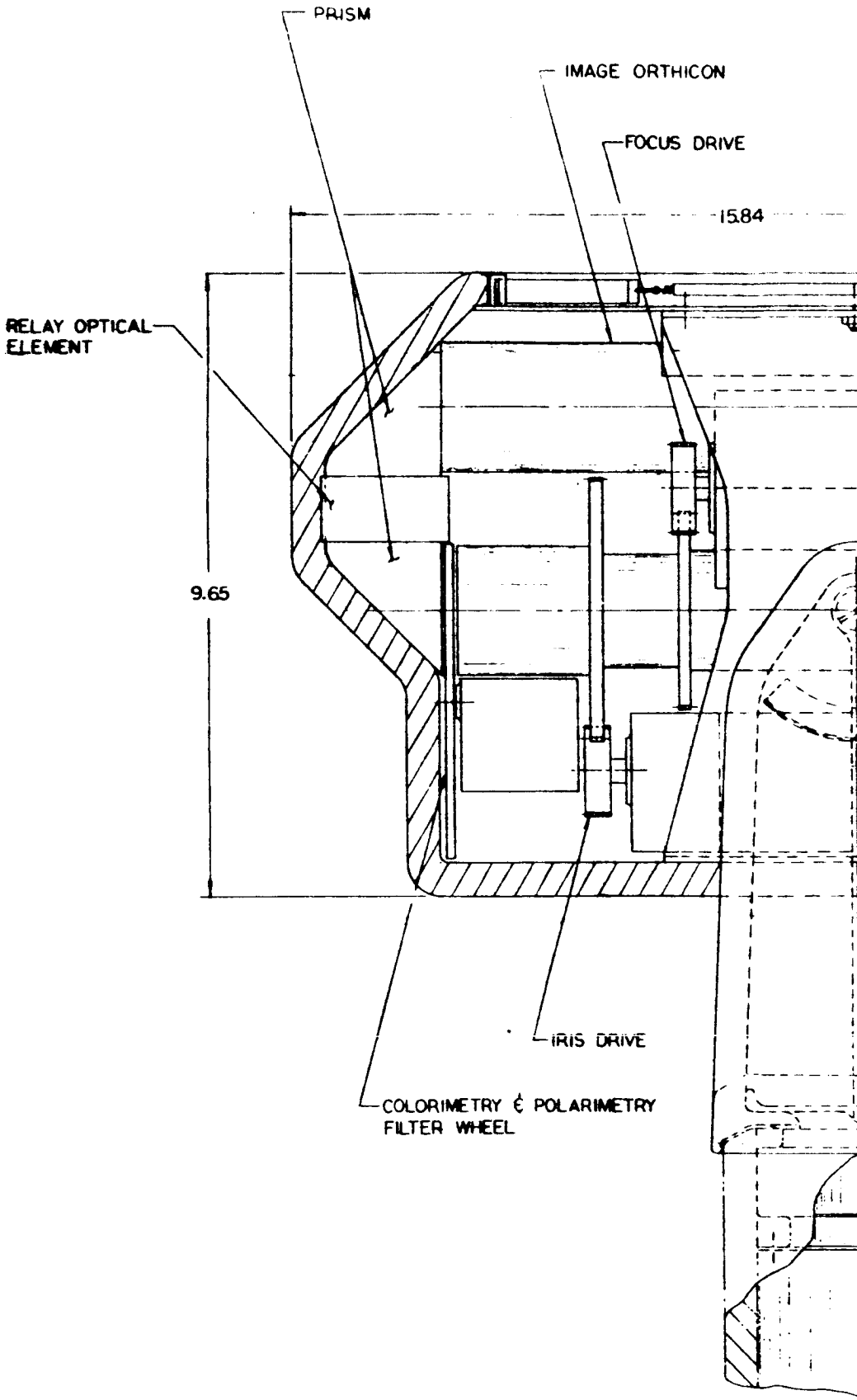

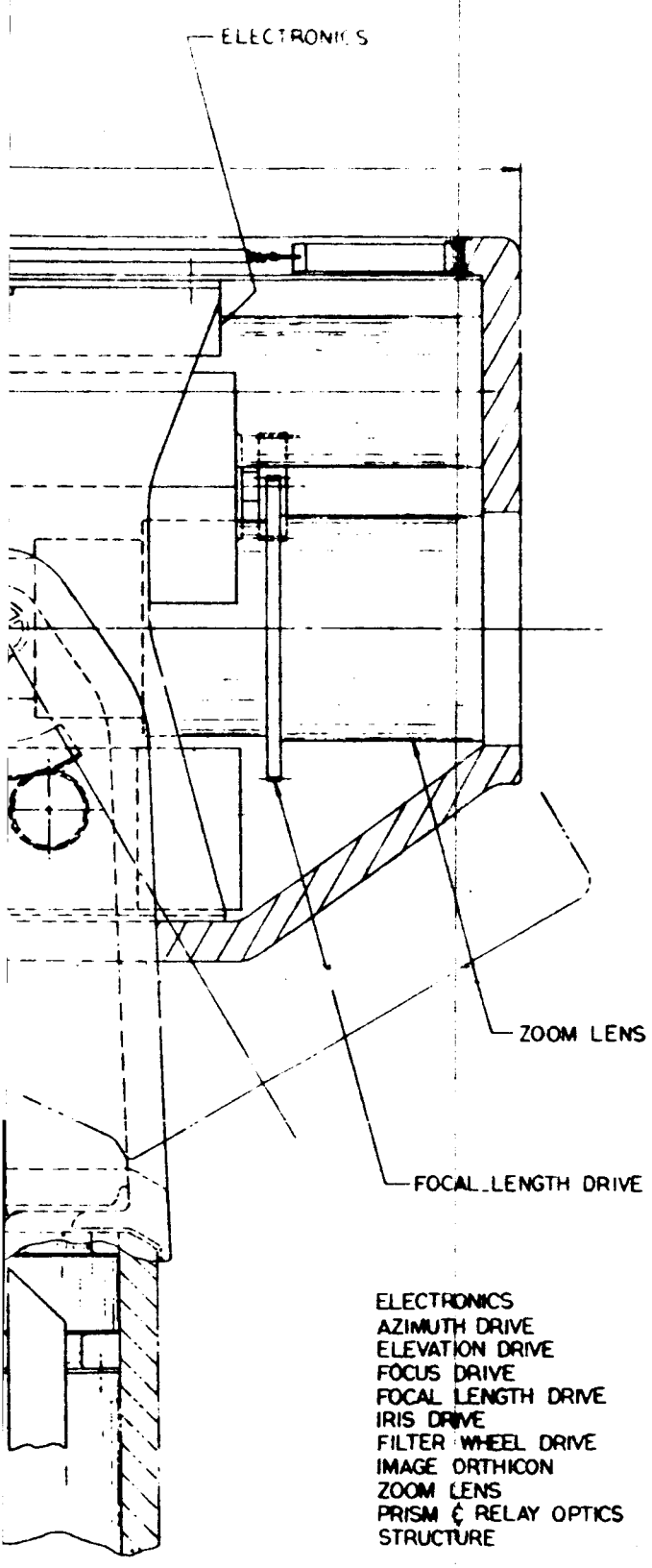

ELECTRONICS	36 OZ.
AZIMUTH DRIVE	20 OZ.
ELEVATION DRIVE	20 OZ.
FOCUS DRIVE	14 OZ.
FOCAL LENGTH DRIVE	20 OZ.
IRIS DRIVE	14 OZ.
FILTER WHEEL DRIVE	14 OZ.
IMAGE ORTHICON	14 OZ.
ZOOM LENS	36 OZ.
PRISM & RELAY OPTICS	8 OZ.
STRUCTURE	80 OZ.
	276 OZ. = 17.25 LBS

Figure 5-6

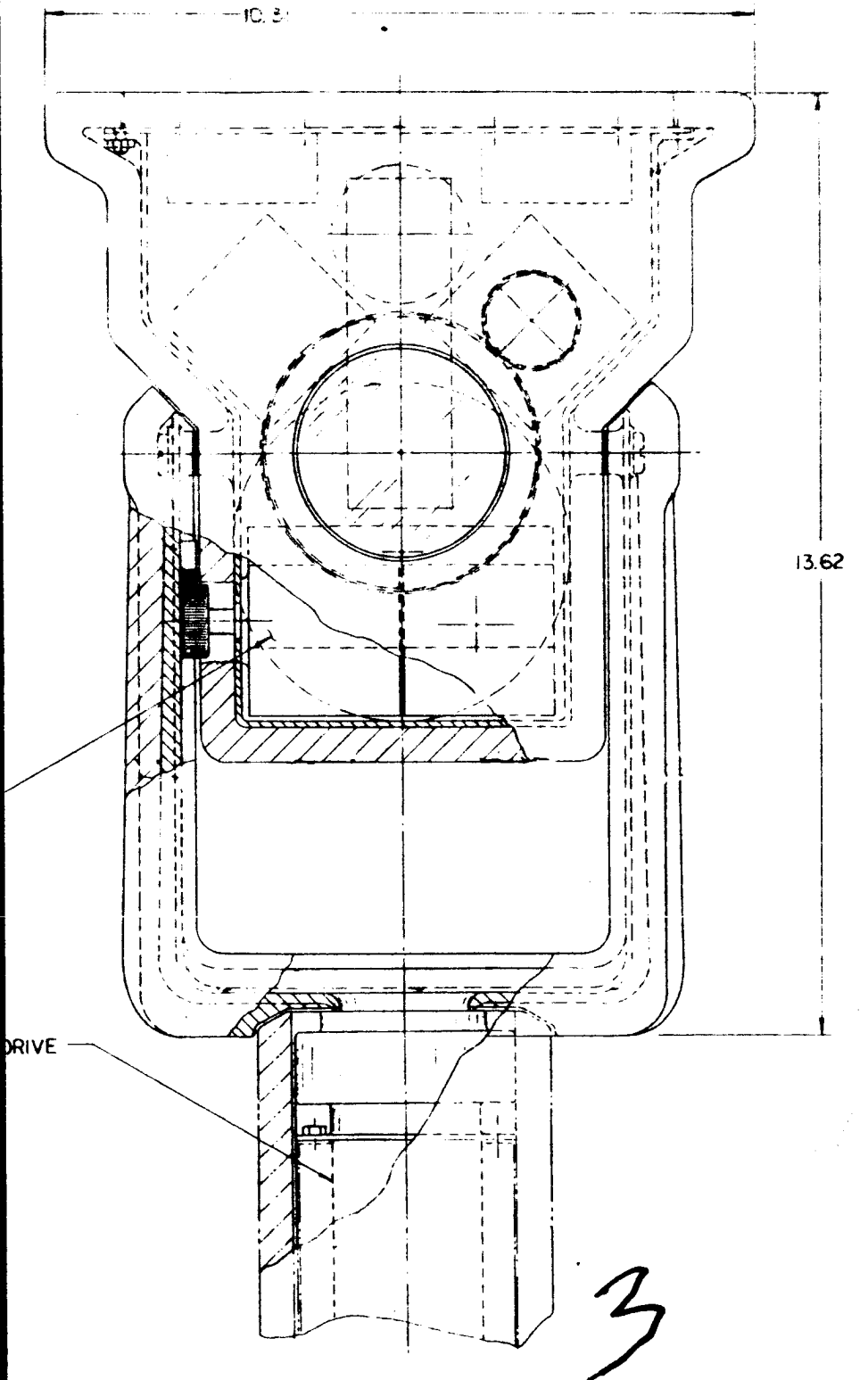

3

SI RV Television Assembly (Zone B)

5-25/5-26

Since the navigation system derived for the 100-lb system depends upon detection of solar angles to determine vehicle heading, operating during lunar night would require the substitution of another sensor for the sun sensor. Several possibilities exist; the function could be replaced by an IR sensitive device used as an earth sensor. The obvious drawback to this type of device during daytime operation is interference from the sun, particularly when it crosses behind the earth. However, at night (when the sun does not appear), an infrared sensor could be effectively used as an earth sensor. Because the earth is fixed in its position with respect to the SLRV point of operation on the moon, an earth sensor would be effective only for missions occurring approximately 10^{o} west of 0^{o} longitude on the moon surface. Star trackers might also be considered; however, as discussed in Volume III, Book 2, these devices are more complex and less reliable than sun sensors. Hence, they are not as desirable for daytime operation. However, they could be used successfully for nighttime operation, although at a penalty in terms of weight and mission time.

The low steady-state temperature which would exist around the vehicle during lunar night affects several subsystems; in particular mechanisms and the properties of materials. It has, for example, been determined that an approximate addition of 4 lb (largely in the traction drive system) would be required to provide a nighttime operational capability in the mobility system. The full impact of nighttime operation on the tracks has not been completely assessed; however, problems in this area may be encountered.

Low temperatures would also affect damping fluids if they are used in the inclinometer. In addition, "wet" lubrications used in sealed bearings and motors would be adversely affected.

Because of the magnitude of the problem, it was not possible to take a thorough look at nighttime operation during the Phase I study. The benefits to be derived from nighttime operation indicate the desirability of extending studies in this area during Phase II.

SECTION 6

SYSTEM DESIGN OF HEAVIER VEHICLES

This section presents the results of a parametric design study of heavier Surveyor Lunar Roving Vehicles. The bounds of the weight category examined are 100 and 150 lb.

For the purposes of the parametric study, the most meaningful parameter is a measure of the increase in the probability of successfully satisfying the SLRV primary mission objective; i.e., verification of the LEM landing site.

The computer evaluation program described in Volume V could be a useful design tool. However, analysis indicates that the computer program should be used only as an evaluation tool. This approach would provide a more comprehensive measure of the effectiveness of the 100-lb system design.

Results of the 100-lb system evaluation have been to aid in the selection of specific functional designs weighing 110, 120, 130, 140 and 150 lb. These designs are evaluated in Section 5, Volume V, to assess the relationship between system weight and probability of success.

6.1 DESIGN OBJECTIVES

Weight is added to the basic SLRV design to produce a significant improvement in the probability of success. The following can result in an increase in the probability of accomplishing the mission:

1. Shorten the mission duration
2. Increase obstacle climbing capability
3. Increase system and subsystem reliability.

The investigation of SLRV system designs weighing more than 100 lb was based on two conditions:

1. The design should include those items or subsystems considered essential but omitted from the basic 100-lb design because of weight limitations; included are safety devices and a marking system.

2. The design should include the addition of weight to various subsystems to cause a significant improvement in the probability of accomplishing the mission. This may be in the form of greater obstacle climbing capability, shorter mission time, and greater reliability in the subsystem designs. Also, the addition of subsystems which will complement existing subsystems must be considered; e. g., including an inertial guidance subsystem in addition to the existing odometer-sun sensor-inclinometer-RF ranging navigation subsystem.

The basic SLRV design without safety and marking weighs 100 lb. A tentative marking system consisting of three 0.5 mil aluminized mylar annular rings, 20 ft in diameter, has been designed (Section 5). On command, stored gas is used to unfold the mylar ring. This marking subsystem design weighs approximately 4 lb, and requires negligible power for deployment.

Tentative design has been completed on a safety subsystem which consists of two powered dummy tracks (equal in size to the mobility tracks) extending in front of the vehicle (Section 5). By measuring the tilt angle of the dummy tracks and the inclination of the support structure, the obstacle height or crevice depth of potential hazards to the SLRV may be determined. This safety subsystem supplements the TV system, and adds approximately 5 pounds to the SLRV system weight. The power requirements for the dummy tracks are 2 watts at all times during vehicle motion.

The addition of these two features increases the weight of the basic SLRV system to about 109 pounds.

Consideration was given to the possibility of increasing system performance through the addition of subsystems which would complement existing subsystems. The navigation subsystem can be supplemented with an inertial guidance subsystem at a weight penalty of approximately 20 pounds. However, such an addition provides little benefit to the basic navigation system other than redundancy for reliability.

A desirable subsystem addition is another vidicon to provide stereo TV capability, and simultaneously provide redundancy in the TV camera system. This is considered further in Section 6.4.

The heavier vehicle designs offer the possibility of increasing the capability of the existing sensors and including other scientific data gathering instruments which are not necessary to fulfill the basic survey mission, but which provide data having general scientific interest concerning the lunar soil characteristics.

In the basic 100-lb design, the penetrometer provided the minimum information about the soil properties necessary to certify a site as suitable for LEM landing. A larger probe tip for the penetrometer would be a desirable addition in the heavier designs, as greater confidence would be gained in the data, and extrapolation to larger areas would be possible. The probe tip diameter in the basic system design is 0.75 in. A tip diameter of 3 in. could be obtained for weight and power increases of about 1 lb and 2 w, respectively.

Because of the weight constraints, other soil characteristic instrumentation could not be included in the 100-lb design. In the heavier designs, such instrumentation devices as a gamma ray densitometer, shear vane meter, jackhammer, and auxiliary wheel might be included.

The gamma ray densitometer provides a measure of the soil density by recording the percentage of gamma radiation scattered and reflected from the surrounding material. The densitometer can be incorporated into the existing penetrometer package without changes in configuration and space requirements, but with an additional weight and power allocation of 1.5 lb and 0.22 w, respectively. The expected accuracy is 20% of the reading.

The shear vane meter provides information about the frictional and cohesive properties of the soil by measuring horizontal or rotary displacement torque. This device can be included in the heavier system design for 1 lb and 8 w.

The jack hammer provides data on the dynamic bearing strength properties of the soil. This would be a supplement to the static data received from the penetrometer, but a considerable weight and power

penalty, as well as a configuration problem is involved. A jack hammer is estimated to weigh 5 lb and to require 5 w.

The auxiliary wheel provides data on the slippage properties of the soil. These data can be obtained by attaching the necessary sensors to the existing odometer wheel in the basic system design. Thus, little weight and power penalty is incurred.

In evaluating the benefit of having each of these soil characteristic measuring devices, the increase in penetrometer tip diameter is the most desirable addition to the heavier vehicle design, with an increase of 1 lb and 2 w. Next in value is the densitometer with an increase of 1.5 lb and 0.22 w. This weight figure may have to be increased if shielding must be included between the densitometer and the RTG power supply. The shear vane meter is next in priority with an increase of 1 lb and 8 w.. Next are the sensors attached to the odometer to provide soil slippage data with a small increase in weight and power. Finally, the jack hammer could be included. This is of lowest priority, and its value traded against the increase in system weight and power caused by its inclusion gives it questionable merit. In the first four additions, the weight additions are cumulative; however, power additions are not necessarily cumulative. RTG size is determined by some combination of transmitter, TV, and mobility requirements. By choosing the sequence of events properly the power increases required by these soil characteristic sensors may be satisfied with little or no increase in RTG capacity. Thus, all of these devices except the jack hammer could be included in the heavier design for approximately 4 lb, and at the most, several watts increase in RTG capacity.

Other subsystems were examined and it was determined that no significant additions could be made to complement existing subsystems, other than those just discussed. Minor improvements in performance can be made in some subsystems with a significant weight penalty. However, these benefits are overshadowed by the large benefits gained by the addition of weight to the transmitter, mobility, scientific payload and TV stereo as discussed in the following sections.

6.2 PARAMETERS AFFECTING MISSION DURATION

This section emphasizes ways requiring the addition of weight to the system rather than a change in operating philosophy. Vehicle reliability

is related to mission duration; therefore, for a given design, a shorter operating time requirement results in a higher probability of success. This is to be distinguished from reliability improvements achieved by changing the design.

There are many ways in which mission time can be reduced with the addition of weight to various subsystems. Some subsystems are considerably more sensitive than others; i.e., the addition of several pounds causes a significant reduction in time to perform a certain function. Others are almost entirely unaffected by the addition of weight. Frequently, the addition of weight to the system is in the form of increased RTG capability, thus making more power available to the subsystem. Generally, an increase in power to a subsystem is accompanied by an increase in weight; e.g., higher transmitter output necessitates a larger TWT. This heavier vehicle trade-off study is premised on the use of an RTG power source, as no design within a 150-lb weight constraint has been conceived that can accomplish the 19-point survey mission without having to survive at least one lunar night.

6.2.1 Data Rate Effects

Parametric data for the transmitter data rate as a function of transmitting system weight is shown in Figure 6-1, for operation with either the 210-ft SFOF facility or the 85-ft DSIF facility. This data rate is expressed in bits per second. A 512 x 512 line digital TV system is assumed, with 4-bit encoding. Thus, there are $512 \times 512 \times 4 = .05 \times 10^6$ bits per frame, and a bit rate of 10^5 bits per second allows a TV frame rate of 10.5 seconds per frame. Frame time as a function of bit rate is shown in Figure 6-1. The transmitting system weight includes both the transmitter proper and that portion of the total RTG weight which is supplying the transmitter input power requirements. The latter is based on an RTG design which yields 1.8 watts of gross power per pound of weight. A power converter efficiency of 80% is assumed, giving:

$$RTG = \frac{P_{input}}{1.8 \times 0.8} = \frac{P_{input}}{1.44} \quad lb$$

as the relationship between the transmitter input power and that portion of the RTG weight which is supplying this power. The transmitted RF power levels are indicated at various places along the curves. The basic 100-lb SLRV design transmits 2 w of RF power and the transmitter plus ΔRTG

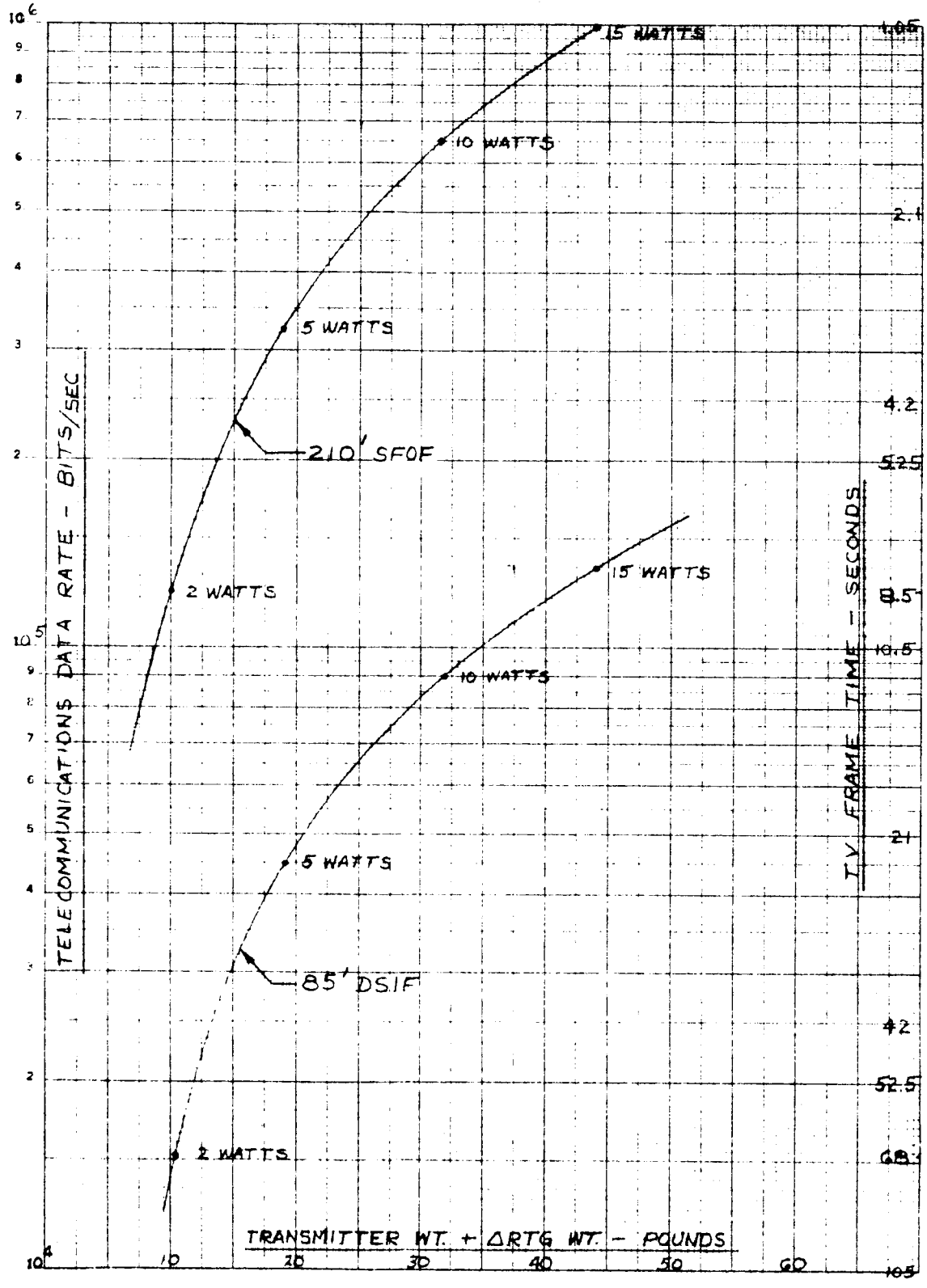

Figure 6-1 Telecommunications Data Rate and Weight Trade-Off

weight is 10 lb. This does not include the weight of the transmitting antenna. From these curves, Figure 6-1, the effect on TV frame time of an increase in transmitting system weight above that of the basic 100-lb system design can be determined, and the consequent change in mission duration calculated.

The mission duration (operational days) as a function of transmitter plus Δ RTG weight is shown in Figure 6-2. Mission duration is based on the complete survey of 19 points in 3-meter travel steps, and also 3-meter steps in the traverse between points. In one point survey, there are a minimum of 830 TV pictures, and a minimum travel distance of 558 meters. In the interpoint traverse, there are a minimum of 167 TV pictures, and a minimum travel distance of 500 meters. In performing the mission time calculations for Figure 6-2, all of the parameters except TV frame time were held constant at the values used for the basic 100-lb design. The minimum time and distance for the various operations involved in completing the mission are modified by factors to account for increases in travel distance caused by the avoidance of surface hazards and also for the abandonment of points that were determined to be unacceptable for LEM after completing part of the survey. These factors are discussed in detail in Section 4, Volume II. The following equation was used to determine the mission times in Figure 6-2;

$$T_M = 19(1.4T_T + 1.8\ T_p)$$

where:

T_M = total operational hours

T_T - minimum hours to traverse between two points

T_p = minimum hours to perform one complete point survey

The multiplying factors in this equation are based on a fairly conservative lunar surface model. The 210-ft SFOF facility is assumed to be available for 11 hours each earth day, and the 85-ft DSIF facilities for either 24 hours per day or 13 hours per day when used in conjunction with the 210 ft SFOF facility. The curves shown in Figure 6-2 are for the three possible ground facility arrangements: 210-ft SFOF only for 11 hours per earth day; 85-ft DSIF only for 24 hours per earth day; or a combination of the two.

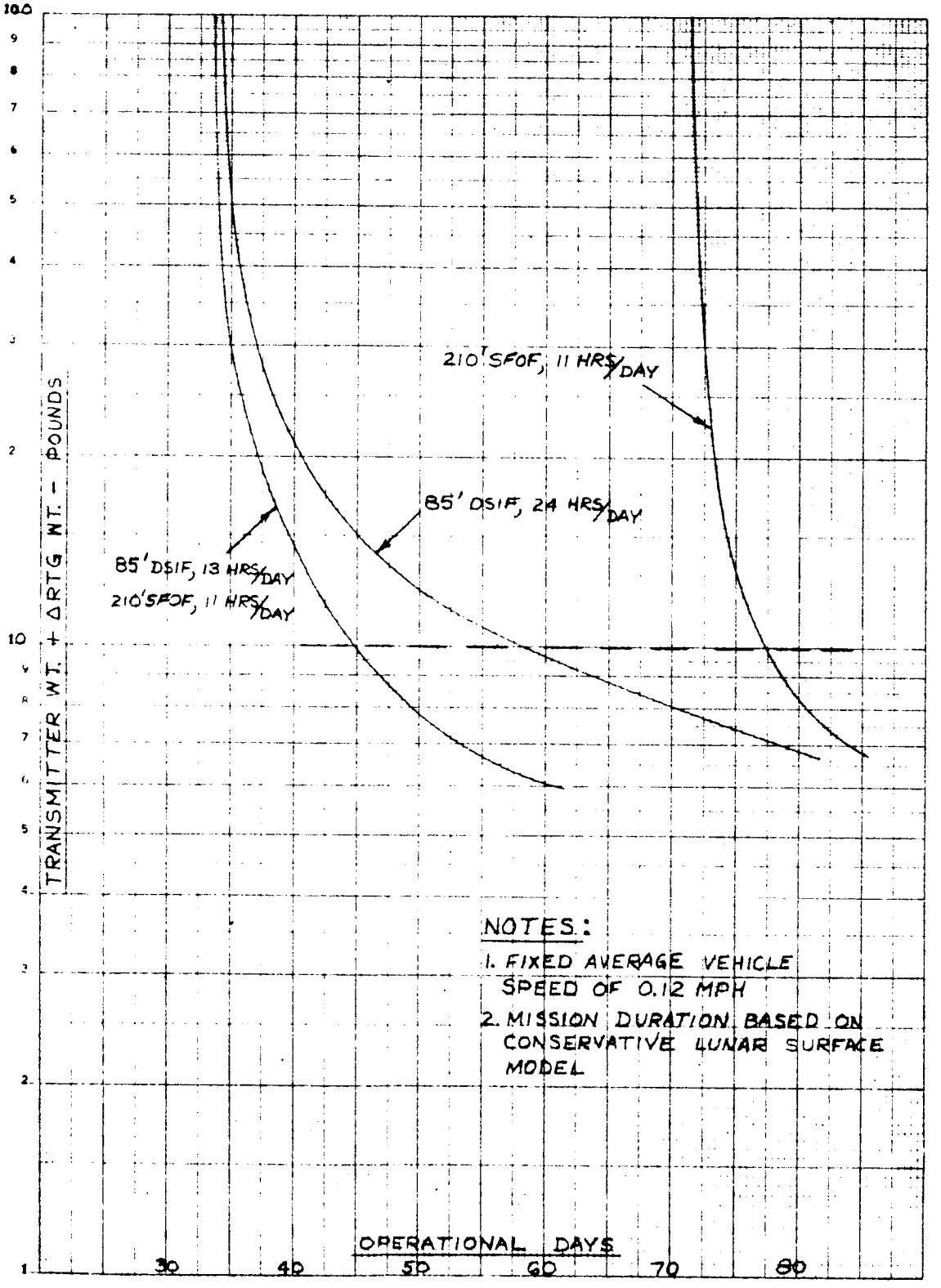

Figure 6-2 Transmitter Weight and Mission Duration Trade-Off

The 85-ft DSIF case is the most sensitive to weight changes. For this case, the addition of 20 lb to the transmitter subsystem reduces operational time by 36%. In every case, however, the addition of more than 20 lbs has little effect in further reducing mission time.

6.2.2 Vehicle Speed Effects

The performance of the transport function is also sensitive to the addition of weight. The transport function consists of the mobility, structure, and deployment subsystems, For considerations relating to shorter mission times, the speed of the mobility subsystem is of primary concern. Parametric data for the heavier designs relating vehicle speed to mobility weight, indicated that there is nearly a linear relationship between speed and input power for a given torque requirement. Accordingly, the graphs shown in Figure 6-3 were generated, based on the mobility power requirements and transport weights of the basic 100-lb system. Increased travel speed is related to the increase in weight of that portion of the RTG supplying the mobility power. This is combined with the total transport weight to arrive at the relationship between transport weight and mission duration for the three possible DSIF modes. The same equation and correction factors were used in calculating mission time as were used in the previous section for the transmitter trade-off data. However, in this case, the variable is vehicle speed rather than TV frame time. Both the composite case (85-ft and 210-ft facilities) and the 210-ft SFOF case are about equally sensitive to weight additions. For these cases, adding 10 lbs to the transport plus Δ RTG weight reduces the mission time 11% from that of the basic 100-lb system. The addition of more than 20 lbs to either case has little effect in further reducing mission time.

6.2.3 Continuous Driving Effect

Mission time can also be reduced by driving nearly continuously between points. However, this requires that TV pictures must be taken while the vehicle is moving; hence, the high-gain steerable antenna must automatically track the earth at all times when the vehicle is moving. This autotracking capability requires the addition of approximately 20 lbs to the system. The reduction is mission time is about 20% for the combined case, and 18% for each of the other two cases. Figure 6-2, shows that the addition of 20 lbs to the transmitter subsystem reduces mission time by 22% for the combined case (85-ft DSIF and 210-ft SFOF), 36% for the 85-ft DSIF only case, and 6.5% for the 210-ft SFOF only case. Thus, if the telecommunications system is designed for either the combined or the 85-ft

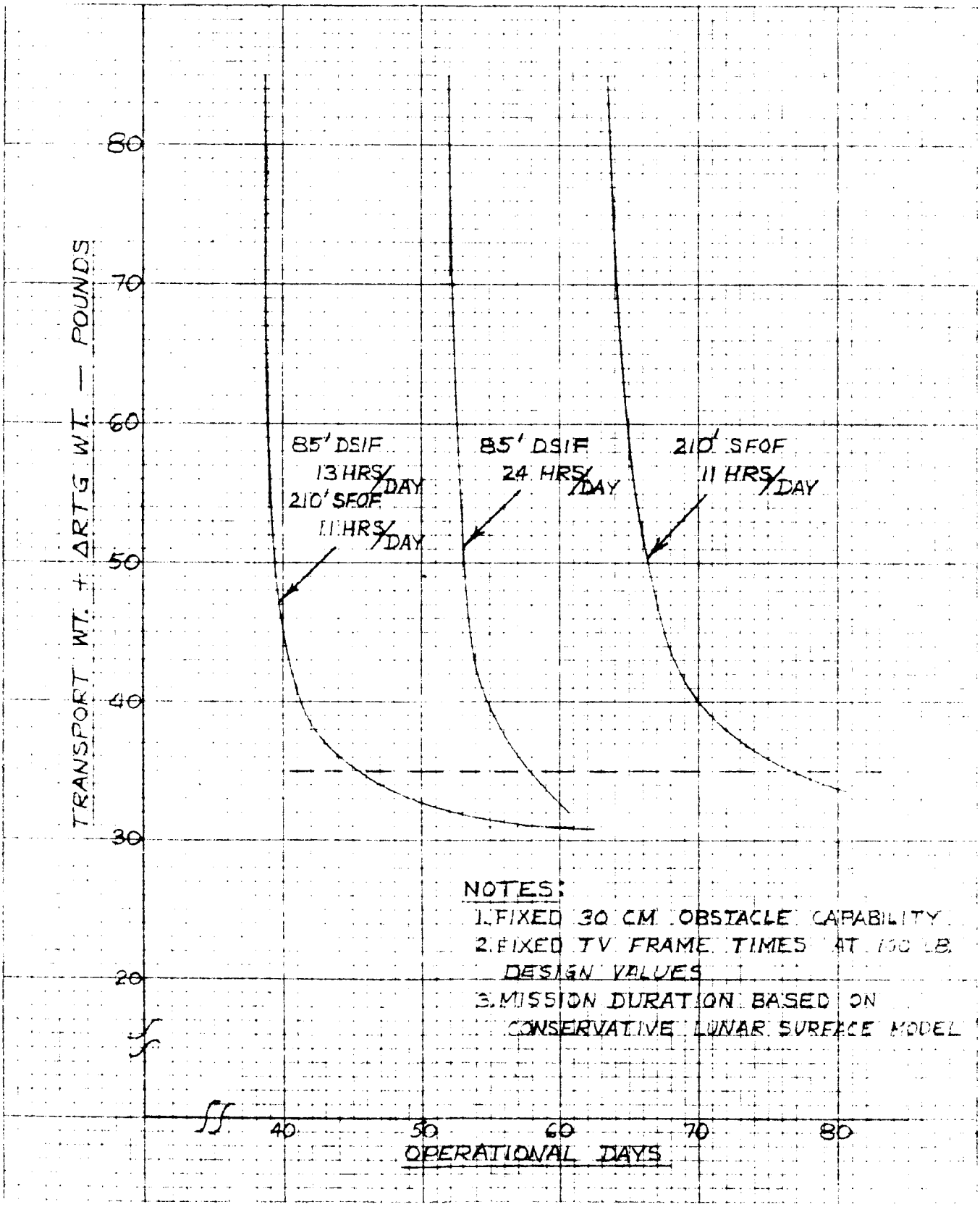

Figure 6-3 Transport Weight and Mission Duration Trade-Off

DSIF only case, the 20 lb causes a greater reduction in mission time when used in the transmitter system. If, however, operation is restricted to the 210-ft SFOF only case, the extra weight should be added in the form of autotracking. Where more than 20 lb can be added to the telecommunications subsystem, consideration must be given to using both means for reducing mission time.

6.2.4 Obstacle Traverse Capability Effect

Some reduction in mission time is achieved by having higher obstacle climbing capability, thus enabling the traverse of otherwise hazardous surface areas, and allowing more straight-line traverses. As part of the SLRV evaluation program, a number of computer runs were made for a variety of lunar surface conditions with a range of obstacle climbing capabilities. The effect of obstacle capability on mission duration is shown in Figure 6-4. The data are related to the weight and design of the basic 100-lb system. The effect on mission duration is shown as the percent above or below the mission duration of the 100-lb design. The graph indicates that above 30 cm, the mission duration is not very sensitive to increased obstacle climbing capability. Below 30 cm, however, there is considerable effect. However, Figure 6-4 does not consider the reduced possibility of encountering impassable terrain with increasing obstacle climbing capability — proportionally more value must be assigned to these systems.

6.2.5 Lunar Night Operation Effects

Another possibility for considerable reduction in mission time is lunar night operation. However, a design for such an operation poses many thermal and optical problems. The low temperature environment necessitates a source of considerably more heating power to maintain electronic equipment within acceptable operating temperature ranges, than is required for lunar night survival. Also, many components such as the traction drive motors, and antenna and TV gimbals, will require more operating power to overcome increased friction at low temperatures. The traction drive mechanism (TDM) would probably require approximately double the power of lunar day operation, and would weigh approximately 20% more. The power and weight increases in the other subsystems cannot be estimated without considerable investigation. The TV operation would perform in a degraded mode, and although "something" would be seen, the value of the information is questionable. Consequently, there

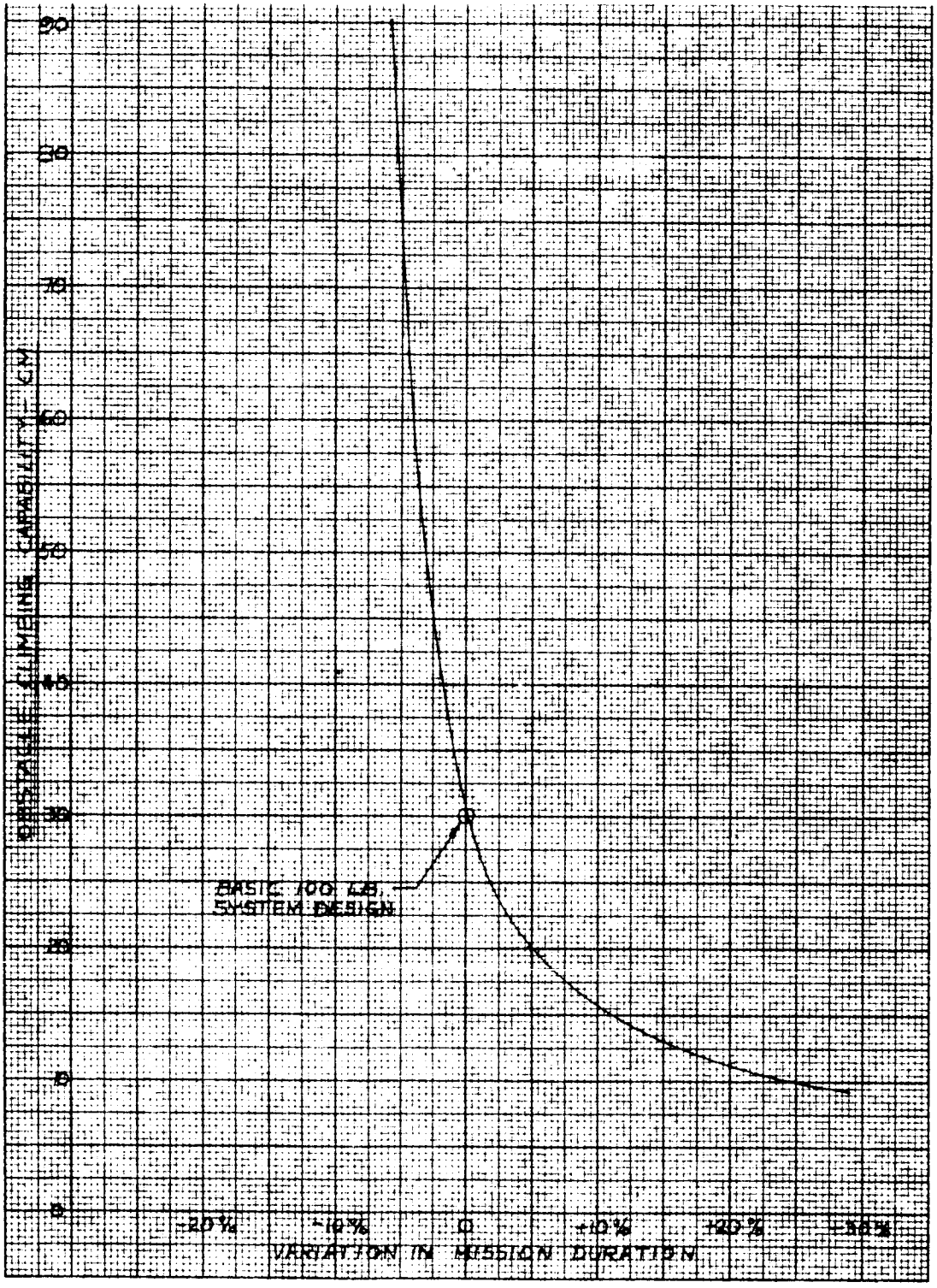

Figure 6-4 Variation in Mission Duration With Obstacle-Climbing Capability

must be a considerable increase in the number of stops for safety reasons. For a given mission duration, an SLRV System having lunar night operation may actually weigh more than a design in which the additional weight is used to supplement lunar day operations with no provisions for lunar night operation.

6.3 PARAMETERS AFFECTING OBSTACLE CLIMBING CAPABILITY

The addition of weight to the SLRV transport system to increase its obstacle climbing capability results in a higher probability of mission success as more of the lunar surface becomes accessible to the SLRV. Hence, travel time and distance can be shortened as fewer detours are necessary, and there is less likelihood of the vehicle encountering impassable terrain. The required obstacle climbing capability for achieving a certain probability of success is dependent on the assumed lunar surface models. For a particular choice of models, a level of obstacle climbing capability is reached beyond which diminishing improvement in probability of success is achieved.

Figures 6-5, 6-6, 6-7 and 6-8 are parametric data pertaining to the transport function of the heavier than 100-lb designs. Figure 6-5 shows mobility subsystem weight (4-track configuration) as a function of obstacle height for a $\pm$ 45° track stop. In Figure 6-6, the vehicle structure weight is shown as a function of obstacle climbing capability. Figure 6-6 is based on designs having up to 100-cm obstacle climbing capability and a maximum of 50 cm undercarriage clearance. Within the space limitations of the Surveyor, a structural fold is essential for vehicles having obstacle climbing capabilities of about 32 cm or more. The structure weights are based on the system weight of the 100-lb design, and Figure 6-6 shows the effect on the structure of supporting the larger tracks necessary for climbing higher obstacles. The effect of vehicle weight on the structure is shown in Figure 6-7. Below a vehicle weight of 110-lb, the structure weight is governed by manufacturing limitations rather than stress. Above 110-lb, the structural weight must be increased to handle the heavier loads. The incremental increases in structure weight with increases in vehicle weight above 100-lb are shown in Figure 6-7.

The deployment subsystem, although not an integral part of the vehicle, is very much dependent on the vehicle design. The relationship between deployment weight and vehicle characteristics is shown in Figure 6-8. For a constant vehicle weight, the deployment weight increases in

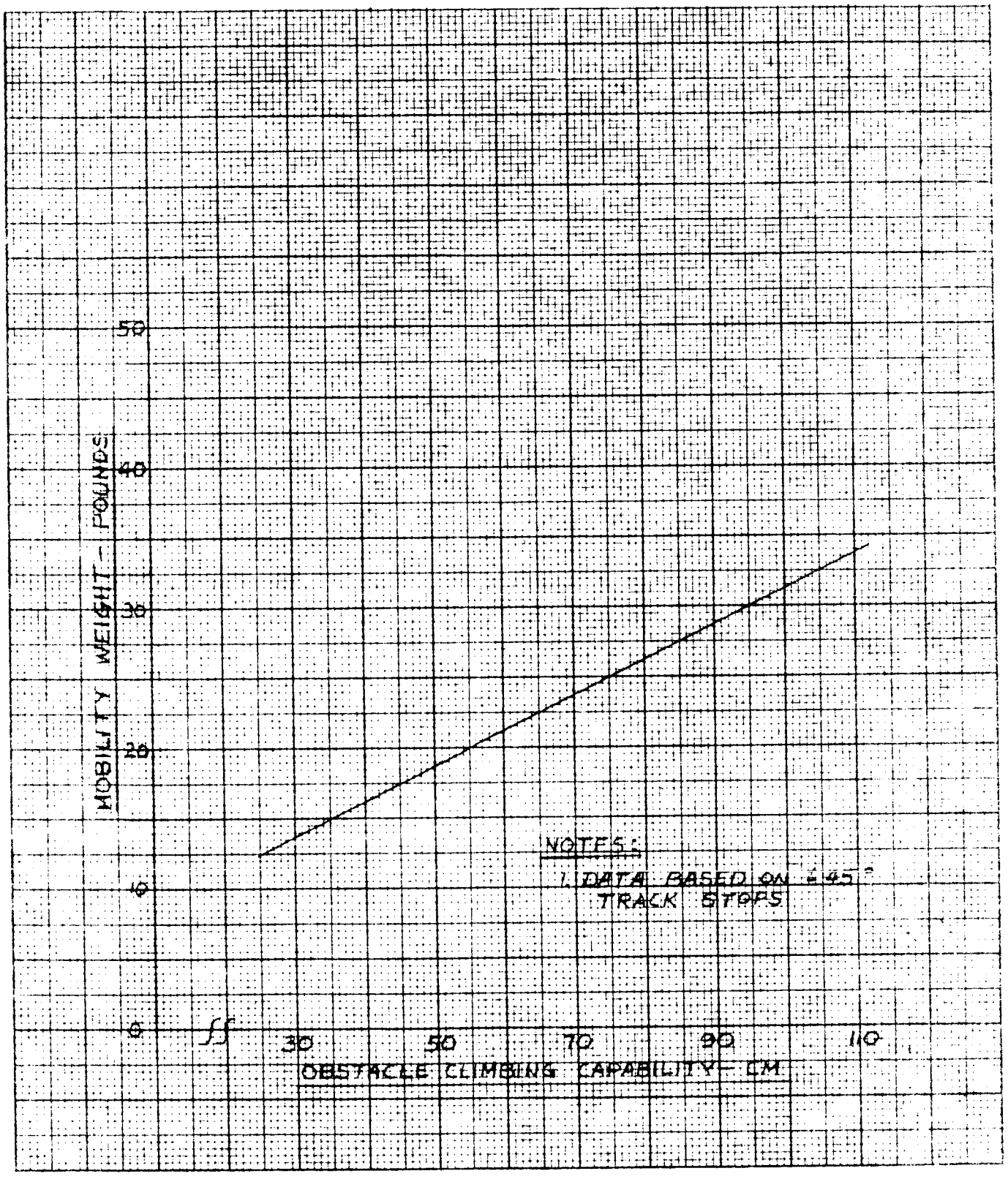

Figure 6-5 Mobility Weight and Obstacle-Climbing Capability

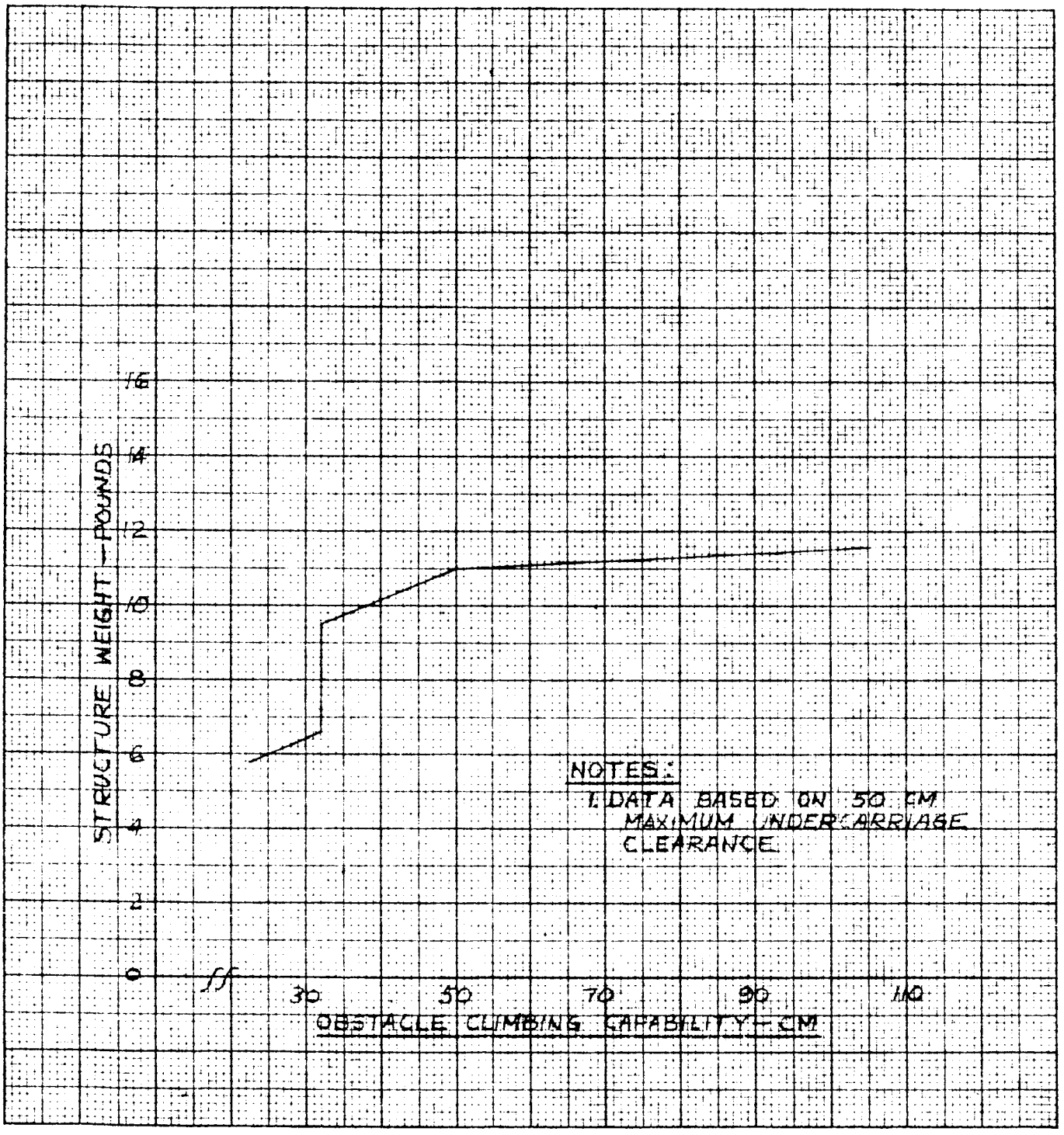

Figure 6-6 Structure, Weight and Obstacle-Climbing Capability

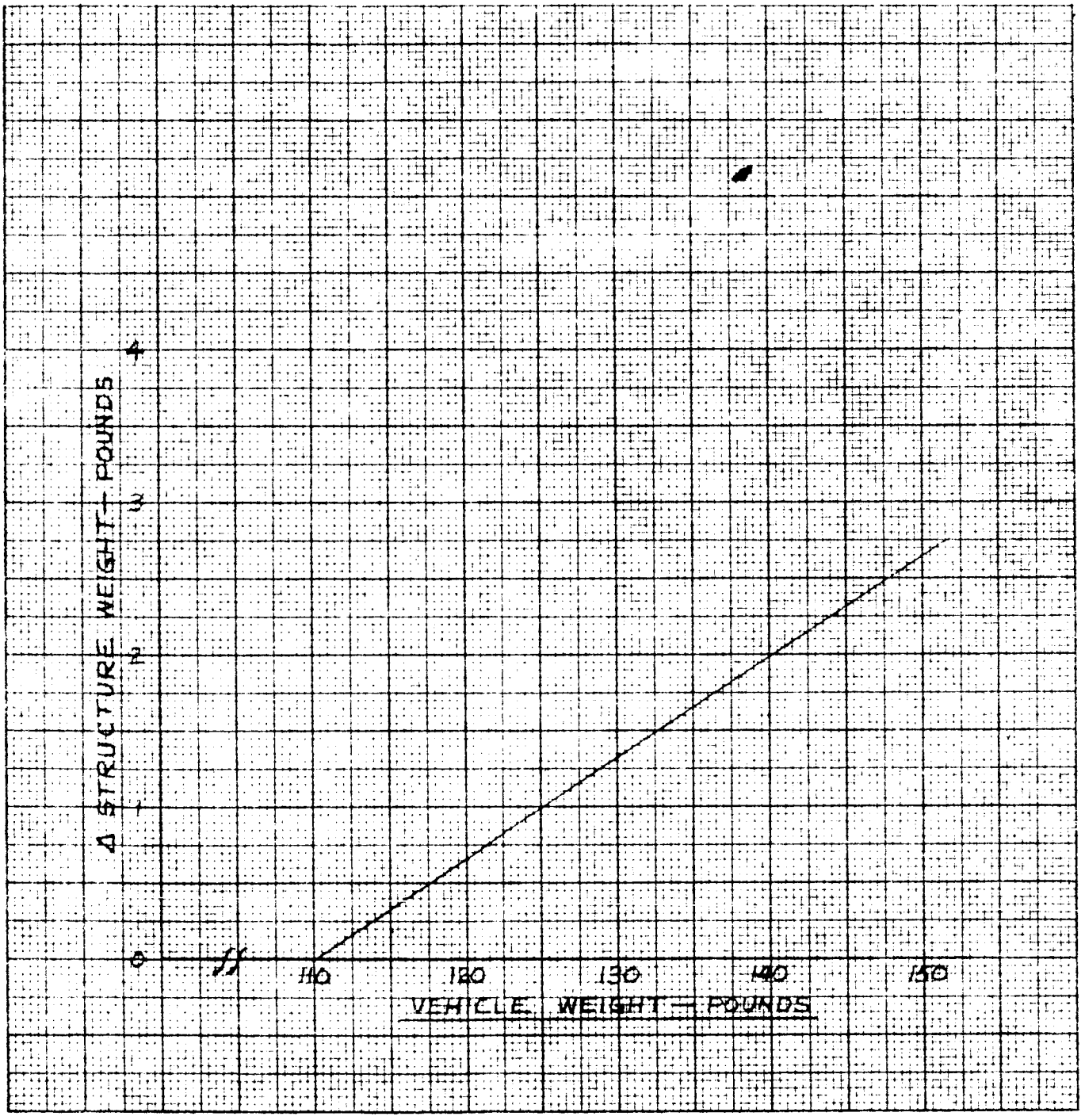

Figure 6-7 Increase in Structure Weight for Vehicles Over 110 Lb

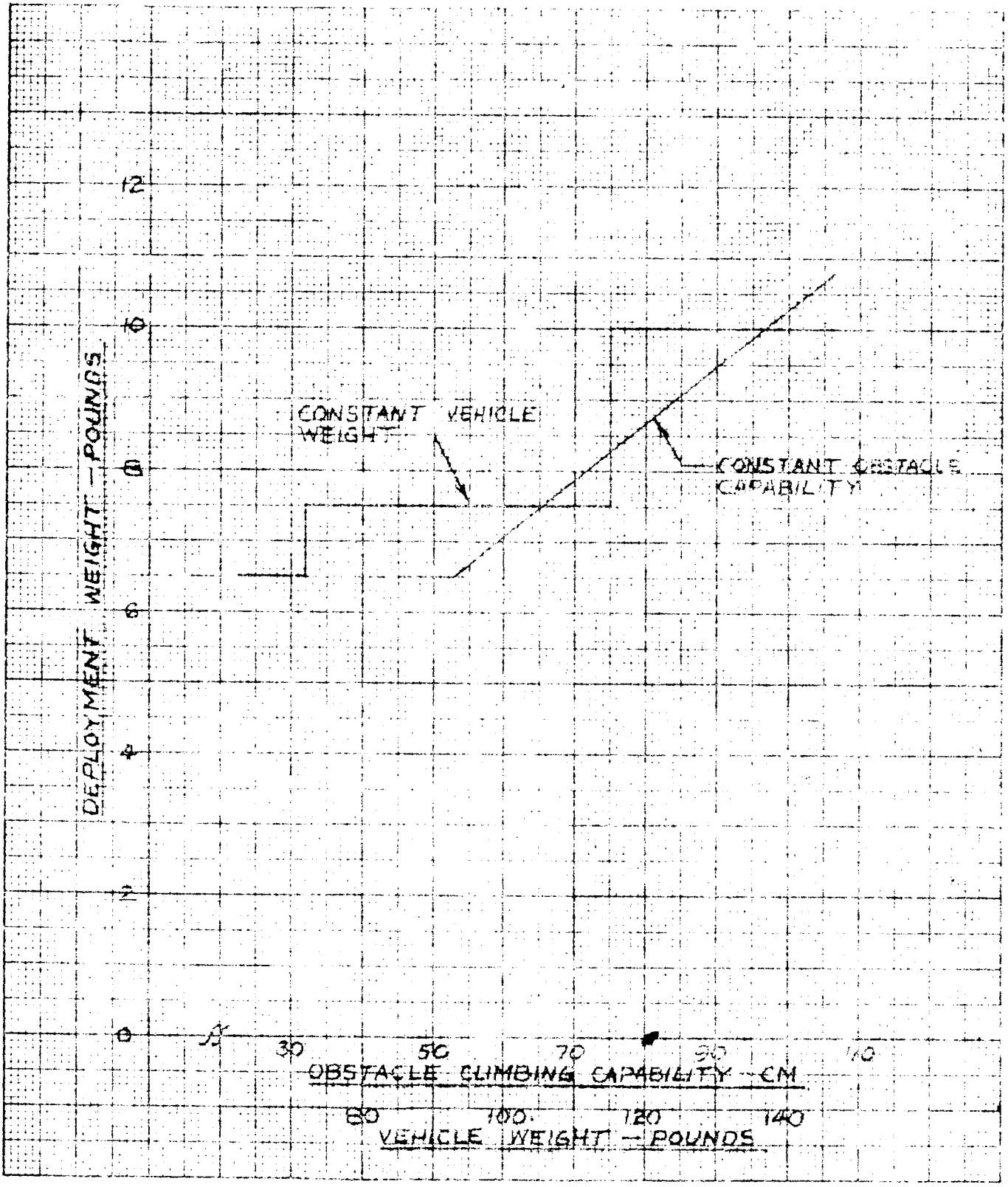

Figure 6-8 Deployment Weight vs Obstacle-Climbing Capability and Vehicle Weight

steps with obstacle capability. For a certain range of track size, the deployment design is essentially fixed. Beyond this range, a new, heavier design is required, and this design remains fixed up to some higher level of obstacle capability. For a fixed obstacle capability, there is a linear relationship between deployment weight and vehicle weight.

The total effect on system weight of increasing the obstacle climbing capability is shown in Figure 6-9, which represents the combined effects of Figures 6-5 through 6-8. A family of graphs is shown, representing various values of the composite non-transport subsystem weights. These include the telecommunications, TV, RTG, etc; i. e., everything in the SLRV System except mobility, structure, and deployment. In the basic 100-lb design, the composite weight of these other subsystems is 70 lb. This does not include safety or marking. The effect on obstacle climbing capability of adding weight to these other subsystems rather than to the transport system for a given system weight is seen. Or conversely, the effect on overall SLRV system weight of adding weight to these other subsystems for a fixed obstacle climbing capability is seen.

The data in this figure are useful for a trade-off study between transport and telecommunications to arrive at the test use of extra weight in achieving the design goals.

6. 4 PARAMETERS AFFECTING RELIABILITY

The third goal for the heavier vehicle is an increase in reliability, which will yield a higher probability of achieving mission success. This goal is directly affected by the two goals discussed previously. In addition, it is concerned with the improvements in reliability resulting from new subsystem designs, higher margins of safety in existing designs, and the addition of redundancy — all of which result in increases in system weight.

A coarse examination of the effects on reliability of adding weight to various critical subsystems was performed with the results shown in Figure 6-10. This first look was only at subsystems where it is known that reliability can be increased through redundancy. There are other subsystems, such as the traction drive motors which are reliability sensitive, but redundancy is not feasible. The curve labeled Basic 110-lb System represents the basic 100-lb system design, plus nine pounds for safety and marking, plus one pound for redundancy in critical circuits in the TV control system, the vehicle command system, and the transmitter coaxial

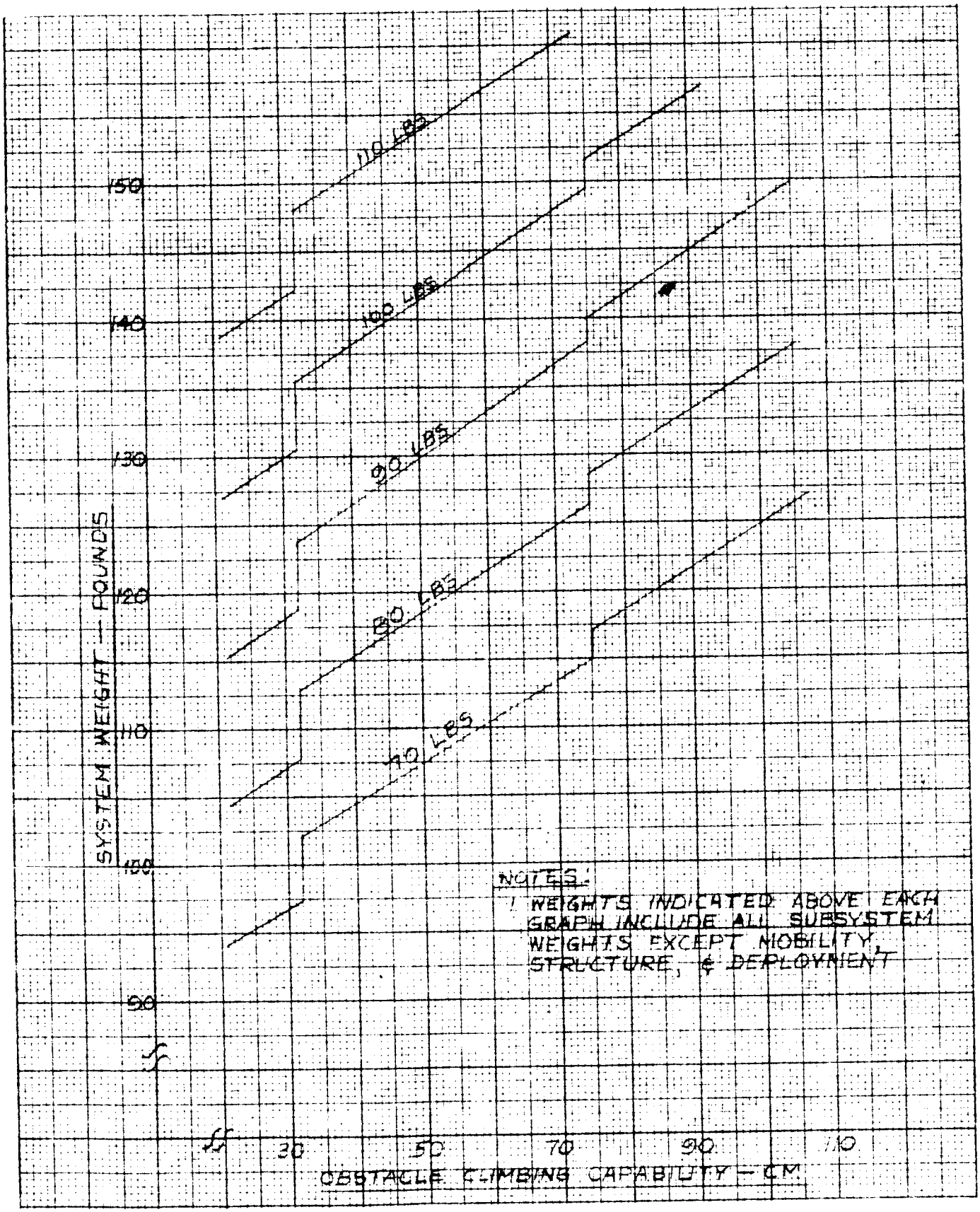

Figure 6-9 System Weight vs Obstacle-Climbing Capability for Various Composite Weights of Non-Transport Subsystems

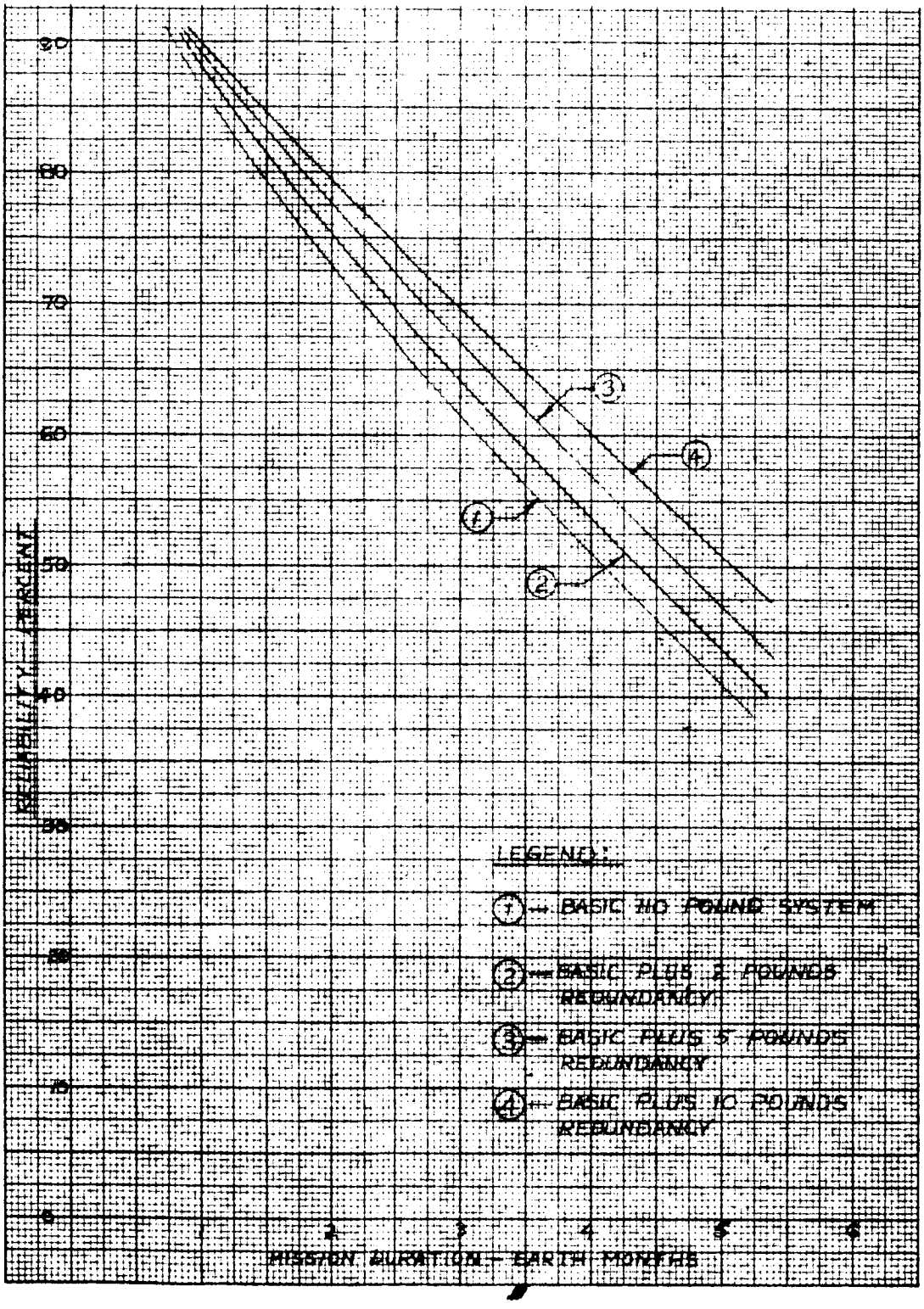

Figure 6-10 Effects on System Reliability of Adding Weight in the Form of Redundancy

switch. Considerable increase in system reliability is achieved with a very small weight penalty in these sensitive items. The curve labeled Basic Plus 2-lb Redundancy includes the redundancy inherent in the basic 110-lb design, plus an increase in track thickness to improve the reliability of the mobility subsystem.

The curve labeled Basic Plus 5-lb Redundancy shows the effect of adding another five lb to provide a redundant TWT in the transmitter. The five lb includes an allowance for structural and thermal plate increases accompanying the redundant additions. At a typical mission duration of three months, the overall system reliability is increased 6% by adding this five lb.

Further increasing the redundant weight to include a dual vidicon in the TV camera subsystem increases the overall system reliability by another 3% at the typical three-month mission point. This is at the expense of another five-lb increase in system weight. Again, the weight increase includes allowance for structural and environmental control increases. The addition of the dual vidicon provides the option of stereo TV capability. This is useful to both the navigation and survey functions and increases confidence in the data obtained from the TV pictures. In addition, stereo TV enables a reduction in decision time, thus causing a small reduction (about 5%) in the overall mission duration. Much of the TV system is shared between the two vidicons, but since this device is one of those most vulnerable to failure, redundancy here will have the most significant effect in increasing the overall reliability of the TV system. If one vidicon fails, the other can be used for monoptic survey and navigation (this is the mode used in the 100-lb design.)

The reliability data presented in Figure 6-10 are used in conjunction with the obstacle climbing capability and mission duration data to perform the final trade-offs in arriving at selected heavier designs.

6.5 TRADE-OFF RESULTS

The primary trade-offs in the heavier that 100-lb design are between mission duration, obstacle climbing capability, and reliability for a given system weight. The parametric data on which this trade-off can be based have been previously discussed. The combined effects on mission duration of increases in the weight of the telecommunications subsystem

and transport subsystem (for faster driving speed) are shown in Figure 6-11. These parametric relationships are based on choosing a value of system weight (> 100 lb), then apportioning the increase over 100 lb between the transmitter and transport subsystems in the combination giving minimum mission duration. For the three DSIF possibilities, the 85-ft DSIF only case is the most sensitive to weight changes. However, since the combined base (85-ft DSIF for 13 hours per day, and 210-ft SFOF for 11 hours per day) gives the shortest mission times, this curve is used in performing the final trade offs.

The results of the trade-off between obstacle climbing capability (Figure 6-9) and mission duration (Figure 6-11) are shown in Figure 6-12 for 10-lb incremental increases in overall system weight between the basic 100-lb design (110 lb with safety and marking) and the 150-lb limit. The system weights shown include nine lbs for safety and marking and one lb for redundancy in subsystems having critical reliability. From this figure, it is seen that for a given obstacle climbing capability, the mission duration becomes less sensitive to increases in system weight beyond 130 lbs. Also, it is seen that for a given mission duration, the obstacle climbing capability is quite sensitive to increases in system weight right up to the 150-lb limit. Thus, if a high obstacle climbing capability is desired for a given system weight, it can be obtained with little sacrifice in mission duration; e. g., with a 140-lb system, the increase in operational days is only 10% when the obstacle climbing capability is doubled from 30 to 60 cm.

To select an optimum system design for each 10-lb increment of system weight from 100 to 150 lbs, a figure-of-merit (FOM) was defined as follows:

$$\text{FOM} \quad \frac{(\text{Obstacle Capability}) \times (\text{Reliability})}{(\text{Weight}) \times (\text{Operational Days})}$$

While the magnitude of the FOM and its dimensions are unimportant, the equation provides a means for selecting the design likely to yield the best overall performance for a given system weight. This approach, although not the only way of defining and selecting optimum systems, provides a convenient means for evaluating the heavier designs based on the essential system design parameters.

For each system weight curve of Figure 6-12, the figure-of-merit is calculated for a number of obstacle capabilities ranging from 30 cm to 120 cm. The operational days corresponding to the selected obstacle

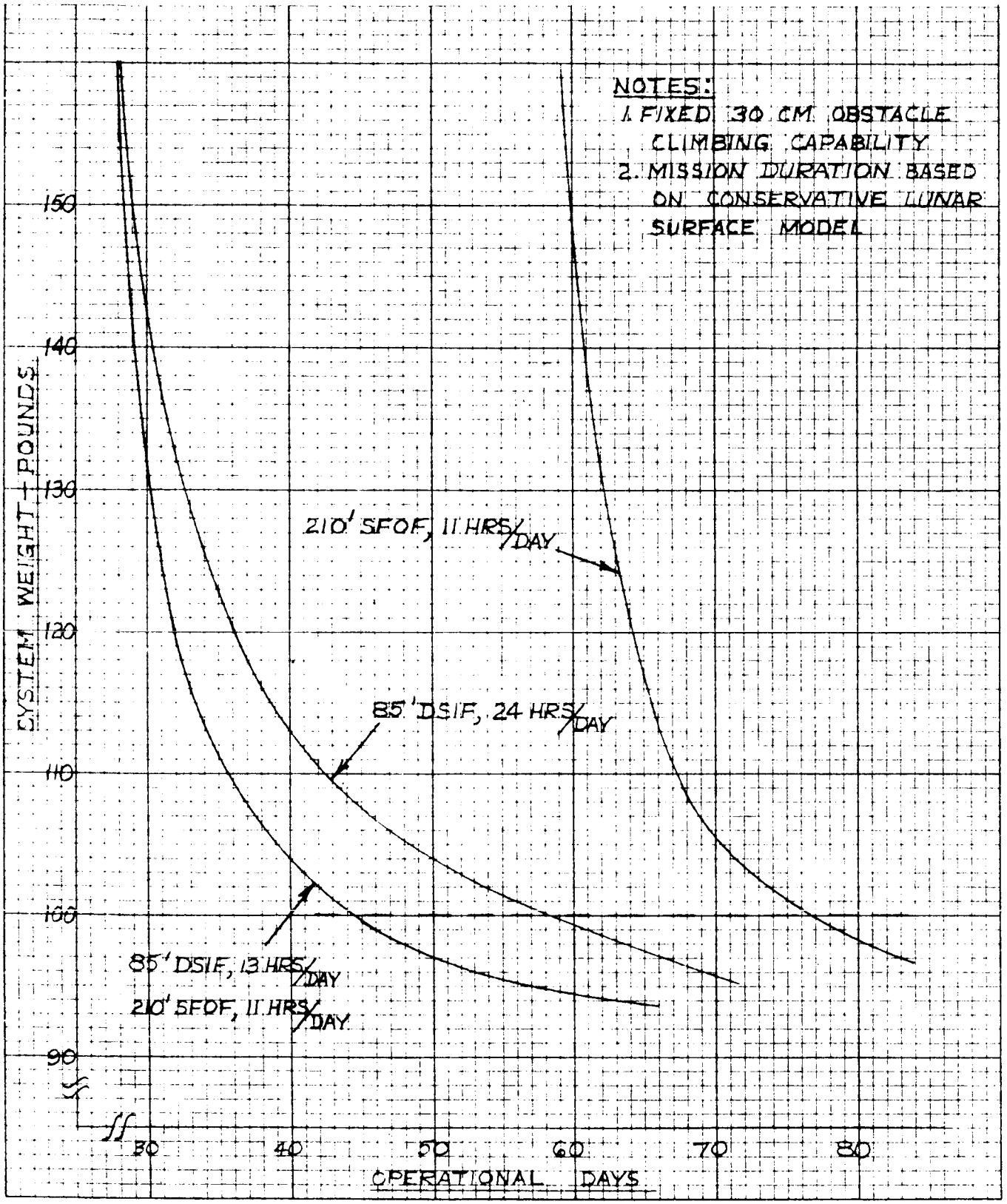

Figure 6-11 Trade-Off Results Between Data Rate and Vehicle Speed for Constant Obstacle Capability

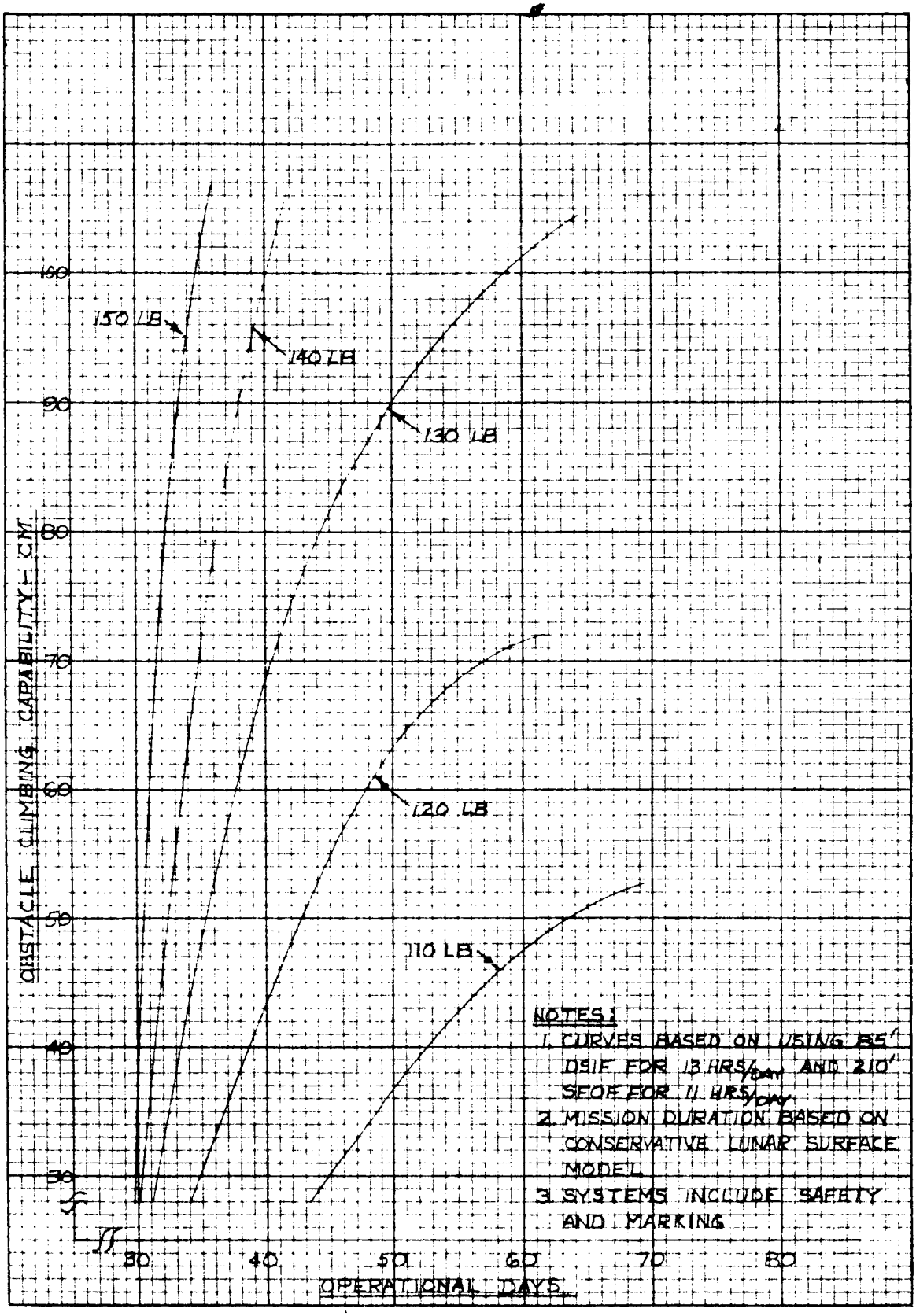

Figure 6-12 Trade-Off Between Obstacle-Climbing Capability and Mission Duration

climbing capability are taken from Figure 6-12. The reliability data are taken from Figure 6-10. The addition of weight for reliability redundancy must be added to the system weight of Figure 6-12, for a given number of operational days. For example, if 10 lbs are added to the 130-lb system for reliability redundancy, the total system weight is 140 lb. However, the 130-lb obstacle capability vs operational days curve of Figure 6-12 is used in calculating the FOM. The FOM results for the 120-lb system design are shown in Figure 6-13 for the addition of 0, 2, 5, and 10 lb for redundancy. The overall weight is held constant at 120 lb. Thus, these weight additions mean that performance is being sacrificed in some other area (obstacle capability and/or mission duration). Each of the FOM curves in Figure 6-13 reaches a peak, but at different values of obstacle climbing capability. Thus, for a given system weight and a given amount of redundancy, an optimum system can be selected. The peaks of the FOM data are given in Table 6-1 for each value of system weight.

TABLE 6-1

FOM DATA PEAKS

System Weight (lb)	Obstacle Capability (cm)	Redundant Weight (lb)	Reliability (%)	Operational Days
110	40	0	52.5	52.5
120	40	10	62	52.5
120	50	5	60	50
120	57	2	50	50
120	60	0	54	48
130	60	10	63	48
130	60	5	68	43
130	60	2	65	40
130	75	0	62	42
140	70	10	71	40.5
140	80	5	68	40
140	90	2	65	40
140	105	0	62	41.5
150	100	10	70.5	40
150	115	5	67.5	41.5
150	110	2	66.0	38
150	115	0	63.5	38

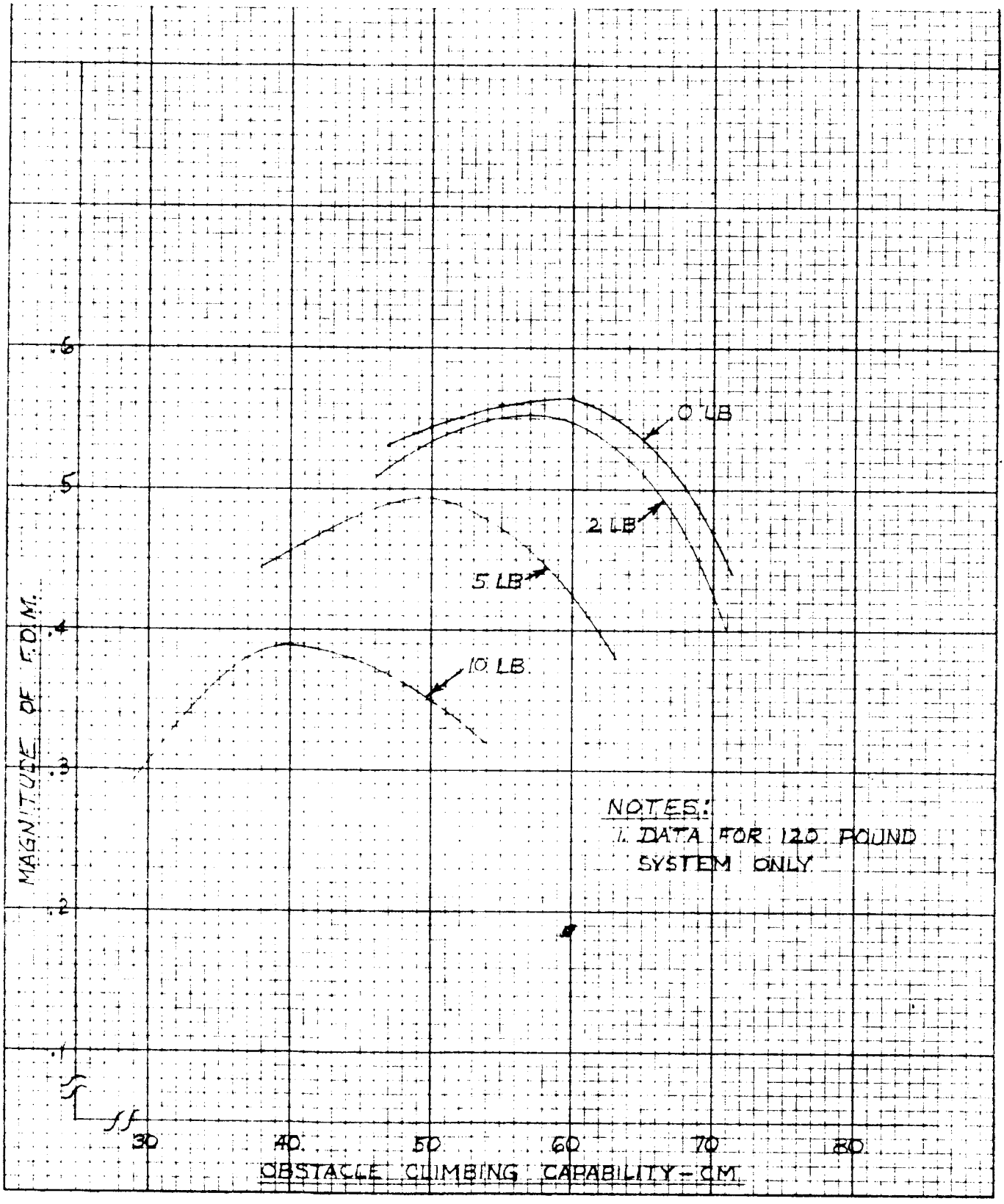

Figure 6-13 Figure of Merit vs Obstacle-Climbing Capability for 120-Lb System Design

II

From these data, it is desirable to select a single system design for each system weight. In arriving at the data presented in Table 6-1, obstacle capability has been traded against reliability and operational days. There is an inherent relationship between reliability and operational days. Increasing mission time increases the probability of subsystem or system failures. Hence, in the final analysis, having a very high obstacle capability at the expense of reliability is not desirable. Since the peaks of the FOM curves for all systems over 120 lb occurred for obstacle capabilities of 60 cm or greater, a final trade will be made between reliability and operational days to select the best choice of redundant weight addition for each system weight. This is justified on the basis that the reliability data used in the previous tradeoffs were not all inclusive, but rather were based on a coarse examination of the most sensitive subsystems, and the effect of the addition of weight in the form of redundancy to these subsystems. Therefore, a shorter mission duration is always desirable, and increases the probability that all subsystems will perform their intended mission. The final tradeoff, then, is made by optimizing the ratio of reliability to optimizing the ratio of reliability to operational days, based on the data in Table 6-1. Dividing reliability in percent by operational days gives the results presented in Table 6-2.

TABLE 6-2

SELECTION PROCESS

System Weight	Redundant Weight Additions 0	2	5	10	Obstacle Capability of Best*
110	1.000	-----	-----	-----	40
120	1.125	1.00	1.20	1.18	50
130	1.475	1.625	1.580	1.310	60
140	1.495	1.625	1.700	1.750	70
150	1.675	1.740	1.625	1.760	100

*Best Choices Are Underlined

The results of this selection process are shown graphically in Figure 6-14. The obstacle capability and mission duration of the five selected designs are presented as a function of system weight in Figure 6-14. All of these system design choices contain the basic subsystems of the original 100-lb design, plus safety and marking subsystems, and at least 1 lb of redundancy in critical plaes such as the TV control system and vehicle command system. Some designs contain additional redundancy as previously discussed.

The characteristics of the five optimum designs for the heavier than 100-lb systems (based on a conservative surface model) are summarized in Table 6-3.

TABLE 6-3

SELECTED CHARACTERISTICS OF DESIGNS OVER 100 LB

System Weight (lb)	Capability (cm)	Reliability (%)	Mission Oper. Days	Duration Earth Months	Redundant[1] Weight-(lb)	Average Travel Speed-MPH
110	40	52.5	52.5	3.83	0	0.07
120	50	60	50	3.75	5	0.07
130	60	65	40	2.90	2	0.18
140	70	71	40.5	2.92	10	0.18
150	100	70.5	40	2.90	10	0.18

[1] The redundant weight additions include the following:

- 0 lb - redundancy in critical circuits of the TV control system, vehicle command system, and transmitter coaxial switch is inherent in the 110-lb design.
- 2 lb - preceding plus an increase in the mobility track reliability.
- 5 lb - preceding plus a redundant TWT in the transmitter.
- 10 lb - preceding plus dual vidicon in the TV camera.

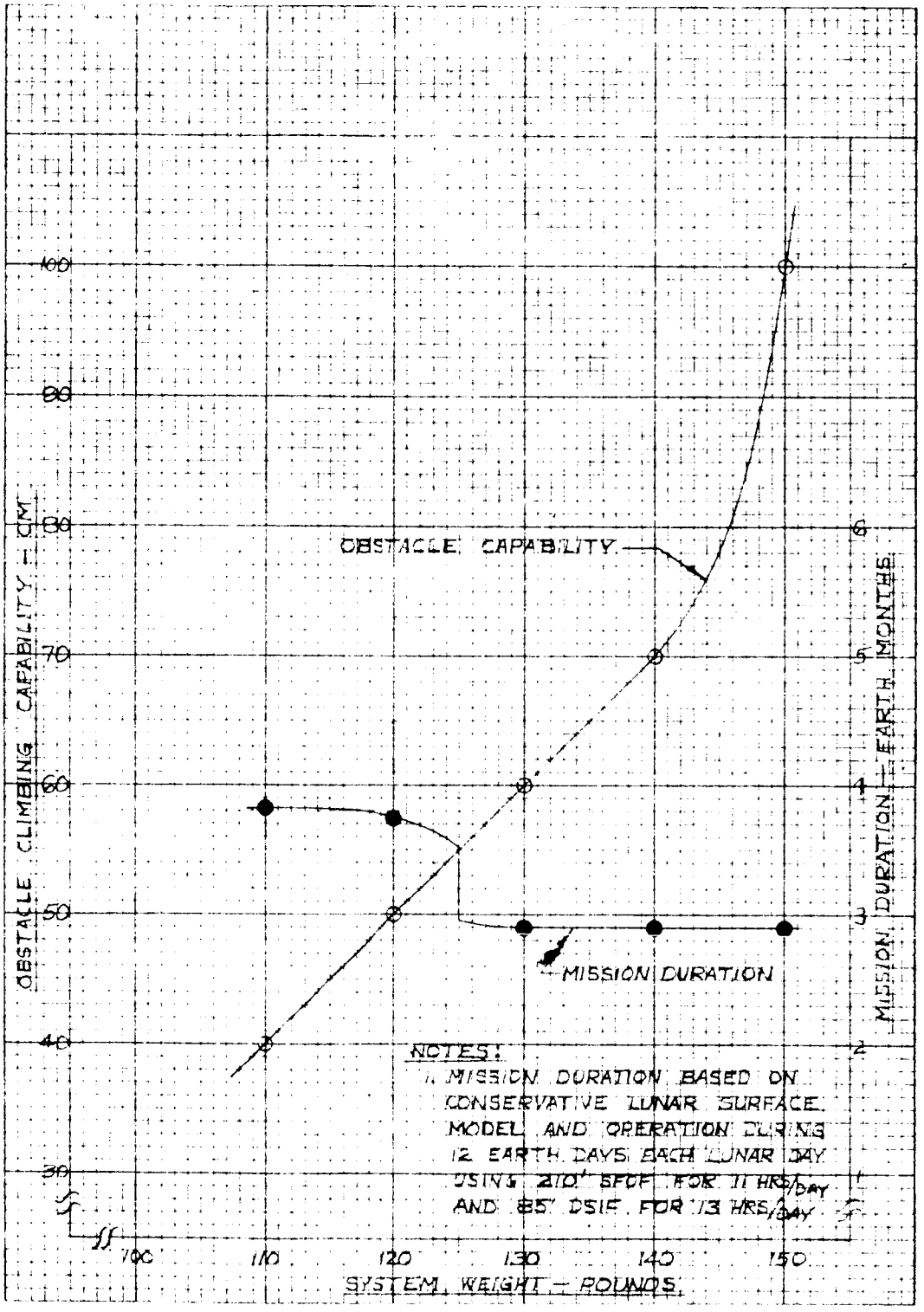

Figure 6-14 Obstacle Capability and Mission Duration of Selected System Designs

The performance evaluation relative to fulfilling the mission objectives of each of these system selections was performed with the aid of the digital computer. The results and conclusions are presented in Volume V, Section 4.

APPENDIX A

IDENTIFICATION OF ACCEPTABLE LANDING POINTS

A.1 INTRODUCTION

The primary objective of the point verification mission is to obtain sufficient lunar surface data to allow verification of the suitability for manned Apollo landing in an area near the spacecraft. When obtained, these data must be presented to the LEM crew such that all acceptable points can be identified by the crew during descent and those points within reach of the LEM capability are made known. Previous studies performed on point identification and marking have considered marking every acceptable point. The obvious drawback to this method is the penalty paid in weight and volume of material required for marking purposes. The study presented in this section is an examination of a method of identification, other than physically marking each acceptable point, and a cursory analysis of the errors involved. These analyses are based on 3 σ error criteria for the establishment of navigation error tolerances and point diameters. If the navigation system provides the necessary performance and the proper point diameter is used, and if each marker satisfies the visual requirements, then a 3σ value (0.997) is assigned to Psi, the probability of identifying a verified point.

A.2 MARKING METHODS

There are two basic methods of marking an acceptable point. One, the active method such as a beacon, has serious disadvantages due to power requirements and reliability problems over extended periods of time. The second, a passive or optical method, has the requirements of long life, good visibility, and extremely low weight and volume if the marking material must be transported from earth.

The active method can be rejected for the following reasons:

1. An active system would require additional equipment on board the LEM; i.e., transmitter and/or receiver, antenna, etc.

2. Any active system required on the lunar surface must be operationally reliable for a period of one year or more.

The second method can be restricted by assuming that it is impractical to mark every acceptable point.

This leaves, as a minimum optical identification scheme, one marked point or landmark and a direction, or two marked points or landmarks and all other acceptable points referenced to them (for example, using the spacecraft and one physically marked point some known distance from it). To clarify a scheme based on two points whose relative positions are known, the following paragraphs examine a nominal LEM trajectory just prior to hover and generate several simple equations to compute the location of acceptable landing points.

A.3 BASIS OF ANALYSIS

One of the nominal trajectories used by NASA for the LEM descent to the lunar surface is described as follows:

1. Detach from Apollo spacecraft in 185 km circular orbit about the moon.

2. Inject into an elliptical orbit with penilune over the landing area and a perilune altitude of 15, 270 meters.

3. At approximately 11 degrees central angle from the landing area, start main retro phase to reduce lateral motion to zero and altitude to 1527 meters above landing area. Time of main retro ≈ 400 seconds.

4. Vertical descent to hover altitude of 153 to 305 meters.

5. Perform any lateral motion required to place craft over landing point.

The trajectory for the last 26 seconds of main retro phase is illustrated in Figure A-1. The last 26 seconds were chosen since this illustrates the approximate LEM position and velocity with respect to the landing point when the ground range is approximately one mile and the depression or look angle to the point is approximately 45 degrees. The larger look angle is desirable because of angle measurements accuracy.

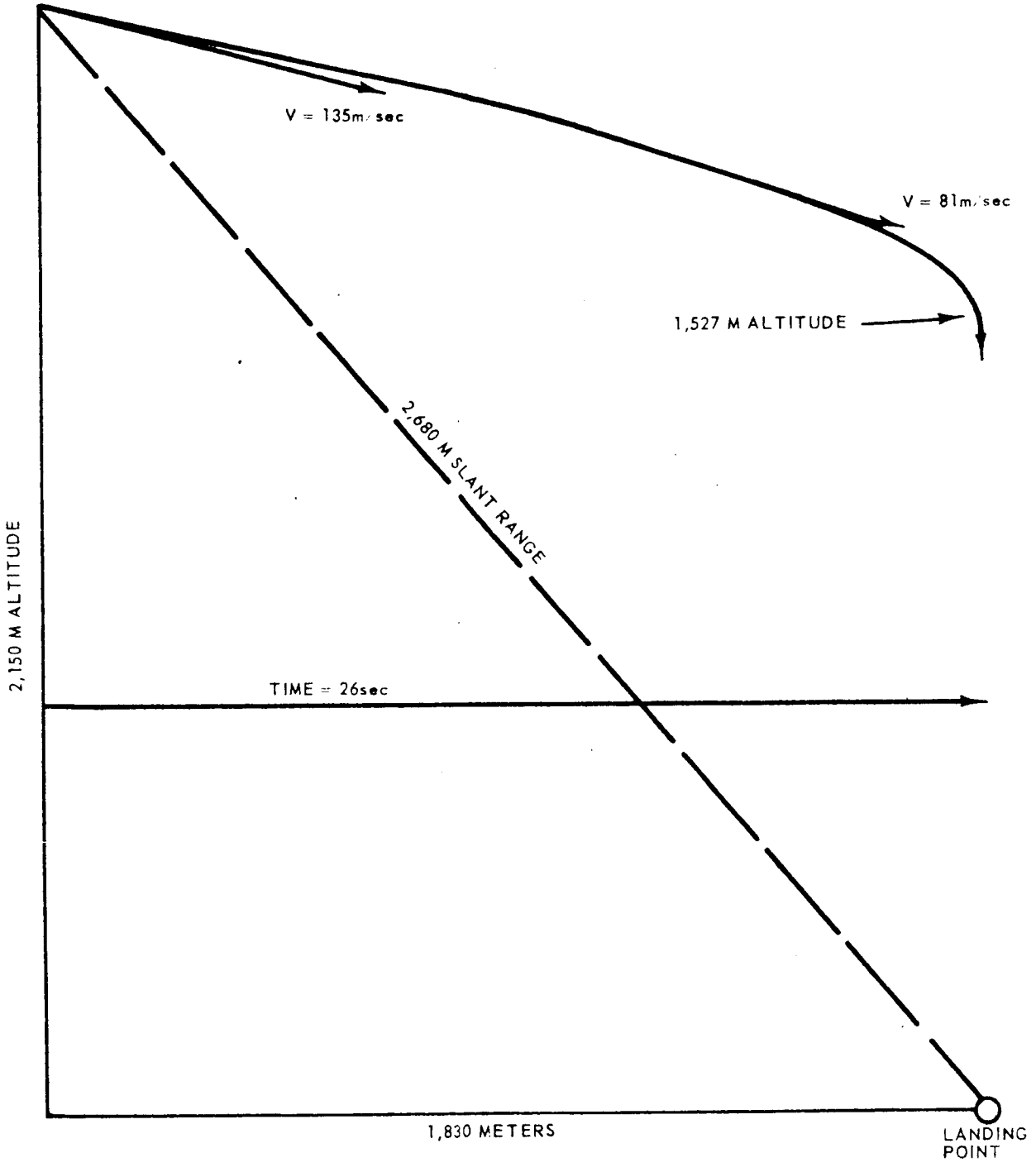

Figure A-1 Trajectory for Final 26 Sec of Main Retro Phase

Assuming that both the spacecraft and marked point are visible at the 2150-meter altitude, the following equations are generated as a possible way of computing an acceptable landing point within the capability of the LEM.

A.4 ANALYSIS

A.4.1 General

The analysis given in the following paragraphs is divided into five areas:

1. Known quantities
2. Measured quantities
3. Computation
4. Procedure
5. Errors

A.4.2 Known Quantities

1. Distance between spacecraft and one landing point (physically marked)
2. The position of other landing points, not marked, relative to the spacecraft and marked landing point; i.e., the position of all acceptable points in the landing area in rectangular coordinates with the origin at the spacecraft and the abscissa through the marked point (see Figure A-2).

A.4.3 Measured Quantities

h = altitude of LEM above lunar surface

η = vertical depression angle to spacecraft from LEM

ψ = vertical depression angle to marked landing point at position (d, o) from LEM.

A.4.4 Computation

Measuring h, η, and ψ, the ground distance from LEM to spacecraft is:

$$R_s = \frac{h}{\tan \eta} \tag{A-1}$$

and the ground distance from LEM to the marked point is

$$R_m = \frac{h}{\tan \psi} \quad . \tag{A-2}$$

Since d is known, three sides of the triangle, spacecraft to marked point to LEM ground projection, are obtainable (see Figure A-3).

The position of the LEM can be computed by

$$\cos \alpha = \frac{d^2 + R_s^2 - R_m^2}{2d\, R_s} \tag{A-3}$$

$$x_l = R_s \cos \alpha \tag{A-4}$$

$$y_l = R_s \sin \alpha \tag{A-5}$$

Computation of α gives a reference direction that can be established within the LEM parallel to the abscissa of the x, y coordinate system.

Based upon the remaining trajectory profile to hover, the hover position (x_h, y_h) can be predicted. The predicted value can be continuously updated by the inertial measurement unit. At this point, the direction and distance to the closest acceptable landing point can be computed:

$$R_{ha}^2 = (x_h - x_a)^2 + (y_h - y_a)^2 \tag{A-6}$$

$$\tan \theta = \frac{(y_h - y_a)}{(x_h - x_a)} \tag{A-7}$$

where θ is the angle from the reference line to the LOS between LEM and landing point.

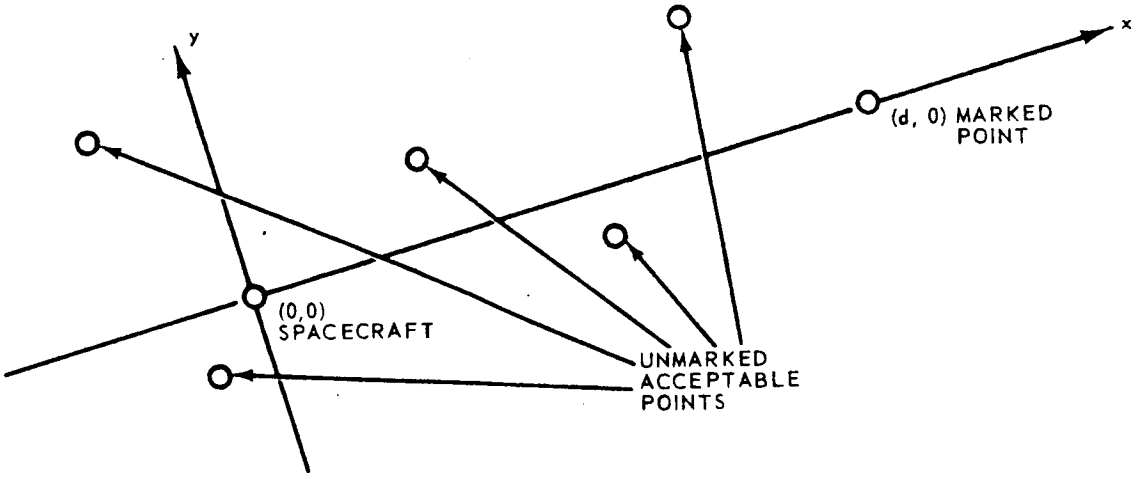

Figure A-2 Typical Landing Area

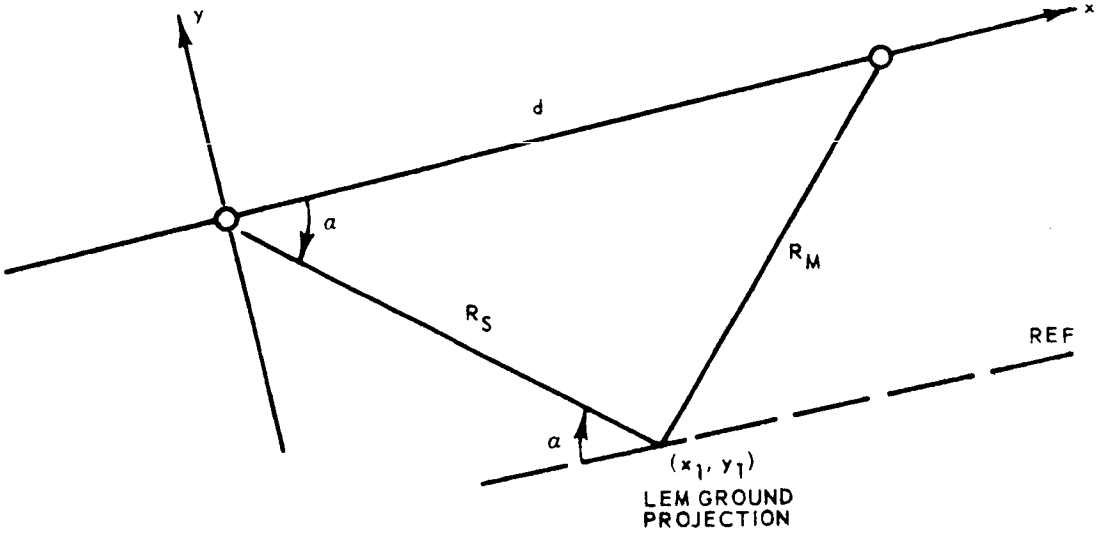

Figure A-3 LEM Position Computation Geometry

A.4.5 Procedure

A procedure is suggested below for landing commencing with the LEM at an altitude of 2150 meters and assuming that at this altitude the spacecraft and the one marked point are easily seen by the crew:

1. Using Optical Measurement Unit (OMU) with direct angle read-out to the computer, measure the depression angles to the spacecraft and marked point.

2. The computer determines the LEM position in the ground plane from the equations given above and the basic reference for measuring all angles at the LEM.

3. The velocity vector of the LEM is computed and updated for the remaining trajectory to hover.

4. The points within the range capability of this hover position are now known to the crew.

5. The distance and direction to the closest acceptable point is computed by Equations (A-6) and (A-7).

A.4.6 Error Analysis

The procedure for determining and landing on an acceptable point contains three basic errors. These errors are broadly defined as:

1. LEM position error: includes the measurement and computation errors used to set up the coordinate system and the platform error in updating to the hover position.

2. LEM guidance error from the moment the lateral motion about the moon is zero to touchdown.

3. Error in relative point location: derived primarily from the SLRV navigation system.

The first two errors are not under the control of the SLRV; however, the feasibility of any scheme must consider them. The third error is of primary importance to the SLRV design. There exists a definite

relationship between the LEM position error and the SLRV navigation error since the measurements used to compute LEM position involve the error in relative marker location.

The LEM position error can be divided into two sources: (1) the error introduced by the Inertial Measurement Unit (IMU) in updating position during the final 1830-meter ground range motion, and (2) the measurement errors in altitude and depression angles. The IMU errors can be approximated by the following.

For the accelerometer; $1/2\ gt^2$ x accelerometer accuracy ≈ 0.3 meter, where g is assumed to be ≈ 6 lunar g's deceleration, t = 26 seconds and the accuracy 1 part in 10^4.

For the gyro: $1/2\ gt^2$ x gyro drift rate $<< 0.3$ meter, where the gyro drift rate is assumed to be on the order of 0.01 degree/hour.

The error in guiding the LEM from the hover position to a selected point (a maximum distance of 305 meters) can again be monitored by the IMU as changes in the LEM position and should be considerably less than the error indicated above. Thus, the LEM guidance error from hover to touch down and the LEM position error due to the IMU can be neglected.

The LEM position error as a function of measurement errors is defined as follows:

1. Altimeter error (Δh), assumed to be 0.1%. At 2150 meters altitude, Δh is equivalent to 2.1 meters.

2. Angular measurement errors ($\Delta\psi$ and $\Delta\eta$) by the Optical Measurement Unit, assumed to be 0.1 degree.

3. SLRV measurement error in distance between markers (Δd), which is a varaible.

The position of the LEM is defined by:

$$x_1 = f_1(h,\ d,\ \eta,\ \psi) \qquad (A\text{-}8)$$

$$y_1 = f_2(h,\ d,\ \eta,\ \psi)$$

However, since bounding the errors is of concern here, only one of the two coordinates need be examined. By assuming values for d and h, and taking the partial derivatives of x_1 with respect to d, h, ψ, and η, the error in the position coordinate can then be determined by

$$\Delta x_1 = \left[\left(\Delta h \frac{\partial x_1}{\partial h} \right)^2 + \left(\Delta d \frac{\partial x_1}{\partial d} \right)^2 + \left(\Delta \psi \frac{\partial x_1}{\partial \psi} \right)^2 + \left(\psi\eta \frac{\partial x_1}{\partial \eta} \right)^2 \right]^{1/2} \quad \text{(A-9)}$$

Before evaluating Equation (A-9), another approach may simplify the computations.

The addition of a third marker to the situation allows the LEM crew to select a triangle with minimum sensitivity.

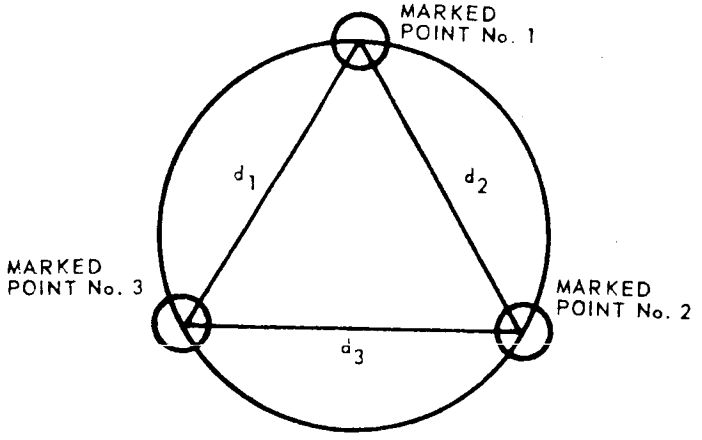

Figure A-4 Three-point Geometry

From Figure II-A-4, the maximum values of ψ and η are where the LEM at hover occurs over the midpoint between two marked points. With a hover altitude of 1500 meters and a d-value of 2000 meters,

$$\psi_{max.} \text{ or } \eta_{max.} = \tan^{-1} \frac{1500}{1000} \approx 56 \text{ degrees.}$$

The minimum value of the depression angles to any marked site occurs at 26 seconds prior to hover:

$$\psi_{min.} \text{ or } \eta_{min.} = \tan^{-1} \frac{2150}{3800} \approx 29 \text{ degrees}$$

The LEM has a capability of measuring slant range to any of the three markers by measuring the angular size of the markers. Assuming an angular uncertainty of 0.1 degree and a maximum slant range of approximately

$$R_{SL_{max}} = \left[(2150)^2 + (1800 + 2000)^2\right]^{1/2} \approx 4400 \text{ meters,}$$

the accuracy of measuring slant range is

$$\frac{4400 \times 0.1^{o}}{57.3} \approx 7.7 \text{ meters.}$$

Slant range can be converted to ground range through altitude or depression angles; i.e.,

$$R_{GND} = (R_{SL}^2 - h^2)^{1/2} = R_{SL} \cos \psi \qquad \text{(A-10)}$$

Using the first expression,

$$\frac{\partial R_{GND}}{\partial h} = - \frac{h}{R_{GND}} \approx \frac{2150}{1000} = 2.15$$

$$\frac{\partial R_{GND}}{\partial R_{SL}} = - \frac{R_{SL}}{R_{GND}} \approx \frac{1800}{1000} = 1.8$$

From before, $\Delta h = 2.1$ meters and the worst case error, R_{GND}, is

$$\Delta R_{GND} = \left[\left(\Delta h \frac{\partial R_{GND}}{\partial h}\right)^2 + \left(\Delta R_{SL} \frac{\partial R_{GND}}{\partial R_{SL}}\right)^2\right]^{1/2} \qquad \text{(A-11)}$$

$$\Delta R_{GND} \approx 14.5 \text{ meters}$$

From Equations (A-3) and (A-4),

$$x_1 = 1/2 \left[d + \frac{1}{d} \left(R_S^2 - R_M^2 \right) \right] \qquad \text{(A-12)}$$

where R_S and R_M are ground ranges to two markers. Thus,

$$\frac{\partial x_1}{\partial R_S} = - \frac{\partial x_1}{\partial R_M} = \frac{R_S}{d} \approx \frac{1800}{2000} = 0.9$$

$$\frac{\partial x_1}{\partial d} = 1/2 \left[1 - \frac{1}{d^2} \left(R_S^2 - R_M^2 \right) \right] = \frac{1}{2} \left[1 - \frac{(0)^2 - (2000)^2}{(2000)^2} = 1.0 \right]$$

These values are computed assuming worst-case conditions. The error in the position coordinate, x_1, can now be computed from

$$\Delta x_1 = \left[\left(\Delta d \frac{\partial x_1}{\partial d} \right)^2 + \left(\Delta R_S \frac{\partial x_1}{\partial R_S} \right)^2 + \left(\Delta R_M \frac{\partial x_1}{\partial R_M} \right)^2 \right]^{1/2} \qquad \text{(A-13)}$$

and from Equation (A-11)

$$\Delta R_S = \Delta R_M = \Delta R_{GND} = 14.5 \text{ meters}$$

$$\Delta x_1 = \left[(\Delta d)^2 + (16.4)^2 \right]^{1/2} \qquad \text{(A 14)}$$

A plot of Δx_1, the error in LEM position coordinate, as a function of Δd, the accuracy in marker position is shown in Figure A-5.

Each landing point will be located to some accuracy with respect to the marker. It is a reasonable assumption that the points can be located to the same accuracy with respect to the marker as the marker can be to an absolute reference. Therefore, the total error can be written as:

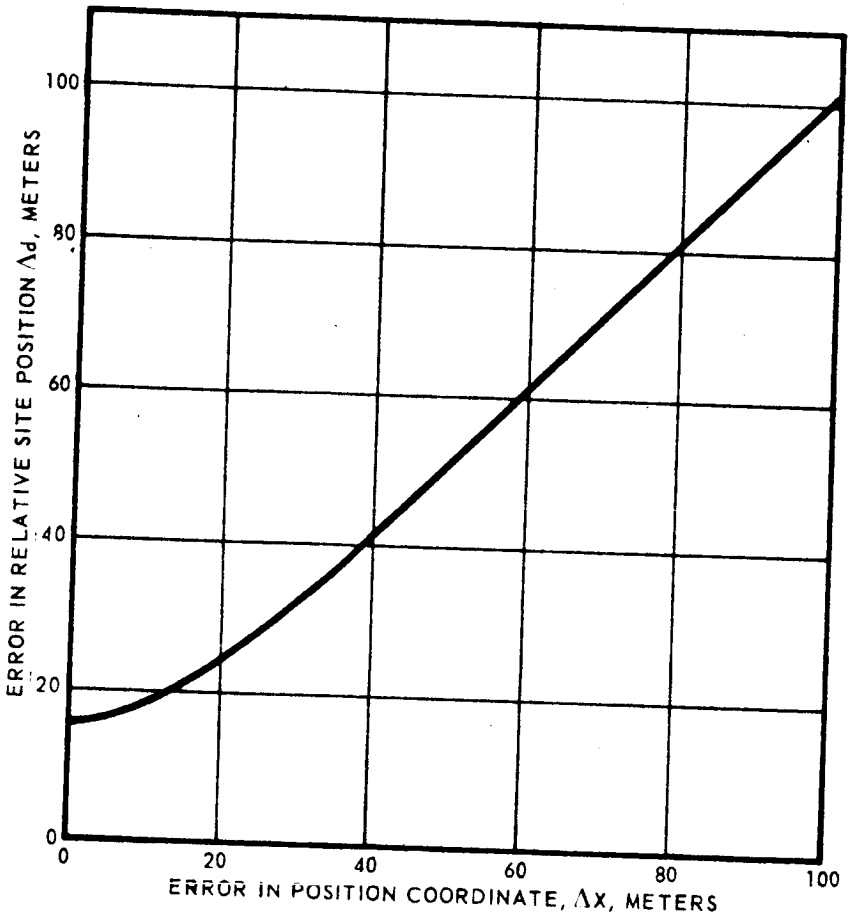

Figure A-5 Position Error as a Function of Relative Site Position Gear

II

$$TE = \left[(\Delta x_1)^2 + (\Delta d)^2\right]^{1/2} \quad \text{(A-15)}$$

or, substituting Equation (A-14)

$$TE = \left[2\,(\Delta d)^2 + (16.4)^2\right]^{1/2} \quad \text{(A-16)}$$

This relationship is shown in Figure A-6, plotting total error as a function of Δd, the relative point location error.

It is necessary that the point diameter equal or exceed the sum of TE plus the LEM footpad span. Assuming a 10-meter LEM span, this relationship is plotted in Figure A-7. Combining Figure A-7, point size as a function of total error, with Figure A-6, total error as a function of point location error, yields the desired result i.e., the point diameter as a function of LRV navigation errors. This is plotted in Figure A-8. The corresponding equation is

$$D = \left[2\,(\Delta d)^2 + (16.4)^2\right]^{1/2} + 10 \quad \text{(A-17)}$$

where

D = point diameter, meters

Δd = point location error, meters.

A.4.7 Point Diameter/Navigation Accuracy Requirement

Equation (A-17) relates the required point diameter as a function of point location error, or SLRV navigation error. The selection of the point diameter involves a conflict between navigation accuracy and internal point vehicle travel. For expedient point survey and verification, it is desirable to use small point diameters. This, however, may require extremely high navigation performance. Preliminary analysis indicated that a 40-meter point diameter with 20-meter location error would be a suitable selection. Accordingly, these values were established as the appropriate system requirement, subject to final validation.

The following conclusions can be reached from this error analysis:

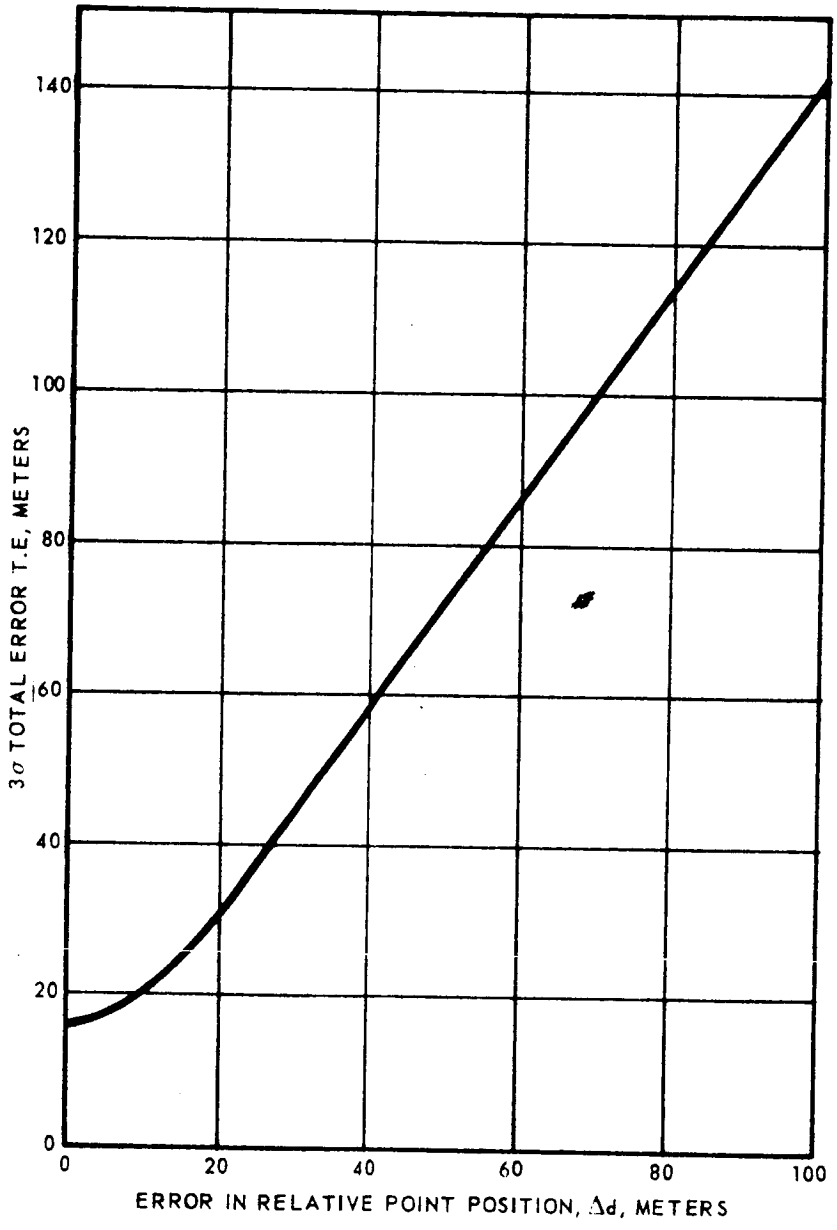

Figure A-6 Total Error as a Function of Relative Site Position Error

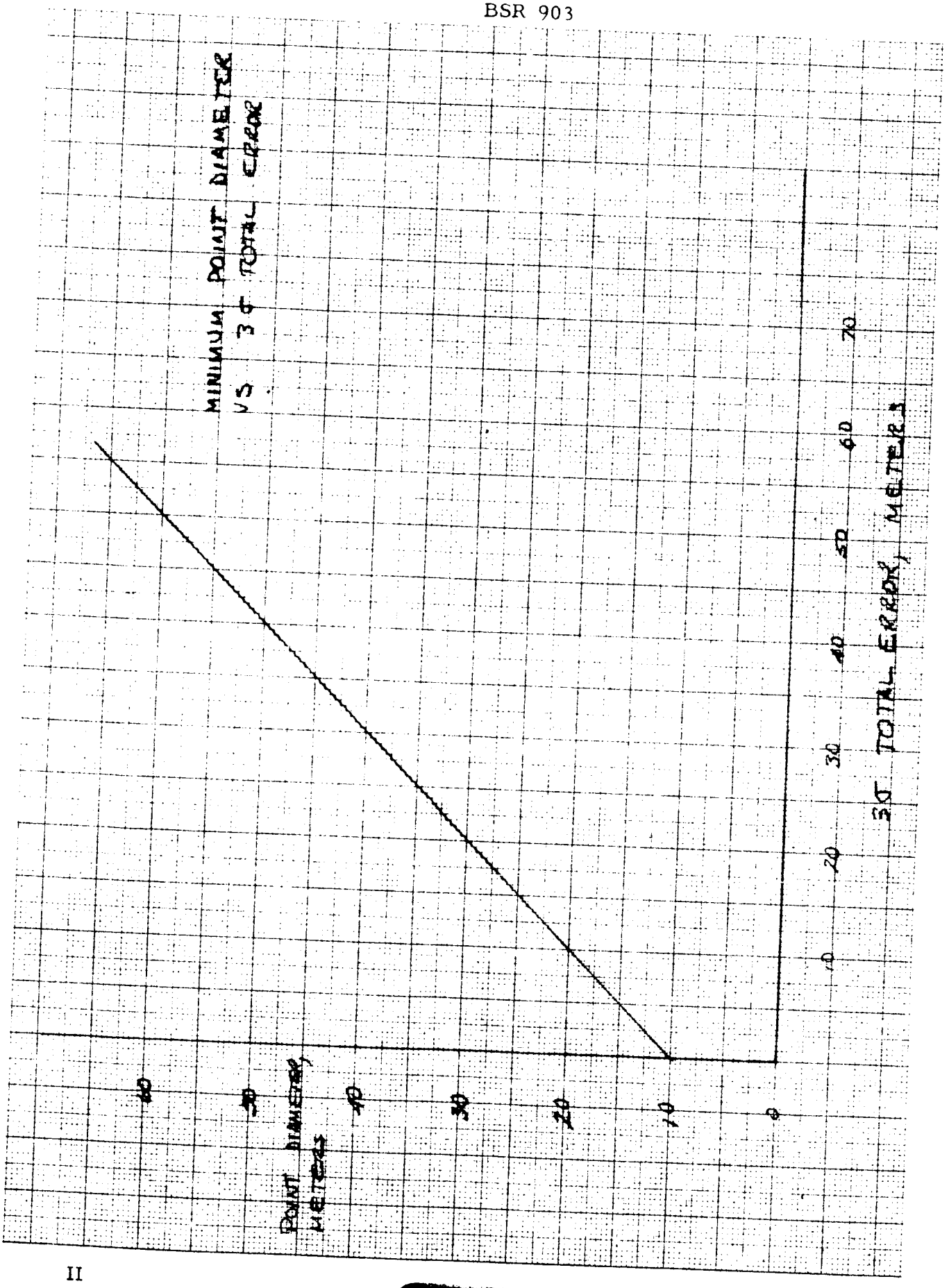

Figure A-7 Minimum Point Diameter vs 3σ Total Error

II

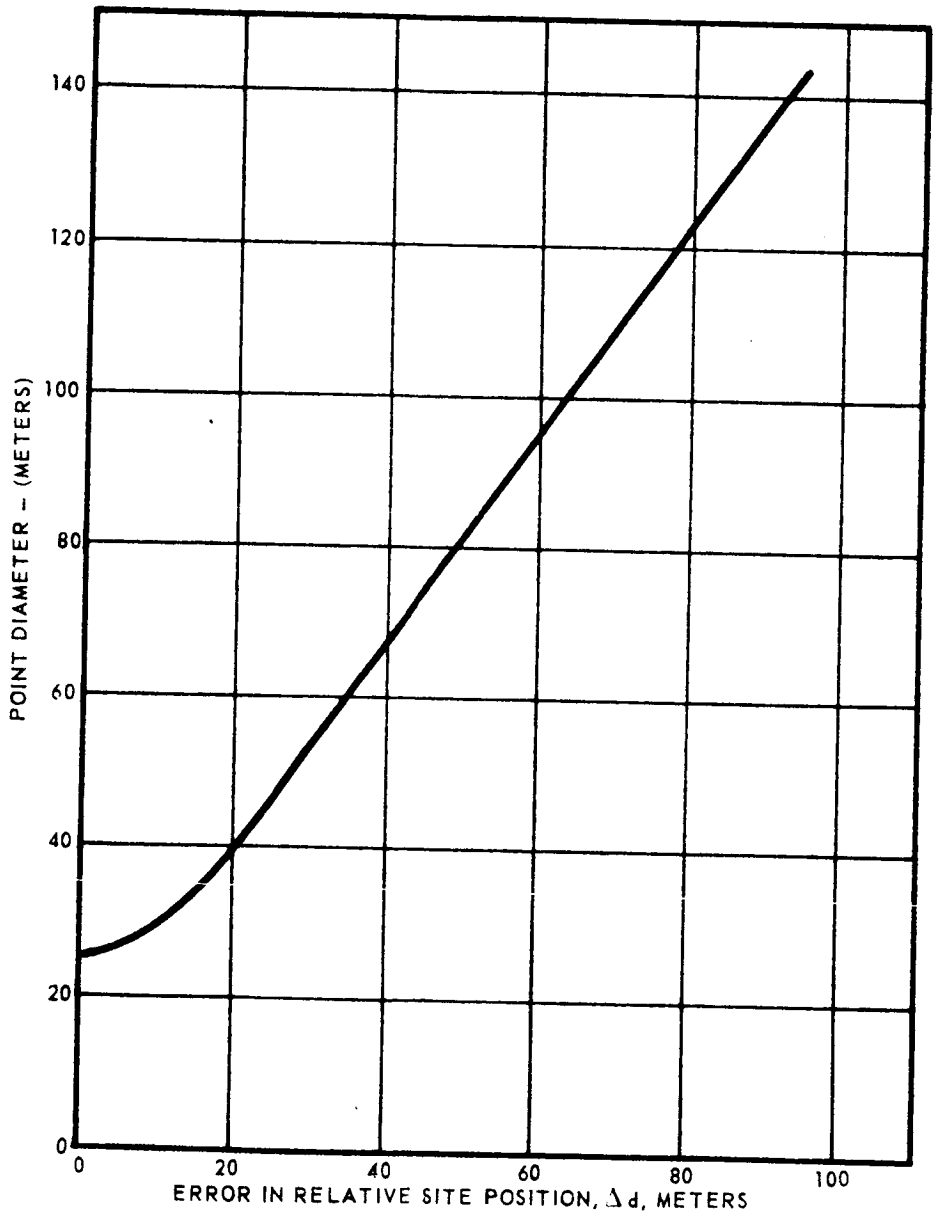

Figure A-8 Point Size as a Function of Relative Point Position Error

1. The guidance and position errors attributable to the LEM primary guidance system are negligible.

2. Using a triangulation scheme as described or one similar to it, error in LEM position is bounded by the curve of Figure A-5.

3. It is possible to identify acceptable landing points without physically marking each point. This allows a tremendous reduction in the amount of marking material required.

4. A relationship has been established between required point size and LRV navigation capability.

A.5 PHYSICAL SITE MARKING

A.5.1 General

The requirements on the marking material and the marking pattern imposed by the LEM optical capabilities are discussed in the following paragraphs. The measurement of the angles indicated in the previous analysis may be performed by one of three methods:

1. TV
2. Human eye
3. Human eye aided by a telescope

A brief description of the resolution and field of view capabilities of each method over the range of interest is given below.

A.5.2 Field of View and Resolution

The field of view of the human eye is limited only by obstruction from the vehicle. The comfortable resolution obtainable by the eye is normally defined as 3 minutes of arc.

Thus,

$$\text{Resolution} = 8.72 \times 10^{-4} \times \text{Range},$$

and at an assumed initial LEM position at which resolution is required (h = 3048 meters, x = 1830 meters), the eye has a resolution capability of 3.1 meters.

A telescope reduces the field of view of the eye but it is assumed to be acceptable. The resolution is assumed to be improved by a factor inversely proportional to the power (P) of the telescope:

$$\text{Resolution} = \frac{8.72 \times 10^{-4} \times \text{Range}}{P}$$

For a nominal telescope of power 50, the resolution obtained by the eye with the telescope is 6.1 cm at the assumed initial point.

Available data pertaining to the Surveyor Lander TV System were used to arrive at quantities approximately equal to those of the LEM TV system. The following two expressions may be written:

$$\text{Field of view} = (0.11)\ \text{Range}$$

$$\text{Resolution} = (1.83 \times 10^{-4})\ \text{Range}$$

Thus, at the initial LEM position, the field of view encloses a square of 392 meters per side and has a resolution capability of 0.65 meters. Figure A-9 summarises the optical resolution capabilities of the LEM.

A.5.3 Detection

A further consideration in marking the point is that of detection. The three optical techniques available to the LEM system must again be considered. The area which must be marked to assure detection is defined as follows:

$$D_c = 2R \left[\frac{E_R}{E_{SB} A_B \cos\psi} \right]^{1/2} \qquad \text{(A-18)}$$

where

D_c = diameter of marked circle

ψ = angle between a normal to the surface and incident radiation vector.

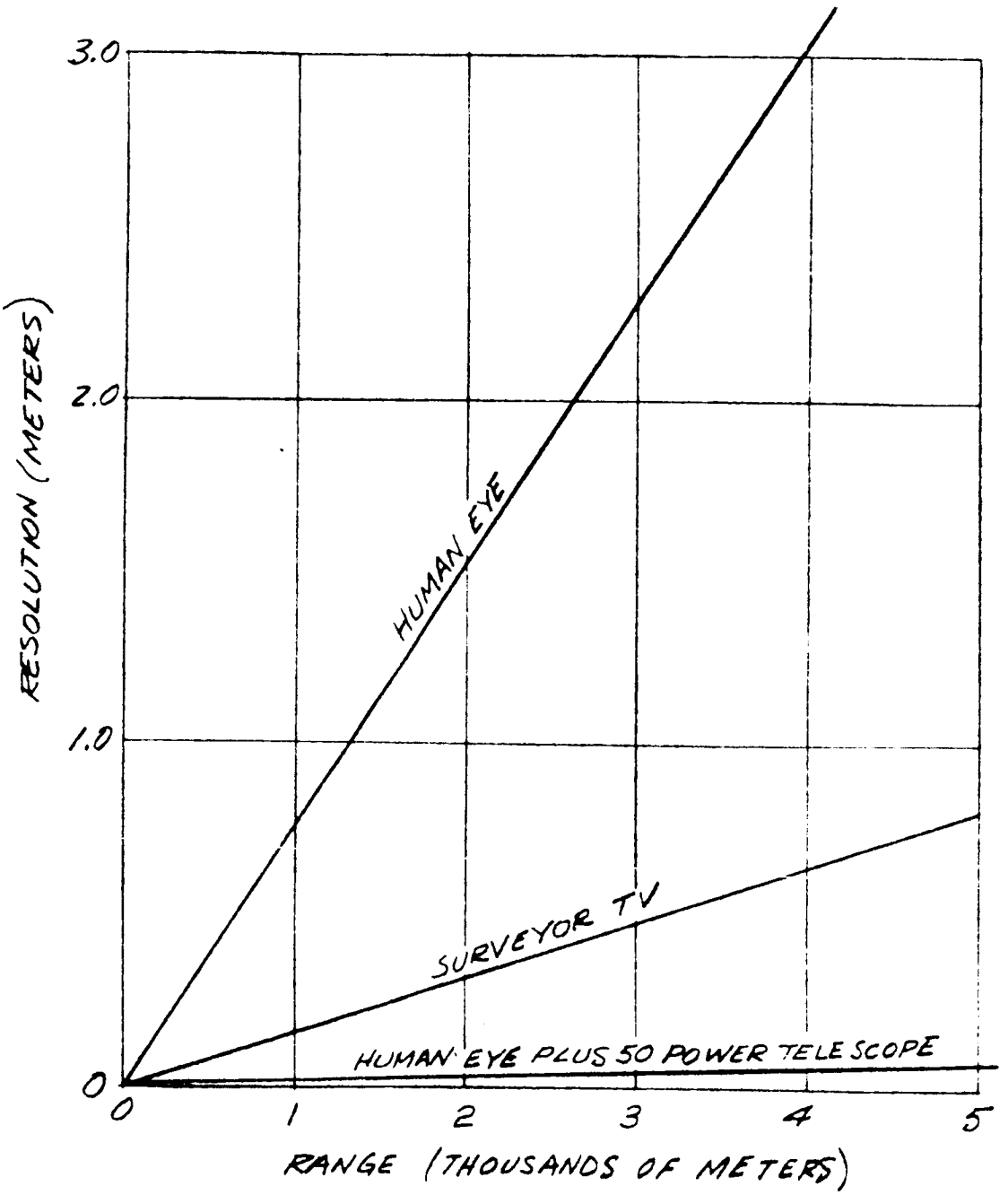

Figure A-9 Optical Resolution vs Range

A_B = albedo of marked area

R = range from which marked point is being viewed

E_{SB} = illumination from sun falling on marked point (on a plane normal to incident radiation)

E_R = minimum illumination required for detection

In the following discussion it is assumed that:

E_{SB} = 15.2 lumens/cm^2 (full moon)

ψ = 0.0 degree

A_B = 1.0

For the human eye, the parameter E_R has been defined, based on experimental data, as a function of background brightness. A background brightness value which was based on the above assumption and a moon albedo of 0.073 yields an E_R of 1×10^{-8} lumen/cm^2. Figure A-8 may be used to determine the required diameter of a marked area as a function of altitude for easy visual detection. This figure is a plot of Equation (A-17) based on the above mentioned assumption and that the calculated value of E_R was increased by a factor of 5 (easy visual detection). This diameter is actually that of a circle of area equal to the projected (normal line of sight) area of the marked area. Thus, at the assumed initial LEM point (h = 3048 meters, x = 1830 meters), the projected area of the marked area must have an equivalent diameter of 0.415 meters.

For the human eye with a telescope, such parameters as the light transmission characteristics of the telescope must be considered, but in general the power of the telescope may be used directly to convert the data of Figure A-10.

At present, the sensitivity of the LEM TV is unknown. Unit information concerning the sensitivity is obtained, it will be assumed that one resolution unit is required for detection.

The detection and resolution capabilities at the initial correction point are summarized in Table A-1.

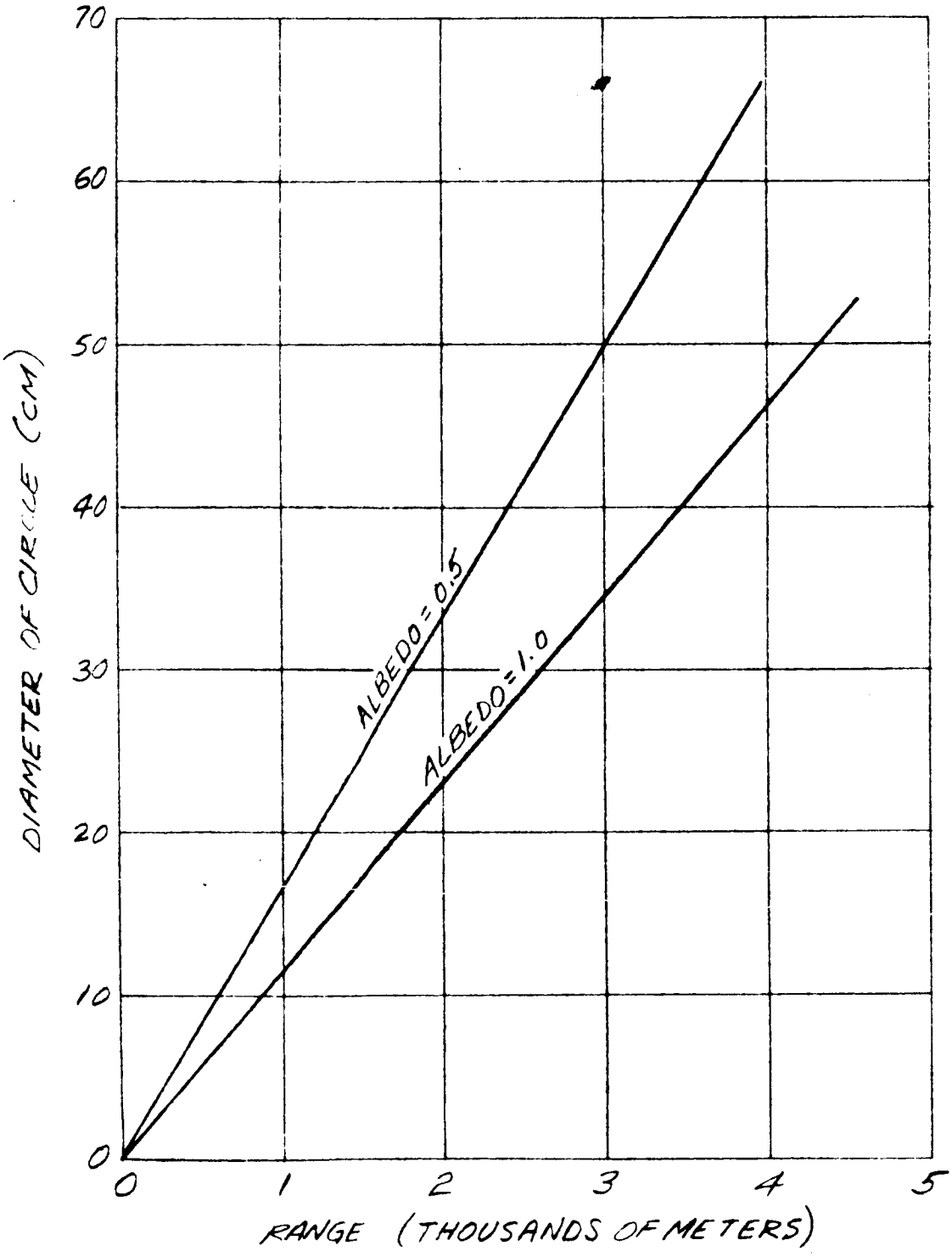

Figure A-10 Required Diameter of Marking Circle as a Function of Range for Easy Visual Detection

TABLE A-1

DETECTION AND RESOLUTION CAPABILITIES AT INITIAL CORRECTION POINT

	Detection (cm)	Resolution (meters)
Human Eye	41.5	3.1
Humay Eye and Telescope	0.823	0.061
TV	65	0.65

A.5.4 Effective Diameter Required for Marked Area

If it is assumed that the maximum marked area is desired for detection (for the purpose of a redundant system), the marking must be performed with no unit area of a diameter less than 0.65 meters.

For resolution, a redundant capability is required of only human eye and telescope and TV techniques. Thus, the resolution unit of the marked area is defined as 0.65 meters. An assumption that the resolution unit is 10 percent of the total marked area yields a required area of size equivalent to a circle of 6.5 meters diameter.

The physical configuration of the LEM also places a restriction on the area to be marked. It is required that the portion of the marked area be visible to the LEM optical system throughout descent. The field of view from a LEM window is defined by (1) horizontal viewing angle euqal to 87^{o}, and (2) vertical viewing angle from -70^{o} to 28^{o}. Additional coverage is possible by the LEM TV; however, for redundancy, -70^{o} is the capability for point observance.

A.5.5 Marking Material Requirements

The marking material must be compatible with the mission requirements. That is, it must meet the transportation requirements on-board the Surveyor in the earth-moon transportation environment, and it must further maintain its marking capabilities on the lunar surface, in the lunar environment, for a minimum duration of one year.

APPENDIX B

PHOTOMETRIC DATA

The photometric data are reduced by computer analysis as follows:

1. An exposure of the scene is made, including an image of the calibration step wedge in the upper corner of the field of view. These data and all pertinent auxiliary angle data (see Section 2.5) are telemetered to earth and stored in computer.

2. SLRV moves to new position and a second exposure with sufficient overlap of the preceding scene is made; image data are again transmitted and stored.

3. The computer constructs a vidicon response curve from known calibration luminances (computed in advance and stored) and average vidicon output from the eight (20 x 20 line) steps in upper corner of scene.

4. Using the vidicon response curve, in absolute luminance units versus volts, the absolute luminance of each scene element is computed.

5. Steps 3. and 4. are repeated for each frame of data.

6. The computer takes at least two luminance values from the same terrain area (it must compute which screen element is being analyzed from vehicle-camera displacements, or a human must be put in the circuit via a computer-driven display to make this decision), and plots these luminances versus relative camera angles (this is equivalent to sensor angle).

7. The computer then performs a least squares fit for these data points to all the photometric functions for the given value of α (the angle between source plane and sensor plane, measured by the SLRV). One method of doing this would be to fit the data to $i = -90^{o}, -80^{o}, -70^{o}, \ldots\ldots\ldots, +80^{o}, +90^{o}$ (19 curves), select the best fit, then fit the data to the 20 curves for $i = (n-10^{o}), (n-9^{o}), \ldots\ldots\ldots, (n+10^{o})$ around this best fit. Thus, for each area investigated 40 comparisons would be required, yielding i^{1} of best fit.

8. The best value for i^{1} is read out. This is the apparent angle of the sun relative to the normal to the surface at that point. The difference between i^{1} and the angle of the sun relative to the local vertical (i) is the component of the surface slope, projected along the line of sight.

$$i^{1} = i = \psi$$

9. These data can then be stored for future use.

10. The $(n+1)^{th}$ scene is compared to the nth, and so on.

There are two possible methods to reduce the vidicon output to luminance plots. The basic problem involved is that of identification of the same area in two successive frames. The change in vehicle and camera orientations should be used to compute the new position of a specific terrain segment if possible. If this procedure is not possible, an observer must view a monitor and instruct the computer as to which portion of the second frame to select and plot with the first data point.

The only additional equipment required for earth-base reduction is a computing facility with a display suitable for data presentation in a readily usable form. If an observer must locate and identify terrain elements in successive frames for real-time aid in control and safety of the vehicle, a display monitor with a luminance sensing device or a sampling of the incoming video signal will be necessary.